ADA 144417

DESIGN AND FABRICATION OF 8-INCH EXTENDED RANGE AMMUNITION

Sabot Technology Study

DISTRIBUTION STATEMENT A
Approved for public release;
Distribution Unlimited

DESIGN AND FABRICATION OF 8-INCH EXTENDED RANGE AMMUNITION

Sabot Technology Study

SABER INDUSTRIES, INCORPORATED
North Troy, Vermont 05859

December 1979
Final Report for Period September 1976 - December 1979

U.S. Army
ARMAMENT RESEARCH AND DEVELOPMENT COMMAND
Dover, New Jersey 07801

FOREWORD

This final report was prepared by Saber Industries, Incorporated (formerly Space Research Corporation), North Troy, Vermont and documents work completed under Contract Number DAAA21-76-C-0543 with the U.S. Army Armament Research and Development Command (ARRADCOM), Dover, New Jersey.

TABLE OF CONTENTS

TABLE OF CONTENTS (Continued)

LIST OF ILLUSTRATIONS

LIST OF ILLUSTRATIONS (Continued)

LIST OF TABLES

1.0 INTRODUCTION

1.1 BACKGROUND

The doctrine of Soviet artillery usage calls for massed fire from heavy deployments of artillery pieces. The quantities of weapons and rate of ammunition expenditure far exceed those employed by NATO allies. Factors of 6:1 have been quoted in open literature. The widely deployed Soviet 130mm M46 field gun is reported to have a maximum range of 27,500 meters, exceeded among currently deployed modern artillery weapons only by the 175mm M107 SP. Thus the artillery of the Nato allies is not only outnumbered but also outranged.

Because NATO artillery is typically more sophisticated and hence more expensive on a per unit basis than Soviet artillery weapons, correction of the numerical inferiority poses a difficult and costly problem. However, the range disadvantage can be corrected at modest cost, and if the artillery of NATO countries can be provided with a range advantage, then this can, to some extent, offset the present numerical deficiencies.

The use of extended range artillery gives the following advantages:

a) An increased range capability allows fewer guns to cover a wider front. More efficient operation is thus possible, since each battery is now capable of responding to more fire missions.

b) Targets deeper in enemy territory can be engaged. While some of these long range targets have larger target location errors, improved payloads can make up for this problem. Further, many target locations such as choke points, are accurately known, and others are area in nature and provide

target rich environments where delivery precision is not so critical for improved payloads. Many area targets are well defended against air attack and are positioned sufficiently rearward from the FEBA so as to be inaccessible to existing artillery.

c) A range advantage over enemy weapons permits suppresive, neutralization and counterbattery fire to be delivered with minimum exposure to return fire.

d) In the modern concept of fluid FEBA's, an improved range allows weapons to be positioned further rearward, giving an added measure of safety against fast breaking incursions.

Several methods of achieving extended range are possible using existing demonstrated technology. Boosted (rocket assisted) projectiles have been developed. Base bleed, a process of base drag reduction, has been demonstrated. Unboosted, purely ballistic projectiles using low drag techniques are a promising low cost alternative to boosted rounds. Spin stabilized subcaliber projectiles have shown range increases in excess of 40% (175mm M107 SP), while analyses of fin-stabilized projectiles indicate even larger increases (greater than 50%) can be achieved in the 8-inch M110E2 SP weapon.

The 8-inch M110E2 is planned to replace the 175mm M107 as the principal heavy artillery piece in the U.S. Army inventory. For this reason, the exploratory development program reported on herein was chosen to focus on the M110E2 weapon system, and to examine and definitize the potential which exists for the defeat of various selected targets at extreme ranges. The program was structured to concentrate on subcaliber projectiles as offering the most promise for success.

1.2 EXTENDED RANGE SYSTEM CRITERIA

Several system criteria were established to guide in evaluation of extended range projectiles. It was decided early on that the payload would be some type or types of submunitions. These might be lethal types, such as AP or AM submunitions or mines, or non-lethal such as electronic packages for communications jammers. As a point of departure, a payload similar to the 155mm M483 submunition cargo was used.

The selected extended range round should be compatible with existing weapons. Battlefield operations may vary for special rounds, so as to allow for a safe sabot discard area, and minor changes in the handling and ramming may be required. However, the basic weapon should be capable of firing either extended range or standard ammunition without change. This includes firing through tubes equipped with muzzle brakes.

An upper performance bound is established by the weapon operating limits. Maximum operational breech pressure must not exceed 40,000 psi and velocity is constrained by muzzle momentum considerations.

In view of the great possible disparity between shot weights and chamber volumes of ERA and standard rounds, special propelling charges are permissible. Although design of a propelling charge was not a part of the scope of work for this effort, some work of necessity was required in order to conduct the test program.

1.3 OBJECTIVES

The primary goal of the effort discussed in this report was the design of an 8-inch extended range subcaliber projectile to carry a target effective payload to a range of greater than forty kilometers when fired from an M110E2 SP howitzer. The design effort included

concepts for the sabot, vehicle, and fins. Following the design and component development phases, it was required to demonstrate the vehicle performance in a flight test.

1.4 PROJECTILE REQUIREMENTS

As previously stated, the selected payload for the 8-inch extended range round was one similar to the 155mm M483. This established the basic size for the projectile. Initial designs made use of concepts for sabotted projectiles previously demonstrated by the Department of Defense as well as the contractor. Earlier demonstrations of dramatic increases in range using sabotted projectile concepts provided the justification for this subcaliber sabot technology study.

Firing a subcaliber projectile requires the use of a sabot, which is a system of structural members affixed around the periphery of the projectile to:

a) Position and structurally support the projectile during the high axial acceleration of a gun launch;

b) Seal or obturate the propellant gases within the launch tube;

c) Minimize balloting of the projectile;

d) Impart rotational acceleration to a spin-stabilized projectile or isolate to a repeatable degree the rotational acceleration transmitted to a fin-stabilized projectile;

e) Discharge from the launch tube and separate from the projectile without disturbing the launch tube or the projectile in its flight.

The basic concept of using a sabot-projectile combination is to result in a total weight less than that of a full caliber round, thus making it possible to obtain a higher muzzle velocity. By then separating and discarding the sabots from the projectile after it emerges from the launch tube, the resultant high velocity, relatively low drag projectile achieves longer ranges and has greater target accessibility. Range increases of greater than 50% can be readily achieved with payloads which are a significant fraction of standard projectile weight.

Required in the development of this round was the compatibility of the projectile to 8-inch weapons including the M110E2 which is fitted with a muzzle brake. Thus, although the gun tube walls limit the natural tendency for the sabot petals to move radially away from the projectile due to spin induced centrifugal forces, there is no such restraint as the sabots pass through the muzzle brake. This radial displacement must then be limited in another manner until the shell exits the muzzle brake. This company has developed for this application a number of techniques which are, in general, dependent upon the geometry of the interface between the petals of the sabot and the projectile, and the spin rate of the sabot and projectile. These techniques are applicable to both high spin rate, spin stabilized and low spin rate, fin stabilized projectiles.

In designing subcaliber projectiles about a chosen payload, there are basic guiding principles to aid in the conceptualization of the sabot-projectile design to attain the most efficient use of the sabots and the longest range from the flight vehicle. For instance the in-bore supports and/or sabots should be placed sufficiently far apart to provide a good wheelbase to reduce the lateral in-bore accelerations of balloting. Also the ratio of total sabot mass to total projectile shot mass should be minimized since this parameter largely determines the amount of kinetic energy lost upon launch due to sabot discard. Additionally, with respect to the vehicle, the shot weight should be as light as possible to attain the highest permissible muzzle velocity.

The cross-sectional projected area of the vehicle should be reduced as much as possible and combined with a good aerodynamic profile to minimize the rate of velocity retardation due to drag and hence result in a longer range. These basic guidelines were integrated early in the conceptual development of the projectile to produce a vehicle design with long range capabilities.

1.5 APPROACH

The initial endeavor in this program was to evaluate previous as well as new sabot designs which offered the potential of successfully launching a subcaliber projectile to extended ranges. Concepts offering hope were evaluated by firing test slugs and recording sabot functioning parameters. The selected concept was then test fired using prototype flight vehicles. Throughout this effort a design program for the basic vehicle was conducted. Although spin stabilized concepts were considered, the main payoff in range appeared to be fin-stabilized rounds and most of the effort was related to such designs. Thus fin design represented a significant portion of the vehicle configuration work. During the test program a satisfactory propelling charge was also developed. After demonstrating component performance, ten rounds were fabricated and flight tested, demonstrating extended range performance. Finally, twenty additional rounds were fabricated and delivered to the Army for further testing.

Specific details of the program are discussed in the following sections of this report. Flight test data supplied by Yuma Proving Ground are presented to validate extended range performance. Finally, recommendations for additional work are outlined, accomplishment of which could complete development of the extended range projectile system and provide the Army with a means to deliver highly effective payloads to ranges significantly beyond 40 kilometers with the existing M110E2 weapon.

2.0 CANDIDATE SABOT DESIGN CONCEPTS

In the conceptual development of the extended range projectile, three basic geometric sabot configurations were considered:

1) Base Pusher Plate Sabot System
2) Center Sabot System
3) Split sabot system

These design concepts are described in the following sections, along with latching and obturation techniques.

2.1 BASE PUSHER PLATE SABOT SYSTEM

In the base pusher plate sabot concept, three examples of which are shown in Figure 1, a thick base plate is utilized to obturate the propelling gas and support the projectile mass ahead of it during acceleration. Additional support, to align the projectile with the axis of the gun tube bore, can be provided at the projectile's mid section, as shown in Figure 1A, or in the region of the nose, as shown in Figure 1B and 1C.

In the concept of Figure 1A, the base pusher plate serves to transmit accelerating forces to the projectile base, creating high stresses in this location, and requires a heavy tail section. However, the base pusher plate shelters the fins from the blast of high pressure propelling gas and unburned propellant grains, providing greater latitude in the fin design.

The center sabot, which provides lateral support and in-bore alignment, is itself supported by the base pusher plate and therefore no grooved connection between the projectile body and the center sabot is necessary. The elimination of the need for these grooves allows for a lighter, thinner body wall design free from groove associated stress concentrations.

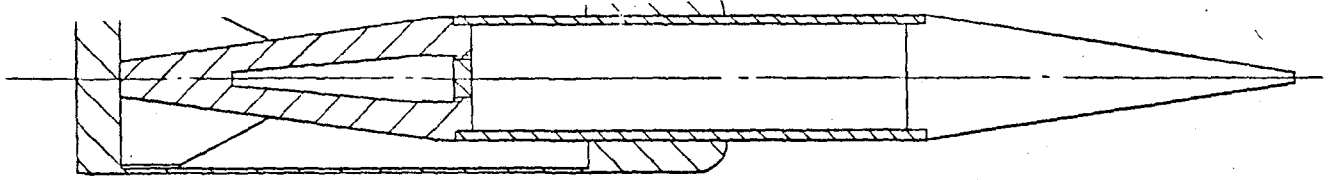

A. Base Pusher Plate with Center Sabot

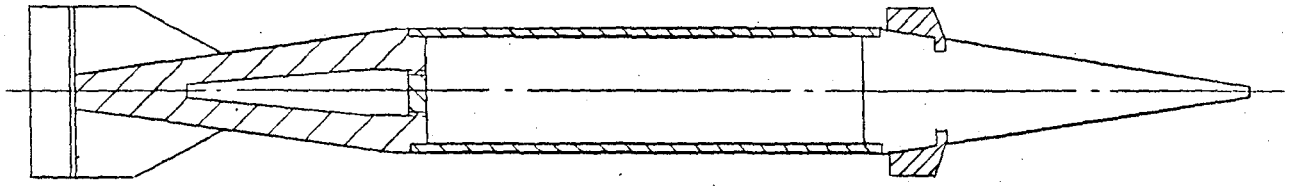

B. Base Pusher Plate with Front Bore Riding Sabot

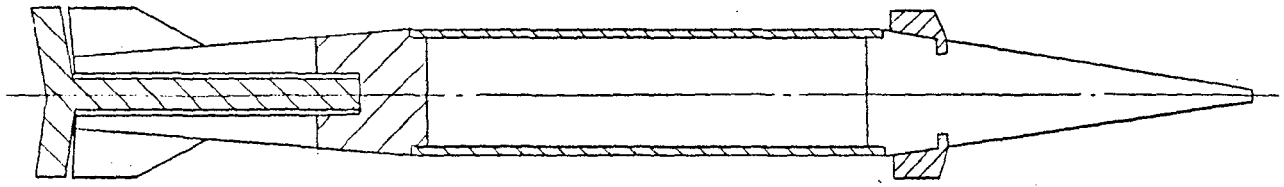

C. Base Pusher Plate and Ram with Front Bore Riding Sabot

Figure 1. Base Pusher Plate Sabot Concepts

The concept of Figure 1B is somewhat of an improvement to the previous case, primarily in that it has a lighter sabot mass. This reduction in weight of the sabot has two effects; it reduces the shot weight of the projectile, allowing higher muzzle velocities, and it reduces the ratio of sabot mass to projectile shot mass, a factor related to the loss of kinetic energy upon projection due to sabot discard. Additionally, the greater axial distance between the base pusher plate and the front sabot gives the projectile a longer wheelbase which is instrumental in reducing in-bore balloting and unwanted projectile dynamics upon muzzle exit.

The concept of Figure 1C not only retains the benefits of the previous two designs but adds one additional improvement. The previous two concepts each requires a massive tail section to support the forward accelerated masses of the body, paylaod and nose. This heavy tail section contributes to a center of gravity position more to the rear, having an adverse effect upon the projectile's stability during flight. In this concept the projectile is supported at the fortified base of its payload section by a shaft extending from the base pusher plate. This adaption to the base pusher plate concept allows the use of a light weight tail section and hence gives the most forward possible position of the center of gravity of the projectile flight configuration.

The principal advantage of the base pusher plate sabot concept is that it has an affinity for conventional ramming with a positive ram stop and shot start pressure. The capability for conventional ramming allows for retention of the projectile at its rammed location at high gun elevation and allows for conventional means of obturation by positioning the obturator at the origin of the rifling.

2.2 CENTER SABOT SYSTEM

Two concepts relating to the center sabot system are illustrated in Figure 2. In this sabot system obturation is maintained behind the center sabot and the loads of acceleration are transmitted to the center sabot by grooves in the projectile body. In-bore alignment can be maintained by either fin-attached bore riders as shown in Figure 2A or by a bore riding front sabot as shown in Figure 2B.

The center sabot configuration of Figure 2A, with bore riding fins, is similar to that used in the 105mm APFSDS-T M735 tank gun kinetic energy ammunition in service and also in the U.S. Navy "Gun-fighter" 8-inch HE projectile. It is characteristic of this concept that a relatively thick body wall is necessary to resist the high chamber pressures behind the center sabot and to accommodate the the required grooved interface between the sabot and projectile. For a specified payload this results in a larger projectile body diameter, a greater shot weight, and a greater frontal cross-sectional area, the results of which are a lower attainable muzzle velocity and a higher drag coefficient, each having an adverse effect on the projectile range of flight.

This configuration, as mentioned earlier, utilizes bore riding fins to ensure bore alignment. To avoid any possibility of the fin tips engaging with the rifling, bore riding tabs spanning two lands of the rifling must be used. These tabs can be either permanently attached, causing added drag during flight, or may be temporarily attached and restrained during muzzle exit from striking the muzzle brake. An additional design consideration in the use of fin bore riding tabs is that they are the lightest means of achieving bore alignment but require the frailest of all components, the fins, to provide this support.

The means of obturation with the center sabot system has become more complicated than the base pusher plate system previously discussed.

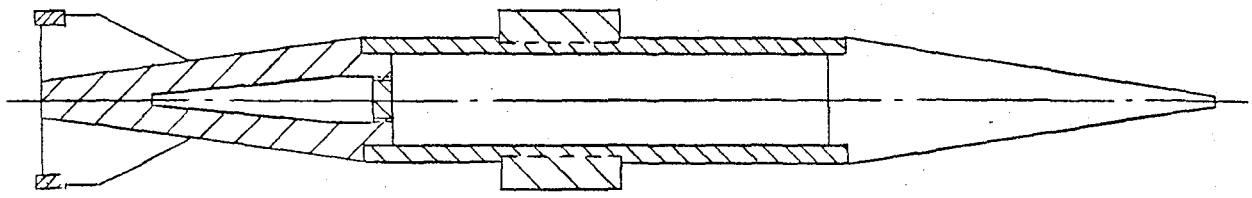

A. Center Sabot with Fin Attached Bore Riders

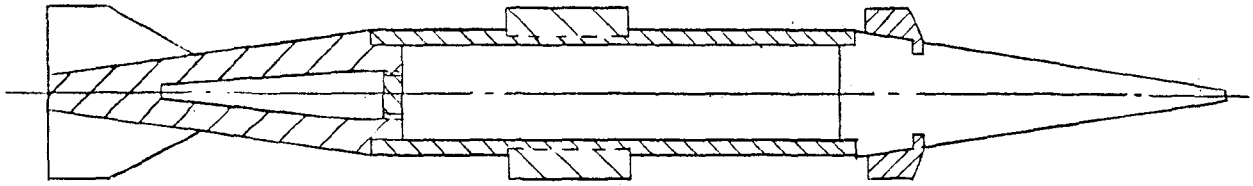

B. Center Sabot with Front Bore Riding Sabot

Figure 2. Center Sabot Concepts

This is so because, for instance, if the center sabot were rammed to engage the rifling at its origin there would not be sufficient chamber volume to attain any reasonable internal ballistic solution. This then means that the center sabot with its obturator must be able to be slid far into the bore of the gun and yet still obturate the propelling gas upon functioning of the gun. The design options to accomplish this will be left to be discussed later.

The concept of Figure 2B relieves the fins of the requirement to provide in-bore lateral support in favor of a much more sturdy system, a front bore rider. This is the principal achievement of this design concept, but it must be recognized that a corresponding increase in the projectile shot weight results. This concept must also use a complex obturation system and just as in the previous center sabot configuration provision for good ramming and shot start pressure characteristics are not inherent features. The promising aspects of these center sabot concepts, however, include a lighter tail section, promoting in-flight stability, and a lighter sabot weight. The lighter sabot weight reduces the shot weight, making available higher muzzle velocities, and reduces the ratio of sabot mass to projectile shot mass, giving prospects of greater ranges than the base pusher plate system.

2.3 SPLIT SABOT SYSTEM

The split sabot system, shown in Figure 3, utilizes a rear sabot mounted behind the body with in-bore alignment maintained by a front bore riding sabot. This effectively combines the weight advantages of both the base pusher plate sabot system and the center sabot system, that is, the thin body of the base pusher plate system, and the lighter tail and sabot weight of the center sabot system.

Because the rear sabot is not interfaced to the body, as shown in Figure 3A, a light weight thin walled body design may be utilized to reduce the weight of adjacent projectile components such as the tail

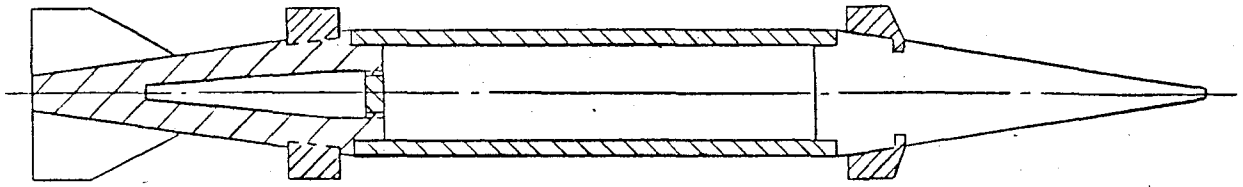

A. Split Sabot System

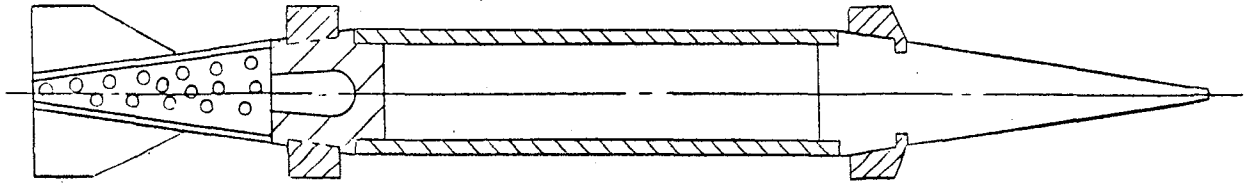

B. Split Sabot System with Ventilated Tail

Figure 3. Split Sabot Concepts

and nose assemblies and to reduce the drag of the flight vehicle. The sabot weight of the split sabot system is much lighter than the base pusher plate system but not as light as the center sabot system with bore riding fins. However, in this case, as in the case of the center sabot system with the front bore riding sabot the fins are not required to provide lateral support.

Again, as in the case of the center sabot system, the massive tail assembly required of the base pusher plate system is not required here, keeping the flight configuration center of gravity more forward and thus improving prospects for stability. In fact, as illustrated in Figure 3B, the tail section may be ventilated to allow the equalization of the pressure created by the propellant gas in the interior of the tail section. This then allows for a substantial reduction of this component's weight, further reducing the shot weight and improving stability.

The disadvantage with the split sabot system, like the center sabot system, is that these design concepts are not readily ameanable to conventional ramming and thus the means of obtaining obturation becomes complicated, as will be discussed later.

Also, in comparison with the center sabot of the center sabot system, the rear sabot is both closer to the central axis of the projectile and in closer proximity to the fins. This means that in order for the rear sabot to avoid contact with the fins during discard, the discard characteristics of the rear sabot must be attenuated over the center sabot.

2.4 SABOT LATCHING CONCEPTS

The application of sabotry to finned projectiles poses special problems. It is essential that the fin stabilized projectile be launched with low residual spin rates. Successful previous designs have used spin rates of between 10 and 50 rps at muzzle exit. Ideally the

muzzle spin rate should be identical with the steady state spin rate induced by fin cant or similar means. This condition implies no tendency either for spin-up or spin-down and produces minimum induced drag losses. However, no matter what muzzle spin rate results, that spin rate must be repeatable from round to round. If large spin rate deviations occur, the accuracy of the projectile will be severely degraded.

The partial spin rates required by fin stabilized projectiles necessitate a decoupling between the projectile and the tube rifling. This decoupling may occur either at the sabot-obturator interface or the sabot-projectile interface. When spin isolation occurs by spin decoupling at the sabot-obturation interface, the resultant advantages will be more control of spin rate, better force transmittal and a low inertia of spinning parts, with the disadvantage that sabot discard will be more difficult because of little centrifugal force. On the other hand, the advantages of spin isolation occuring at the sabot-projectile interface are better obturation, easier sabot to projectile latching and improved sabot discard which is enhanced by spin. Disadvantages of this technique are that the sabot-projectile interface is a bearing surface, making it more difficult to transmit acceleration, and closer tolerances and surface finish control of sabot and projectile parts are required. The approach considered best is to decouple principally at the obturator-sabot interface because although full spin sabots (sabot-projectile interface spin decoupling) are easier to design for clean discard, the sabot-projectile interface must be a bearing surface capable of transmitting accelerating forces but decouple the torque. This is difficult to do without transmitting excessive spin rates to the projectiles.

In the case of the base pusher plate the means of discard are self-evident. But in order that the sabot petals of the center and split sabot systems be restrained against lateral movement during handling and in-bore motion, while discarding freely after passing through the muzzle brake, special provisions must be made. For the front bore riding sabot of each sabot system, a simple inertial latch may be

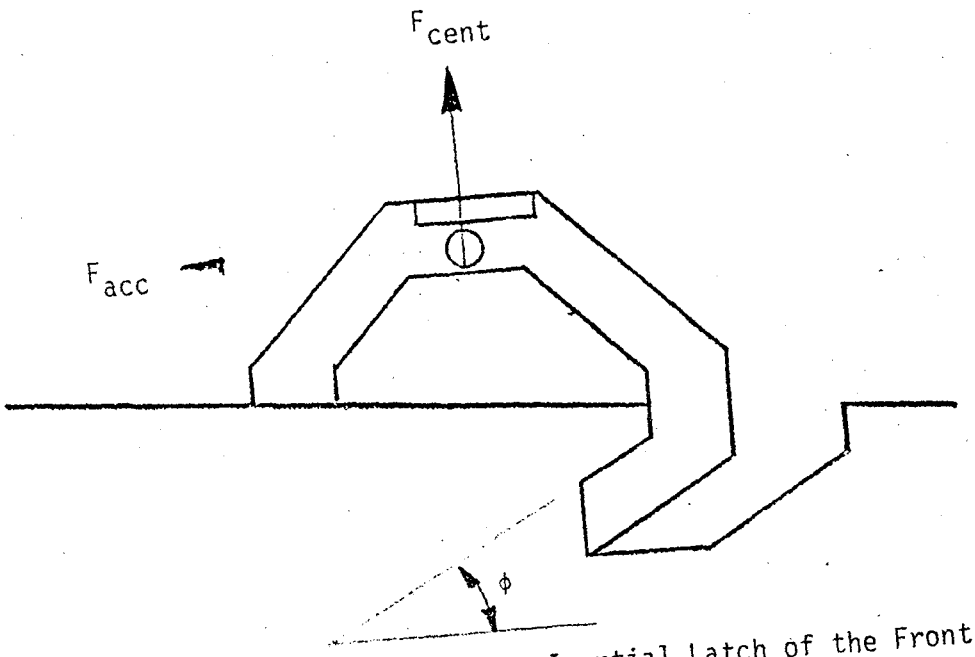

Figure 4A. Diagram showing the Inertial Latch of the Front Bore Riding Sabot and Loads during In-bore Travel

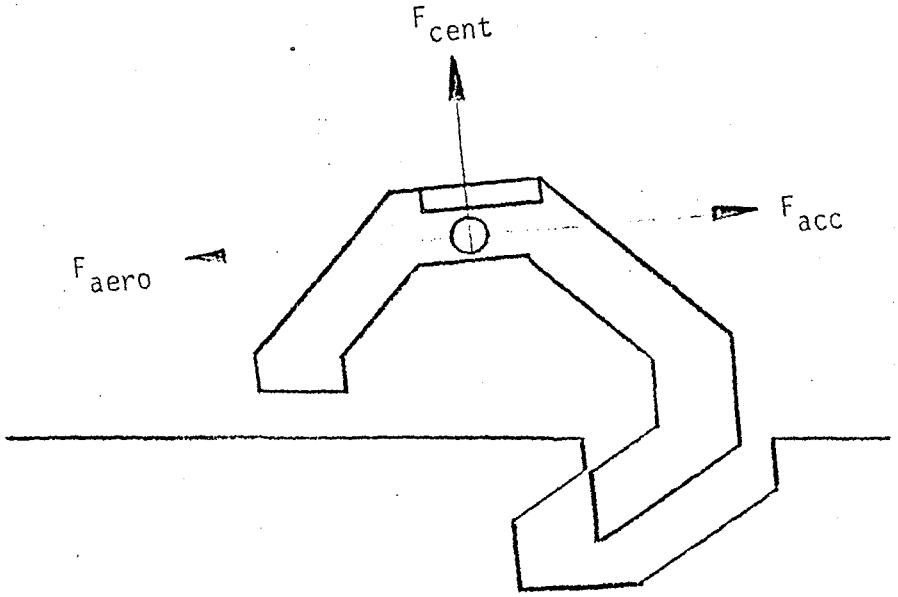

Figure 4B. Diagram showing the Inertial Latch of the Front Bore Riding Sabot and Loads during Deceleration after Muzzle Exit.

employed. The operation of this concept may be visualized by reference to Figure 4. During in-bore travel, inertial loads (F_{acc}) cause the rider to set back against the angled groove in the body. The angle of this groove (ϕ) is usually selected so that the component of set-back force (F_{acc}) overcomes the component of centrifugal force (F_{cent}). The front rider is thus restrained during the firing cycle. The projectile will continue to accelerate until the obturation seal formed by the rear sabot is broken. Shortly after this time, the projectile will begin to decelerate. Three principal forces shown in Figure 4B are now acting on the rider petals:

a) Centrifugal forces, tending to force the petal forwards and outwards along the angled surface.

b) Deceleration forces, driving the petals forward.

c) Aerodynamic forces acting to maintain the rider in a rearward position.

The latch angle of the rider-projectile interface is chosen so that in this situation, centrifugal forces will cause the radial motion of the sabot petals out of contact with the groove and away from the projectile, thus achieving discard. In low spin projectiles this technique may need to be augmented by aerodynamic forces.

For sabot systems involving a center sabot or the rear portion of the split sabot system shown in Figures 2 and 3, a modified buttress groove has been found suitable, as shown in Figure 5. The principal of operation is similar to that for the front rider, except that the latch is directed in the opposite direction. For this sabot, gun gas pressure (P) provides the dominant force. The latch rake angle (θ) is chosen so that the component of gun gas pressure provides a net inward force, overcoming the centrifugal force tending to drive the petals outward. The critical design condition for the latch angle is that existing during traverse of the muzzle brake. It is necessary to hold the sabot latch even under the low base pressures which exist at muzzle brake

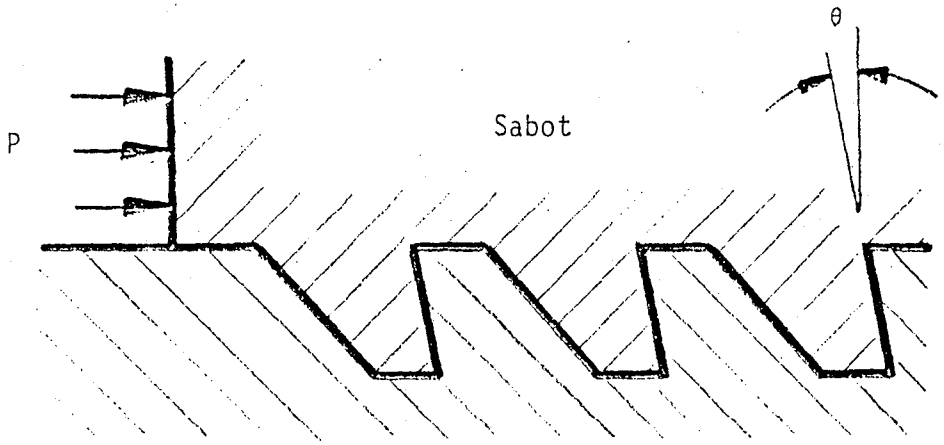

Figure 5. Latching System for Center or Rear Sabots

exit. Depending on the design of the brake and its efficiency, the pressure is estimated to be between about 15 percent and 50 percent of true muzzle pressure, i.e., between about 2000 and 5000 psi. Discard in this case is effected by centrifugal and aerodynamic forces.

2.5 OBTURATION CONCEPTS

The self-evident means of attaining obturation with the base pusher plate is sharply contrasted by the complex means of achieving obturation in the center and split sabot systems. In fact the successful implementation of the center and split sabot concepts is dependent upon the formulation of a successful obturator design to meet special requirements.

First, since the rearmost sabot is positioned far into the bore of the gun, provision must be made to allow the obturator to slide past the origin of rifling and yet still provide obturation upon exposure to the propelling gas. Second, the obturator must discard upon muzzle exit to allow the separation of the sabots.

To satisfy these requirements, two obturator configurations can be considered. The first is the use of a pre-engraved obturator, shown in Figure 6, such as was used in the U.S. Navy "Gunfighter" 8-inch HE projectile. In this concept a rubber obturator is pre-engraved which allows the obturator to interface with the rifling upon insertion into the bore. Upon exposure to the high pressure chamber gas the rubber obturator is forced to expand over the sabot and engage the rifling with force to obturate the gas. An obturator of this material would have to be cut into segments to allow separation. But to maintain obturation these cuts must take the shape of a labyrinth, as shown.

Another obturator design is an engravable ring obturator, shown in Figure 7 and similar to that employed on the 152mm APFSDS M579 KE

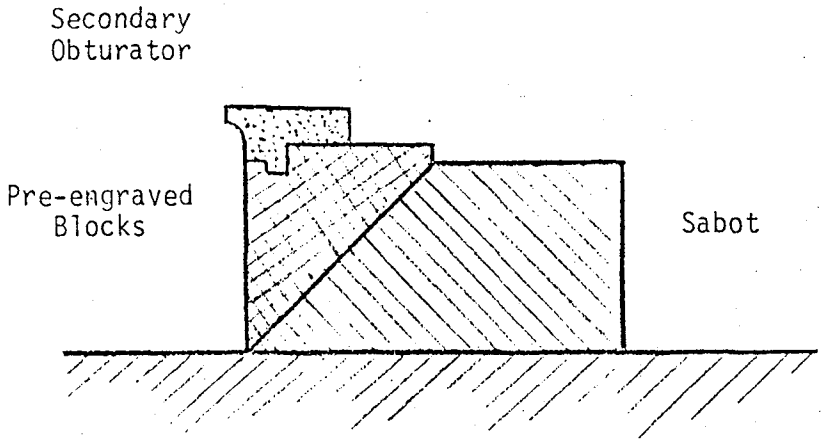

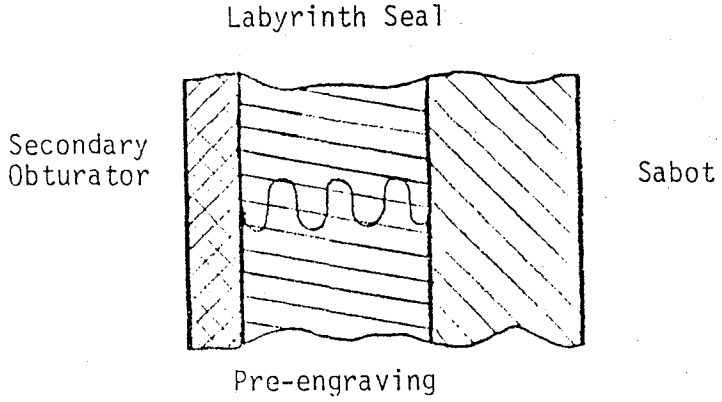

Figure 6. Pre-engraved Obturator showing Gas Sealing Labyrinth cut to allow Discard

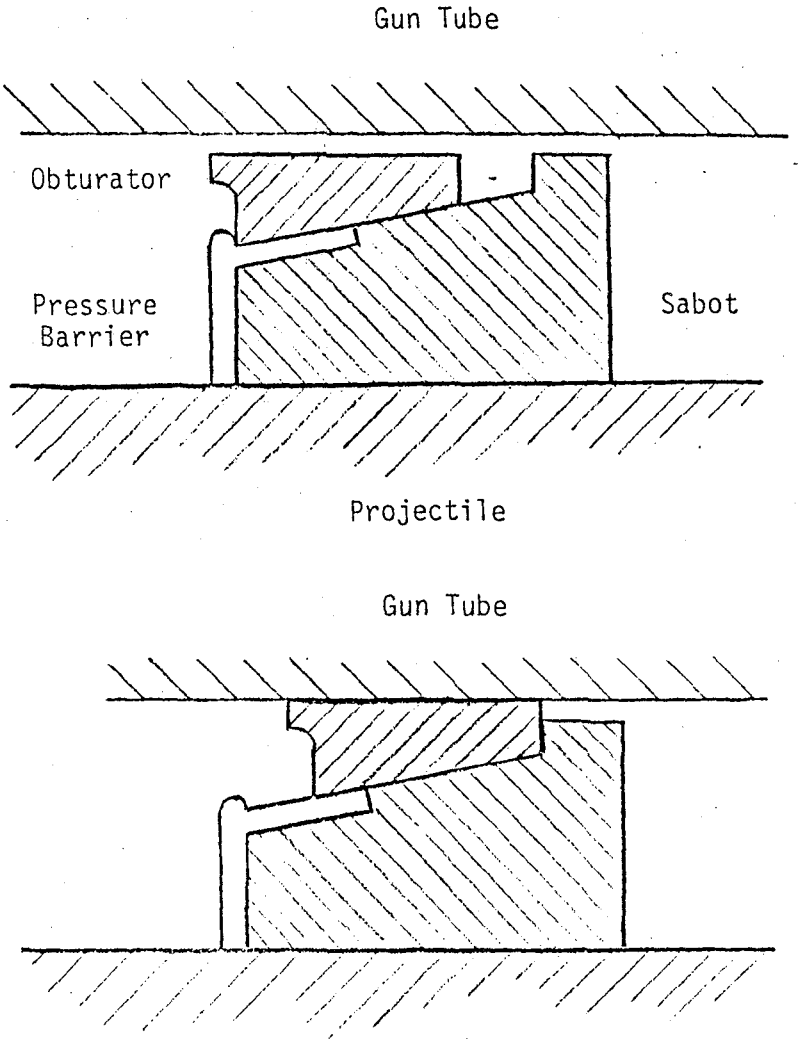

Figure 7. Engravable Ring Obturator shown in the Top Diagram with the Obturator recessed away from the Gun Tube Wall. The lower Diagram shows the Obturator expanded over the Sabot under Breech Pressure to contact with the Gun Wall

projectile, which under the action of the high gas pressure is driven forward over a conical surface of the sabot and expanded outward to be engraved by the rifling of the tube and thus achieve obturation. The discard of this obturator is achieved by fracturing upon muzzle exit.

The pre-engraved obturator has the advantage that obturation is assured at all gas pressures, whereas in the engravable obturator some finite delay occurs before a gas tight seal is achieved. The engraved obturator, however, is more complex and costly and requires additional handling, incorporating a method of indexing to match the obturator grooves with the lands of the gun tube rifling to prevent binding during insertion of the round. This is a major disadvantage of the pre-engraved obturator concept.

3.0 SABOT DESIGN AND EVALUATION

The sabot concepts described and illustrated in the previous section were studied to determine which configurations were most contributory to the design goals of an extended range projectile. From these concepts several configurations were selected for an internal ballistic test. To accomplish this test a versatile subcaliber test slug was designed to be used as a test bed for these concepts. Non discarding sabots were used in this test because the purpose of this test was to collect internal ballistic measurements and the discard of the sabots is characteristic to the external ballistic regime. With the data collected in this test a discarding sabot was designed and applied to a preferred sabot configuration for further testing and development with the test slug. Testing was done in a step-by-step process to evaluate the discarding characteristics of the sabots first with the gun without the muzzle brake and then with the gun fitted with a muzzle brake. For these tests, a non-functional or dummy muzzle brake was designed to represent the internal contour of the functional or "standard" muzzle brake supplied by the U.S. Army. The purpose of the dummy muzzle brake was to avoid unnecessary damage to the standard muzzle brake while developing the discarding sabot design for use on the extended range projectile and further testing described in latter sections.

3.1 PRELIMINARY EVALUATION OF SABOT DESIGN CONCEPTS

Each of the configurations of the three basic sabot systems - base pusher plate sabot, center sabot, and split sabot - described earlier were evaluated for application to the extended range projectile.

Essential in the stability of a spin or fin stabilized projectile is the relative position of the center of gravity to its aerodynamic center of pressure. In a fin stabilized projectile stability is achieved if the center of gravity is located more forward, toward the nose, than the center of pressure. The axial location of the center of pressure varies with mach number, being most forward at the highest mach number in

the supersonic regime. This means that upon muzzle exit, where the projectile has its highest velocity, stability will be least at this time in its supersonic flight and most susceptable to disturbances due to sabot discard. Because the muzzle of the gun is the origin of the projectile's exterior ballistic trajectory, any variation at this point will cause a large deviation between the target and impact.

The position of the aerodynamic center of pressure is constant (for equal mach numbers) for two projectiles if the aerodynamic profile is unchanged. If stability is to be improved it may be accomplished by either moving the center of pressure backwards away from the center of gravity or the center of gravity may be moved forward away from the center of pressure. But to move the center of pressure backwards for a gain in stability would require the aerodynamic profile to be modified with the addition of high drag appendages (in addition to the fins) at the base of the vehicle. This approach however does not provide a sound basis for a long range projectile design. Thus the approach taken here is to maintain the least drag possible and to increase stability by moving the center of gravity as far forward as possible. The position of the center of gravity, in fact, was a very important consideration in the evaluation of the sabot design concepts.

Both base pusher plate sabot versions shown in Figure 1A and 1B requiring heavy steel tail sections to transmit high launch accelerations were immediately rejected. These two configurations were rejected not only because of the high projectile shot weight resulting from the steel pusher plate and steel tail sections but also because the massive tail sections moved the center of gravity too far back.

The inability of these two sabot configurations to meet stability requirements was the impetus toward the conceptualization of the configuration shown in Figure 1C. The result of the preliminary analysis of this configuration indicated that this base plate and ram would weigh approximately 45 lbs. and require an ultra high strength steel with a 250,000 psi

yield strength to project a 125 lb. flight vehicle at a breech pressure of 40 kpsi. Considering the base sabot alone without regard to the front sabot, the ratio of sabot mass to shot mass would be 0.25, in other words one-fourth of the total kinetic energy imparted to the projectile during launch would be lost upon the inflight discard of this pusher sabot part and decreasing the flight weight of the projectile does not significantly reduce the weight of the sabot part. Thus although stability of the flight vehicle is not jeopardized by this design, the low maximum allowed muzzle velocity (due to the high shot weight) and the poor efficiency in the use of available energy were not desired for consideration in an extended range projectile.

The four configurations of the center sabot and split sabot systems shown in Figures 2 and 3 respectively were considered as viable concepts contributory to the goal of an extended range projectile. It will be noted here, however, that preference was accorded to the split sabot system shown in Figure 3A for eventual use on the extended range projectile. Preference was given to the split sabot system over the center sabot system because it afforded the use of a thin-walled, light weight body.

There was, however, a concern associated at this time with the use of the split sabot system because of the close proximity of the rear sabot to the fins. When compared with the center sabot system the rear sabot of the split sabot system is only a short distance ahead of the fins and also a bit closer in radial distance to the longitudinal axis of the projectile. The closer proximity of the rear sabot to the fins in these two ways are disadvantageous to the discard of the sabot without striking the fins. The center sabot on the other hand with its greater distance from the fins is in a better position for discard without fin interference and for this reason was maintained as an alternate design consideration.

The ventilated tail boom, shown in the split sabot configuration of Figure 3B, is generally applicable to all configurations although it is more difficult to apply to the center sabot configuration utilizing

fin bore riders shown in Figure 2A. The purpose of this concept was to lighten the tail section to gain stability and its use was considered only when necessary due to the uncertain aerodynamics of the ventilating holes.

Thus to prepare for the design of the extended range projectile although the split sabot configuration of Figure 3A was favored the center sabot system and the ventilated tail boom were designated for internal ballistic testing.

With regard to the obturator design, the engravable ring obturator of Figure 7 was considered to be the better choice for application than the pre-engraved obturator of Figure 6. The engravable obturator was preferred because of its freedom from the extra handling upon insertion necessary for the pre-engraved obturator and because of its simplicity of manufacture.

3.2 TEST SLUG DESIGN

Before any testing could be done some means of evaluating these concepts in actual gun firings was required. To meet this need, a test slug was designed giving an early internal ballistic representation of the expected properties of the final vehicle. This test slug was not designed to be a structural or aerodynamic representation of the expected configuration. Instead, it was designed with sufficiently massive parts (having a total weight expected of the final projectile) such that the structural adequacy of this test slug was ensured and would not be a variable from test to test. This approach was taken because it was intended to use this basic test slug design not only as a model for internal ballistic studies of different sabot configurations but also as a test bed for the development of the sabot design as well as several other design concepts. This decoupling of vehicle strucure considerations from the mechanisms intimate with in-bore operations simplified the isolation of cause and effect in tests of these parts.

Another consideration in the design of the test slug was economy. In order to reduce the cost of the test slug no attempt was made to simulate the aerodynamics of the expected final projectile. This then eliminated the cost of machining aerodynamic noses and fins.

One further economic consideration in the design of the test slug was its versatility to fulfill the needs of many tests without the need of major redesigns of the organization or materials of its structure. To meet this need interchangeability of many of its main components was required.

Thus the design philosophy encompassed the following ideals:

a) Provide an internal ballistic model representing the expected characteristics of the final projectile design.

b) Decouple the structural adequacy of the test slug from the development of other design concepts.

c) Provide an inexpensive test platform for the development of design concepts.

The test slug design was comprised of a conical finless tail assembly, a cylindrical body assembly, and a blunt nose. With this design, there was the capability of giving an internal ballistic representation of each of the four sabot configurations of Figures 2 and 3 as shown in Figures 8 through 10 plus a representation of the center sabot system combined with the ventilated tail boom as shown in Figure 11.

As mentioned earlier, the ventilated tail boom represents the concept of improving stability by reducing the tail weight. By allowing the gas pressure to equalize on the interior with the exterior, the need for the thick walls required of the closed tail boom pressure vessels is eliminated and the aft weight of the vehicle as well as the total weight is significantly reduced. As an example a weight reduction

NOTES

1. APPLY A LIGHT COATING OF SILICONE GREASE, MIL-G-23567, ON TAPERED SURFACE OF ITEM 4, PRIOR TO INSTALLATION OF ITEM 5.
2. HEAT ITEM 5 IN BOILING WATER FOR 10 TO 20 MINUTES PRIOR TO INSTALLATION. INSTALL ITEM 5 BY APPLYING A FORCE OVER ITS ENTIRE REAR FACE.

CLASSIFICATION OF CHARACTERISTICS (WR43A)
CRITICAL –
MAJOR –
MINOR –

LTR	DESCRIPTION	DATE

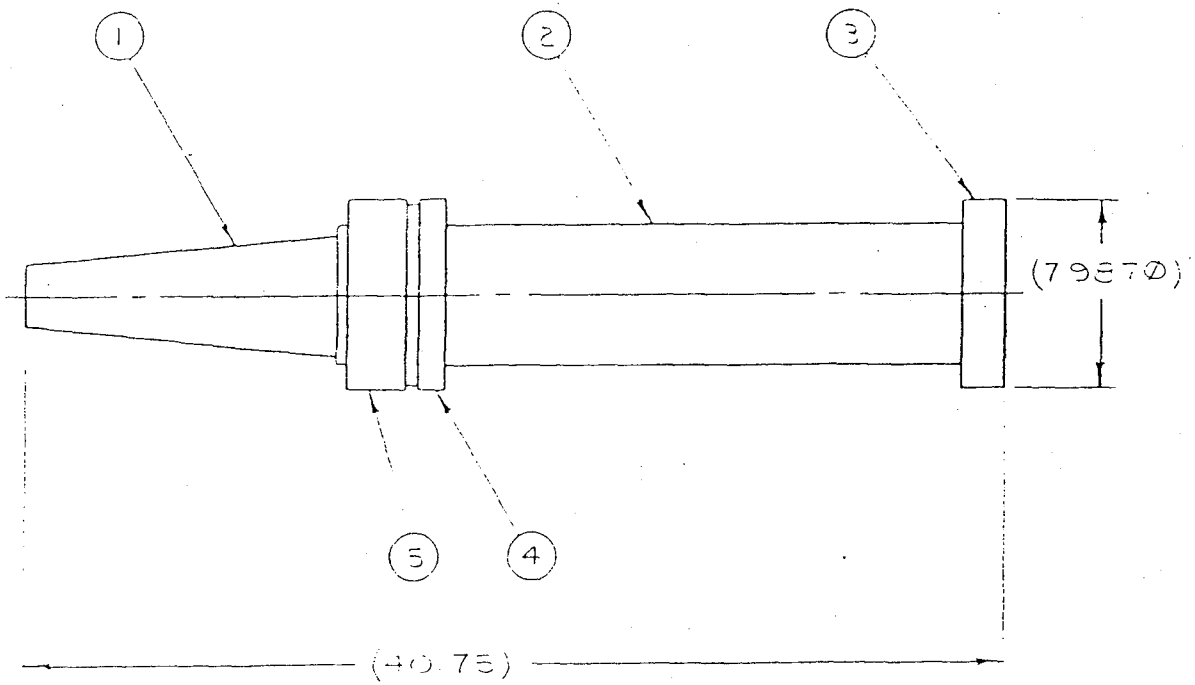

ITEM NO	PART NO.	TITLE
5	D22974	BAND
4	D22973	SABOT
3	C22972	NOSE
2	C22959	BODY
1	D22958	SOLID FIN 3

PARTS LIST

		UNLESS OTHERWISE SPECIFIED DIMENSIONS ARE IN INCHES	ORIGINAL DATE OF DRAWING		SPACE RESEARCH CORPOR
		TOLERANCES ON DECIMALS			NORTH TROY, VERMONT
		ANGLES	PREP	4 APR 77	TEST SLUG ASSY
		MATERIAL	CHK		
			ENGR		(SOLID FIN – REAR SA
	TEST SLUG	HEAT TREATMENT.	SUBMITTED		
FINAL	8"-155MM				SIZE C | CODE IDENT NO. 30478 | C22977
NEXT ASSY	USED ON	FINAL PROTECTIVE FINISH	APPROVED		SCALE 1/4 | SHEET
APPLICATION					

Figure 8. Test Vehicle Type C

NOTES

1. APPLY A LIGHT COATING OF SILICONE GREASE, MIL-S-21567, TO TAPERED SURFACE OF ITEM 4, PRIOR TO INSTALLATION, OF ITEM 5.
2. HEAT ITEM 5 IN BOILING WATER FOR 10 TO 30 MINUTES PRIOR TO INSTALLATION. INSTALL ITEM 5 BY APPLYING A FORCE OVER ITS ENTIRE REAR FACE.

CLASSIFICATION OF CHARACTERISTICS (WR43A)
CRITICAL –
MAJOR –
MINOR –

REVISIONS	
LTR	DESCRIPTION

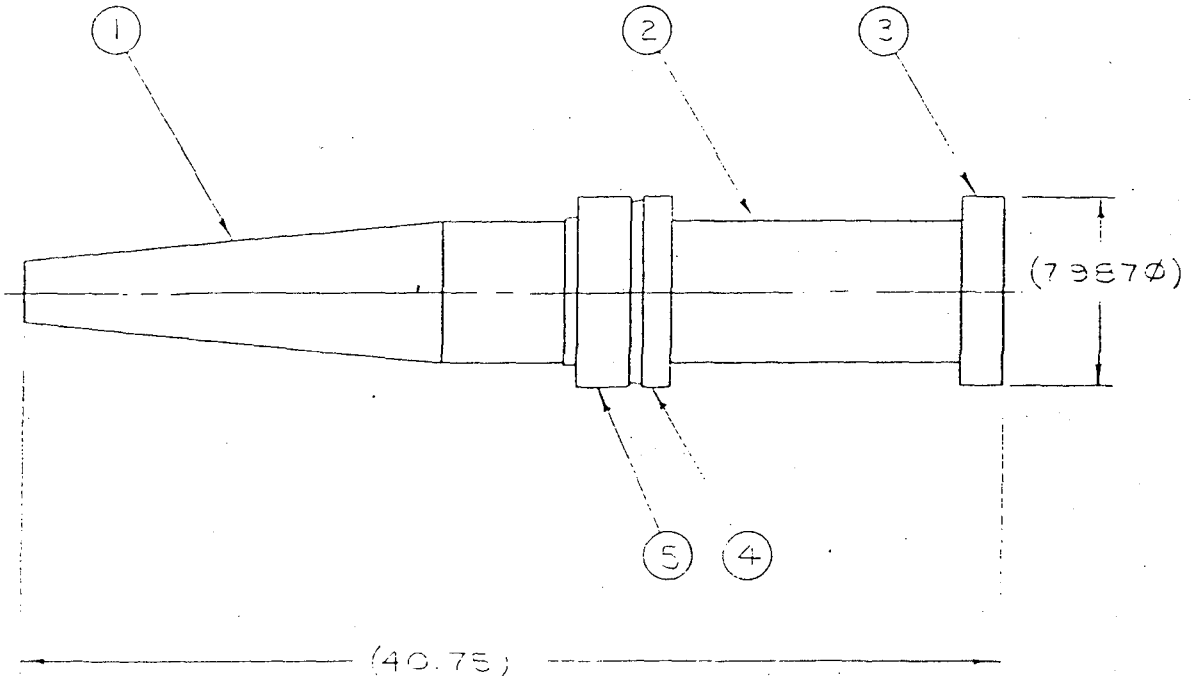

ITEM NO.	PART NO.	TITLE
5	D22974	SABOT
4	D22973	SABOT
3	D22972	NOSE
2	D22971	BODY
1	D22957	SOLID FIN S.

PARTS LIST

Figure 9. Test Vehicle Type D

		UNLESS OTHERWISE SPECIFIED DIMENSIONS ARE IN INCHES
		TOLERANCES ON DECIMALS
		ANGLES
		MATERIAL
	TEST SLUG	HEAT TREATMENT
FINAL	8.155 mm	
NEXT ASSY	USED ON	FINAL PROTECTIVE FINISH
APPLICATION		

ORIGINAL DATE OF DRAWING

PREP		SAPRT
CHK		
ENGR		

SUBMITTED

APPROVED

SPACE RESEARCH CORPOR.
NORTH TROY VERMONT

TEST SLUG ASSY
(SOLID FIN – CNTR SAB

SIZE	CODE IDENT NO.	
C	30478	C22978

SCALE 1/4 SHEET

NOTES

1. APPLY [illegible] GREASE [illegible] SURFACES OF ITEM 4, PRIOR TO INSTALLATION OF ITEM 5.

2. HEAT ITEM 5 IN BOILING WATER FOR 10 TO 20 MINUTES PRIOR TO INSTALLATION. INSTALL ITEM 5 BY APPLYING A FORCE OVER ITS ENTIRE REAR FACE.

CLASSIFICATION OF CHARACTERISTICS (WR 43A)

CRITICAL	–
MAJOR	–
MINOR	–

LTR	DESCRIPTION	DATE

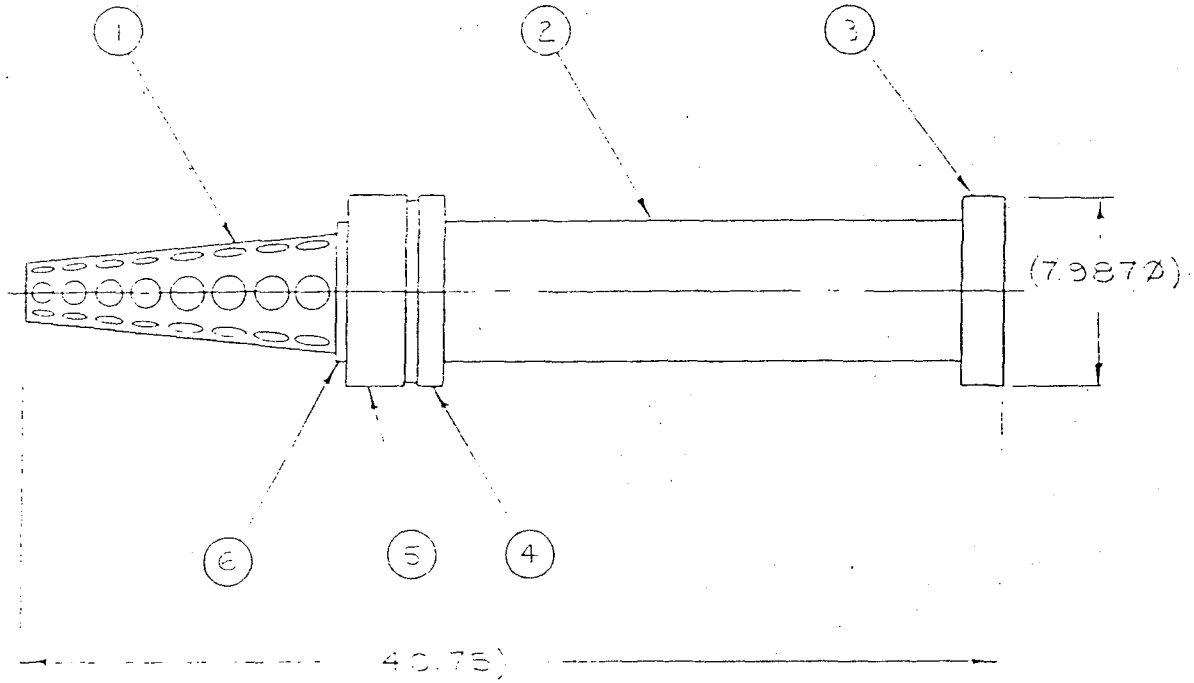

ITEM NO.	PART NO.	TITLE
6	C22955	CLOSURE
5	D22974	BAND
4	D22973	SABOT
3	C22972	NOSE
2	C22959	BODY
1	D22954	VENT. FIN 3

PARTS LIST

Figure 10. Test Vehicle Type B

		UNLESS OTHERWISE SPECIFIED DIMENSIONS ARE IN INCHES	ORIGINAL DATE OF DRAWING	SPACE RESEARCH CORPOR NORTH TROY VERMONT
		TOLERANCES ON DECIMALS		
		ANGLES	PREP [illegible] 4APR77	TEST SLUG ASSY
		MATERIAL	CHK	
			ENGR [illegible] 13 Apr 77	(VENT FIN - REAR SA
	TEST SLUG	HEAT TREATMENT	SUBMITTED	SIZE C | CODE IDENT NO 30478 | C22975
FINAL	8 - 155MM			
NEXT ASSY	USED ON	FINAL PROTECTIVE FINISH	APPROVED	SCALE 1/4 | SHEE
APPLICATION				

NOTES:

1. APPLY A LIGHT COATING OF SILICONE GREASE, MIL-G-21547, ON TAPERED SURFACE OF ITEM 4, PRIOR TO INSTALLATION OF ITEM 5.
2. HEAT ITEM 4 IN BOILING WATER FOR 10 TO 20 MINUTES PRIOR TO INSTALLATION. INSTALL ITEM 5 BY APPLYING A FORCE OVER ITS ENTIRE REAR FACE.

CLASSIFICATION OF CHARACTERISTICS (WR43A)
CRITICAL -
MAJOR -
MINOR -

LTR	DESCRIPTION	DATE

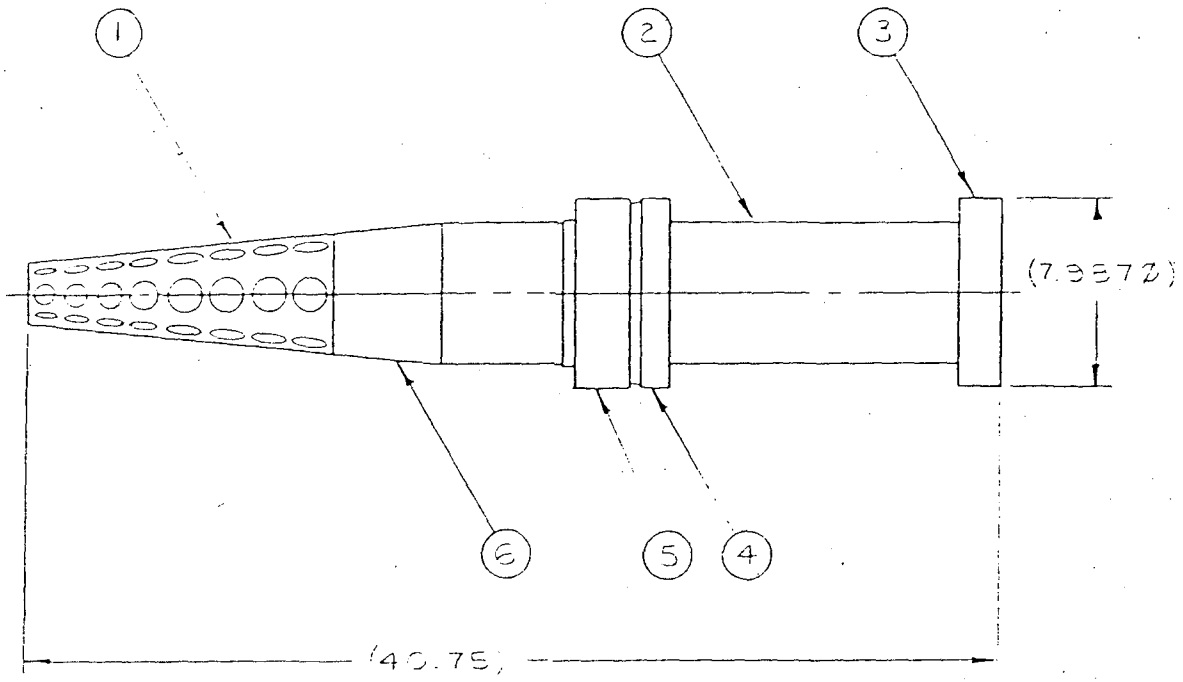

ITEM NO.	PART NO.	TITLE
6	C22956	CLOSURE
5	D22974	BAND
4	D22973	SABOT
3	C22972	NOSE
2	C22971	BODY
1	D22954	VENT. FIN

PARTS LIST

Figure 11. Test Vehicle Type A

		UNLESS OTHERWISE SPECIFIED DIMENSIONS ARE IN INCHES
		TOLERANCES ON DECIMALS
		ANGLES
		MATERIAL
	TEST SLUG	HEAT TREATMENT
FINAL	8-155MM	
NEXT ASSY	USED ON	FINAL PROTECTIVE FINISH

ORIGINAL DATE OF DRAWING: March 77

PREP	[illegible]	SEPT 77
CHK		
ENGR	[illegible]	[illegible]
SUBMITTED		
APPROVED		

SPACE RESEARCH CORPO
NORTH TROY, VERMONT

TEST SLUG ASS
(VENT FIN - CNTR S

SIZE	CODE IDENT NO.	
C	30478	C22976

SCALE 1/4 SHEE

of nearly eight pounds was realized in the test slug and two to five pounds in later utilizations. This weight reduction in addition to the gain in stability makes available a higher maximum muzzle velocity and hence a greater range.

Initially the front bore rider sabot was modeled as flange integral with the blunt nose. This was done to allow the interior ballistics testing to begin because discarding sabots are unnecessary in these tests and information which evolves from these tests is useful in their design. Also in later testing it would simplify the identification of the results during the development of the rear discarding sabots. The flange was later replaced by a discarding front sabot during tests concentrating upon that aspect of the sabot design development. It should be noted here that the use of the front bore rider sabot in the center sabot system configuration did not eliminate the consideration of using bore riding fins for support but instead it duplicated their function in the finless test slug configuration.

Similarly, the rear sabot of the split sabot system and the center sabot were initially modeled as collars screwed into place. Again, during tests involving concentration on rear sabot separation dynamics, these non-discarding collars were replaced by discarding sabots. Both of these sabot systems were designed to utilize the engravable obturator design rather than a pre-engraved obturator.

The design of the test slug in the split sabot, closed boom configuration is such as to match the weight and axial moment of inertia expected of the final projectile as closely as possible while the center of gravity was matched to a lesser degree. In this configuration the nominal physical properties of the test slug are given in Table 1.

The location of the center of gravity has much more influence in the external ballistic trajectory than the internal ballistic trajectory. Variations in the weight of projectiles alter measurements pertaining to interior ballistics to a much greater degree. The significance of the axial moment of intertia is great in this application for spin rate

TABLE 1. 8-INCH /155MM TEST SLUG PHYSICAL PROPERTIES

ITEM	UNITS	VALUE
Total weight (w/sabots)	lbm	140.0
Tail section weight	lbm	21.5
Body weight	lbm	80.0
Nose weight	lbm	25.0
Rear sabot weight	lbm	10.0
Front sabot weight	lbm	3.5
Axial moment of inertia (w/out sabots)	lbm-in^2	700.0
Maximum diameter	in.	5.8
Overal length	in.	42.0
CG position from base (w/out sabots)	in.	27.9

measurements required for the design of the sabotry.

Variations in the physical properties of the different test slug designs were expected to correspondingly match the changes in the physical properties between the same differences of design in the final projectile.

A stress analysis was done for the test slug of both the split sabot and center sabot configurations during gun launch. The highest load for either configuration resulted at the interface between the body and tail section of the center sabot configuration. A Von Mises equivalent stress of 125 kpsi was calculated for this projectile with a weight of 140 lbs. accelerated by a breech pressure of 40 kpsi to 11,800 g's. The split sabot configuration's highest equivalent stress was also at this same location but was calculated to be 105 kpsi at the same conditions. Making an allowance for localized yielding and for the dynamic nature of the loading, normalized AISI 4140 steel, with a yield strength of 85 kpsi and a tensile strength of 155 kpsi was considered adequate for the body.

Also, because of the direct contact, stresses in the area of contact with the body in the tail should be similar. However, the state of stress for the tail in this area is approximately triaxial (i.e. hydrostatic pressure) and 7075-T6 aluminum with a yield strength of 70 kpsi and a tensile strength of 80 kpsi was used. Mild steel was used for the blunt nose and 7075-T6 aluminum was used for all discarding sabot designs, to resist the shear involved, as well as all non-discarding collars.

Drawings of the various components used with the test slug are contained in Appendix A for reference.

3.3 TEST PROPELLING CHARGE DESIGN

A propelling charge was also designed for use in the Internal Ballistic Test and subsequent testing. The physical size of the charge was limited by the dimensions of the XM201 cannon chamber. The diameter of the chamber measured 8.485 inches with the origin of the rifling located

51.0 inches from the breech face. With the closing of the breech, the mushroom protrudes into the chamber 11.0 inches (including an attached piezoelectric gage).

To make available the largest volume possible for the test charge, the test slugs and ensuing test vehicles in all tests were rammed to a measured distance of 51.0 inches from the breech face thus allowing a maximum charge length of 40.0 inches. The maximum allowed charge dimensions, held in all tests, were a length of 40.0 inches and a circumference of 25.0 inches (8.0 inch diameter). Within these dimensions the largest amount of propellant that could be utilized was 62.0 pounds.

A charge and its components are shown in the sectional diagram of Figure 12. The propelling charge used an easily adjustable cloth bag to accomodate various charge weights. The charge incorporates a cardboard liner to provide shaping and rigidity. Let it be noted here that initially the charge comprised 62.0 lbs. of M30A1 0.085 inch multiperforated triple base propellant and a 1.0 ounce black powder based pad igniter until a high pressure was recorded in Shot Number 512 when the propellant weight was generally reduced to 58.0 lbs., and the base pad was increased in weight to 3.0 ounces of black powder. The core igniter of 5.0 ounces of black powder supported by a 28.0 inch long nitrocellulose igniter tube was used consistently throughout.

3.4 INTERNAL BALLISTICS TEST

Each of the four test slug configurations were tested with various propelling charge weights to measure ballistic performance and for the determination of the charge. The pertinent results of this test are summarized in Table 2.

The resulting breech pressures from the various charge weights are plotted for each test slug as shown in Figure 13. Similarly the muzzle velocity and breech pressure data were correlated to give the curves in Figure 14.

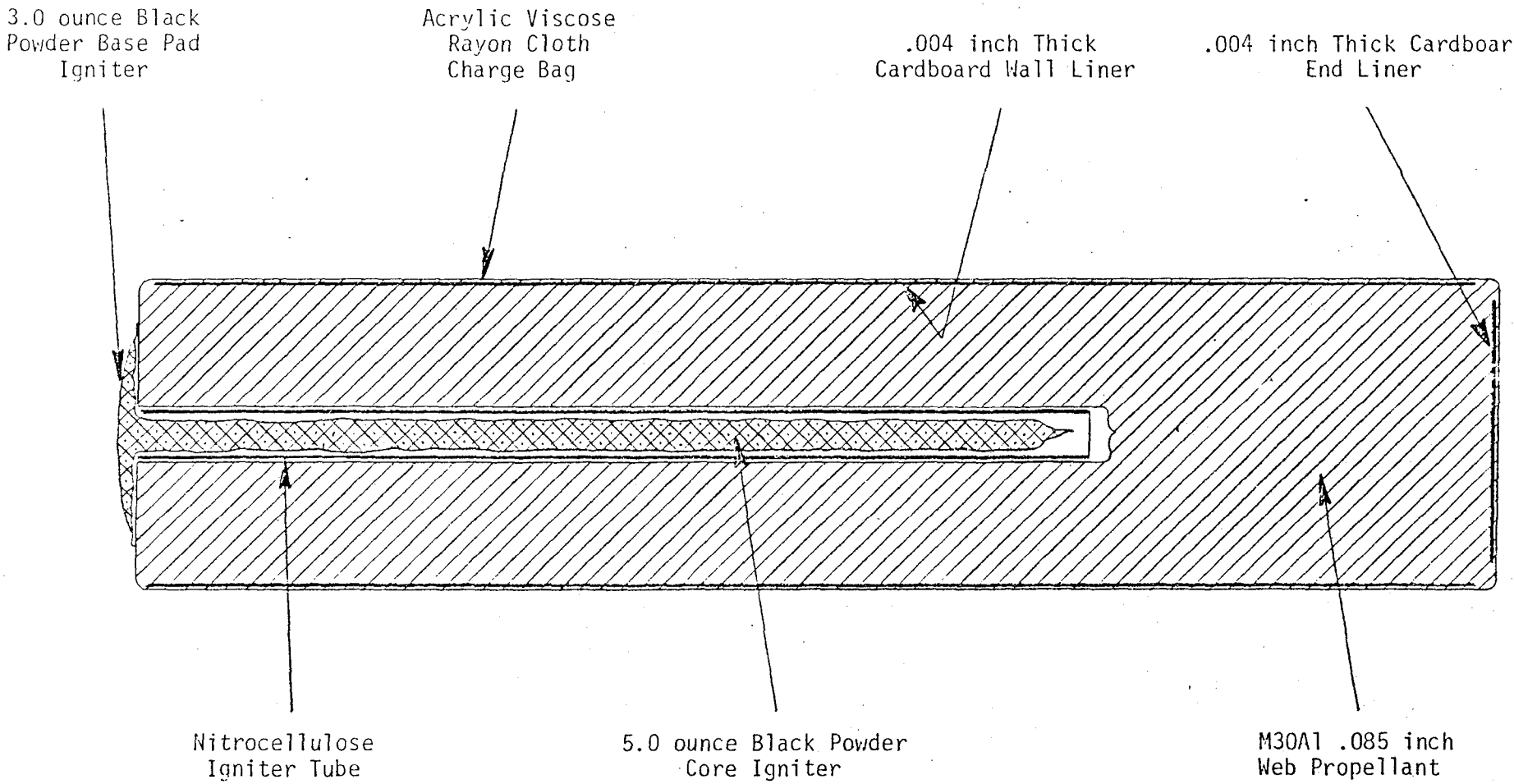

Figure 12. 8-inch Test Propelling Charge
Length 40.0 in.; Diameter 8.0 in.

TABLE 2. 8"/155 INTERNAL BALLISTICS FIRINGS

DATE	SHOT NO.	VEHICLE[1] TYPE & SERIAL NO.	VEHICLE WEIGHT (lbs)	CHARGE[2] WEIGHT (lbs)	BREECH PRESSURE (kpsi)	MUZZLE VELOCITY (fps)		SPIN RATE (RPS)
						Smear 1	Smear 2	
9 June	462	C-3	129.96	30	>10	1591	1585	-
	463	C-2	130.04	35	>10	1772	1775	-
	464	C-5	129.90	40	>10	1926	1942	-
	465	C-1	129.42	45	14.8	2224	2224	-
	466	C-4	130.2	50	18.3	2413	2409	10.5
	467	C-6	129.91	55	21.5	2620	2605	10.5
	468	C-7	129.97	60	27.0	2879	2877	11.8
	469	C-8	129.86	62	31.2	3043	3047	10.8
16 June	470	D-5	137.69	50	22.5	2640	2641	-
	471	D-7	138.18	55	28.4	2860	2857	8.7
	472	D-2	137.62	60	32.7	3022	3006	9.6
	473	D-3	137.62	62	38.7	3179	3178	-
	474	A-4	136.75	50	20.2	2481	2460	-
	475	A-7	136.95	55	26.2	2769	2785	-
	476	A-5	136.87	60	33.4	3109	3052	9.4
	477	A-1	136.75	62	34.4	3059	3047	-
20 June	478	B-7	128.69	50	20.6	2600	2581	7.5
	479	B-1	128.94	55	22.7	2707	2700	8.6
	480	B-2	129.00	60	28.5	2981	2973	-
	481	B-3	128.75	62	29.0	2977	2966	-

NOTES [1] Type D - Split Sabot, Closed Boom - Chamber Volume - 2635 $in.^3$
Type C - Split Sabot, Open Boom - Chamber Volume - 2885 $in.^3$
Type B - Center Sabot, Closed Boom - Chamber Volume - 3110 $in.^3$
Type A - Center Sabot, Open Boom - Chamber Volume - 3360 $in.^3$

[2] Shot No's 462-469 - Propellant M30A1 .091 WEB
Shot No's 470-481 - Propellant M30A1 .085 WEB

[3] Ram Depth - 51 inches

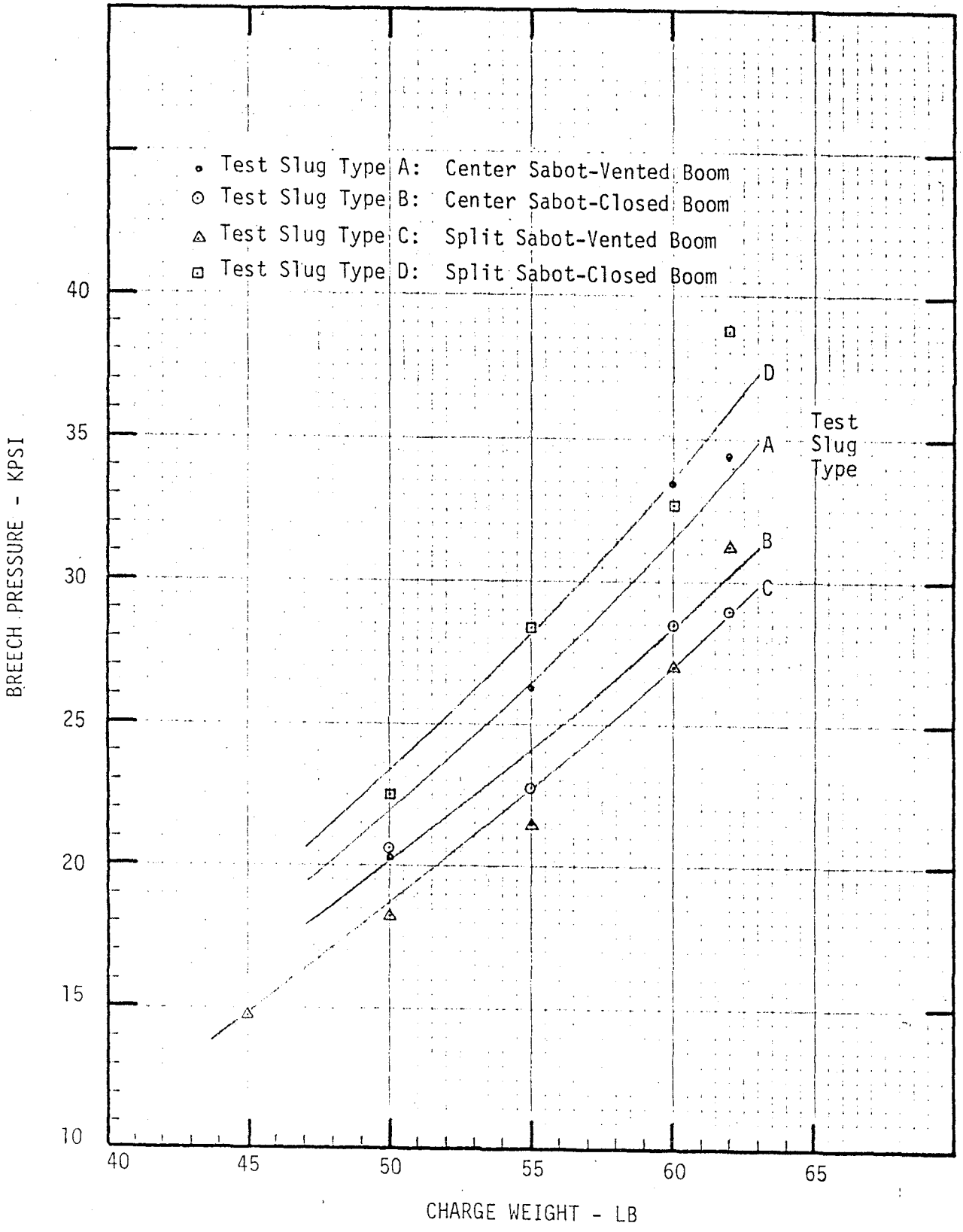

Figure 13. Breech Pressure vs Charge Weight Results for Internal Ballistic Test

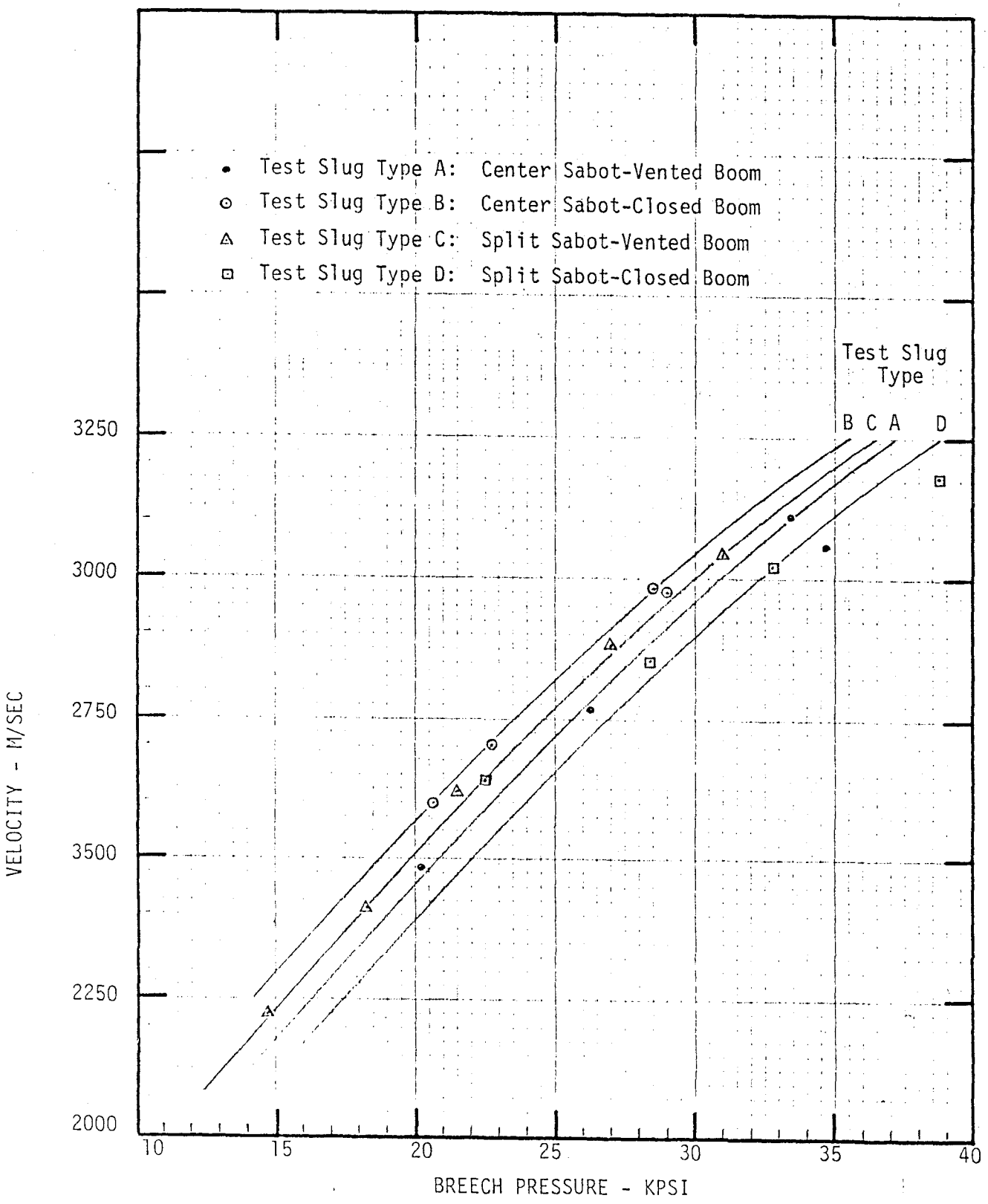

Figure 14. Velocity vs Breech Pressure Results For Internal Ballistic Test

While obturation during this test was not viewed as satisfactory for the final version, the resultant spin rates, given in Table 2, were within the desired range and obturation performance exhibited in Shot Number 467 shown in Figure 15 showed good results for a first effort. Figure 15 shows some gas escaping from the muzzle ahead of the vehicle as may be expected from this obturation design. In operation some breech gas will pass by the obturator as it is forced to slide and expand over the conical ramp of the sabot until it engages with the rifling and seals. Examples of photographic results of the other configurations are shown for Shot Number 472 in Figure 16, Shot Number 476 in Figure 17, and Shot Number 478 in Figure 18.

In the sabot development tests to come, it was desired to operate at pressures at least equivalent to the 40 kpsi working pressure of the XM201 gun tube. The required charge, determined from this test, was the maximum possible charge weight of 62.01 lbs. of M30A1 multiperforated .085 inch web triple base propellant when used with the split sabot system and closed tail boom.

As shown in Table 2 the spin rates were fairly constant between designs. This is not surprising in view of the fact that each design tested used the same obturator and means of spin isolation, namely obturator-sabot interface decoupling. These measurements however gave the required data for sabot-projectile latching design.

3.5 SABOT DESIGN

During launch, a sabot design must; position and structurally support the projectile, obturate the breech gas, minimize balloting, transmit acceleration and spin, pass through a muzzle brake (in this design), and discard from the projectile without disturbance. In this design then the sabots must properly interact with the three different environments of the; launch tube, muzzle brake, and free atmosphere where in each case the nature of the loads change. Additionally, in a split sabot design, the loads upon the front bore riding sabot are different from those acting on the obturating rear sabot. The main

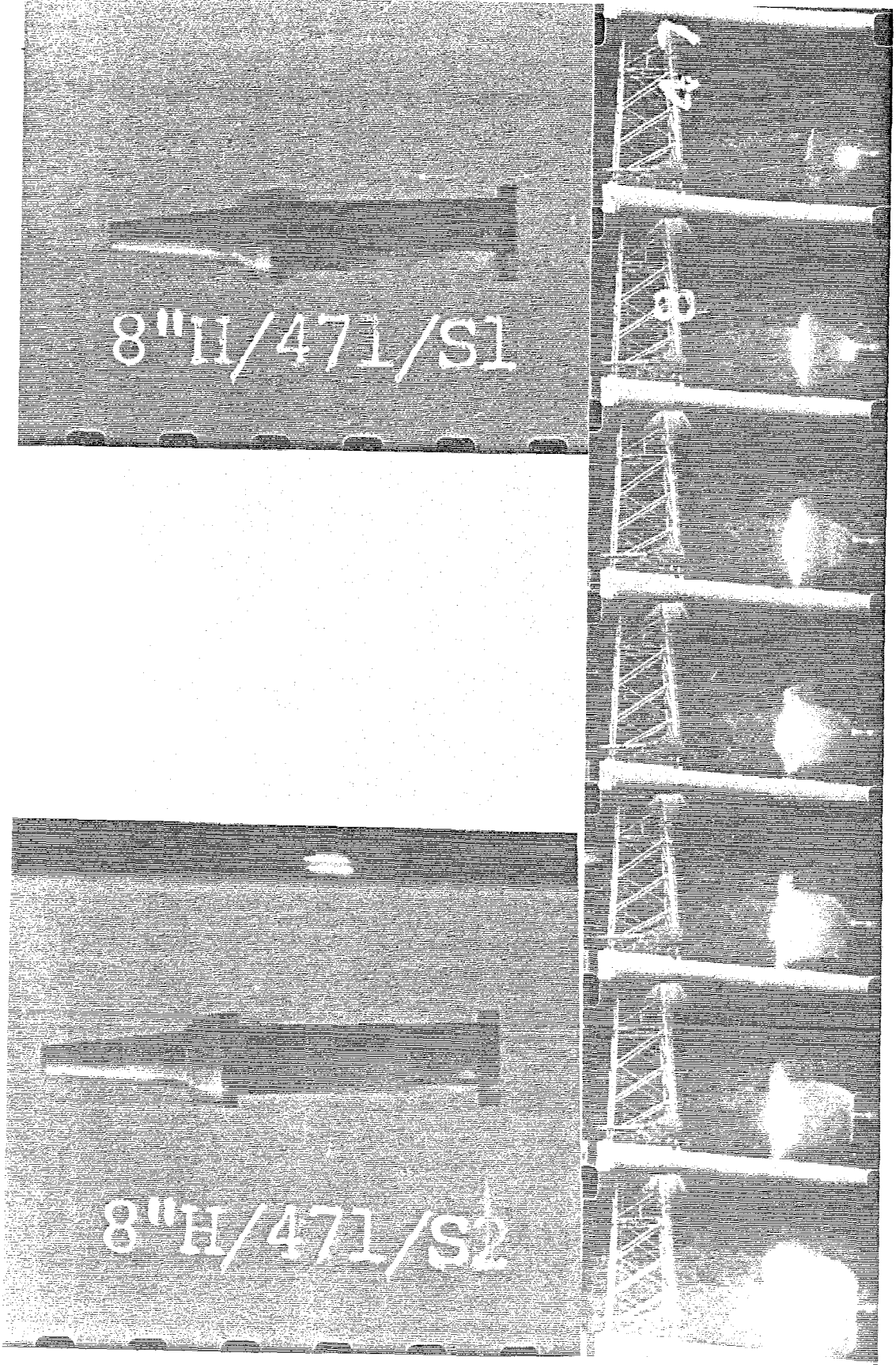

Figure 15. Photographic Results for a Type C Vehicle of Shot Number 467

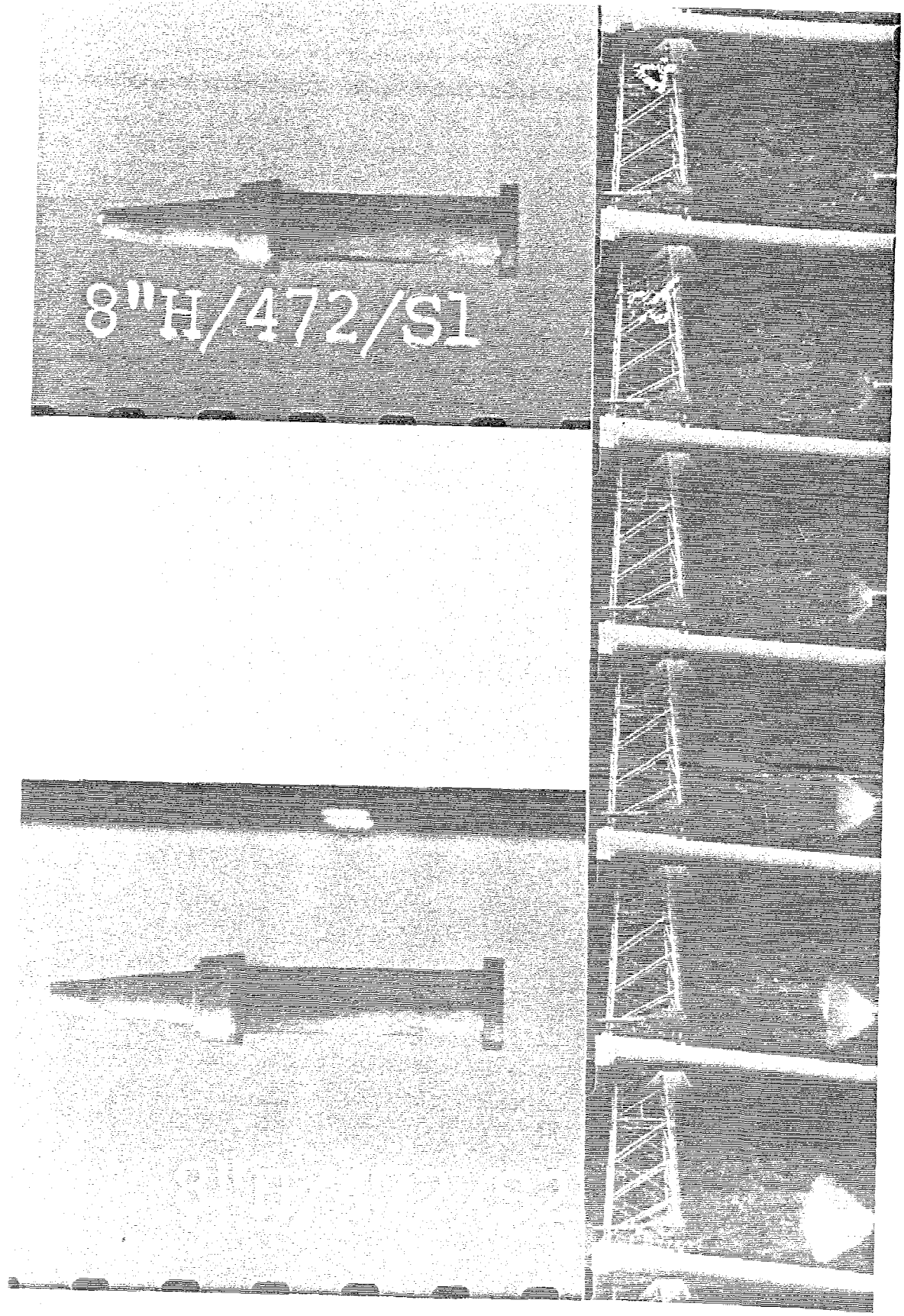

Figure 16. Photographic Results for a Type D Vehicle of Shot No. 472

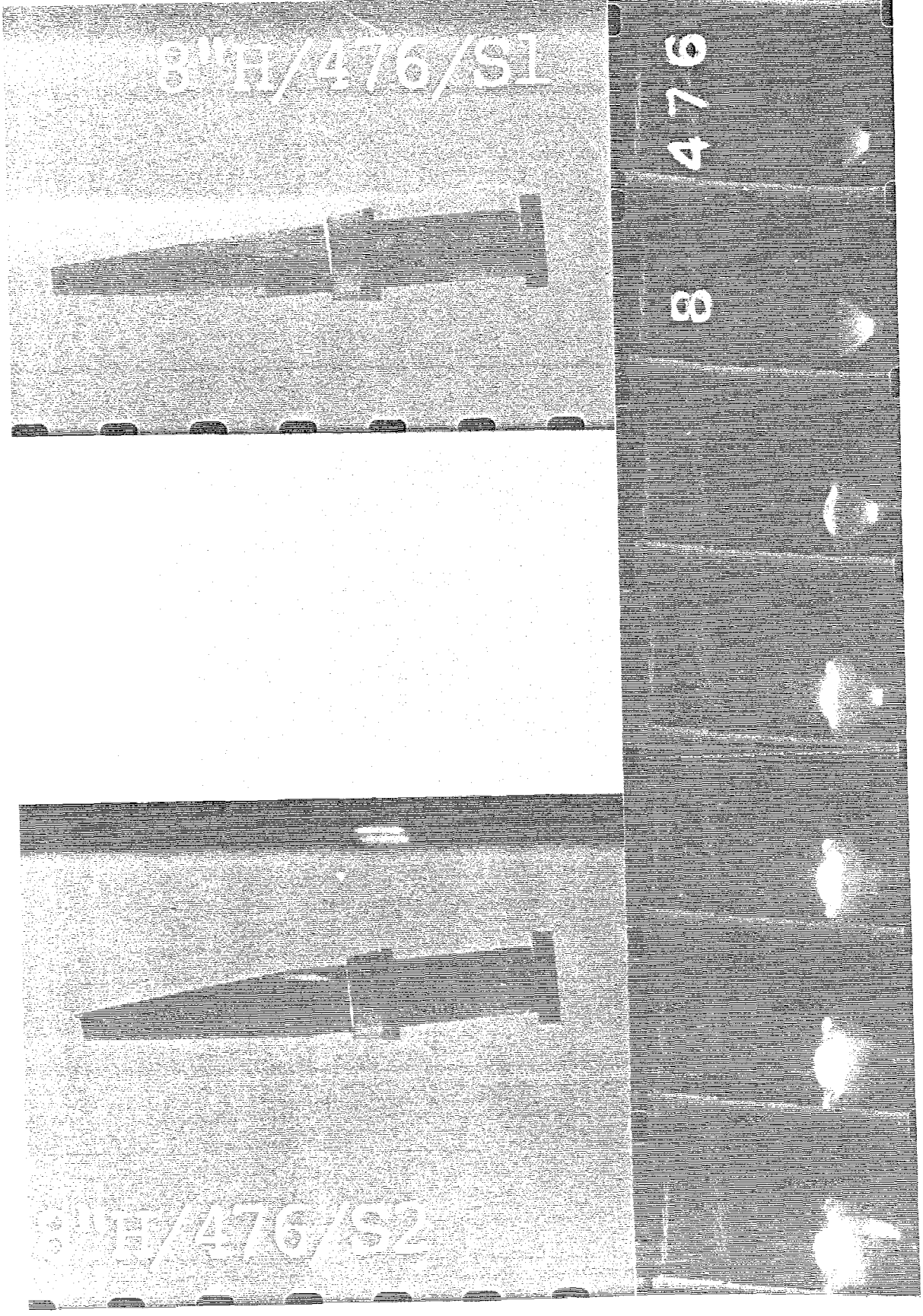

Figure 17. Photographic Results for a Type A Vehicle of Shot No. 476

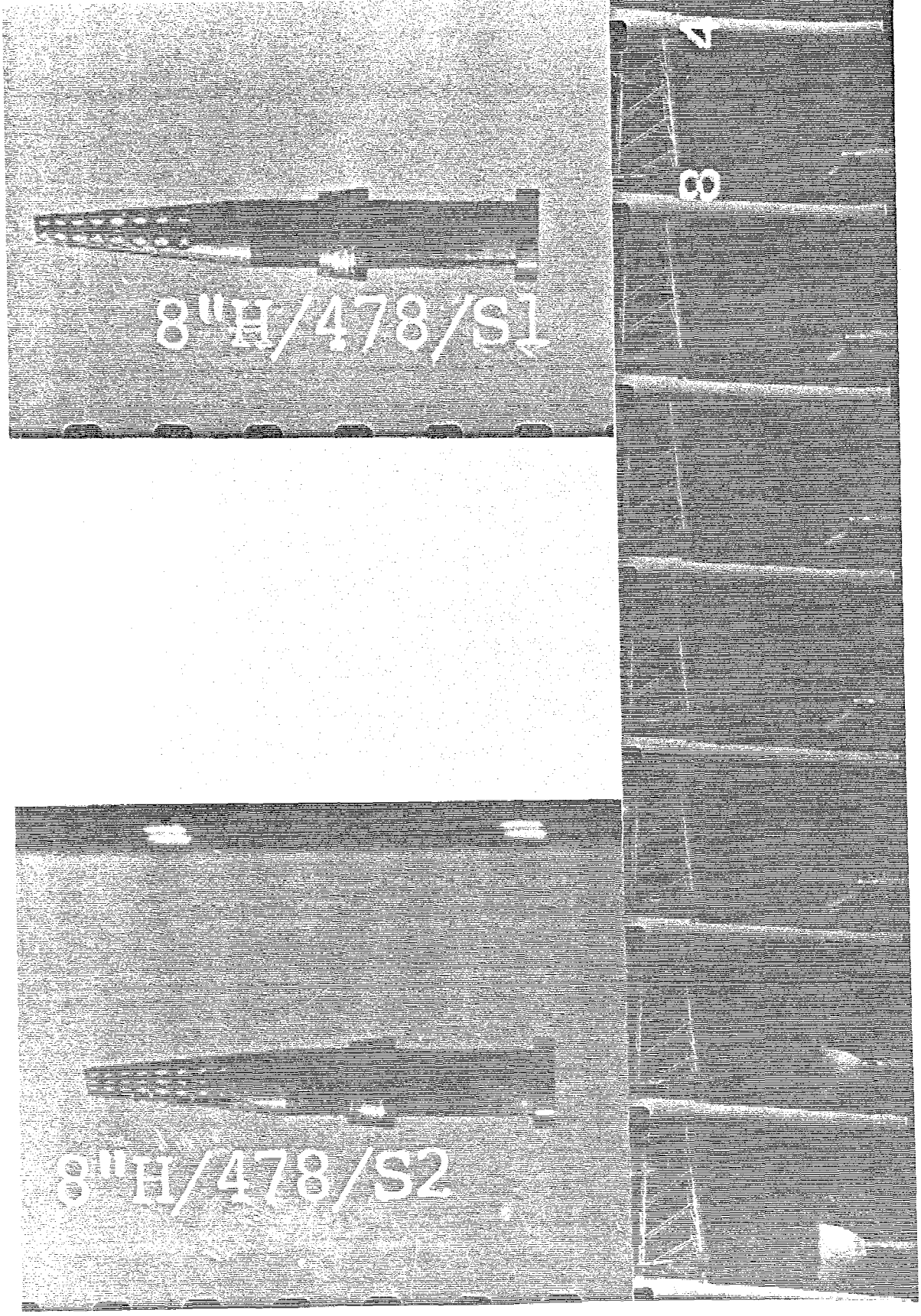

Figure 18. Photographic Results for a Type B Vehicle of Shot No. 478

obturating center sabot of the center sabot configuration is intrinsically the same in analysis as the obturating rear sabot of the split sabot configuration. For this reason the approach of this analysis is toward the more general split sabot configuration as it considers the front sabot and is applicable to the center sabot configuration.

3.5.1 Front Sabot Loads

During acceleration in the gun tube the front sabot is subjected to an inertia load directed opposite to the direction of travel and a centrifugal load directed radially away from the projectile axis. The inertial load is easily restrained by a front sabot latch while the centrifugal force is opposed by the walls of the gun tube.

It is important that good obturation of the propellant gas behind the rear sabot be achieved. In the event that imperfect obturation is experienced, the gun gas pressure on the rear of the front sabot could tend to dislodge the front sabot in the barrel or muzzle brake. Ventilation of the front sabot by drilled holes was considered necessary in order to prevent the build up of gas pressure between the front and rear sabots. The drilled holes also lighten the front sabot, reducing the ration of sabot mass to projectile shot mass.

The distance between the front sabot and rear sabot is approximately 24 inches in the test slugs and 22.88 inches in the final design. This is greater than the distance between the gun tube muzzle and the end of the muzzle brake (15 in.) so the front sabot is clear of the muzzle brake before the rear sabot exits the gun tube. Thus, as the front sabot enters the muzzle brake it is still being accelerated by the obturated propellant gas and has developed its maximum spin-generated centrifugal force. Also neglecting the initial gas which passes by the obturator as it seals, the front sabot is not exposed to any back pressure of the propellant gas but at this time begins to come under the influence of an aerodynamic pressure.

After the projectile has exited from the muzzle brake, the loads acting on the front sabot are the same as those given above except that the load of acceleration is removed and replaced by deceleration due to the termination of obturation. The centrifugal force and aerodynamic pressure continue to act on the front sabot. The load on the front sabot due to the muzzle blast and efflux is not considered here but it is realized the effect of this load would be to beneficially speed the separation of the front sabot after muzzle brake exit.

Expressions for the various loads which are assumed to act on the front sabot while it is in the muzzle brake are as follows:

$$F_c = M_f r_f \omega_f^2/g$$

$$F_a = M_f D$$

$$F_d = 1/2 \rho \frac{V^2}{144} A_f$$

The load due to the dynamic pressure is assumed to be equal to the dynamic pressure times the frontal area of the sabot (as projected on a plane perpendicular to the projectile axis).

The above loads can be resolved into components normal to and parallel to the thrust flange(s) of the sabot-projectile interface (the flange which is shown in Figure 19 to be oriented at an angle ϕ to the projectile axis). The parallel component of the force is oriented outwards and therefore tends to cause release of the front sabot.

$$N_f = M_f r_f \omega_f^2/g \cos \phi + M_f D \sin \phi + 1/2 \rho V^2/144 A_f \cos \beta$$

Where $\beta = \alpha - \phi$

$$P_f = M_f r_f \omega_f^2/g \sin \phi - M_f D \cos \phi - 1/2 \rho V^2/144 A_f \sin \beta$$

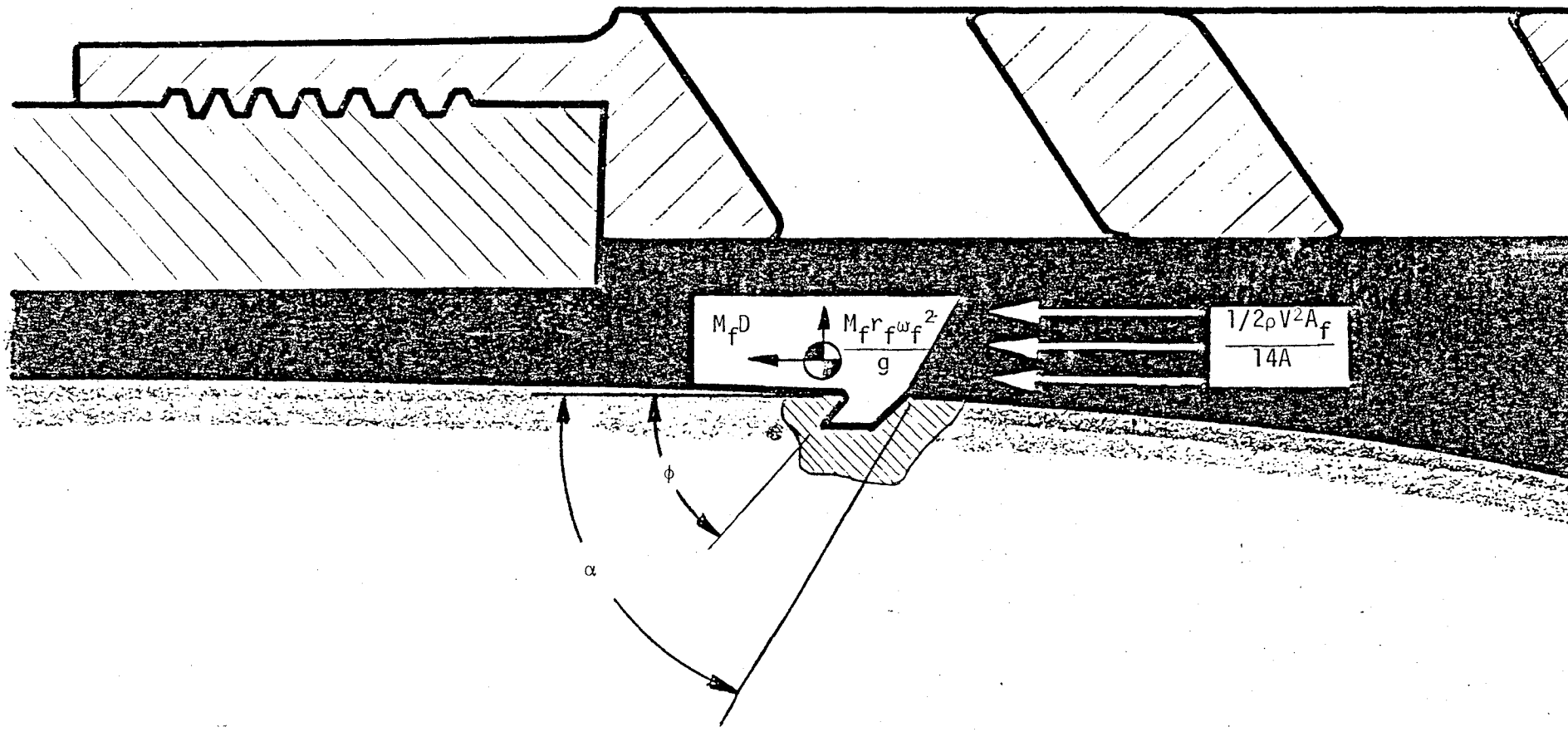

Figure 19. Loads on Front Sabot While in Muzzle Brake

Friction exists on the thrust flange of the sabot-projectile interface due to the normal force between the parts. The retention force is defined as the difference between the friction force which resists release and the force parallel to the thrust flange which tries to cause release of the front sabot.

$$A_f = \mu_f N_f - P_f$$

After the projectile is clear of the muzzle brake the load on the front sabot due to acceleration of the projectile is removed. The normal and parallel components of the forces are then:

$$N_f = M_f \omega^2 r_f / g \cos \phi + 1/2 \rho V^2 / 144 A_f \cos \beta$$

$$P_f = M_f \omega^2 r_f / g \sin \alpha - 1/2 \rho V^2 / 144 A_f \sin \beta$$

The release force is defined as the difference between the parallel force and the friction force.

$$B_f = P_f - \mu_f N_f$$

For a particular set of operating conditions, a satisfactory design is one for which A_f and B_f are both positive.

3.5.2 Rear Sabot Loads

Figure 20 shows the loads that act on the rear sabot while it is in the muzzle brake. In addition to the loads due to acceleration of the projectile and due to centrifugal force, which act on the front sabot, the rear sabot is exposed to the residual gun gas pressure which exists while the rear sabot is in the muzzle brake. This pressure tends to push the rear sabot forward; hence the latching orientation of the rear sabot-projectile interface or "teeth" is opposite to that of the front sabot-projectile interface. The pressure on the front face of the rear

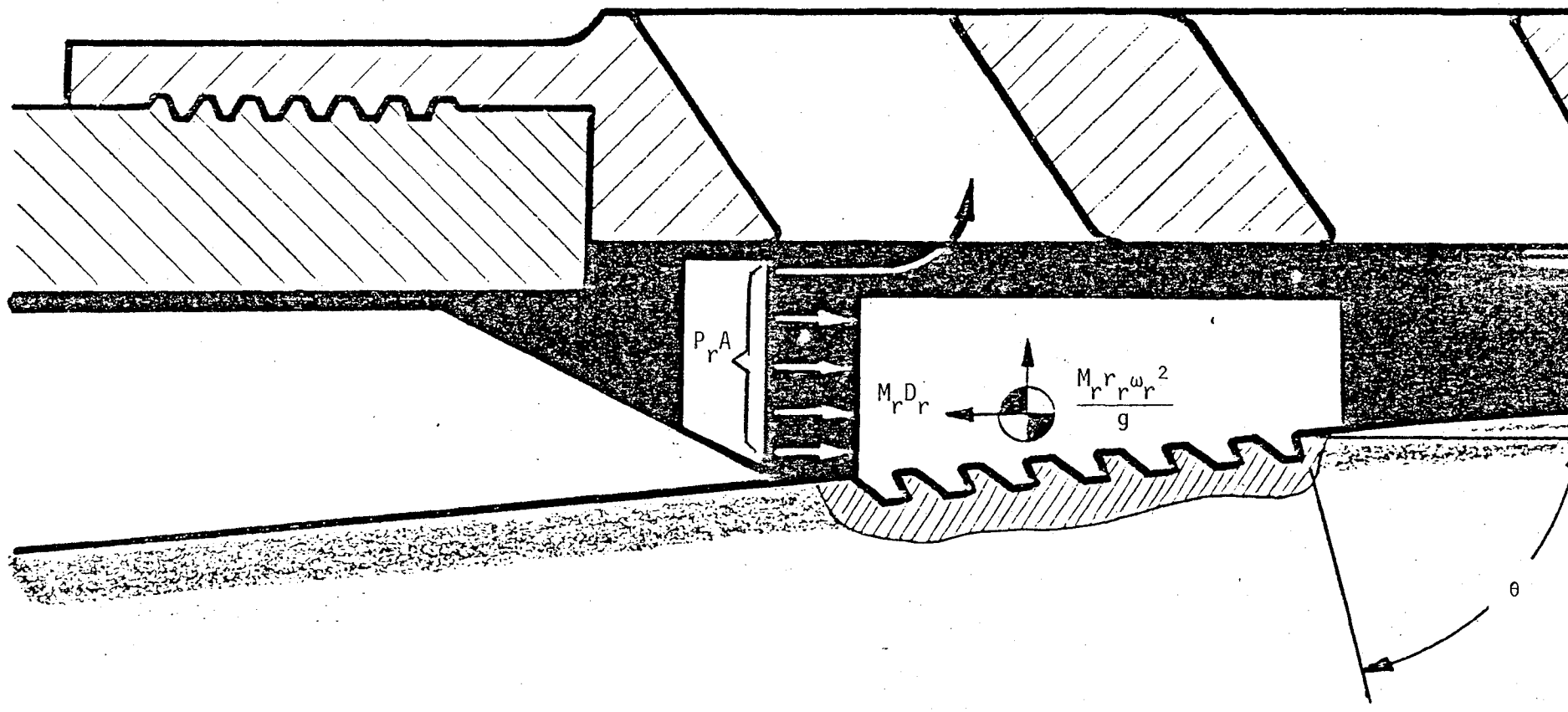

Figure 20. Loads on Rear Sabot While in Muzzle Brake

sabot due to the impingement of the free stream is neglected in the analysis. While the rear sabot is in the muzzle brake, the gun gas pressure is much greater than the aerodynamic pressure and so it is reasonable to neglect the latter. After exit from the muzzle brake, the neglect of the aerodynamic pressure results in a conservative calculation of the release loads.

It is noted that the complex dynamic nature of the gas flow in the muzzle brake is not considered in the analysis. A single value of the pressure acting on the base of the rear sabot is assumed.

The expressions for the loads that are considered to act on the rear sabot are:

$$R_c = M_r r_r \omega_r^2/g$$

$$R_p = P_r A$$

$$R_a = M_r D_r$$

As in the case of the front sabot, the above loads are resolved into components normal to and parallel to the thrust flange(s) of the sabot-projectile interface.

$$N_r = M_r r_r \omega_r^2/g \cos\theta + (PA - M_r D_r) \sin\theta$$

$$P_r = M_r r_r \omega_r^2/g \sin\theta - PA - M_r D_r) \cos\theta$$

Again following the approach used for the front sabot, the retention force is defined as:

$$A_r = \mu_r N_r - P_r$$

After the rear sabot is clear of the muzzle brake, the centrifugal load is the only one that is assumed to act. The normal and parallel components of this force are:

$$N_r = M_r r_r \omega_r^2/g \cos \theta$$

$$P_r = M_r r_r \omega_r^2/g \sin \theta$$

The release force is defined as:

$$B_r = P_r - \mu_r N_r$$

3.6 EVALUATION OF RETENTION AND RELEASE LOADS FOR THE FRONT AND REAR SABOTS

The calculation of the retention and release loads for the sabotry requires a knowledge of the internal ballistic conditions that pertain at the muzzle. A preliminary internal ballistic trajectory for an assumed projectile configuration was determined using the method of Baer-Frankel[1]. The assumed conditions were a shot weight of 140 lbm., a charge weight of 65 lb. of M30 .085 web and a shot start pressure of 0 psi. The appropriate chamber volume for the two piece sabot, closed boom configuration was used. The calculation estimates a maximum breech pressure of 43,171 psi and a muzzle velocity of 3,437 ft/sec. The internal ballistic parameters required for calculation of the sabot loads are included in Table 3. Other parameters required for the calculations are also included in Table 3. Parameters which have no set value through the calculations are defined; however, no values for these parameters appear in the tabulation.

---

[1] P.G. Baer and J. M. Frankel, "The Simulation of the Interior Ballistic Performance of Guns by Digital Computer Program," Ballistic Research Laboratories Report No. 1183; December, 1962

TABLE 3. PARAMETERS FOR CALCULATION OF RETENTION AND RELEASE LOADS OF FRONT AND REAR SABOTS

PARAMETER	DESCRIPTION	UNITS	VALUE
P	Base Pressure at Muzzle	psi	12,179.
D	Acceleration at Muzzle	g's	3,470.
V	Muzzle Velocity	ft/sec	3,437.
ω_f	Angular Velocity, Front Sabot	rad/sec	-
r_f	C.G. Radius, Front Sabot Segment	in.	3.0
m_f	Mass of Front Sabot	lbn.	2.7
g	Acceleration due to Gravity	$\frac{\text{lbm - in.}}{\text{lb. - sec}^2}$	386.04
ρ	Density of Air	slugs/in.^{3}	.002377
A_f	Frontal Area, Front Sabot	in.^{2}	30.6
F_c	Centrifugal Force, Front Sabot	lb.	-
F_a	Acceleration Force, Front Sabot	lb.	-
F_d	Dynamic Force, Front Sabot	lb.	-
ϕ	Front Latch Angle from Horizontal	degrees	-
α	Front Surface Angle from Horizontal	degrees	-
N_f	Normal Force, Front Sabot, in Muzzle brake	lb.	-
P_f	Parallel Force, Front Sabot, in Muzzle Brake	lb.	-
N_f'	Normal force, Front Sabot, Free Flight	lb.	-
P_f'	Parallel Force, Front Sabot, Free Flight	lb.	-
μ_f	Coefficient of Friction, Front Sabot - Body	-	.61
A_f	Retention Force, Front	lb.	-

TABLE 3. PARAMETERS FOR CALCULATION OF RETNETION AND RELEASE LOADS OF FRONT AND REAR SABOTS (CONT'D)

PARAMETER	DESCRIPTION	UNITS	VALUE
B_f	Release Force, Front Sabot	lb.	-
ω_r	Angular Velocity, Rear Velocity	rad/sec	-
r_r	C.G. Radius, Rear Sabot Segment	in.	2.8
M_r	Mass of Rear Sabot	lbm.	7.7
D_r	Acceleration, Rear Sabot in Muzzle Brake	g's	359
A	Area of Rear of Rear Sabot	in^2	30.6
P_m	Pressure, Rear Sabot in Muzzle Brake	psi	1000
R_c	Centrifugal Force, Rear Sabot	lb.	-
R_p	Base Pressure Force, Rear Sabot	lb.	-
R_a	Acceleration Force, Rear Sabot	lb.	-
Θ	Rear Latch Angle from Horizontal	degrees	-
N_r	Normal Force, Rear Sabot in Muzzle brake	lb.	-
P_r	Parallel Force, Rear Sabot in Muzzle brake	lb.	-
N_r'	Normal Force, Rear Sabot, Free Flight	lb.	-
P_r'	Parallel Force, Rear Sabot, Free Flight	lb.	-
μ_r	Coefficient of Friction, Rear Sabot - Body	-	.61
A_r	Retention Force, Rear Sabot	lb.	-
B_r	Release Force, Rear Sabot	lb.	-
r	Gun Bore Radius	in.	.4
W	Shot Weight	lbm.	140.

The values of several of the parameters listed in Table 3 require discussion. The values of the coefficients of friction between the sabots (front and rear) and the body of the projectile have been assigned assuming an interface of aluminum on steel. According to Marks and Baumister[2] a value of .61 is appropriate for the coefficient of static friction between unlubricated aluminum and steel. The pressure which is maintained behind the rear sabot up until it exits the muzzle brake is not well known. A value of 1,000 psi, which is believed to be conservative, is therefore assigned to this parameter. The acceleration of the projectile at this time is determined from:

$$D_r = \frac{\pi r^2 p_m}{W}$$

As this projectile is to be a low spin rate projectile, the calculations of the retention and release forces for the sabots has been made assuming partial spin up. The full spin rate for a muzzle velocity of 3,437 ft/sec. for a rifling twist of 1 in. 20 is 1,620 rad/sec. (258 rps).

Figures 21 and 22 are plots of the retention and release loads for the front sabot. In each of the graphs, the loads are plotted versus the latch angle of the interface between the front sabot and the boyd. For Figure 21, the front face of the front sabot has been taken to be perpendicular to the projectile axis. For Figure 22, the front face of the front sabot has been taken to be inclined at 60° to the projectile axis. Figure 23 is a plot of the retention and release loads for the rear sabot. The loads are plotted versus the latch angle of the rear sabot - body interface

---

[2] L. S. Marks and T. Baumister, "Standard Handbook for Mechanical Engineers," Seventh Edition, McGraw Hill; 1967

Figure 21. Retention and Release Loads for Front Sabot vs Latch Angle for Two Spin Rates ($\alpha = 90^{o}$)

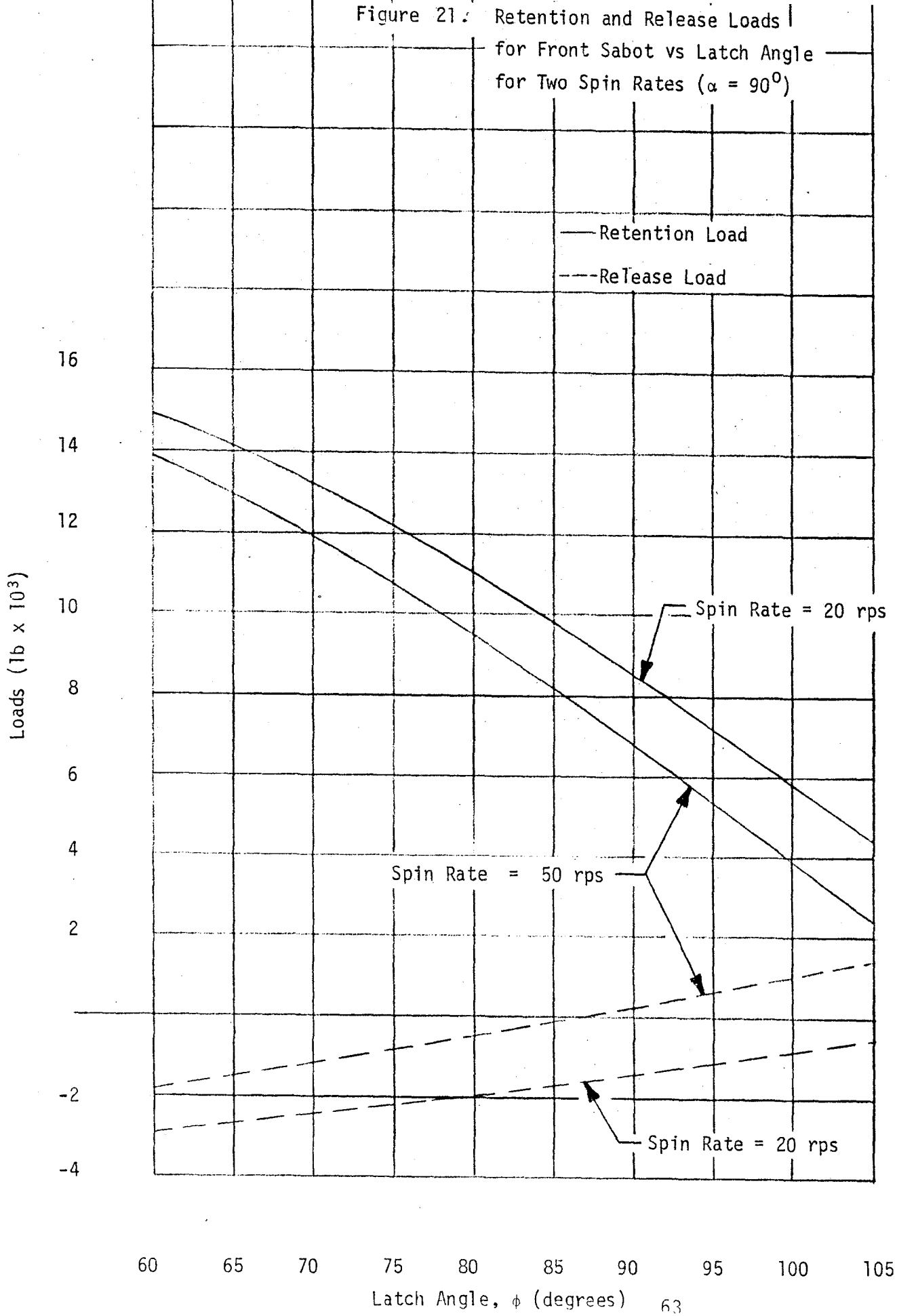

Figure 22. Retention and Release Loads for Front Sabot vs Latch Angle for Two SpinRRates ($\alpha = 60^{o}$)

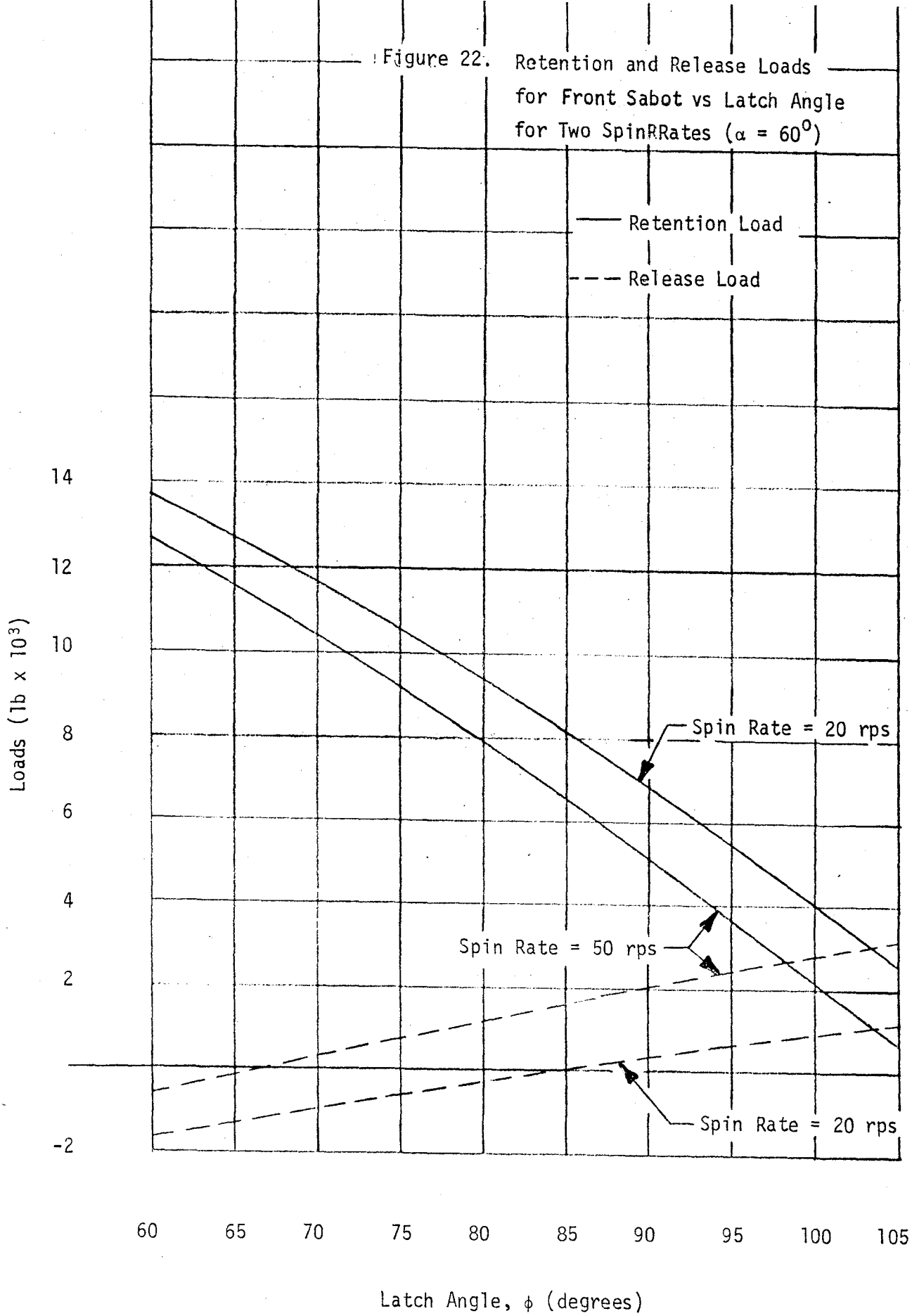

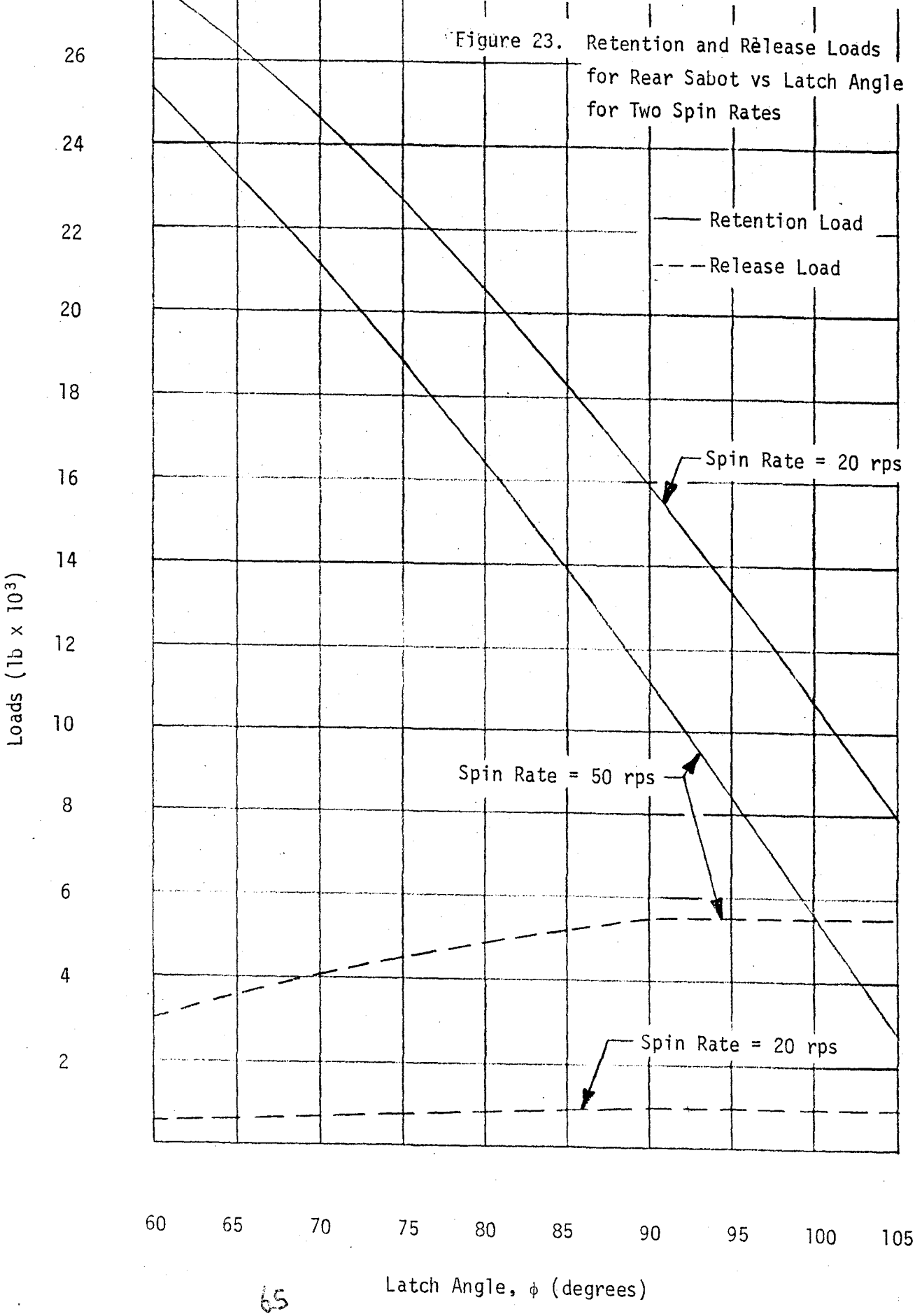

Figure 23. Retention and Release Loads for Rear Sabot vs Latch Angle for Two Spin Rates

From Figure 21, it can be seen that for the case of a perpendicular front face the release loads for the front sabot are low for all angles of the latch, even for angles above 90°. In fact, for a spin rate of 20 rps, the release load is in all cases negative. In order to achieve positive values of the release loads for a spin rate of 20 rps, it is necessary to do either of two things:

a) reduce the coefficinet of friction on the front sabot-projectile interface.

b) utilize a portion of the aerodynamic load for separation (i.e. incline the front face of the front sabot).

The values of the loads on the front and rear sabots due to centrifugal force, acceleration and dynamic and gun gas pressure are shown in Table 4 for the two cases of spin rate considered.

From Table 4, it can be seen that the value of the aerodynamic force on the front sabot is higher than that of the centrifugal force, particularly so for the lower spin rate case. This causes the normal force on the front sabot-projectile interface to be high. Correspondingly, the resistance to separation due to friction is also high. Reduction of the coefficient of friction between the front sabot and projectile body could alleviate this.

In Figure 22, the effect of inclining the front face of the front sabot at an angle of 60° from the projectile axis is considered. It can be seen that the values of the release loads are increased over those calculated for the case of a perpendicular front face. The values of the retention loads are reduced somewhat also. Based on the results presented in Figure 22, it is considered that a good starting point for the design of the front sabot would be with an unlubricated interface between the front sabot and body, a latch angle between 90° and 100° and an angle of inclination of the front face of 60°.

TABLE 4. VALUES OF LOADS ACTING ON FRONT AND REAR SABOTS FOR TWO SPIN RATES

LOAD PARAMETER	LOAD - (lbs.)	
	(Spin Rate = 50 rps)	Spin Rate = 20 rps
F_c	2,069.	333.
F_a	11,799.	11,799.
F_d	2,983.	2,983.
R_c	5,506	887.
R_p	30,600.	30,600.
R_a	2,764.	2,764.

In Figure 23, it can be seen that both the retention and release loads for the rear sabot are positive for all latch angles between 60° and 105°. For latch angles of greater than 90°, however, there is no increase in the release force although the retention force continues to decrease. This is due to the fact that the normal force on the latch (after exit from the muzzle brake) is zero for latch angles of 90° and greater. For this reason it is not considered appropriate to utilize a latch angle for the rear sabot of greater than 90°. From the results shown in Figure 23, it is considered that a good starting point in the design of the rear sabot latch would be with an unlubricated interface and a latch angle of between 70° and 80°.

Due to the uncertainty in the values of some of the parameters that were used in the analysis and due to the simplifying assumptions that were made, it is to be emphasized that the above are simply starting points in what was an iterative sequence of firing trials and design improvements.

3.7 PROTOTYPE SABOT TESTS

With the establishment of the sabot prototype design, testing began to determine their performance and verify the designs. The test procedure of the sabot structure and discard performance was based upon a principle of isolation. That is, tests were planned to focus upon one advancement at a time toward verifying the design of the sabot system.

The test plan was to develop the front sabot and rear sabot designs independently from each other by the use of non-discarding sabots. These tests were to be done without a muzzle brake.

Later each sabot was introduced to the muzzle brake independently from each other and then finally combined. For use in these tests a dummy muzzle brake was designed to avoid any unnecessary damage to the Army supplied muzzle brake (Dwg. No. WTV-F26323).

The dummy muzzle brake was designed to duplicate the internal contour of the Watervliet muzzle brake which must be avoided by the discarding sabot petals. The dummy muzzle brake is shown in Figure 24.

The first sabot test explored the capability of the front sabot. The test was conducted utilizing a test slug fitted with a non-discarding rear sabot collar and a discarding front sabot assembly. The front sabot (see Dwg. C24119 of Appendix A) had a latch angle of 90° and a front face inclination of 60°. The bore riding surface was gilding metal swaged onto the sabot and segmented to coincide with the splits in the sabot. To retain the sabot on the vehicle during handling and loading, a narrow polypropylene ring is sweated onto the sabot. The total weight of the front sabot for test slug use was 4.26 lbs. Photographic data of this test showed the front sabot petals to separate from the test slug. The test results are given in Table 5.

The rear sabot tests utilized a test slug assembly with a non-discarding front bore rider and discarding rear sabots. Again, a self-engraving slip obturator was used rather than a pre-engraved driving band. A total of five test slugs were fired encompassing four iterations in the rear sabot design as shown in Figures 25 and 26. The final configuration is sketched in Figure 26A and pertinent test results are included in Table 5.

This rear sabot design composed of four segmented petals had a 90° latch angle to its grooves. It made use of an inclined forward face to increase aerodynamic loads for separation. Obturation was accomplished with a high density polypropylene secondary obturator weakened by eight saw cuts. The driving band was high density polypropylene engravable slip obturator.

The next test series investigated the sabotry discard characteristics within the region of the muzzle brake. The dummy muzzle brake was used during these tests for the three test slug configurations. These

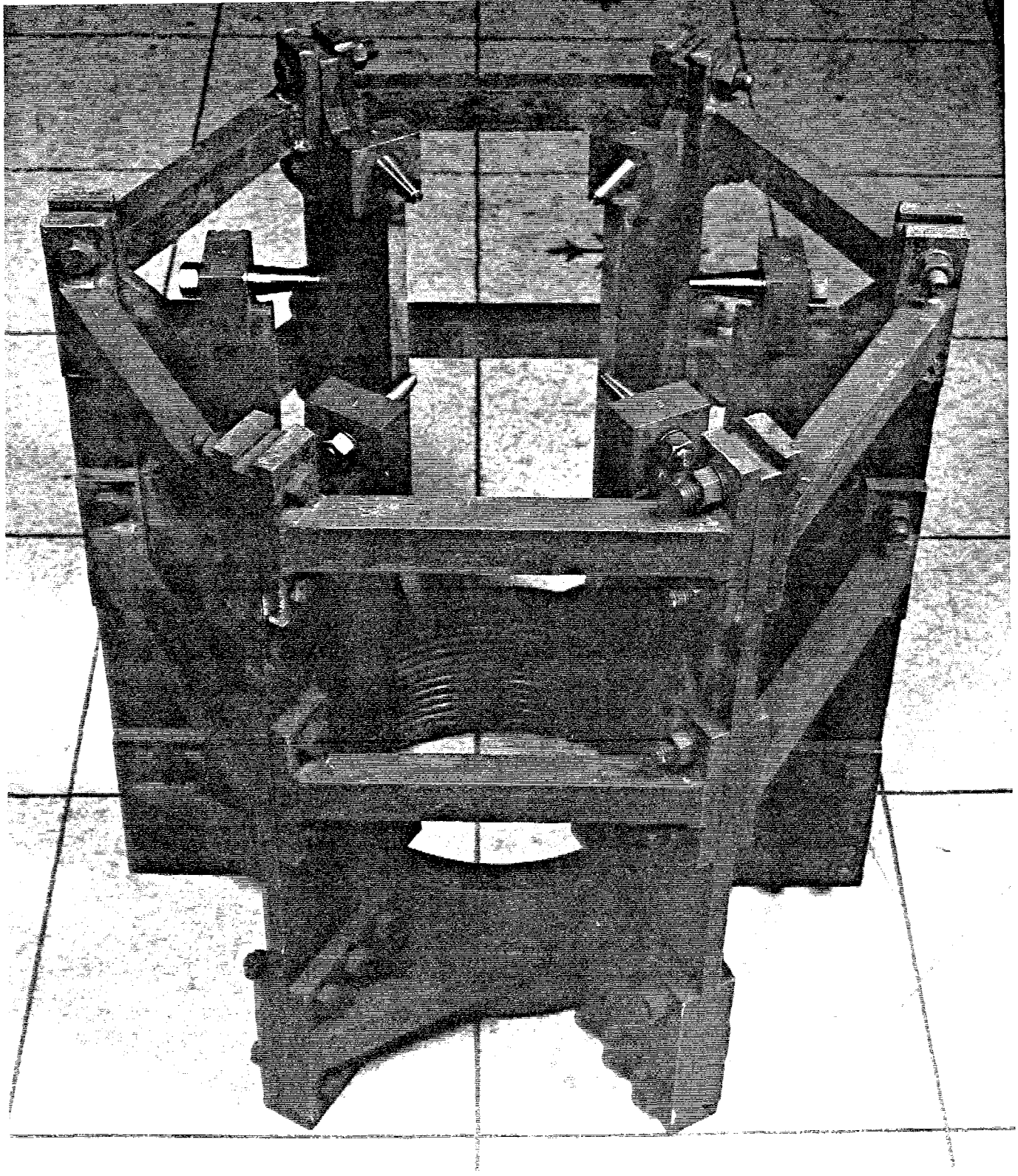

Figure 24. Dummy Muzzle Brake

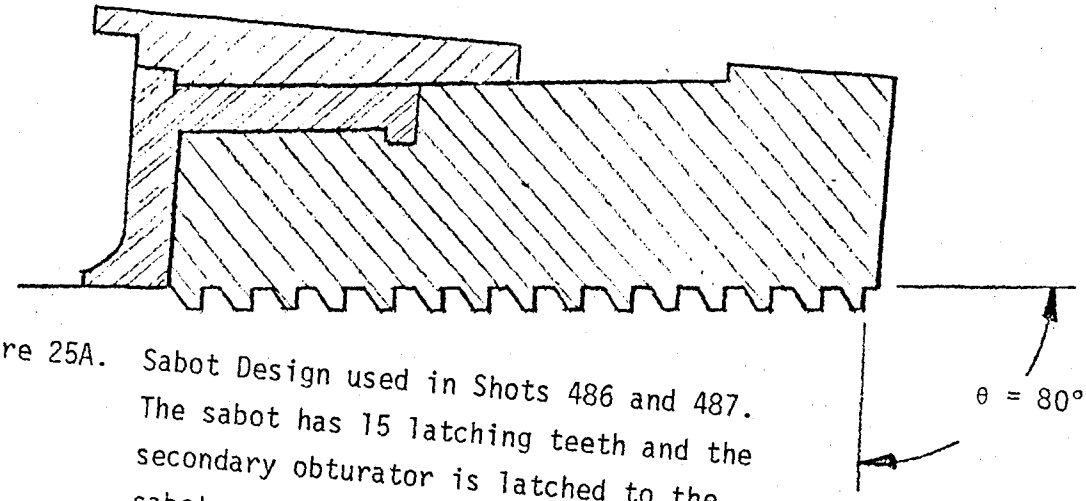

Figure 25A. Sabot Design used in Shots 486 and 487. The sabot has 15 latching teeth and the secondary obturator is latched to the sabot.

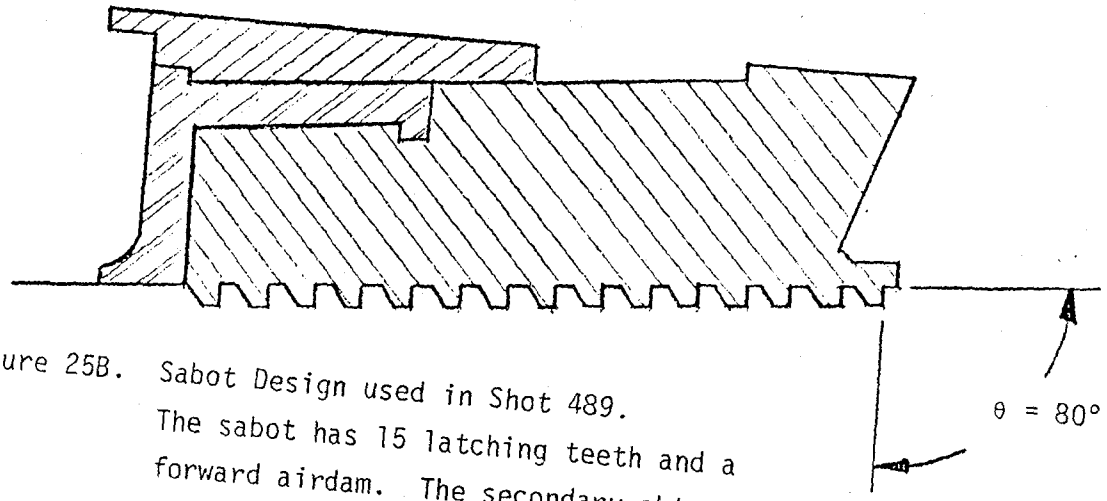

Figure 25B. Sabot Design used in Shot 489. The sabot has 15 latching teeth and a forward airdam. The secondary obturator is latched to the sabot and was weakened by four cuts.

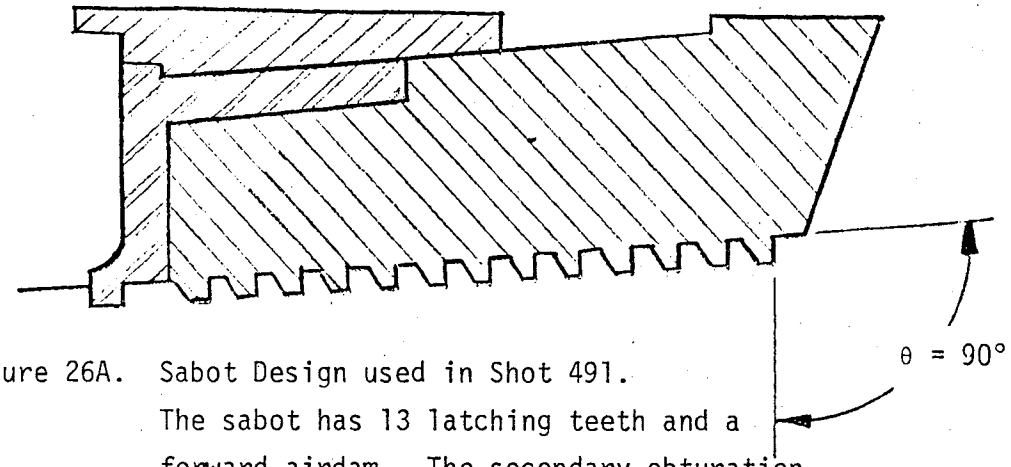

Figure 26A. Sabot Design used in Shot 491. The sabot has 13 latching teeth and a forward airdam. The secondary obturation is secured to the projectile and weakened by eight cuts.

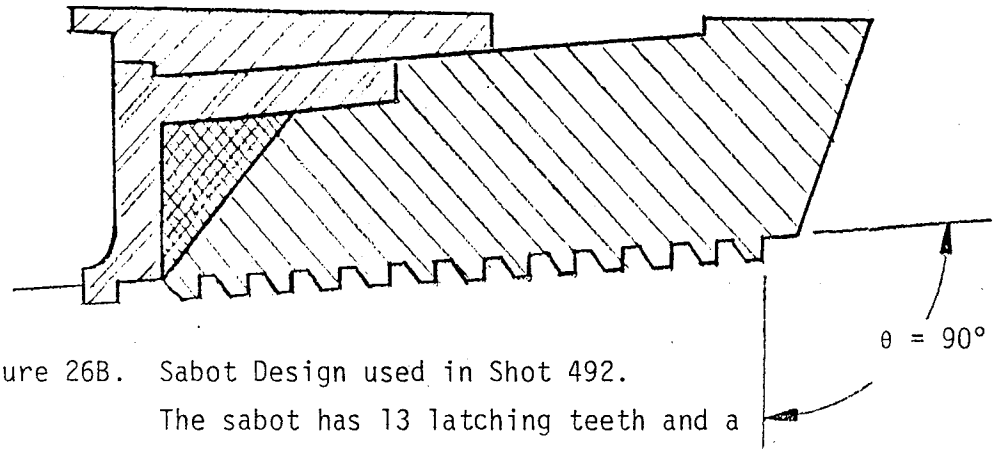

Figure 26B. Sabot Design used in Shot 492. The sabot has 13 latching teeth and a forward airdam. The secondary obturation is latched to the projectile and is weakened by eight cuts. This design shows a block included under the secondary obturator to help fracture the secondary obturator.

TABLE 5. SABOT DISCARD TESTS USING TEST SLUGS

SHOT NO.	DATE	TEST SLUG		BREECH[1] PRESSURE (kpsi)	MUZZLE[2] VELOCITY (fps)	SPIN RATE (rps)	COMMENTS
		NO.	Wt (lbs)				
FRONT SABOT DISCARD TEST WITHOUT MUZZLE BRAKE							
483	8/77	1A	137.13	34.2	3114	19	Front Sabot Discard
483	8/77	6A	137.13	34.3	3133	22	Front Sabot Discard
REAR SABOT DISCARD TEST WITHOUT MUZZLE BRAKE							
486	10/77	D6	136.44	31.4	-	-	No Results
487	10/77	D8	136.38	29.6	2965	-	No Rear Sabot Discard
489	10/77	C5	136.0	33.7	3098	-	No Rear Sabot Discard
491	11/77	D2	135.19	32.5	3083	-	Rear Sabot Discard
492	11/77	D3	136.0	33.5	3077	-	Rear Sabot Discard
FRONT SABOT DISCARD TEST WITH DUMMY MUZZLE BRAKE							
494	12/77	A4	136.87	34.7	3047	-	Loss of Obturation, Muzzle Brake Impacts
497	1/78	A8	137.25	36.8	3174	-	No Muzzle Brake Impacts
REAR SABOT DISCARD TEST WITH DUMMY MUZZLE BRAKE							
500	2/78	4	136.0	35.9	3014	-	No Muzzle Brake Impacts
501	2/78	6	136.0	33.7	3070	-	No Muzzle Brake Impacts
COMBINED FRONT & REAR SABOT DISCARD TEST WITH DUMMY MUZZLE BRAKE							
503	2/78	7	135.25	38.1	3208	-	No Muzzle Brake Impacts
504	2/78	8	135.25	36.9	3217	-	No Muzzle Brake Impacts

[1] Measurement by Three M-11 Gages

[2] Measurement by Smear Camera Films

Projectile Ram: 51 inches

Propelling Charge: 62.0 lbs. M30A1 .085 inch Web, Lot KAU 7/76

configurations listed in the order of testing, utilized a discarding front sabot only, then a discarding rear sabot only, and finally in the last tests of this series, combined front and rear discarding sabots.

The tests were satisfactory in each category even though poor obturation was seen in most tests. The tabulated data is shown in Table 5. Figures 27 through 29 show sample smear camera results for the front sabot discard, rear sabot discard, and front and rear sabot discard, respectively. The three smear cameras in each figure were located 15, 30, and 50 feet down range from the muzzle. The extent of the obturation can be noted from the first smear camera at the top of each figure.

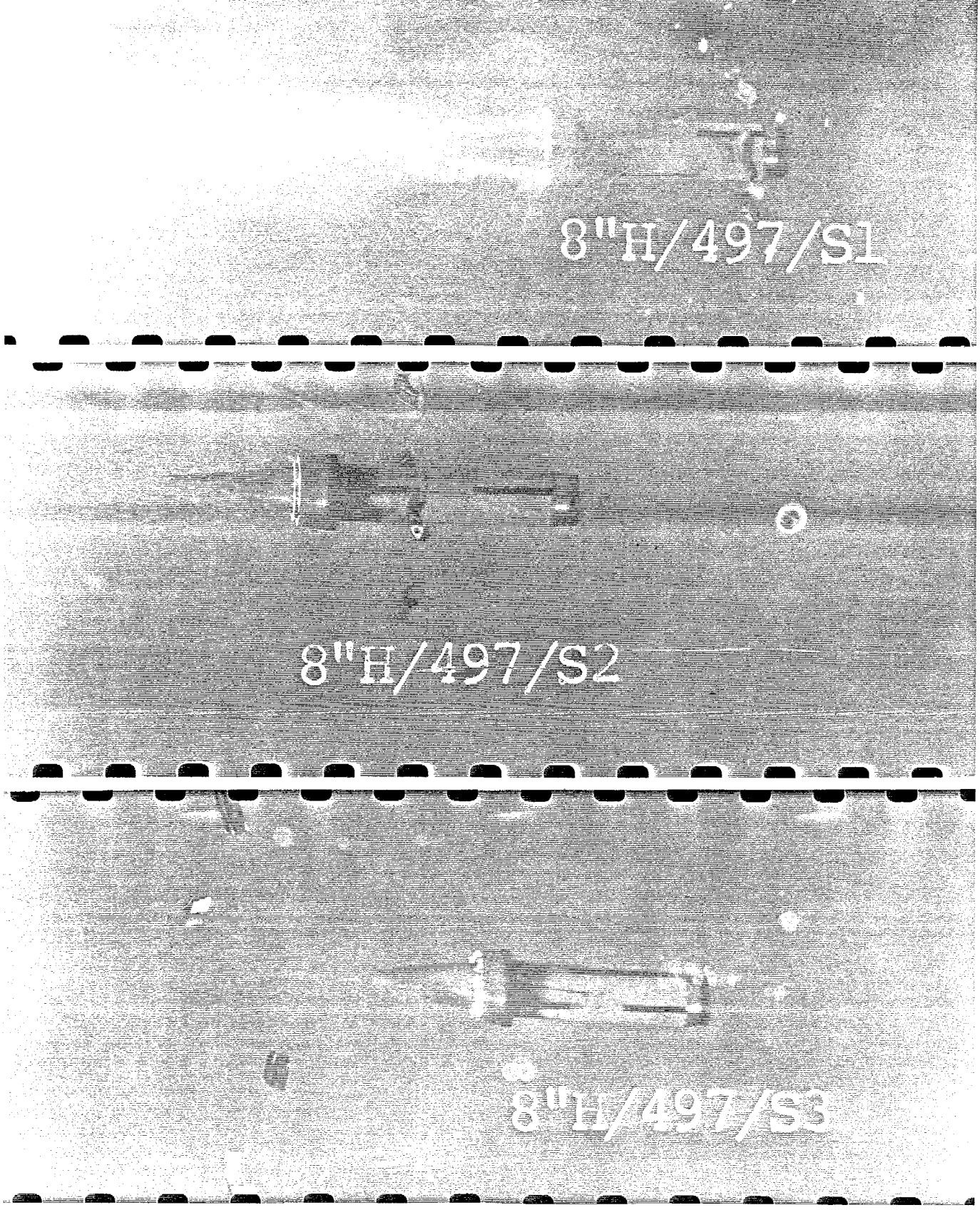

Figure 27. Smear Photographs of the Front Sabot Discard of Shot No. 497

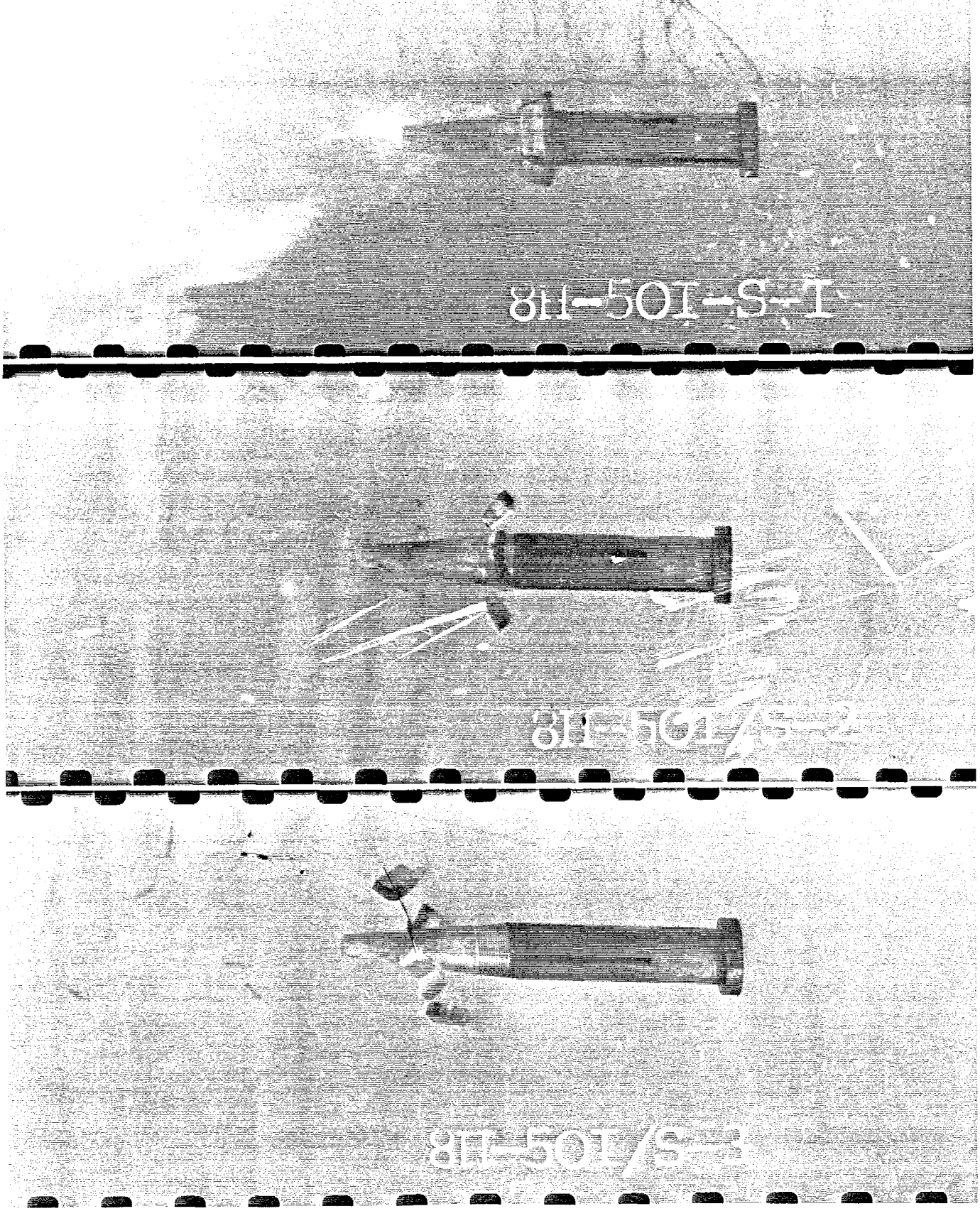

Figure 28. Smear Camera Photographs showing Rear Sabot Discard of Shot No. 501

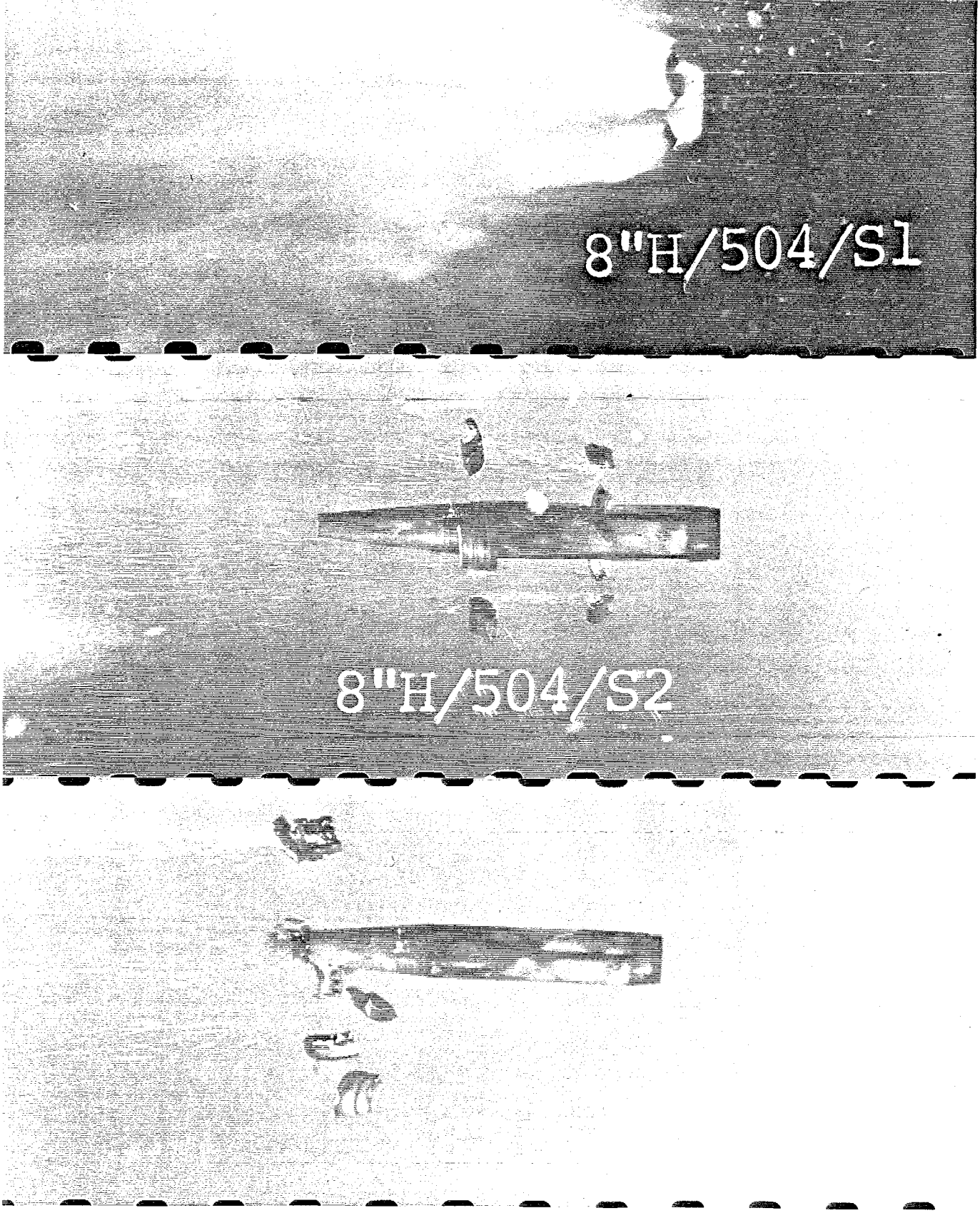

Figure 29. Smear Camera Photographs showing Discard of both Front and Rear Sabots during Shot No. 504

4.0 TEST VEHICLE CONFIGURATION

Upon the successful conclusion of the initial sabot design tests the next operation in this development project was the design of an efficient extended range cargo carrying projectile and the incorporation of the sabot design therein. Necessarily, then, decisions were made to give direction to the impetus of the work to be done, particularly with regard to the sabot configuration and the method of obturation.

Of the three basic sabot configurations (base pusher sabot, center sabot, and split sabot) the split sabot system was felt to offer more to the primary goal of an extended range vehicle. The base pusher sabot as pointed out earlier was clearly too heavy and thus was eliminated as an option. The additional weight of this design restricts the maximum muzzle velocity of the round by the muzzle momentum limit of the gun recoil system to lower values.

The center sabot configuration, using fin attached bore-riders has the lightest total sabot weight of the three configurations. This design, however, requires a larger diameter body with a thicker wall not only to accommodate the sabot latching grooves and resulting stress concentrations but also to give strength while under the influence of the rearward high breech pressure. The center sabot configuration, in comparison to the split sabot configuration gives a lower sabot mass but higher shot mass and hence lower muzzle velocities. This configuration also results in a shorter in-bore travel reducing the momentum transfer of the expanding propellant gas to the projectile.

With respect to balloting, the split sabot system is better for two reasons. First it has a greater wheel base for better in-bore alignment and second its wheelbase brackets the projectile's center of gravity promoting better in-bore projectile stability without in-bore support by the fins. In the center sabot configuration where both support points are located behind the projectile's center of gravity the balloting loads are supported by the fins requiring them to be stronger and hence heavier, having an adverse effect on projectile

total drag and center of gravity location. Thus the selected design approach was the split sabot system.

It was also deduced that the engravable sliding obturator as used in the test slug design presented greater benefits than the pre-engraved obturator. The concern in the use of the pre-engraved obturator was the additional handling of the round required during ramming to interface the gun tube rifling with the obturator engraving. The sliding self-engraving obturator on the other hand eliminates this additional complexity because it does not interfere with the rifling and is simply slid into place.

It was then decided that the extended range vehicle concept would make use of a split sabot system with a self-engraving obturator.

Several design iterations were made where the intentions of each design was to increase the maximum range capability by reducing the total shot weight and place the center of gravity generally far forward to maintain a good margin of stability. The design developed here represents a successful balance between the choice of shot weight, center of gravity and margin of stability.

4.1 PROPOSED PROJECTILE DESIGN DESCRIPTION

The design of this extended range subcaliber fin-stabilized cargo shell is shown in the sketch of Figure 30. This shell is designed to carry a payload similar to the 155mm M483A1 projectile already developed and in operation. The principal feature of this extended range design other than the use of sabots is the use of an ultra-high strength 4140 steel body having a thin skin and permitting a small body diameter of only 5.478 inches (139mm). This not only reduces the weight of the vehicle but gives the minimum projected frontal area of the shell possible for lower drag.

PARTS LIST

1. FINS
2. REAR SABOT CARRIER
3. REAR SABOT
4. BODY
5. FRONT SABOT
6. SPACER, BODY
7. PAYLOAD
8. PUSHER PLATE
9. FRONT SABOT CARRIER
10. FUZE W/EXPULSION CHARGE
11. WINDSHIELD

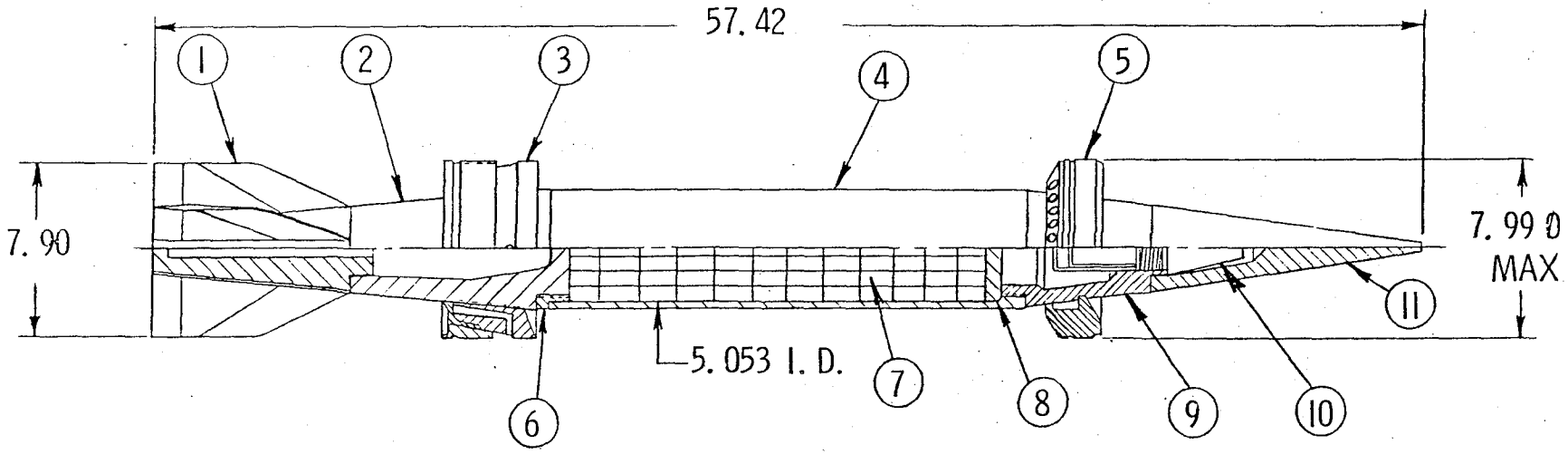

Figure 30. Proposed 8-inch Subcaliber Fin Stabilized Extended Range Projectile shown with Submunition Payload

The design of the cargo shell is divided into four major functional sections. These are;

1) The aft section comprised of the fins, a tail boom, a rear sabot carrier and a body spacer. The rear sabot carrier is that part of the aft section which is grooved to interface with the rear sabot petals.

2) The body section which includes not only the thin-skin body but all payload components and ejection plate.

3) The forebody section having as its components; the front sabot carrier, the fuze and expulsion charge, and the windshield. The front sabot carrier is grooved to accept the front sabot, petals, and it also accepts the fuze and expulsion charge, and provides the expansion cavity for the expulsion charge.

4) Sabots including front and rear which are broken down as follows:

   a. The rear sabot is comprised of the sabot petals, a pressure barrier or secondary obturator, and a main obturator.

   b. The front sabot which includes the sabot petals, a bore riding surface, and a retaining ring.

The aft section utilizes a 6061 aluminum welded fin assembly with six fins having a root chord length of 9.0 inches and a tip chord length of 4.5 inches. The fins have a 0.5 degree angle of cant to vehicle axis to retain projectile spin and minimize fin drag upon launch. The fins have a total diametral span of 7.90 inches. The fins are welded to a 6061 aluminum truncated conical fin boom having a 5.19 degree taper which is threaded for mating to the rear sabot carrier.

The 7075-T6 Aluminum rear sabot carrier is located just forward of the fin weldment and has thirteen grooves which latch the rear sabot petals. Because of the high bearing loads upon launch a hardened 4140 steel (HRC 48 minimum) bearing washer or body spacer is threaded onto the rear sabot carrier as an interface to the thin body. This body spacer distributes the high loads of the forward supported members during launch over a larger area of the rear sabot carrier to give a much more sound foundation. With this body spacer the launch load at 50 kpsi breech pressure is 93.5 kpsi on the rear sabot carrier.

The body, which starts at 18.0 inches from the base, is made of 4140 hardened steel (HRC 56) and tapers on the outside from 5.478 inches (139mm) to 5.346 inches over a length of 21.67 inches. The body provides a cylindrical payload cavity having a diameter of 5.053 inches and a length of 19.67 inches. The 0.17 degree taper of the body exterior was implemented to reduce the weight of the body and to produce a constant stress design during launch. This body design however does not have the longitudinal groove as on the M483 body because of the low launch spin. An ejection plate is located in the front of the payload section for payload expulsion.

Threaded to the front of the body is the front sabot carrier which is made from 1018 mild steel. The front sabot carrier provides the latching groove of the front sabot. It also receives the fuze and expulsion charge and forms the expansion cavity for the expulsion charge.

Upon assembling the fuze to the front sabot carrier a mild steel (1018) windshield is threaded onto the front sabot carrier covering the fuze. The windshield completes the aerodynamic shape and provides ballast for proper center of gravity placement.

The aerodynamic shape of the nose is a 3/4 power curve extending over the entire length (17.75 inches) of the windshield and front sabot

The rear sabot is segmented into four 7075-T6 Aluminum sabot petals located 13.79 inches from the base and latched to the rear sabot carrier with thirteen parallel buttress teeth. A weakened polypropylene pressure barrier or secondary obturator is sweated about the sabot petals. Over this a polypropylene slip driving band is sweated into place for obturation of the breech gas.

The front sabot is likewise constructed of four hardcoat anodized 7075-T6 Aluminum sabot petals held in place by a thin narrow polypropylene retaining ring during handling. The front sabots are latched by a groove in the front sabot carrier located 41.67 inches from the base. Each front sabot petal has five 5/16 inch holes drilled through it to lighten its weight and prevent gas pressure build up between the front and rear sabots.

The capabilities of this design have been demonstrated in tests of representative vehicles. It is upon these tests that the representation of this vehicle design capabilities are made.

4.2 8-INCH SUBCALIBER CARGO SHELL TEST VEHICLE DESIGN

A test vehicle was designed to perform in a similar manner as the proposed design in both the internal and external ballistic domains. The design of this test vehicle shown is in the schematic drawing of Figure 31 and the photograph of Figure 32. The particular ways in which this test vehicle models the proposed vehicle are discussed below.

This test vehicle represents the proposed vehicle design by making use of many of the actual components intended for use in the proposed vehicle. Those components which have been designed to model components of the proposed vehicle are the test vehicle body and payload. All other components are accurately represented by the description given in the previous sections dealing with the proposed design.

ARTS LIST

1. FINS
2. REAR SABOT CARRIER
3. REAR SABOT
4. BODY
5. FRONT SABOT
6. WINDSHIELD
7. SPACER BODY
8. DUMMY PAYLOAD
9. PAYLOAD BALLAST
10. HEX HD BOLT
11. FRONT SABOT CARRIER
12. INERT FUZE

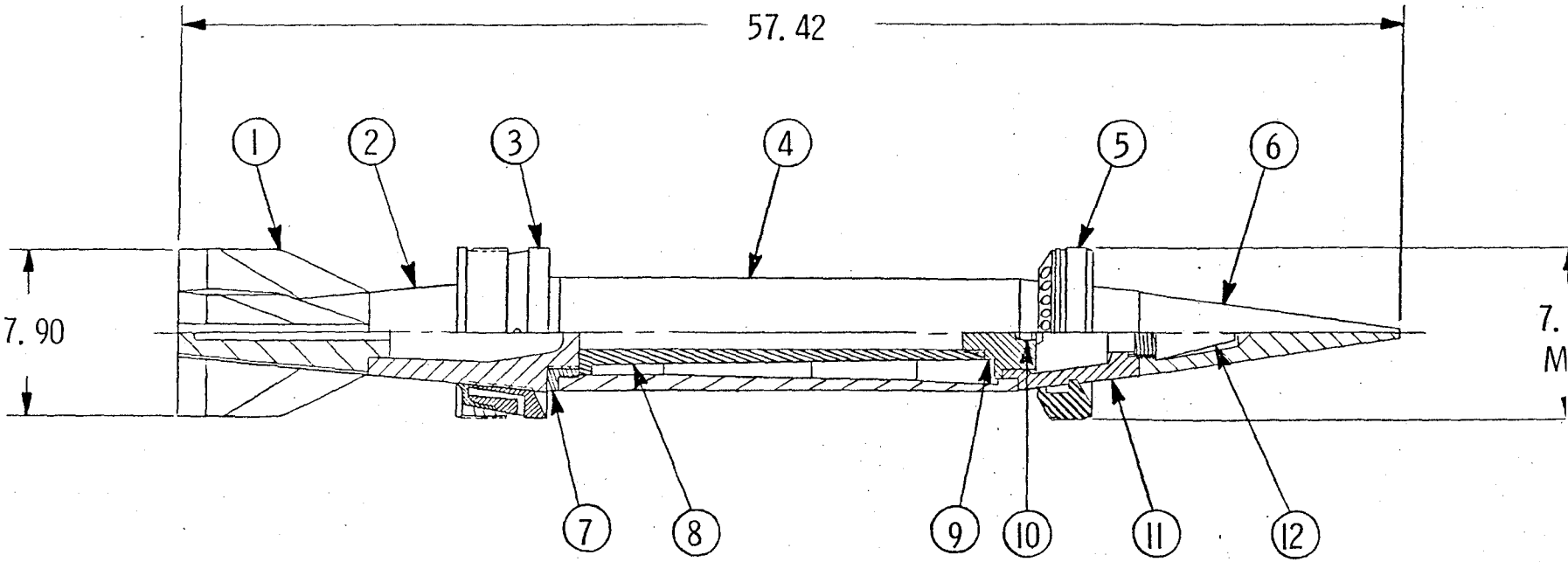

Figure 31. 8-inch Subcaliber Fin Stabilized Test Vehicle

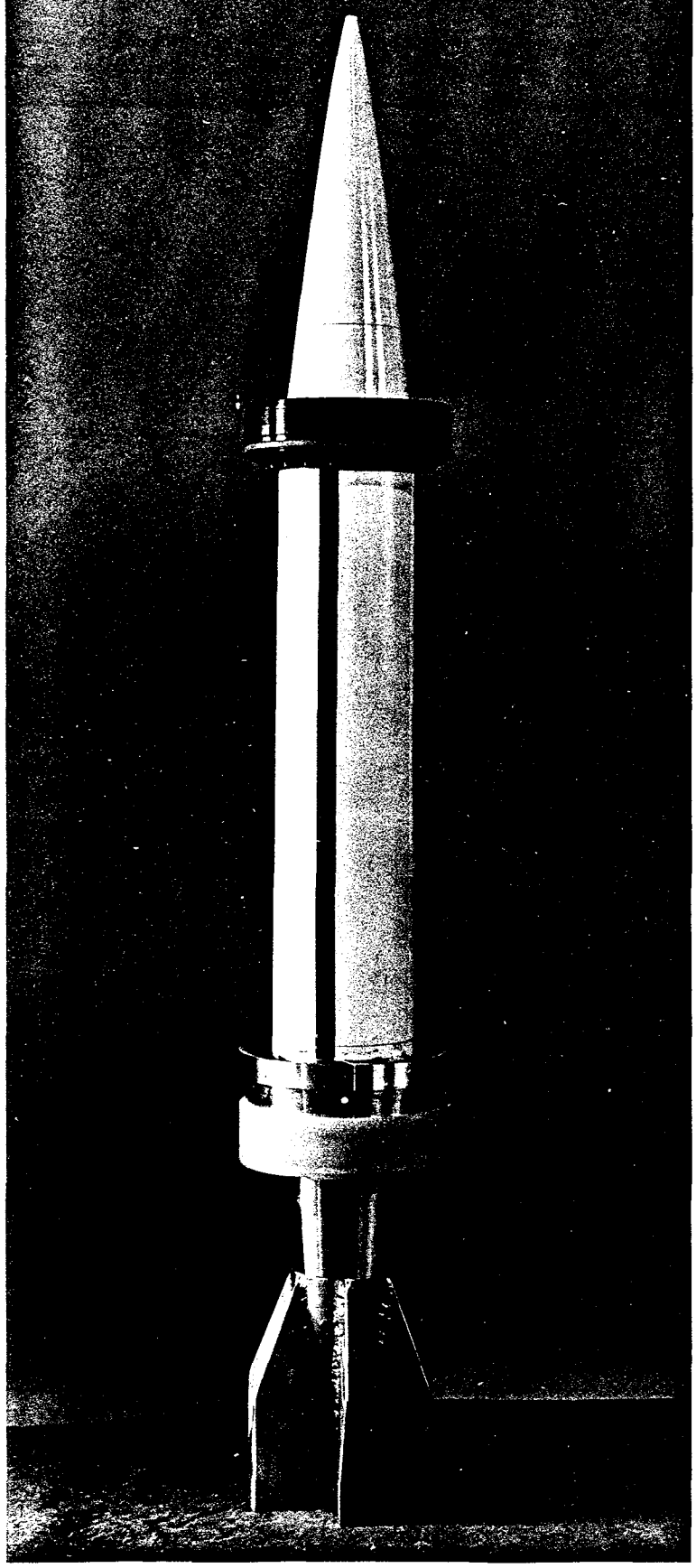

Figure 32. Photograph of 8-inch Test Vehicle used in Design Development Testing

The test vehicle makes use of a thicker lower strength 4140 steel body which by its increased weight over the thin body of the proposed vehicle is made to simulate the weight of a fraction of the payload. A dummy payload assembly is also included in the test vehicle which represents the weight of the remaining fraction of the payload and adjusts the center of gravity. These components represent the major differences between the two designs.

As shown in Figure 31, the test vehicle body has several internal tapers. This has been done to prevent the body wall from exceeding the weight and center of gravity requirements of the body and payload components of the proposed vehicle design. The specific tapers shown produce a fairly uniformly stressed body wall under the acceleration of the breech gases. This principle applied here, as in the case of the proposed vehicle design, prevents the over loading at the base of the body wall, makes efficient use of the component's material and effectively demonstrates this principle to be used in the proposed vehicle design.

In the proposed vehicle's body design, constant stress over the length of the body is achieved by the external taper, while its internal payload cavity must be straight to allow payload ejection. The test vehicle on the other hand has the same external taper for reasons of modeling but makes use of additional internal tapers to present a constant stress design.

The aft section including the rear sabot is similar. Two minor differences exist here however. First, the test vehicle uses a hardened steel body spacer, as the proposed vehicle, but in the test vehicle this body spacer is threaded to the body, where in the proposed vehicle it would be press fitted to the thin body and pinned in place. Second, because of the thicker and heavier body wall of the test vehicle its body spacer must distribute a larger load upon launch and thus has a larger bearing area. The body spacer of the test vehicle is threaded to the rear sabot carrier with a 3.5 inch diameter thread rather than the 4.25 inch diameter thread of the proposed vehicle.

The nose assembly is the same as intended for the proposed vehicle including the front sabot and is described by the description of the proposed vehicle components presented earlier.

The mass properties of the test vehicle are shown in Table 6. In this table the nominal weights of the components are given as calculated along with the pertinent nominal flight and shot properties.

4.3 FINITE ELEMENT STRESS ANALYSIS

The stresses in the test vehicle were investigated with the use of a computer aided finite element stress analysis. In this analysis the loading parameters as given in Table 7 were placed upon the finite element grid of Figure 33.

To keep the size of the stiffness matrix with the bounds of the program, the fins, rear sabot of payload assembly, front sabot, windshield, and fuze were all modeled simply as masses mathematically attached to the appropriate element nodes. That is, although the internal stresses of these components were not calculated the inertial effects of these components on the main frame of the test vehicle were not neglected. These components are therefore listed in Table 7 as inertial loads supported by the test vehicle structure.

In this analysis, the test vehicle design was evaluated with a breech pressure of 50,358 psi. The test vehicle was evaluated to an overpressure of more than 10 kpsi to reveal the most extreme loads that this design would be exposed to in the event of a mishap in the chamber of the gun during launch.

TABLE 6. 8"-155MM CARGO SHELL COMPONENT SUMMARY

COMPONENT	WEIGHT (lbs)
Fuze	1.7408
Front Sabot Carrier and Windshield	31.390
Body	50.565
Dummy Payload	14.080
Body Spacer	3.271
Rear Sabot Carrier	11.844
Fin Boom	7.0274
Fins (Est.)	3.2286
Flight Properties	
Weight (lbs)	123.15
C.G. in from base	29.694
I_{xx} about C.G. (lb-in^2)	499.842
I_{yy} about C.G. (lb-in^2)	21930
Shot Properties	
Sabot Weight	13.292
Shot Weight	136.44

TABLE 7. FINITE ELEMENT ANALYSIS LOADING CONDITIONS FOR THE 8 INCH-155MM CARGO SHELL MOD 4

Total Shell Wt. (lbs.)	136.58
Breech Pressure (psi)	50,358
Base Pressure (psi) (from LeDucs equation)	41,359
Acceleration (g)	15,287

Figure 33. Finite Element Analysis Grid of the 8 inch-155 mm Cargo Shell Mod 4

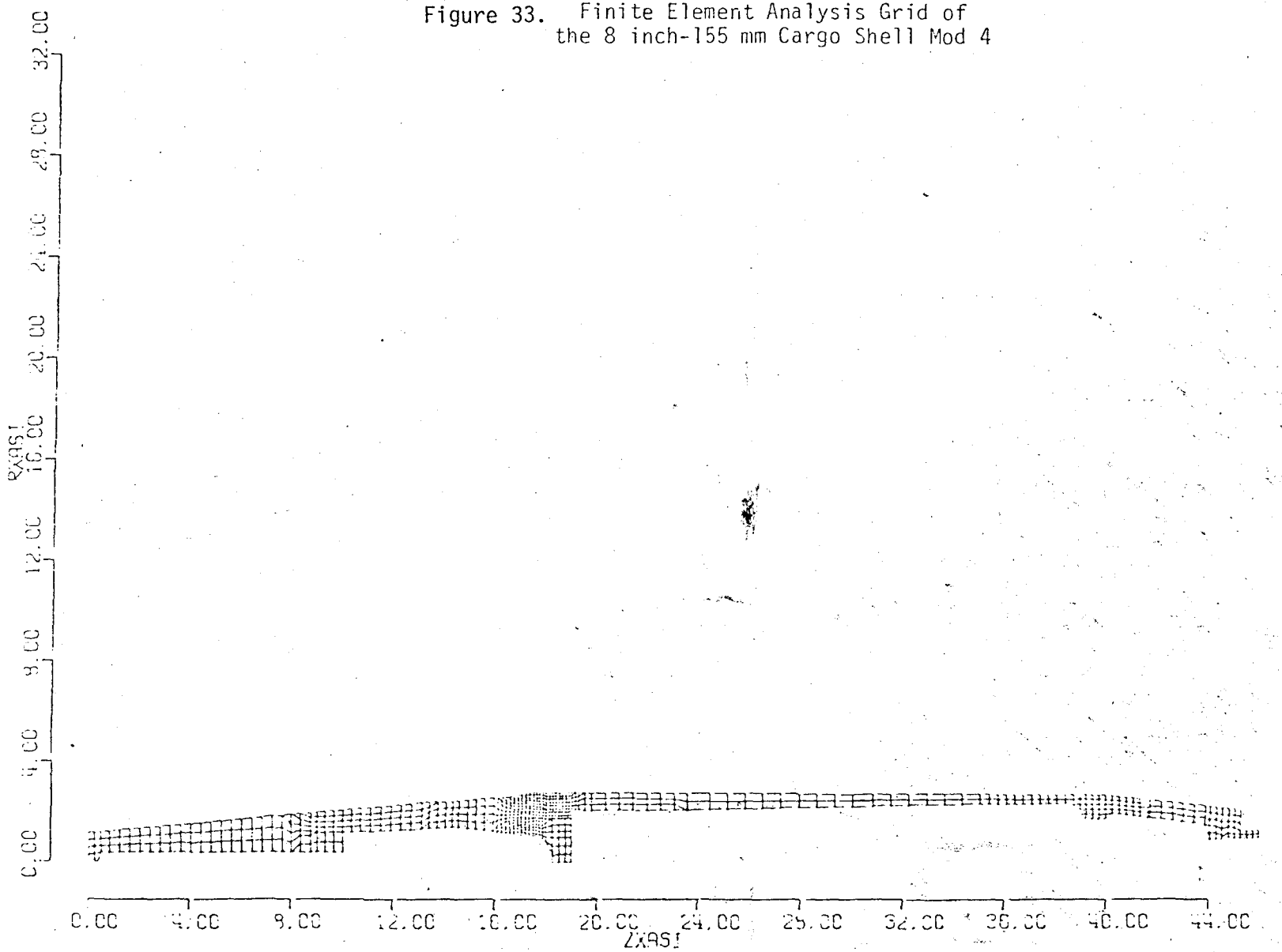

DRAWING
CASE NO.
09/80 F20/60
34-0

A breech pressure (P_b) of 50,358 psi exerts a pressure on the base (P_{base}) of the accelerating projectile of 41,359 psi as determined by Leducs formula given as;

$$P_{base} = \frac{P_{breech}}{1 + \frac{CW}{2W_s}}$$

where Cw is the charge weight and W_s is the shot weight of the vehicle. The accleration (a) is determined to be 15,287 g's by Newton's Law;

$$a = \frac{P_{base}\ \pi D^2}{4W_s}$$

Figure 34 shows the plot of the maximum equivalent stress in the cross section of the shell versus its axial location. The largest component of the equivalent stress is the axial stress, a direct result of the acceleration, shown in Figure 35. Other components are the radial, tangential and shear stresses similarly plotted in Figures 36, 37 and 38 respectively. The highest equivalent stress of 226,000 psi as shown in Figure 34 has an axial location of 17.9 inches placing that stress within the body spacer at the body interface.

Figures 39 to 44 show enlarged views of sections of the shell with the equivalent stress contours plotted. From these figures it is evident that the highest stresses occur at the rear sabot carrier-body interface shown in Figure 41. As a note to the reader the body is made of 4140 steel heat treated to a yield strength of 140 kpsi and an ultimate strength of 156 kpsi. The body spacer is also of 4140 steel heat treated to a hardness of 48 to 50 Rockwell C with a yield strength of 220,000 psi and an ultimate strength of 257,000 psi. The rear sabot carrier is machined from 7075-T6 Aluminum with a yield strength of 73 kpsi and an ultimate strength of 83 kpsi.

Although the stresses on the shoulder of the rear sabot carrier are high, the loading upon these elements are nearly hydrostatic and

MAR. 30 1979
DRAWING F24760
CASE NO. 34-0

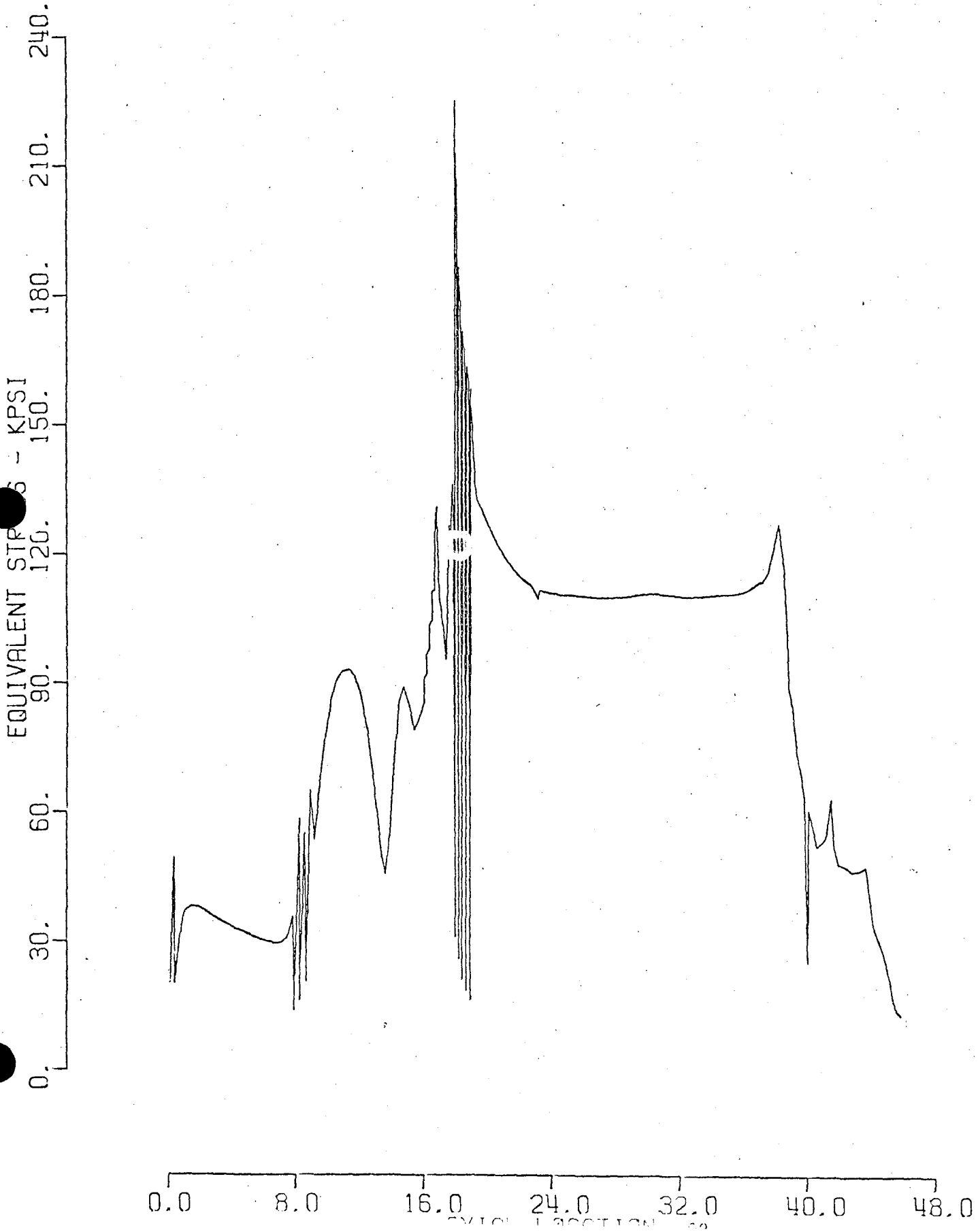

MAR. 30 1979
DRAWING F24760
CASE NO. 34-0

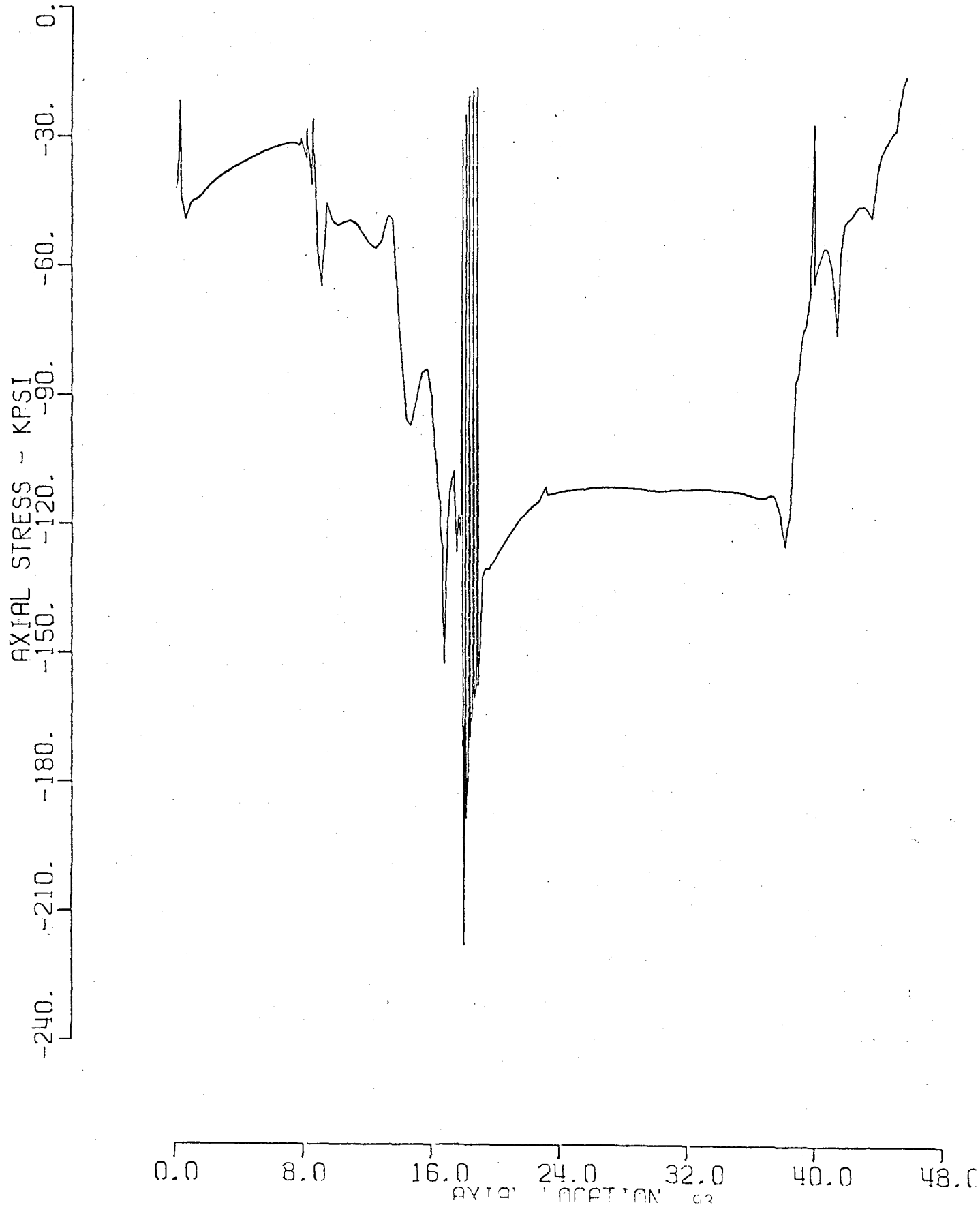

Figure 30. BIN-135MM CARGO SHELL HOD, 4
MAR. 30 1979
DRAWING F24760
CASE NO. 34-0

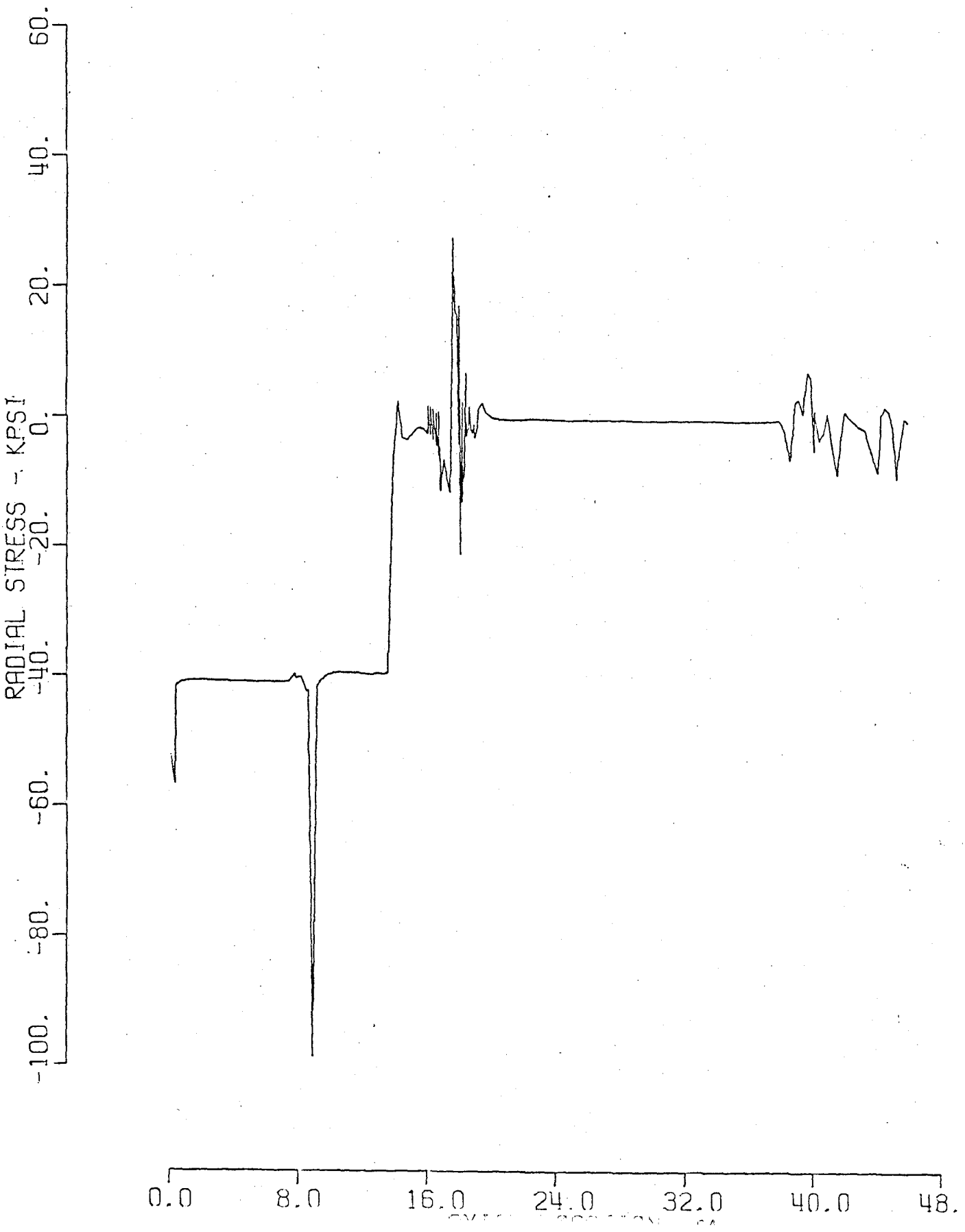

MAR. 30 1979
DRAWING F24760
CASE NO. 34-0

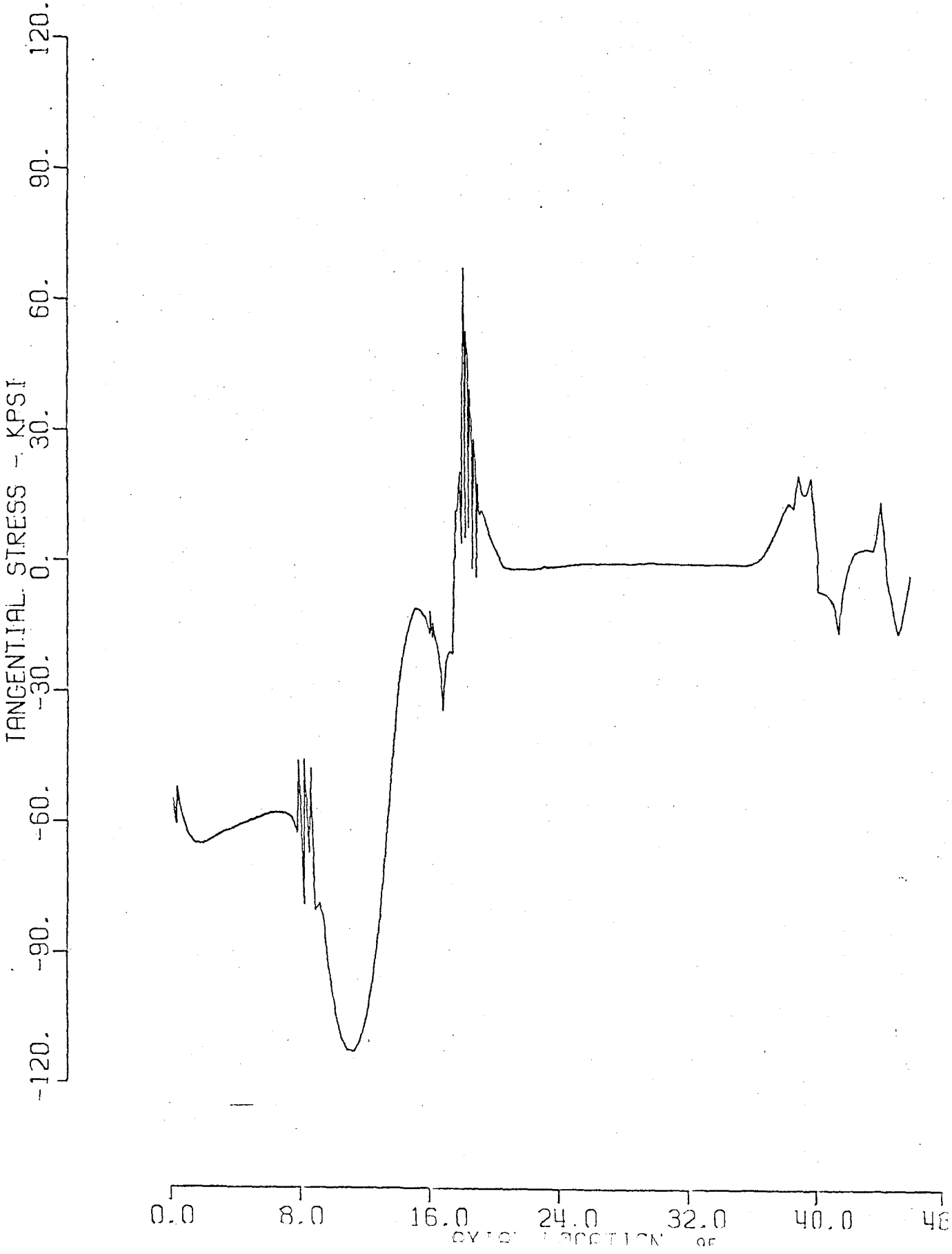

MAR. 30 1979
DRAWING
CASE NO.

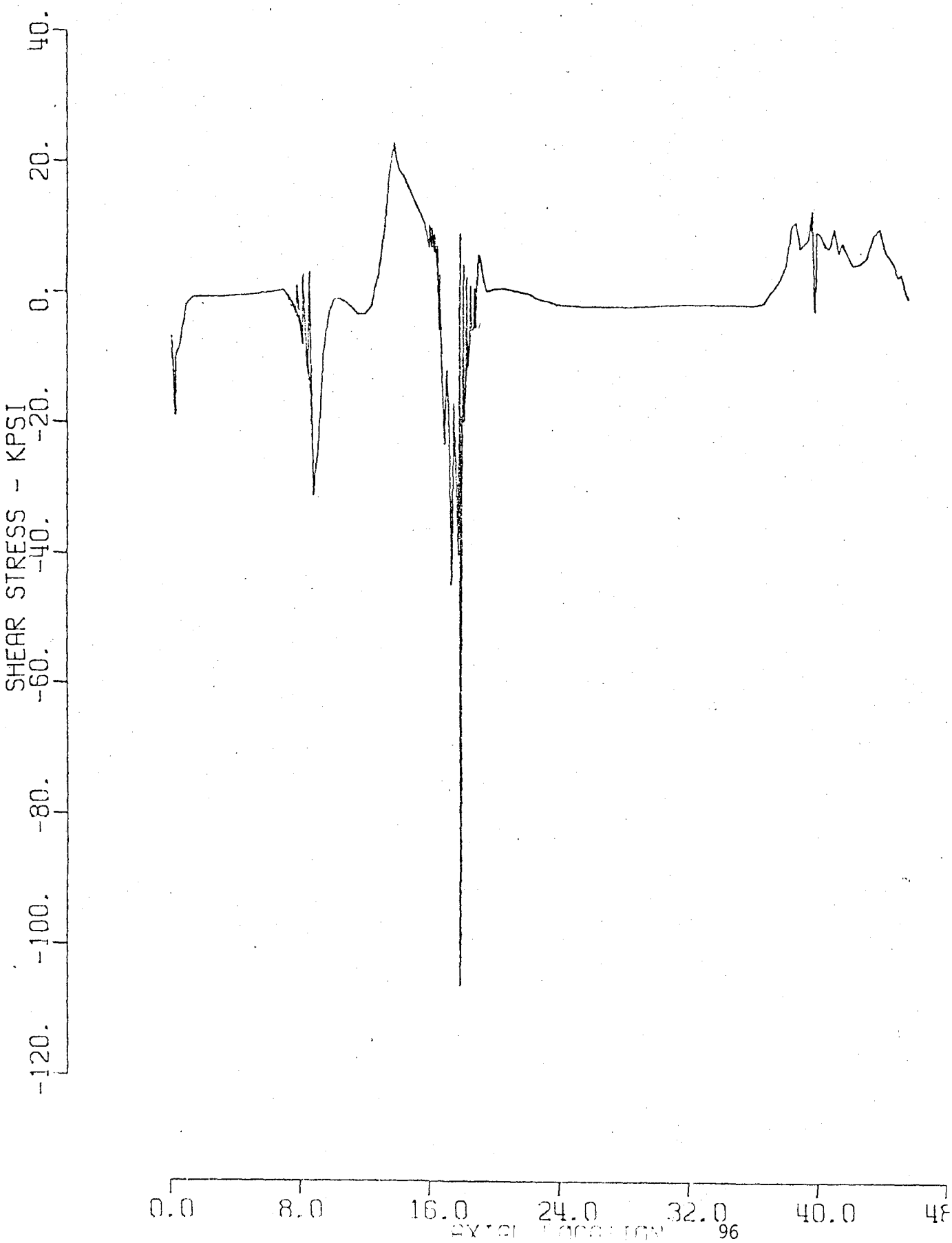

Figure 39. Equivalent Stress Contours (kpsi) of Section 1 resulting from a 50.4 kpsi Breech Pressure

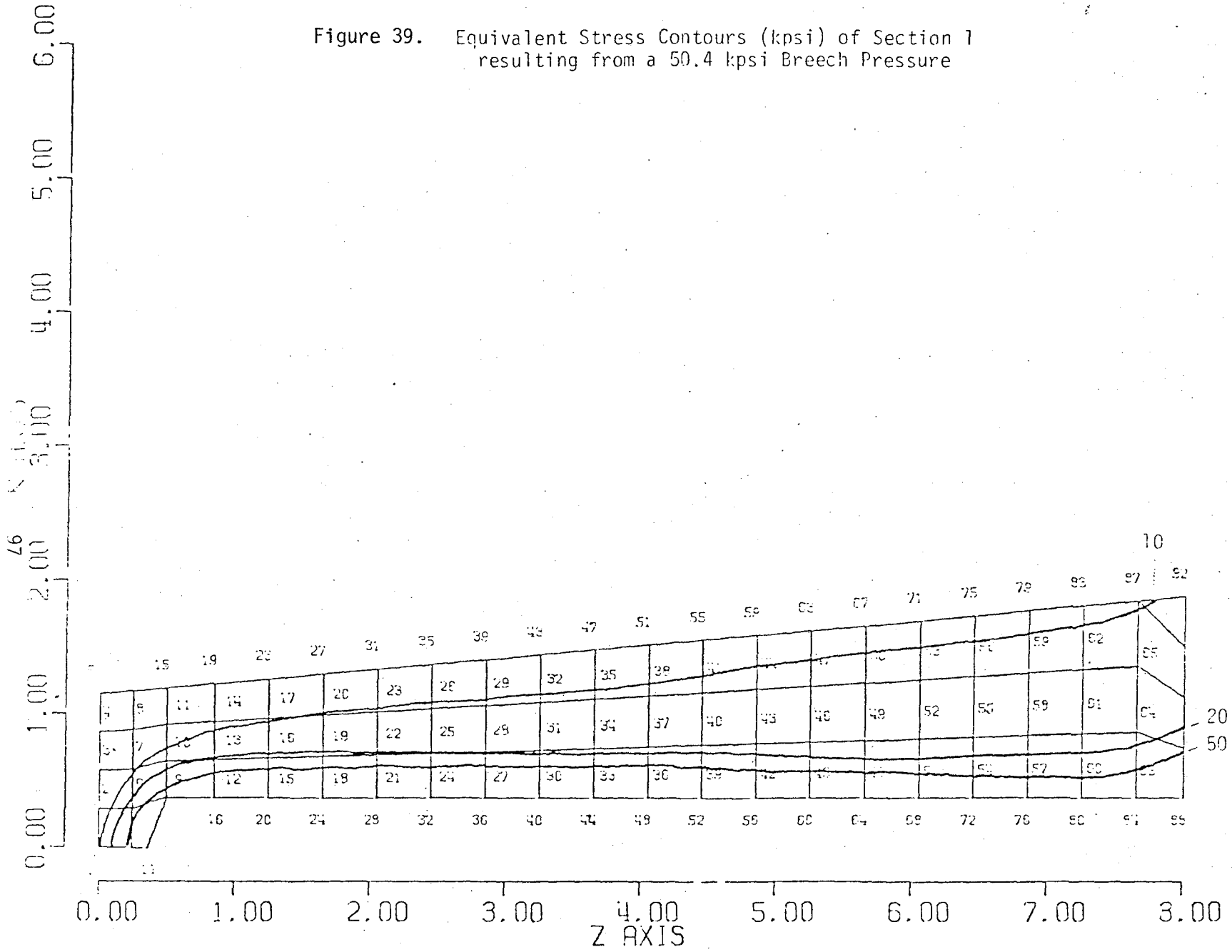

FEB. 26 1979 F211760
DRAWING
CASE NO. 314-0

Figure 40. Equivalent Stress Contours (kpsi) of Section 2 resulting from a 50.4 kpsi Breech Pressure

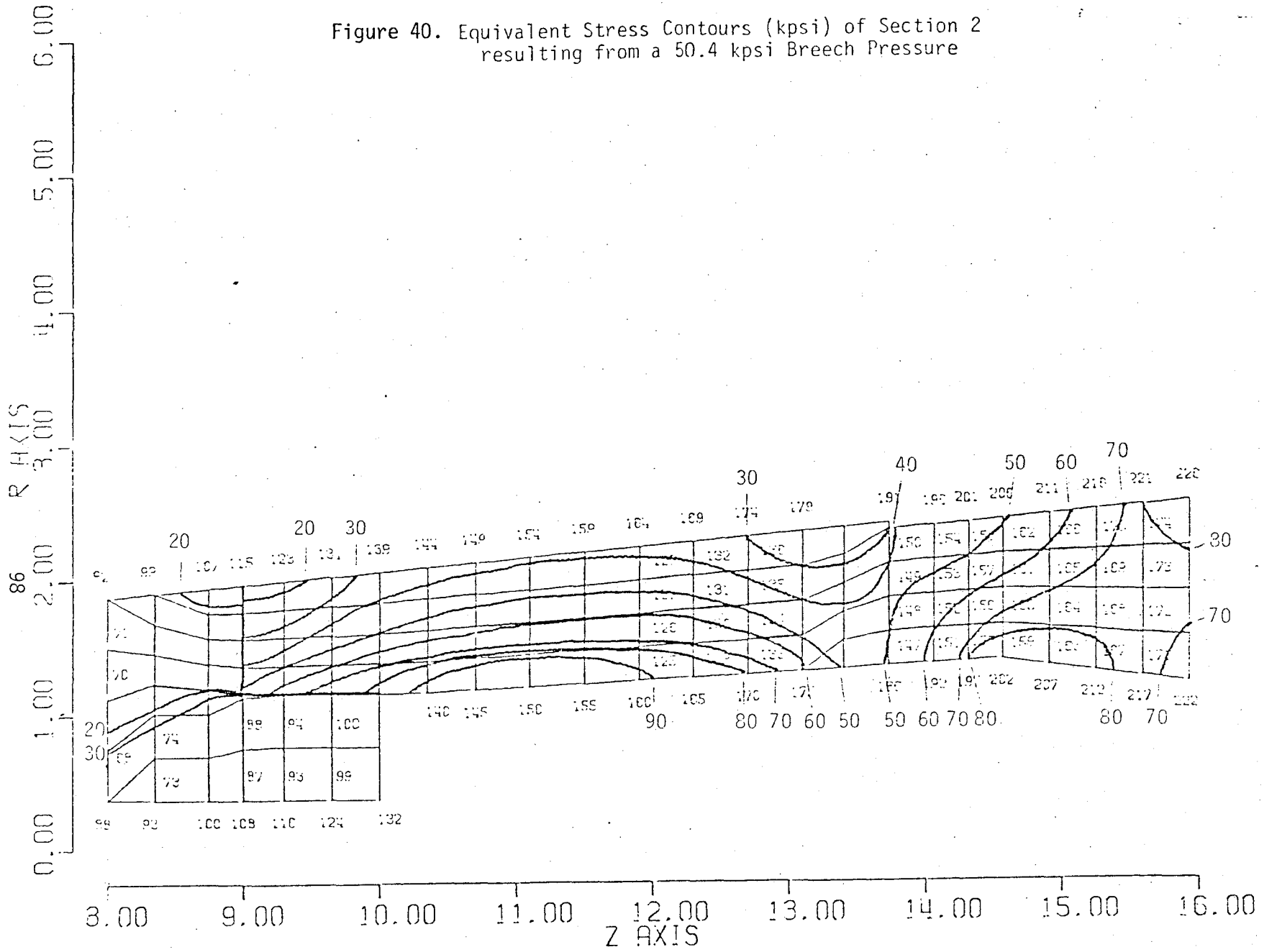

Figure 41. Equivalent Stress Contours (kpsi) of Section 3 resulting from a 50.4 kpsi Breech Pressure

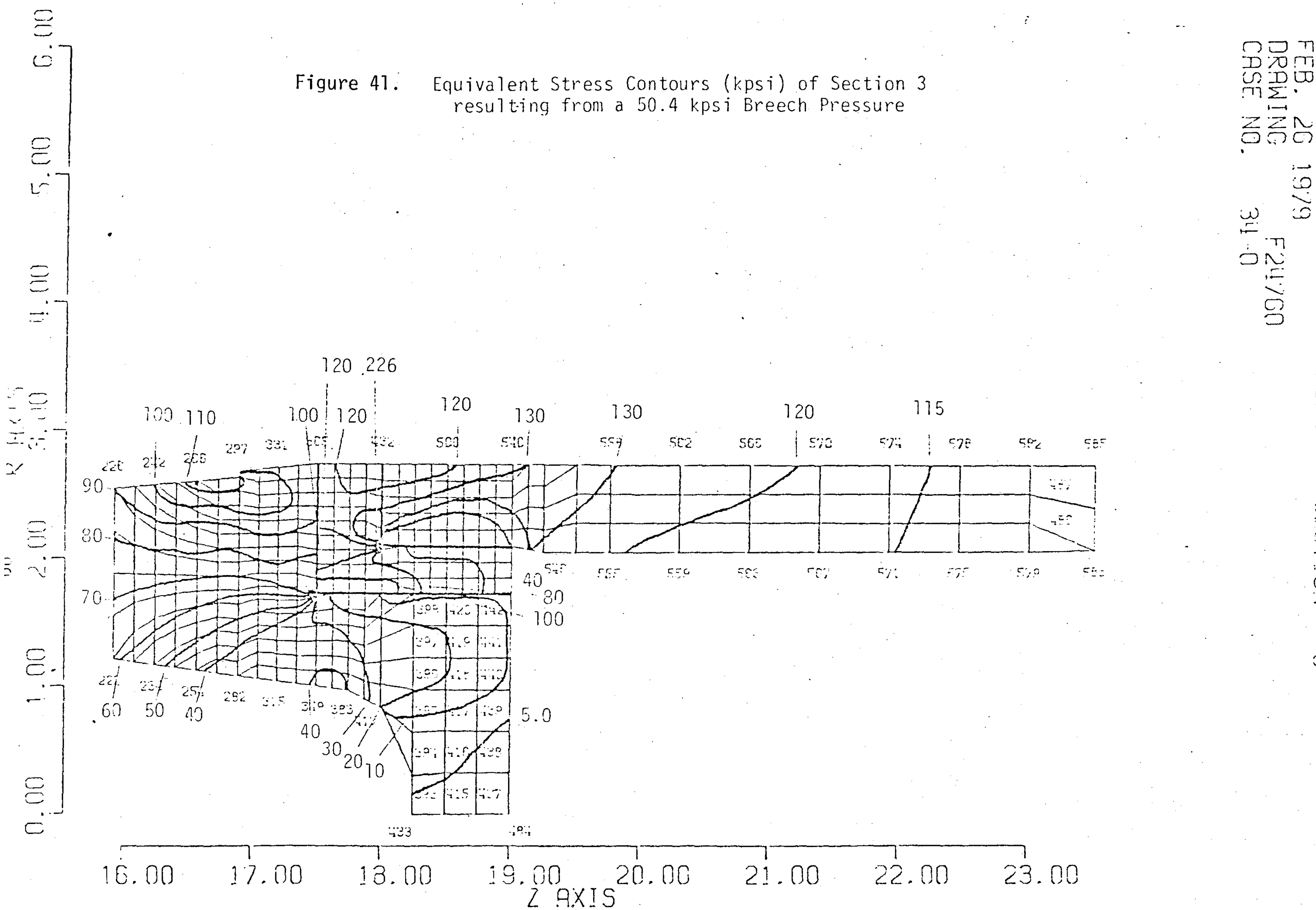

Figure 42. Equivalent Stress Contours (kpsi) of Section 4 resulting from a 50.4 kpsi Breech Pressure

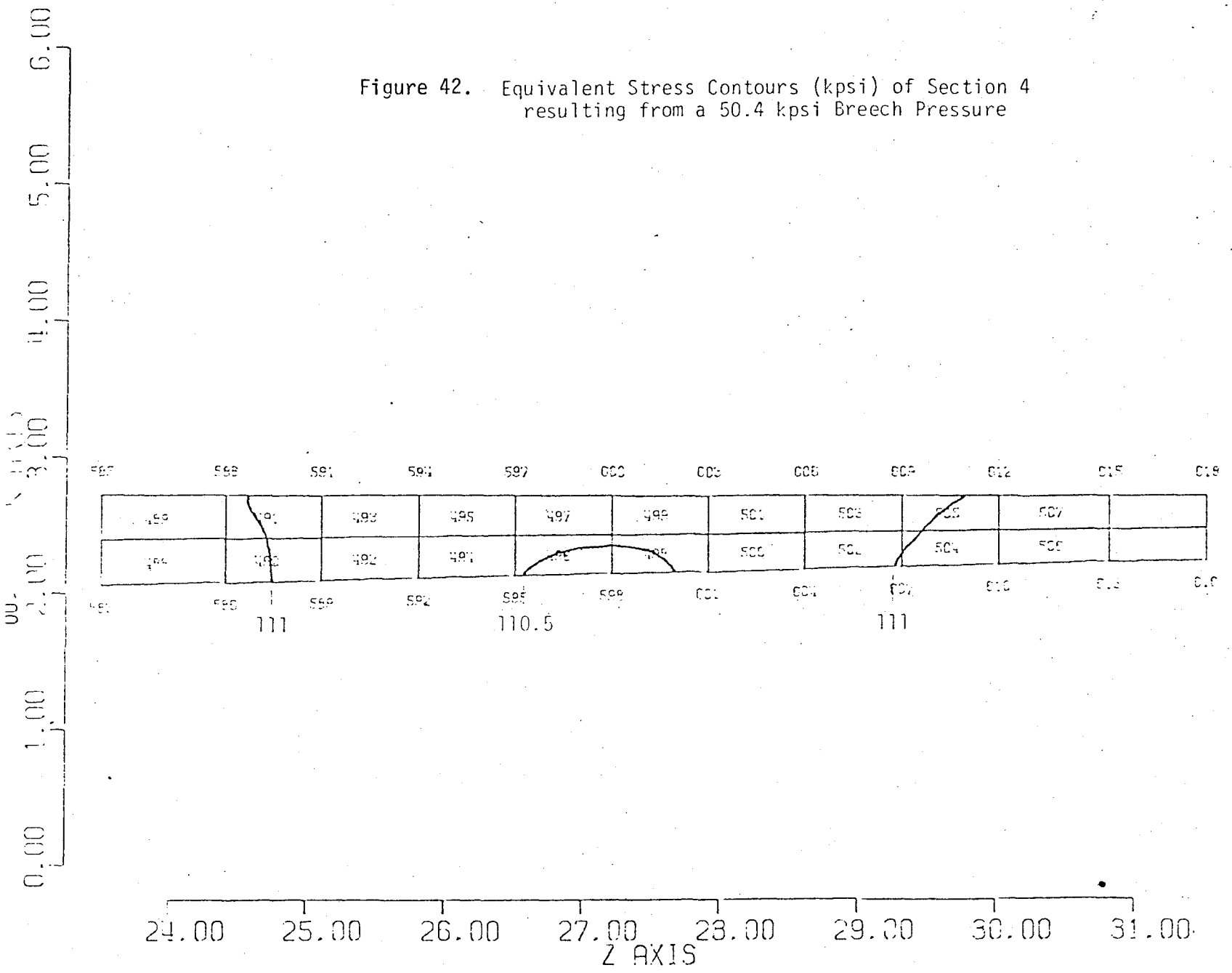

Figure 43. Equivalent Stress Contours (kpsi) of Section 5 resulting from a 50.4 kpsi Breech Pressure

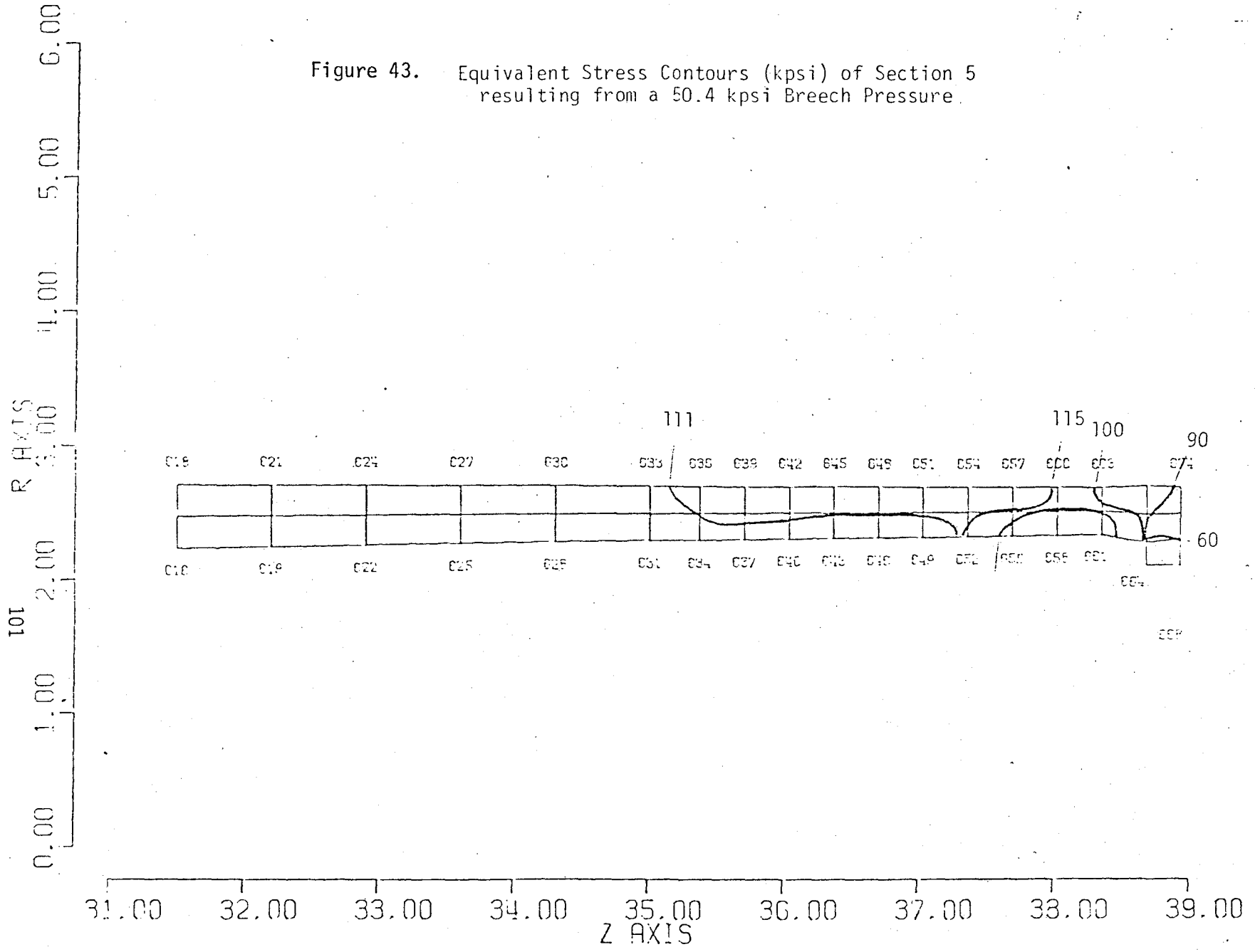

DRAWING F247/60
CASE NO. 34-0

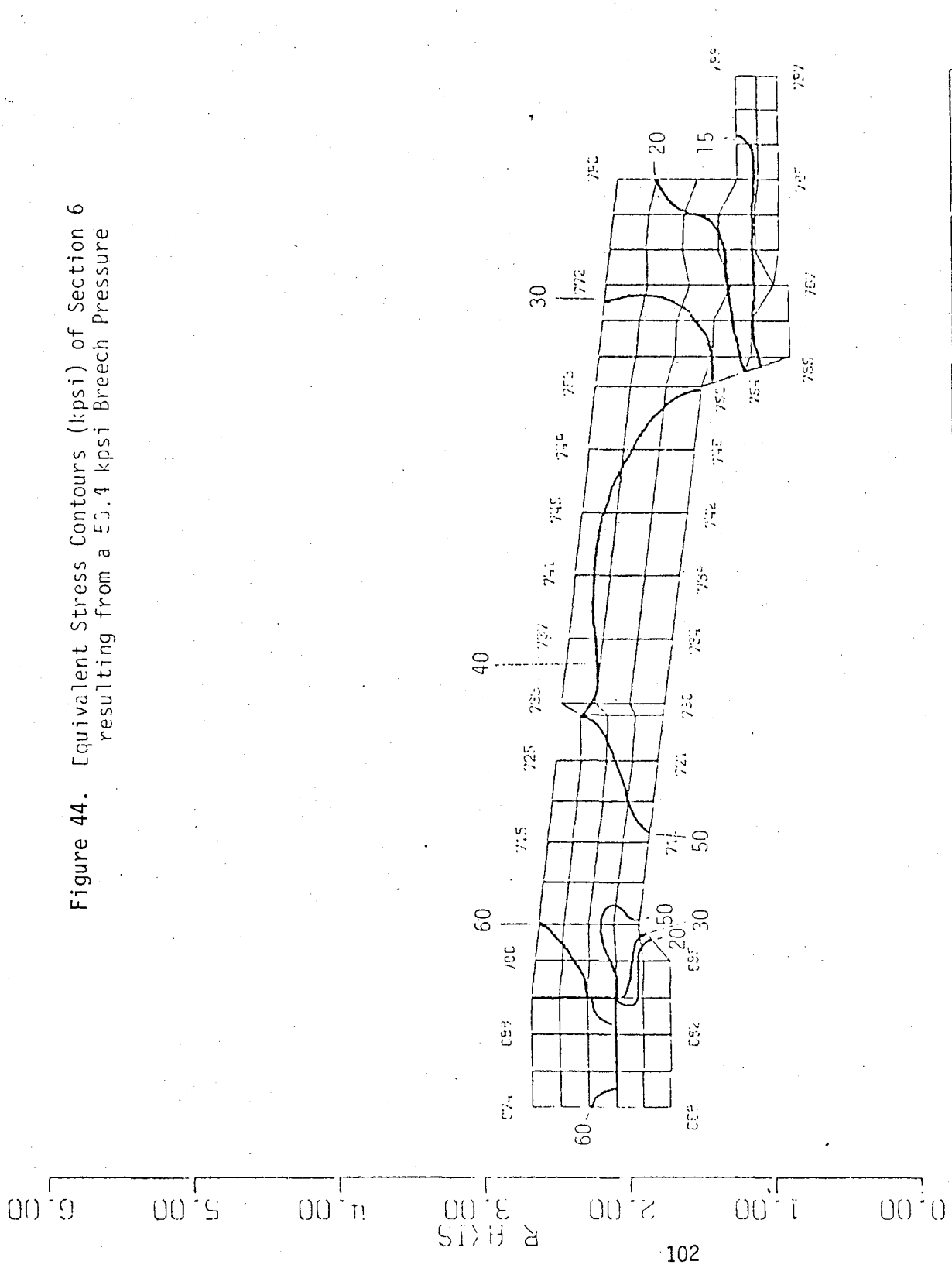

Figure 44. Equivalent Stress Contours (kpsi) of Section 6 resulting from a 55.4 kpsi Breech Pressure

the design has been confirmed through actual firings. It may be useful here to show a comparison of the level of bearing stresses upon this shoulder between the test vehicle design and the prototype design.

This shoulder provides a support foundation to the forward supported inertial loads of the body spacer, body wall, front sabot carrier, front sabot, fuze and windshield. The total mass of these components when multiplied by the maximum acceleration will give the maximum inertial load on the shoulder. The payload weight in both the test vehicle and the proposed design are not supported by this shoulder. This load when divided by the annular bearing area of the shoulder will give the maximum average bearing pressure on that bearing area. This is represented by the equation

$$\sigma_b = \frac{4W_f a}{\pi(Do^2-Di^2)}$$

where σ_b is the bearing pressure (psi), W_f is the forward supported weight (lbs.), a is the maximum acceleration (g), and Do and Di represent the outer and inner diameters of the annular area (in.).

Then from Table 6 the sum of the forward supported weights is 86.97 lbs. and from Table 7 the acceleration can be 15,290 g's. The test vehicle has a body spacer with outer and inner diameters of 5.478 and 3.50 inches respectively. The bearing pressure on the rear sabot carrier is then calculated to be 95,340 psi.

The proposed vehicle design has a body weight of 18.19 lbs. and uses a body spacer having a weight of 2.99 lbs. The body spacer threads onto the rear sabot carrier with a 4.25 inch thread and thus the annular bearing area of rear sabot carrier shoulder has an outer diameter of 5.478 inches and an inner diameter of 4.25 inches.

Making the appropriate substitutions into Table 6 the forward supported weight is found to be 54.31 lbs. At the same acceleration

the bearing pressure is found to be 88,500 psi. This essentially shows that the load upon the rear sabot carrier shoulder of the proposed design will be less than the load carried in the test vehicle design.

4.4 PROPELLING CHARGE REQUIREMENTS

An internal ballistic study was done to determine an optimized propelling charge for the 8-inch subcaliber fin stabilized cargo shell. Specifically, the objective of this study was to define an optimized propelling charge for this projectile (having a fixed aerodynamic shape), to maximize the range as the shot weight is allowed to vary. If the aerodynamic shape of the projectile is fixed then the external ballistic characteristics are constant even though the shot weight may vary. This means that under these conditions, the projectile range will be directly related to the attained muzzle velocity and for this reason comparisons will be made of muzzle velocities rather than ranges. In the solution of this problem certain conditions and constraints were imposed as follows to bound the possible solutions;

Conditions:
1) M110E2 Gun
2) M30A1 Multiperforated Propellant
3) Chamber Volume 2635 in^3.

Constraints:
1) Charge Weight $\leq$ 62 lbs.
2) Breech Pressure $\leq$ 40,000 psi
3) Muzzle Momentum $\leq$ 22,090 lb./sec.
4) 130 lb. $\leq$ shot weight $\leq$ 170 lb.

For each projectile shot weight there exists a unique propelling charge as defined by its charge weight and web size which will result in the highest possible muzzle velocity without exceeding the muzzle momentum limit. These solutions are obtained from the governing internal ballistic equations. Three constraints limit the number of possible solutions which are the maximum permissible charge weight, a breech pressure of 40,000 psi, and a specific range of projectile shot weights.

These internal ballistic solutions for several charge weights are graphed in Figure 3 (light solid curves).

By the internal ballistic solution alone the optimized propelling charge would consist of 62 pounds of propellant of the appropriate web size, but there is one additional constraint upon the solutions that must be considered. This is that the maximum allowable muzzle momentum (MM) is determined according to the equation.

$$MM = \frac{W_s V_o + 4700\ C_w}{g}$$

where W_s is the projectile shot weight, V_o is the muzzle velocity, C_w is the charge weight and g is the gravitational constant. Note that this equation is independent of the propellant web size.

The solutions to this equation are plotted (dashed curves) in Figure 45 for various charge weights where the muzzle momentum is set to the maximum allowable.

The locus of points formed by the intercept of the two sets of curves represents the upper limit on the velocity (i.e. range) potential when the governing internal ballistic equations and the muzzle momentum limit are simultaneously imposed.

Figure 46 indicates the resulting optimum propelling charge solution from Figure 45 as defined by the charge weight and web size for a projectile of varying shot weight.

Figure 45 shows that not until the shot weight is reduced to about 122.5 lbs. does the charge weight reach the constraint of the maximum allowable 62 lbs. Thus is is not possible to utilize the full ballistic potential of the gun due to the muzzle momentum limitation until the projectile shot weight is reduced to 122.5 lbs. or below. Figure 45 also shows that as the shot weight of the projectile decreases the muzzle velocity and hence the maximum range increases.

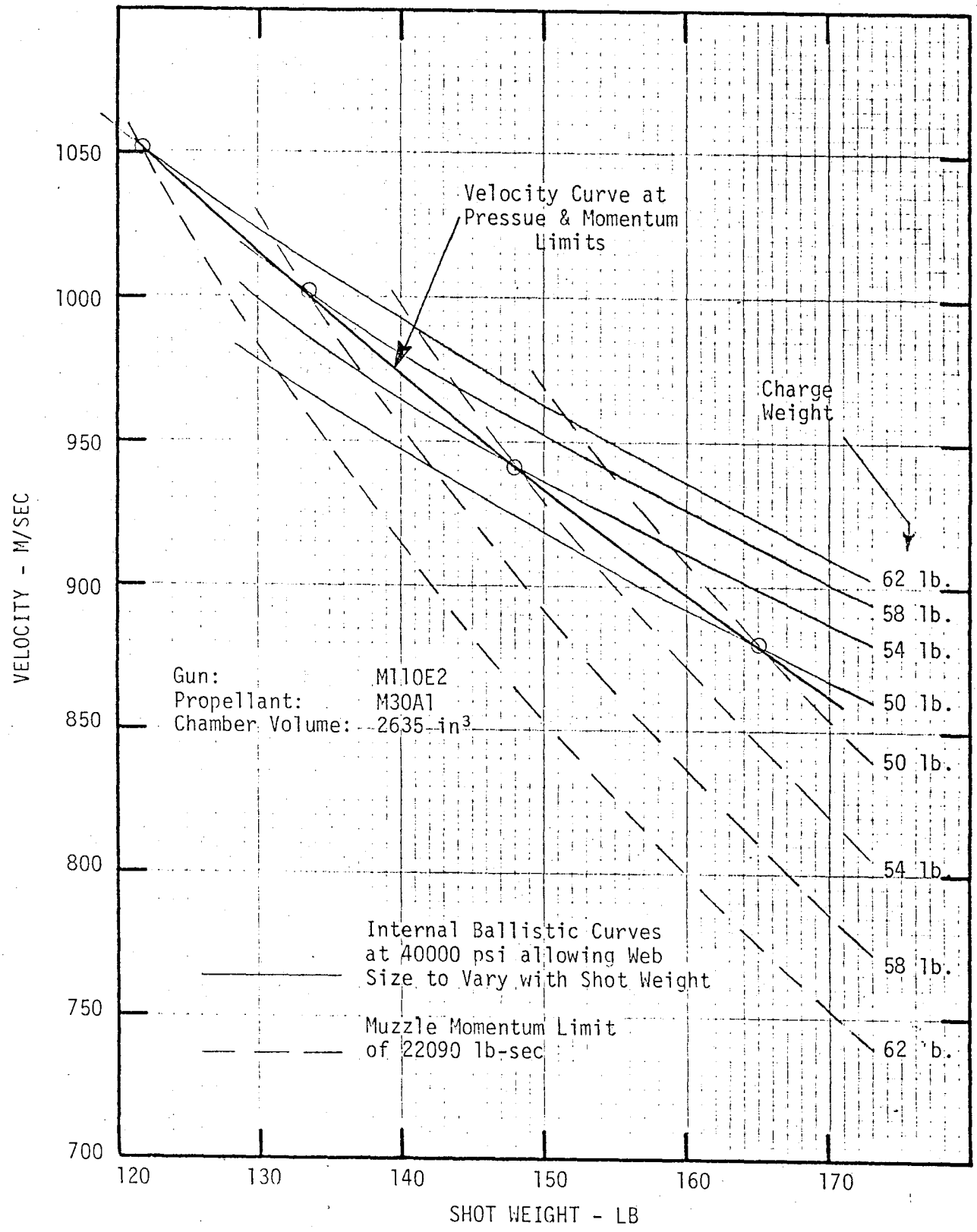

Figure 45. Velocity vs Shot Weight for Optimum Charge Determination

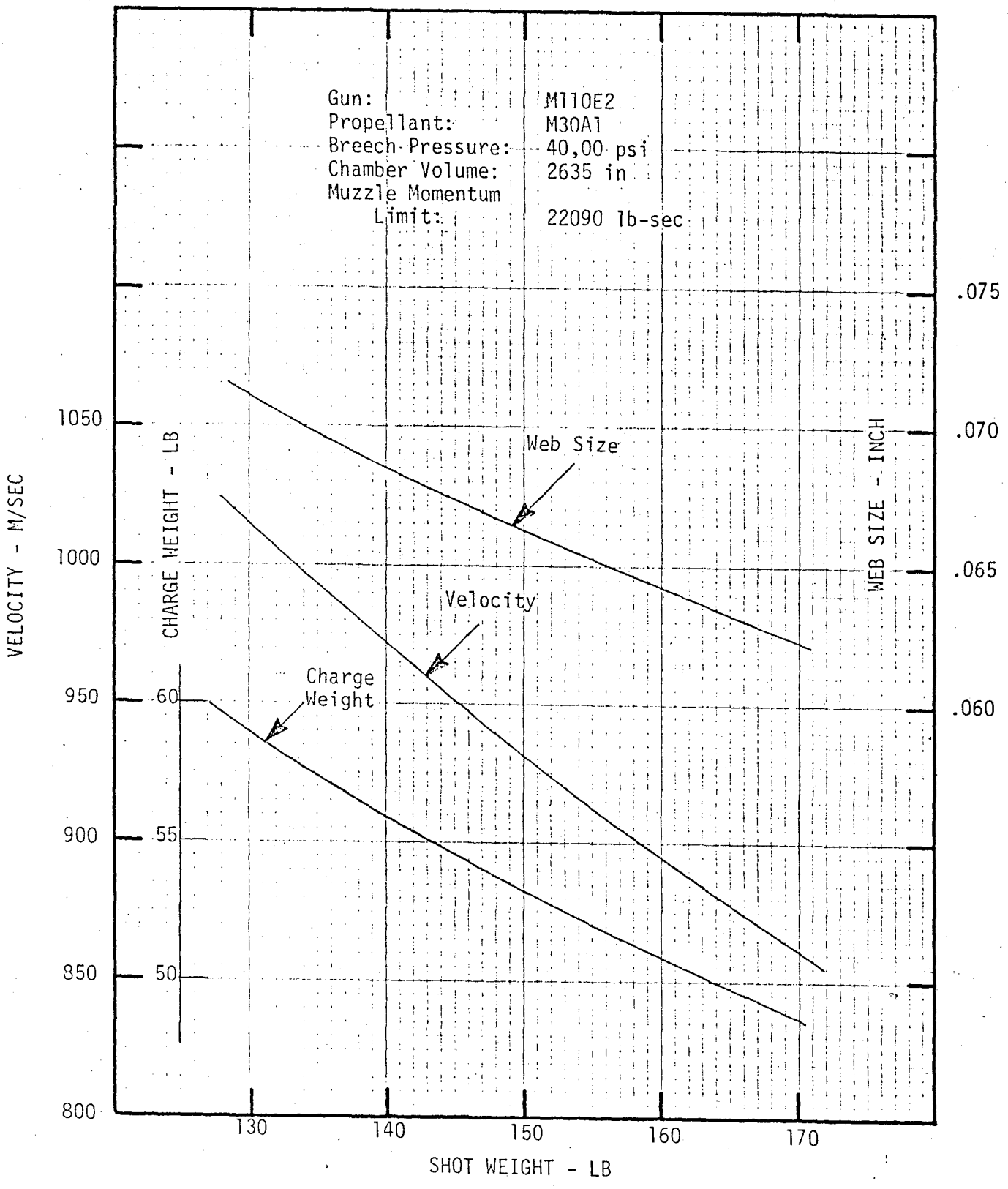

Figure 46. Optimum Charge Ballistic Solution for Charge Weight, Velocity, and Web Size

Figure 46 indicates that optimum web sizes lie between .074 and .063 for the range of projectile shot weights.

4.5 TEST PROPELLING CHARGE

In this contract a propelling charge design was not a requirement, however in order to accomplish the testing required, a propelling charge was designed solely for test purposes. An effort was made to obtain a supply of M30A1 multiperforated propellant with a web size close to the values specified in the previous section such as 0.078 inch which was being produced in great quantities for the 155mm XM203 propelling charge, but none could be had. Then because of the unavailability of a propellant of a closer web size and because of the immediate supply of a sufficient quantity of M30A1 MP propellant with a 0.085 inch web, an internal ballistic study similar to that of the previous section was conducted to study the prospects of its use in a test propelling charge.

The objective of this study then was to define a propelling charge for this projectile to maximize the muzzle velocity as the shot weight of the projectile was allowed to vary. Conditions and constraints imposed upon the solution of this problem were as follows:

Conditions:
1) M110E2 Gun
2) M30A1 .085 Web Multiperforated Propellant
3) Chamber Volume 2635 in^3.

Constraints:
1) Charge Weight $\leq$ 62 lbs.
2) Breech Pressure $\leq$ 40,000 psi
3) Muzzle Momentum $\leq$ 22,090 lb./sec.
4) 130 lb. $\leq$ Shot Weight $\leq$ 170 lb.

In this case a propelling charge was defined with respect to its charge weight which would give the highest possible muzzle velocity without exceeding the muzzle momentum limit. The internal ballistic solutions (solid curves) are plotted in Figure 47 for various charge weights. Here the propellant web size has been fixed and the breech

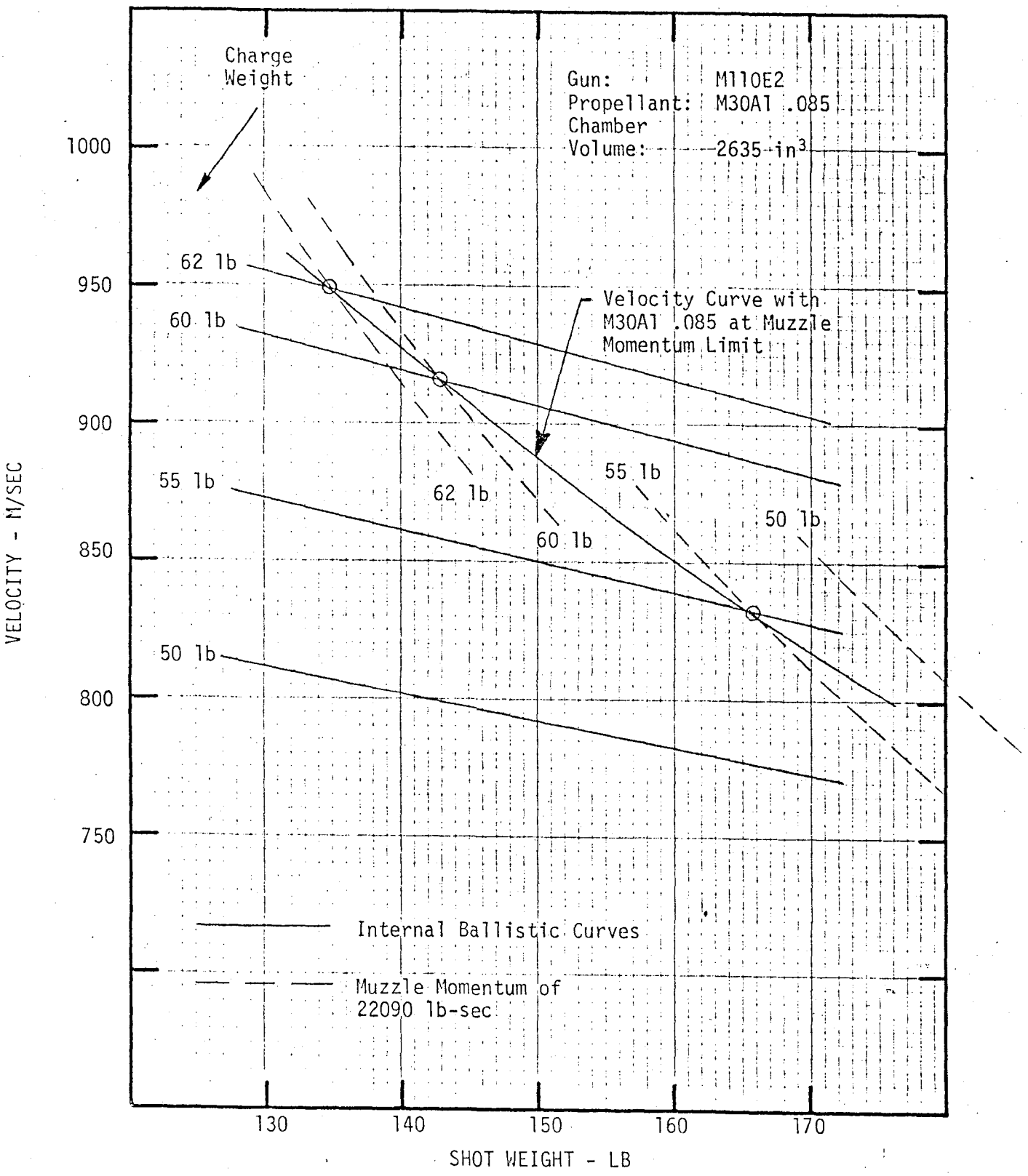

Figure 47. Velocity vs Shot Weight for Optimum Charge Determination of M30A1 .085 inch Web Propellant

pressure is the independent variable although it is limited to a maximum of 40,000 psi. The curves defining the maximum muzzle momentum for various charge weights (see previous section) are also plotted as dashed curves in Figure 47.

The locus of points formed by the interception of these curves describes the maximum attainable muzzle velocity for charges of various weights of the 0.085 inch web propellant as the projectile shot weight varies.

Figure 48 defines the propelling charge with respect to charge weight and the expected breech pressure for a projectile of various shot weights.

From Figure 47 it is determined that for a projectile with a shot weight of 135 lbs., the highest possible muzzle velocity attainable without exceeding the muzzle momentum limit is achieved with a charge of 62 lbs. of propellant. Figure 48 also shows that the breech pressures are lower than the full potential of the gun.

This study verifed the test charge design described in Section 3.3 which resulted from the Internal Ballistic tests of the test slugs.

4.6 STABILITY AND PERFORMANCE ANALYSIS

An aerodynamic stability and performance analysis was conducted for the 8-inch subcaliber projectile. The results of this analysis applies to both the proposed design and the test vehicle design. The analysis was based upon the following projectile configuration;

1) Forebody : 3/4 power law body of 3.341 calibers length of 17.75 inches and a diameter that varies from 0.4 to 5.48 inches.

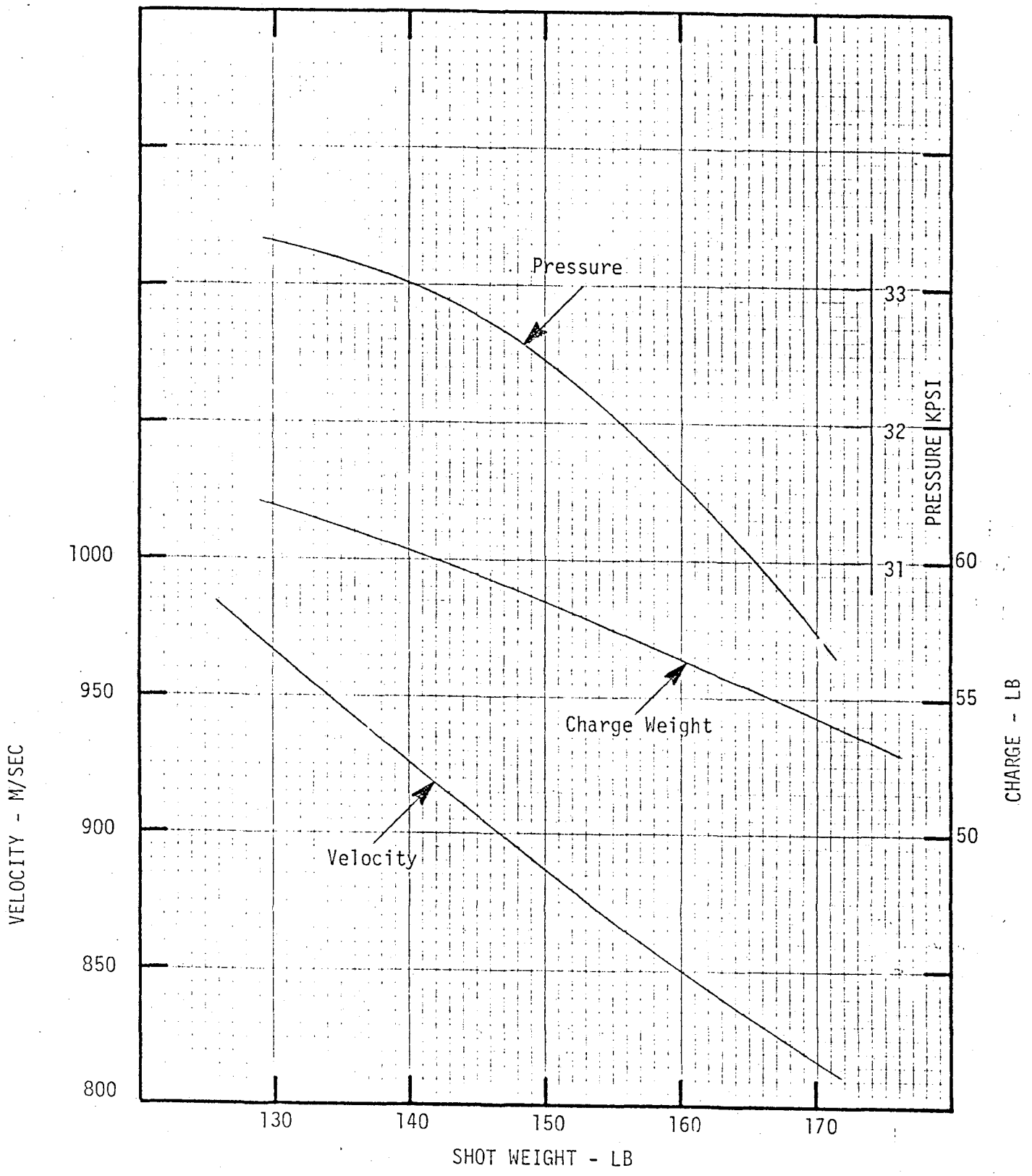

Figure 48. Optimum Charge Ballistic Solution for M30A1 .085 Web Propellant

2) Body : Cylindrical
length 22.17 inches having a reference diameter of 5.48 inches.

3) Afterbody : Boattail of angle 5.19°
length of 17.50 inches with a diameter that varies between 5.48 to 2.30 inches.

4) Stabilizer : 6 fins at the base of the boattail
root chord length (C_r) is 9.0 inches
tip chord length (C_t) is 4.5 inches
Total span (b) is 7.9 inches.

5) Shell Dimensions : Length (L) = 57.42 inches, diameter (D) = 5.48 inches.

The fineness ratio of the forebody affects both the static margin (i.e., the distance between the center of pressure, X'_{cp}, and the center of gravity, X_{cg}) and the drag, C_{D_o}. A calculation was made for two forebody length of 3.341 calibers, as specified in the projectile description above, and 4.5 calibers. The increase in fineness ratio, 4D, from 3.341 calibers to 4.5 calibers represents a change in the actual length of the forebody from 17.75 inches to 23.91 inches and a corresponding reduction of the cylindrical body.

Based upon these two configurations the stability and zero lift drag (C_{D_o}) calculations give the results of Table 8. These results were obtained using the 2nd-order shock expansion method for the forebody (with afterbody effect) and the Royal Aeronautical Society "Data Sheets", as well as the U.S. Stability and Control DATCOM for the boattail with the stabilizer.

These results show not only the aerodynamic properties for the vehicle configuration of the proposed vehicle and test vehicle designs but also show that the center of pressure moves backward by about 2.5 inches, with the stabilizing movement increasing by roughly 50 percent,

TABLE 8

	FOREBODY LENGTH (CALIBER)	MACH NUMBER			
		1.5	2.0	2.5	3.0
C_{N_α}	3.341 4.5	4.746 4.626	4.984 4.828	5.024 4.849	4.951 4.766
X'_{CP} [1]	3.341 4.5	25.3 22.9	25.7 23.1	25.7 23.1	26.1 23.5
C_{D_o}	3.341 4.5	0.315 0.279	0.261 0.230	0.233 0.195	0.195 0.168
$C_{M_{\alpha_{cg}}}$	3.341 4.5	22.31 32.84	21.43 33.31	21.60 33.46	19.31 30.98

[1] X'_{CP} is measured in inches from the projectile base

whereas the drag has been reduced by approximately 11 to 14 percent, in the case of an increase of the forebody length by 6.16 inches but keeping the same vehicle overall length of 57.42 inches.

This change is not possible, however in the present configuration because of the already thin wall at the front of the body without altering the payload configuration.

Calculations have been made to check the optimum size of the fins. Assuming a ration of tip chord to root chord (C_t:C_r) of 0.5, the tip chord has been varied from 2 to 7 inches over the range of Mach 1.5 to 3.0. The location of the center of pressure (X'_{cp}) for the shell indicates an optimum fin configuration is obtained for tip chords between 4 and 5 inches in length.

Similarly a reduction of the boattail length with total body length and base diameter unchanged does not improve stability or performance.

In conclusion, with regard to this study, the present configuration with a 3/4 power law forebody of 17.75 inches gives a center of pressure position of 25 to 26 inches from the projectile base for Mach numbers over the range of 1.5 to 3.0. It has been determined that the present fin configuration (having a tip chord length of 4.5 inches and a root chord length of 9.0 inches) and boattail configuration represent an optimum regarding stability. Also it has been determined that a possibility exists to reduce the drag by about 11 to 14 percent if the payload configuration could be altered, but this has not been pursued here.

4.7 STABILIZER DESIGN

This 8-inch subcaliber projectile makes use of a stabilizer composed of six fins machined from one-half inch thick 6061 Aluminum plate and welded to a 6061 Aluminum fin boom.

In welding the fins to the boom, the weld area is abrasively cleaned with a stainless steel wire brush and the assembly is then preheated to a temperature no greater than 300 degress Fahrenheit. The fin assembly is secured in a fixture to maintain the position of the fins and TIG welded using an inert gas shield composed of 75 percent Helium and 25 percent Argon at an efflux rate of 30 to 40 cubic feet perminute. A two percent thoriated 1/8 inch diameter tungsten electrode is used to apply 200 to 220 amps of current. A 3/32 inch diameter 5356 aluminum weld rod is used, applying very slowly to allow a well developed puddle. The temperature of the mid section of the fin is not allowed to exceed 400 degrees Fahrenheit so as not to reduce the aluminum temper below the T4 condition.

In finned projectile designs, ranging from a simple arrow to large rockets, it is most often advantageous to have some amount of inherent spin in its trajectory to average out any asymetrics it may have and so reduce their affect upon the trajectory. Thus it is so in this case, but there is one additional consideration to be made as the specific rate of spin to be chosen.

In the internal ballistic regime of its trajectory, the motion of a projectile with regard to its spin is unaffected by its fins except for the inertial loads they cause. Thus the initial rate of spin of the projectile is for the most part independent of fin design. The fins begin to do work only after the projectile has entered the external ballistic regime of its trajectory. It is at this time that the fins will begin to show their effect upon the projectile spin rate. If a fin design causes the projectile spin rate to change either faster or slower it does so because it has generated lift. In any wing or fin design when there is lift there is drag. So the best approach to reduce the drag of the fins is design them in such a way that they conform to the spin of the projectile and have a minimum effect upon the projectile spin as it exits the gun tube.

The fins in this design have a zero-lift aerodynamic shape, and are canted with respect to the longitudinal shell axis to conform to the projectile spin rate upon muzzle exit. This angular offset has been calculated from the following equation which relates the angular offset to the equilibrium roll rate:

$$\alpha = \frac{360}{12} \frac{rP}{V_o} \quad \text{degrees}$$

Here, the radial distance to the fins aerodynamic center (r), is equated to 2.60 inches, the radial distance to the fins geometric center because of its zero-lift profile. The equilibrium spin rate (P) has been measured as 20 rps and the muzzle velocity can be represented as 3200 fps. The angular offset is then calculated to be approximately 0.5 degrees. At this offset angle to the projectile axis the zero-lift fin should have an angle of attach of zero to the free airstream and cause no lift generated drag.

4.8 8-INCH SUBCALIBER TEST VEHICLE DESIGN TESTS AND RESULTS

4.8.1 INTRODUCTION

Previous testing chiefly concerned the development of a sabot design using an internal ballistically representation blunt-nosed test slug. Although the test bed function of the test slug was again called upon during the final fin structural tests, the structural testing here was accomplished with the test vehicle, an aerodynamically shaped structural representation of the proposed cargo shell design. The terms test slug and test vehicle are not used interchangeably.

Throughout much of the testing of the test vehicle design that follows, test objectives were consolidated rather than isolated as in the sabot development test phase. This consolidation was an inherent feature to the overall goal of testing the test vehicle, wholly like the proposed design. The objectives of this test phase were;

1) Measurement of pertinent vehicle characteristics

2) Structural testing of the test vehicle design

3) Structural testing and development of a fin design

4) Testing of sabot separation performance with regard to interaction with the muzzle brake and fins

5) Testing of general design changes and innovations

Because of the continuous interdependency of the test objectives, the presentation of the test results of this phase of testing will be to present a complete compilation of the tests and make reference to that compilation, along with pointing out additional highlights, how each of the test objectives were satisfied. This will give a better organized presentation than a chronologically oriented study as was possible in the sabot development test phase. A complete tabulation of the conditions and the results of all tests conducted within the premise of the above objectives is presented in Table 9.

As indicated in Table 9 seven different fin designs were tested. To aid in the presentation of the reaults associated with the testing of these designs, each is referred to with a design letter identification as shown in Table 10. This table also tabulated a basic description of each fin type.

4.8.2 TEST INSTRUMENTATION & MEASUREMENTS

To examine how the first objective, the measurement of pertinent vehicle characteristics, was achieved it will be necessary to explain the general test set-up and instrumentation.

The tests were conducted using an 8-inch M110E2 self-propelled howitzer (fitted with an XM201 tube, Serial Number 8). Of all tests three muzzle fixtures were used; a thrust collar Dwg. WTV-F26789 here

TABLE 9. COMPONENT DEVELOPMENT TEST RESULTS SUMMARY

SHOT NO.	DATE	PROPELLANT				PROJECTILE				RAM (in)	MUZZLE FIXTURE	RECOIL (in)	BREECH PRESSURE (kpsi)	MUZZLE VELOCITY (fps)	SPIN RATE (rps)
		Type	Web Size (in)	Lot	Weight (lbs)	Type	Mod	Weight (lbs)	Fin Type						
505	7/78	M30A1	.085	KAU 7/76	35.0	M106	-	195.8	-	45 1/4	ring	-	25.9	-	-
506	7/78	M30A1	.085	KAU 7/76	35.0	M106	-	194.3	-	45 1/4	ring	62 1/4	26.0	2233	-
507	7/78	M30A1	.085	KAU 7/76	62.0	T.V.#5	2	135.0	A	51	dummy	62 3/4	41.0	3287	17.5
508	7/78	M30A1	.085	KAU 7/76	62.0	T.V.#6	2	135.0	A	51	standard	62 1/2	39.3	3266	19.5
509	9/78	M30A1	.085	KAU 7/76	35.0	M106	-	196.0	-	45 3/8	standard	61 1/2	25.2	-	-
510	9/78	M30A1	.085	KAU 7/76	62.0	T.V.#2	2/3	134.5	B	51	standard	69	36.2	3204	23.4
511	10/78	M30A1	.091	KAU 8/76	36.0	M106	-	198.5	-	45 1/8	standard	64	21.9	-	-
512	10/78	M30A1	.085	KAU 7/76	62.0	T.V.#4	2/3	134.5	C	51 1/16	standard	67	50.7	3394[1]	-
513	10/78	M30A1	.085	KAU 7/76	55.0	T.V.#1	3	137.4	D	51	dummy	68 1/4	28.4	2905	17.7
514	10/78	M30A1	.091	KAU 8/76	36.0	M106	-	195.0	-	45 1/4	dummy	64 3/4	22.7	-	-
517	1/79	M30A1	.091	KAU 8/76	36.0	M106	-	200.5	-	45	standard	63 1/4	22.6	-	-
518	1/79	M30A1	.091	KAU 8/76	36.0	M106	-	199.8	-	45	standard	62 1/2	20.9	-	-
519	1/79	M30A1	.085	KAU 7/76	58.0	T.V.#3A	3	132.6	D	51	standard	67 1/2	36.7	3216	31.0
520	1/79	M30A1	.091	KAU 8/76	36.0	M106	-	200.3	-	45	standard	61 1/2	20.3	-	-
521	1/79	M30A1	.085	KAU 7/76	58.0	T.V.#4A	3	132.4	C	51	standard	67 1/2	39.2	3239	24.4
522	2/79	M30A1	.091	KAU 8/76	36.0	M106	-	199.5	-	45	standard	62 3/4	22.5	-	-
523	2/79	M30A1	.091	KAU 8/76	36.0	M106	-	200.0	-	45 1/3	standard	63 1/2	22.1	-	-
524	2/79	M30A1	.085	KAU 7/76	58.0	T.V.#13A	4	131.0	None	51	standard	67	43.5	3198	-
525	2/79	M30A1	.091	KAU 8/76	36.0	M106	-	199.8	-	45 3/8	standard	63 3/4	24.1	-	-
526	2/79	M30A1	.085	KAU 7/76	58.0	T.V.#14A	4	131.5	None	51	standard	67	32.7	3136	35.7
527	3/79	NQM	.044	CAD 7135	20.5	M106	-	199.8	-	45 1/2	ring	51 1/2	23.1	-	-
528	3/79	NQM	.044	CAD 7135	25.0	M106	-	200.0	-	45	ring	58 1/2	31.9	-	-
529	3/79	NQM	.044	CAD 7135	29.0	M106	-	199.8	-	45 1/2	ring	58 1/2	41.7	-	-
530	3/79	NQM	.044	CAD 7135	44.0	T.V.#3	2/3	134.0	B	51	ring	56 1/2	29.3	2174	-
531	3/79	NQM	.044	CAD 7135	20.5	M106	-	199.8	-	45 1/4	standard	49 1/2	23.9	-	-
532	3/79	NQM	.044	CAD 7135	49.0	T.S.#1	-	132.1	None	51	standard	61 1/2	50.8	3190	-
533	3/79	NQM	.044	CAD 7135	45.5	T.S.#2	-	135.5	F	51	standard	61 1/2	44.3	3003	-
534	3/79	NQM	.044	CAD 7135	45.0	T.S.#3	-	135.4	F	51 1/8	standard	60 1/2	44.0	2958	-
535	3/79	NQM	.044	CAD 7135	20.5	M106	-	200.3	-	45 1/8	standard	49 1/4	23.5	-	-
536	3/79	NQM	.044	CAD 7135	45.0	T.S.#4	-	134.5	E	51	standard	60 1/2	43.7	2974	-
537	3/79	NQM	.044	CAD 7135	45.0	T.S.#5	-	134.6	E	51	standard	58 1/2	40.1	2870	-
538	3/79	NQM	.044	CAD 7135	45.0	T.V.#11A	4	135.0	G	51	standard	60	42.9	2968	-
539	5/79	M30A1	.091	KAU 8/76	36.0	M106	-	199.9	-	45 1/8	standard	62	23.1	-	-
540	5/79	M30A1	.085	KAU 7/76	36.0	M106	-	199.8	-	45 1/8	standard	64	28.2	-	-
541	5/79	M30A1	.085	RAD-E-7	36.0	M106	-	199.8	-	45	standard	63 1/4	24.7	-	-
542	5/79	M30A1	.085	RAD-E-7	58.0	T.V.#8A	4	134.5	F	51	standard	66 1/4	32.0	3096	19.1
543	5/79	M30A1	.085	RAD-E-7	60.0	T.V.#9A	4	134.6	F	51	standard	66 1/2	33.3	3138	14.5
544	5/79	M30A1	.085	KAU 7/76 RAD-E-7	49.8 8.2	T.V.#10A	4	134.8	F	51	standard	65	35.3	3158	16.5

TABLE 10. FIN DESIGN DESIGNATION

DESIGN	DRAWING	LEADING EDGE		FIN TIP THICKNESS	FIN ROOT THICKNESS
		ANGLE	THICKNESS		
A	B24701	0°	0.250"	0.250"	0.250"
B	D24735	2° 45'	0.024"	0.147"	0.250"
C	D24755	4°	0.075"	0.250"	0.250"
D	D24756	3° 30'	0.065"	0.200"	0.250"
E	D24761	4°	0.075"	0.250"	0.250"
F	D24762	6° 8'	0.075"	0.350"	0.400"
G	D24763	8°	0.075"	0.450"	0.500"

called muzzle ring, a dummy muzzle brake (described previously) and what will be referred to as the "standard" muzzle brake, supplied by Watervliet Arsenal (Dwg. WTV-F26323).

In all cases the breech pressure was measured with three M11 copper crusher gages and the test vehicle's muzzle exit condition was recorded by three smear cameras, located 15, 30, and 50 feet down the gun line from the muzzle.

The film from the smear cameras was used to supply the following information:

1) Muzzle Velocity
2) Vehicle Spin Rate
3) Structural Integrity
4) Sabot Discard Performance

The results of the first test vehicle structural test (Shots 506 to 508) will be presented here to aid in the discussion of how the test measurements were derived from the instrumentation results. Figure 49 to 51 show the smear camera results for Shot Numbers 506, 507, and 508.

The muzzle velocity (V_o) was determined from the smear film to an accuracy generally of ±15 feet per second by the equation

$$V_o = \frac{L}{\ell} V_{fm}$$

where L is the actual vehicle length, ℓ is the vehicle film image length and V_{fm} is the film speed. A doppler radar was used during the first test in an attempt to accurately measure the muzzle velocity. A linear regression analysis of the resulting data showed high standard errors when compared with the velocity measurement of an M106 shell, as presented in Table 11. Because of these high standard errors, the velocity measurements were not accepted as representative of the test vehicle and its use was discontinued. The cause for these poor results was the inability

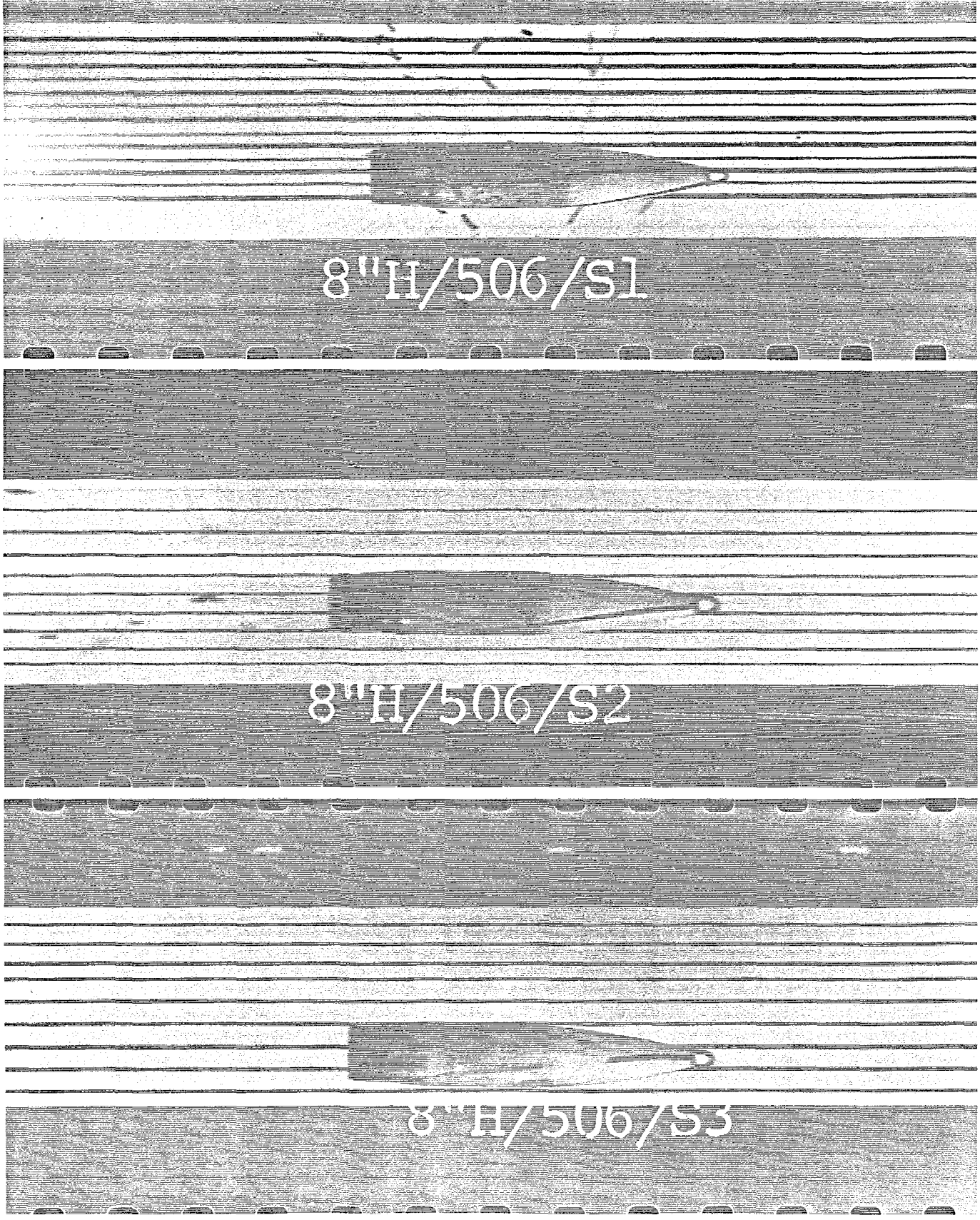

Figure 49. M106 Warming Round Smear Photos for Shot 506

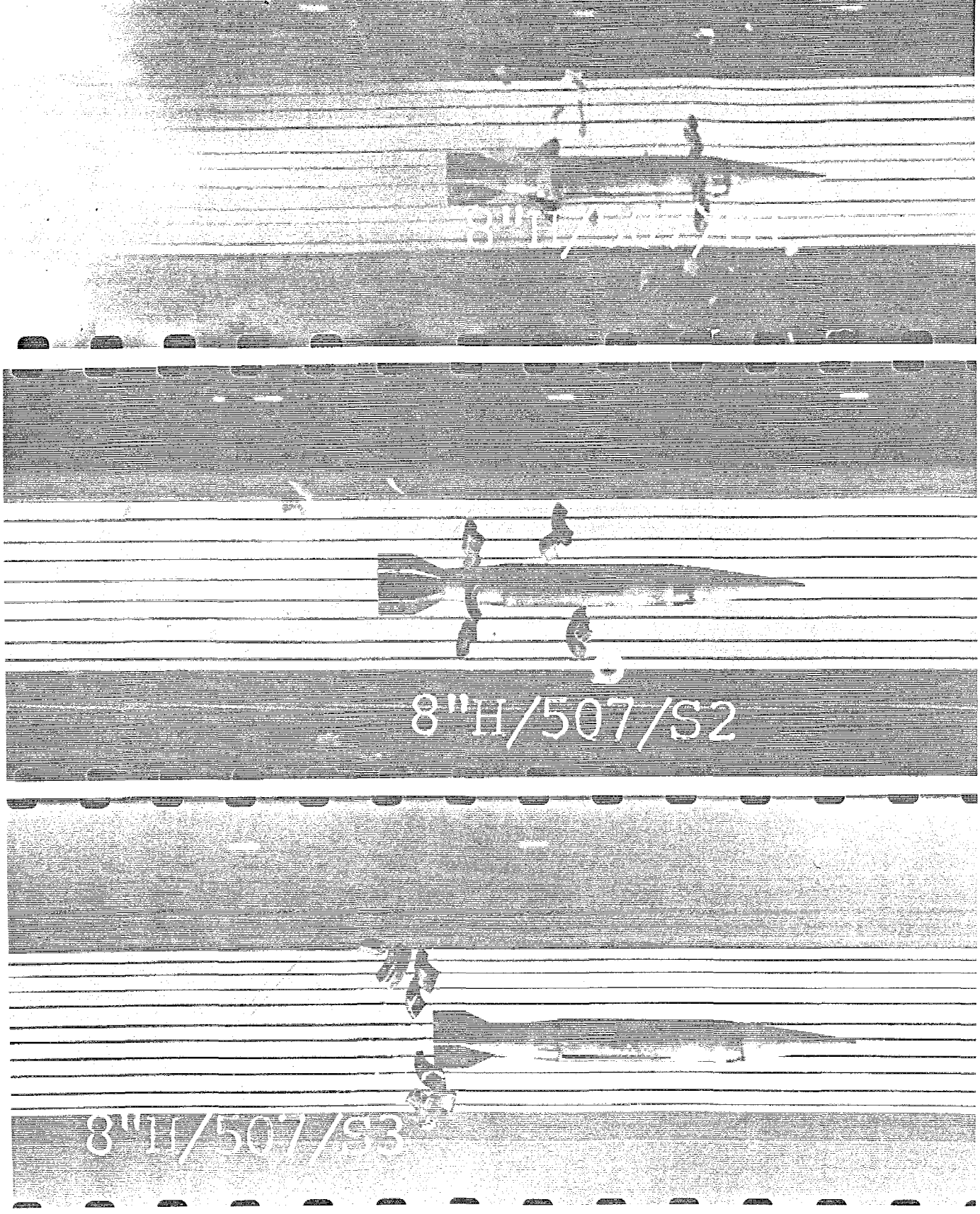

Figure 50. Test Vehicle Shot No. 507 Smear Photo Sequence

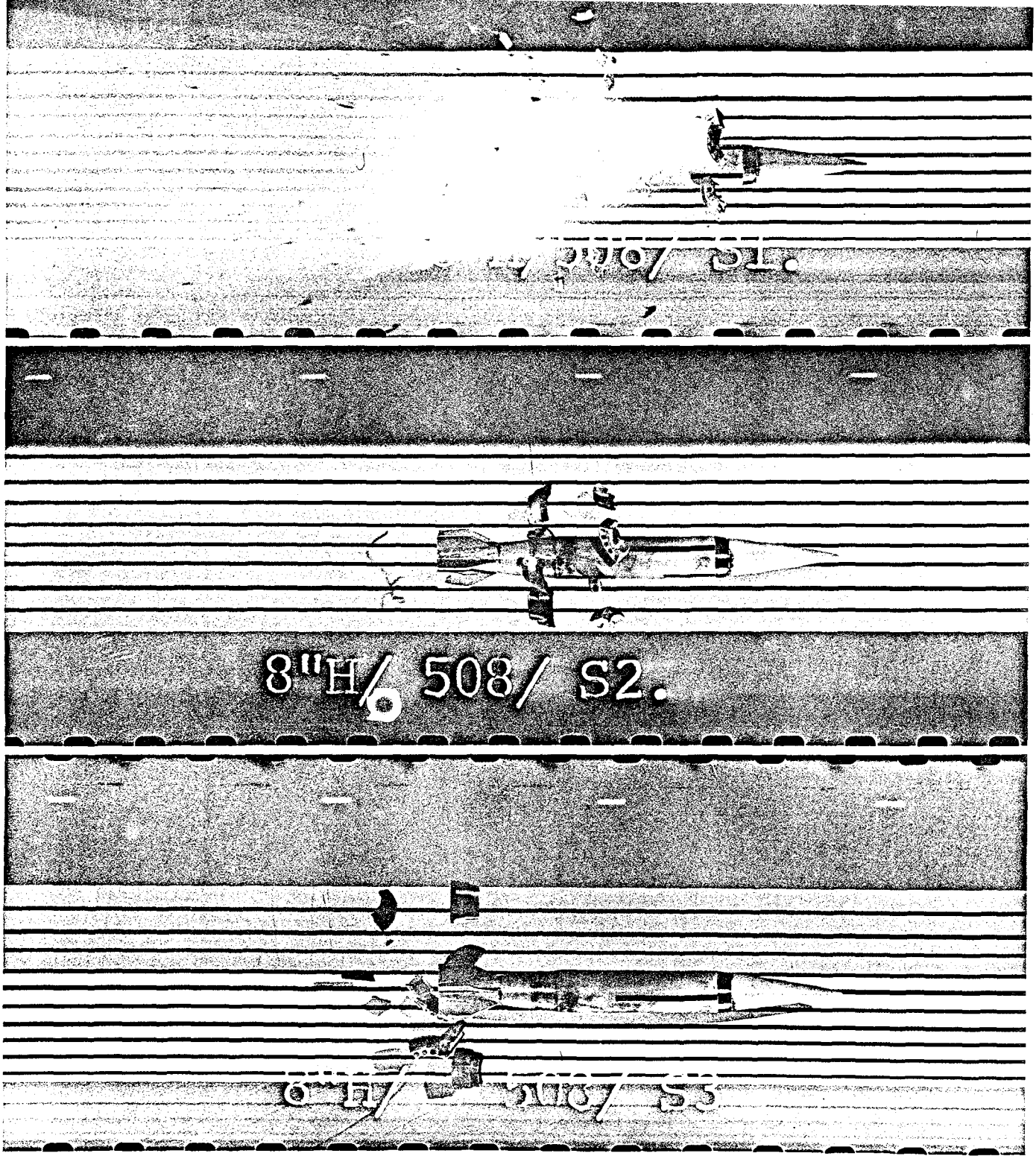

Figure 51. Test Vehicle Shot No. 508 Smear Photo Sequence

TABLE 11. COMPARISON OF MUZZLE VELOCITY MEASUREMENT DATA

		DOPPLER DATA		SMEAR PHOTO DATA		
Shot No.	Projectile	Muzzle Velocity fps	Standard Error fps	S1 fps	S2 fps	S3 fps
506	M106	2233	0.29	2263	2250	2240
507	Test Vehicle	2932	175.	-	3286	3288
508	Test Vehicle	2754	158.	3265	3269	3265

of the doppler radar to distinguish the test vehicle from the "cloud" of decelerating sabot petals.

Test vehicles were painted with a sequence of unique stripes on the body exterior as shown in the smear photos. Together, with these stripes and the averaged velocity results, obtained from the smear camera films, the spin rate ($\dot{\theta}$) was determined from the equation

$$\dot{\theta} = \Delta\theta \frac{V}{d}$$

where $\Delta\theta$ represents the number of revolutions over the interval of distance d for which V represents the average velocity.

The smear film also presented valuable photographic evidence of the structural conditions of the shell and its components as well as the motion of the discarding sabot petals relative to the fins. For instance in Figures 50 and 51 the discarding of the sabot petals is very regular and clean without disturbing the projectile or interfering with the fins. Close examination of Figure 50 shows no structural impairment of the components as a result of the gun launch. Upon examination of Figure 51, however, two structural deficiencies can be seen. First a guilding metal bore rider, swaged to the front sabot petals has separated from a front sabot petal shown in the third smear photo as a dark rectangular shape about one-half inch behind the fins. Second, again in the third smear camera photograph the horizontal fin is shown to be slightly bent.

The guilding metal front bore riders were used in a majority of the tests but were later replaced by a hard coat anodized surface applied to the front sabot petal.

Also, the bent fin of test vehicle number 6 (Shot No. 508) was shown to exist upon loading the vehicle into the breech by Figure 52. The vehicle can be identified by the number 6 marked on the shell and located in the photograph just to the right of the witness mark. Figure 52 also gives a view of the "A" design fins used in this test.

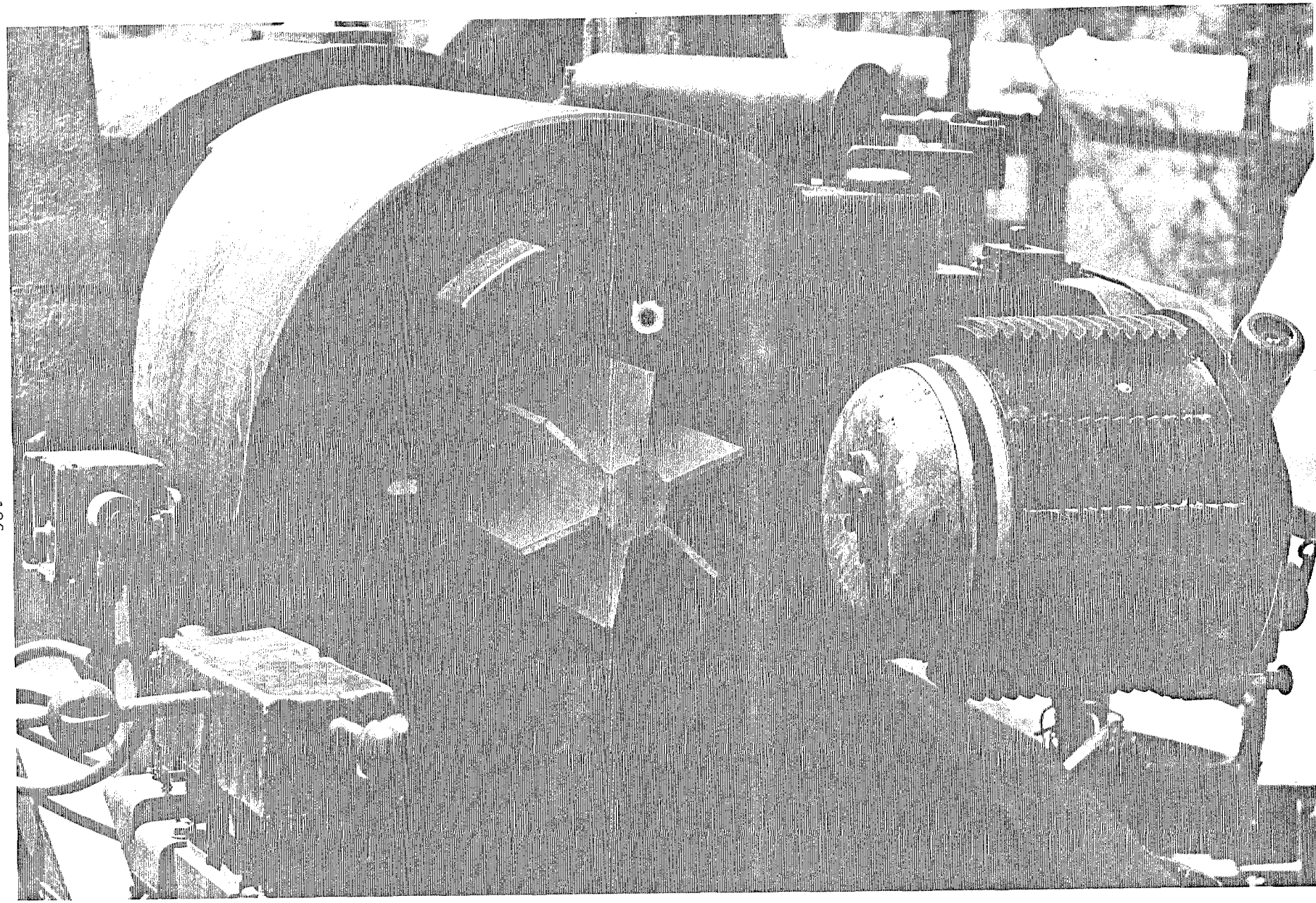

Figure 52. Photo of Test Vehicle No. 6 in Breech

Thus it was found through the photographic data collected that this test was structurally successful.

A high speed framing camera was used to record the muzzle gas efflux sequence relative to the moment of vehicle muzzle exit as an indication of the quality of propellant gas obturation. Again supplying the results of this first structural test, Figure 53 and 54 show the framing camera photographs of Shots 506, 507, and 508. A sign of good obturation is that the nose of the projectile is seen to exit the muzzle before an efflux of gas. Figure 53 shows the obturation performance of a M106 (Shot 506), where is is seen that a small amount of gas efflux occurs before the projectile's nose is visible. Using the obturation quality of the M106 as a standard, the quality of obturation of the test vehicles, shown in Figure 54, is very good. The results of Shots 507 and 508 show the vehicle nose exits the muzzle ahead of the gas efflux. The dummy muzzle brake is shown in place for Shot 507 and for 508 the standard muzzle brake is seen.

The dummy muzzle brake, described earlier, was used to avoid any unnecessary damage to the standard muzzle brake during sabot development. Likewise, it was also used during this phase of testing at any time that it was felt sabot-muzzle brake strikes may occur. But because the gas dynamics and thus the pressure distribution differ altogether between the dummy and standard muzzle brakes, as shown in Figure 54, it was unavoidable that the sabot performance needed to be qualified with the standard muzzle brake. The smear photographs give a strong indication that no sabot-muzzle brake impacts occurred. This, however was confirmed here, as in all tests, by an examination of the muzzle brake after each shot.

The breech pressure measurements, as mentioned earlier were measured with three M11 copper crusher gages, and ram distance and recoil distance were measured for all shots and are recorded in Table 9. The shot weights of all vehicles were also measured and are given in Table 9.

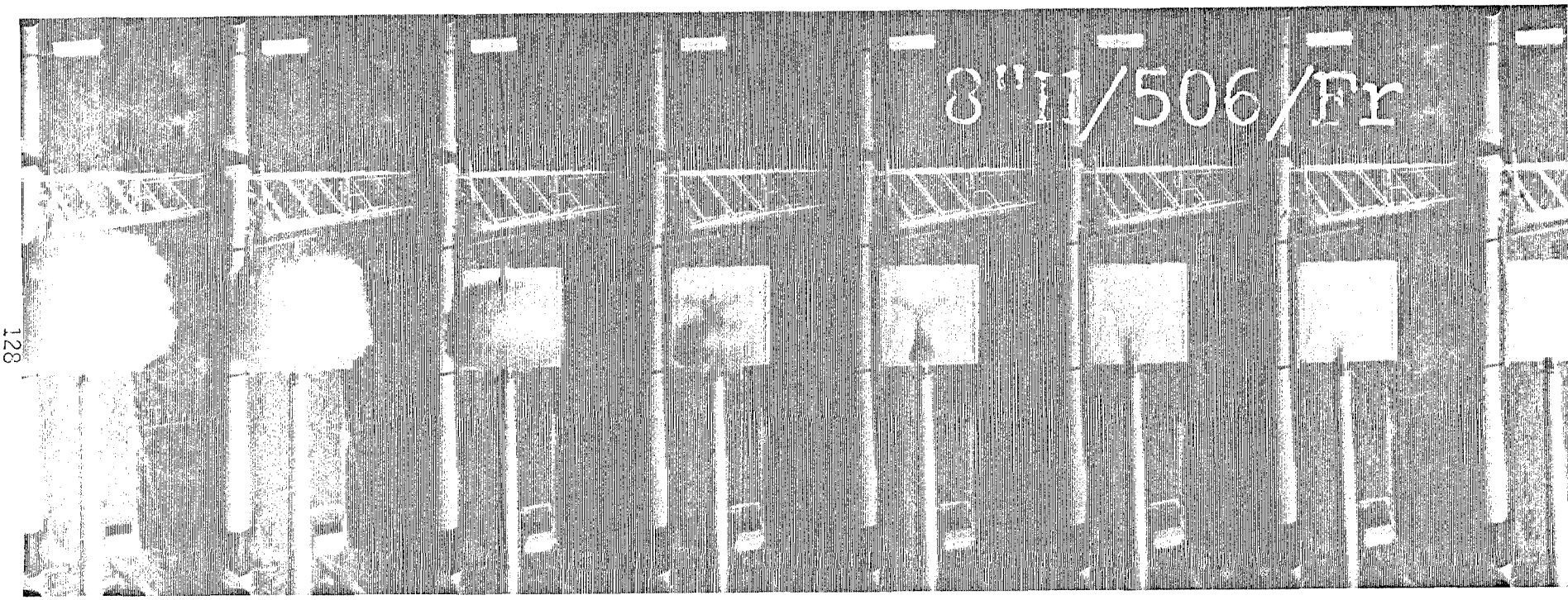

Figure 53. M106 Warming Round Framing Camera Film of Shot No. 506

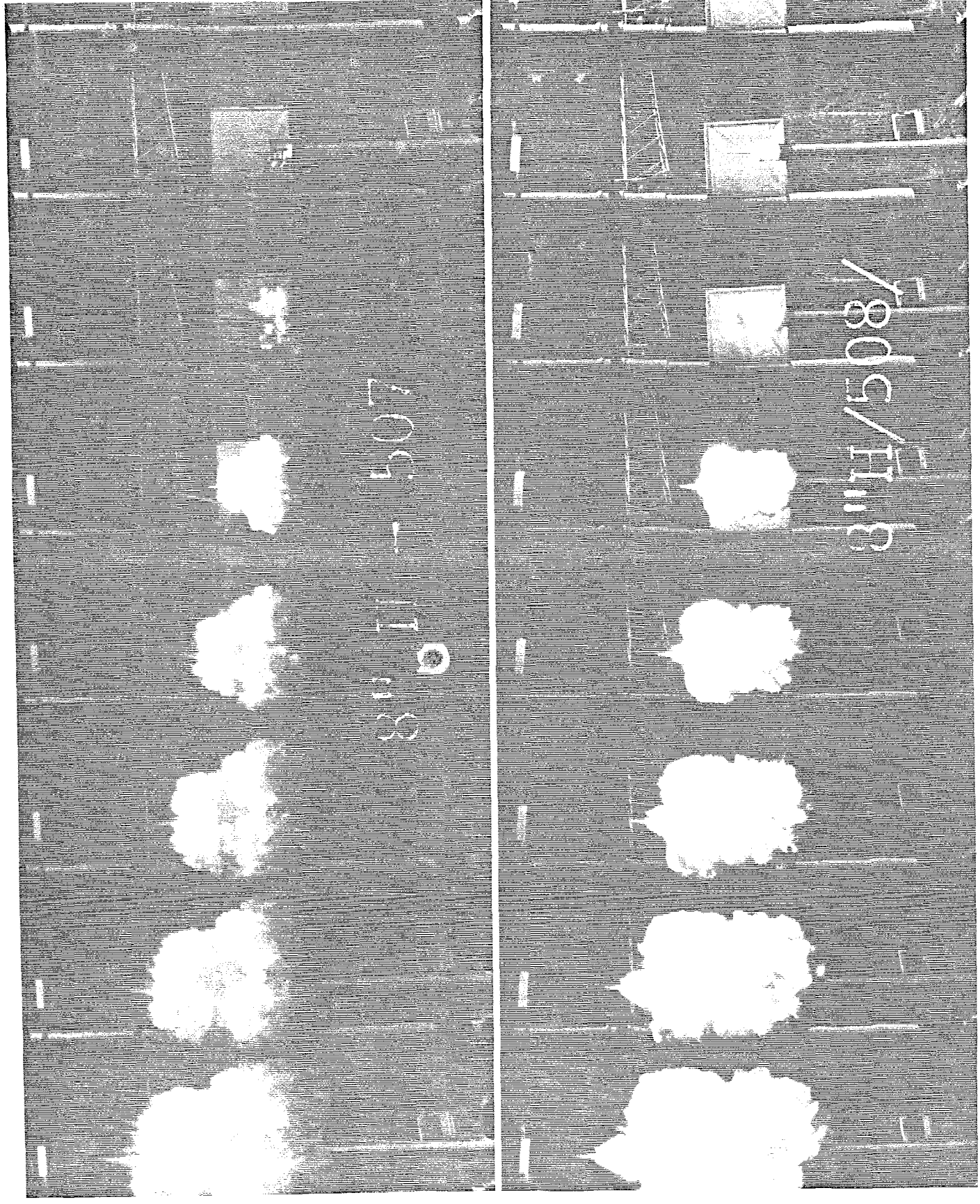

Figure 54. Framing Photos of Test Vehicles of Shot Nos. 507 and 508

4.8.3 Structural Test Results

Structural testing of the test vehicle design was an inherent objective to all shots involving a test vehicle. A fault in the early test vehicle design was revealed by two structural failures occuring in Shots 512 and 521. This failure was located at the body rear sabot carrier interface. Figure 55 presents the smear camera results showing the rear sabot carrier failure of Shot 521.

The test vehicle design at this time did not include the hardened body spacer. After the implementation of this design modification to the test vehicle design no further structural failures were recorded which would show any design inadequacies in this area. A stress analysis has been presented showing the stresses in this area with the inclusion of the body spacers.

This structural failure is attributable to the fact that in this test vehicle design a thicker, heavier body wall has been used which models not only the weight of the proposed design body wall but also a large fraction of its payload weight. This accumulation of additional weight in the body wall, particular to the test vehicle design, requires greater support by the rear sabot carrier. In the proposed design the weight to be supported by this area of the rear sabot carrier is greatly reduced and lower stresses prove to result as pointed out in the stress analysis discussion.

Through this phase of testing no other structural modifications were necessary and the overall design, with this modification, has been found to be sound.

Front and rear sabot petals recovered after testing throughout all phases of testing have shown no deformation in the latching areas.

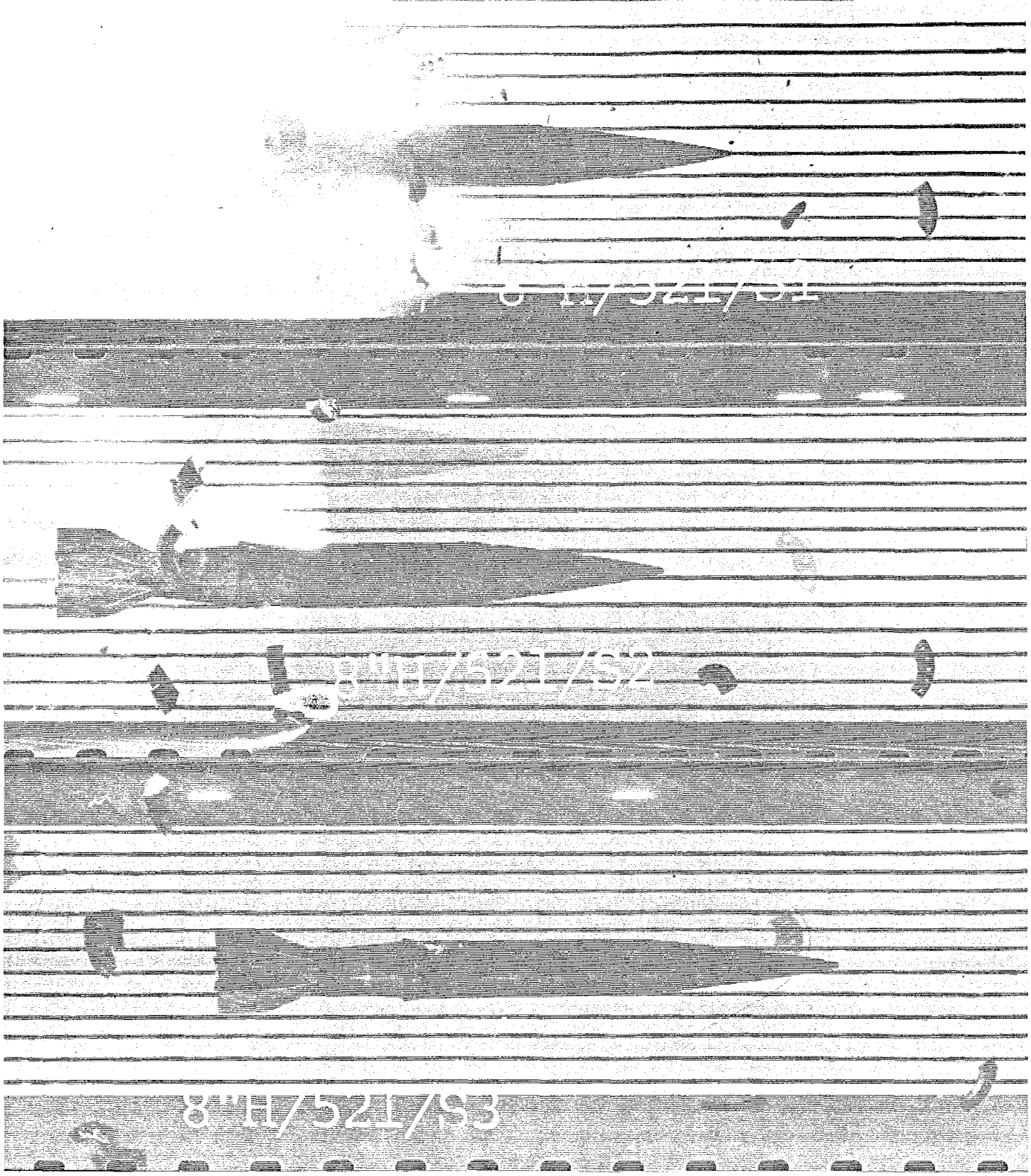

Figure 55. Smear Photograph Sequence of Shot 521 showing Structural Failure

4.8.4 Structural Fin Test Results

4.8.4.1 Fin Welding

Throughout these tests the loss of fins due to fin weld fractures did not present itself as a problem in the test vehicle design. However, many welding techniques were used to improve the weld quality and to reduce the effect of welding on the temper of the aluminum fins and fin boom.

A goal in the development of the welding procedure was to reduce the preheat conditioning temperature as low as possible, without giving rise to weld cracks, to prevent the heat added during welding from seriously impairing the temper of the aluminum.

The final welding procedure, as described previously had a preheat temperature of no greater than 300 degrees Fahrenheit and during the welding the temperature was not allowed to exceed 450 ± 50 degrees Fahrenheit. Using this welding procedure the 6061 fins and fin boom maintained a T4 temper (Postweld hardness was measured to be HRF 35-77), while the threaded connection maintained a strength nearly equal to the T6 temper (Postweld hardness was measured to be HRF 72-86).

4.8.4.2 Fin Design Structural Tests

During this phase of testing seven fin designs were tested and are identified by letter designations as given in Table 10. Table 9 indicates all tests involving these fin designs. It can be noted that at least one structural failure of each fin design occurred in Shot Number 505 to 530 involving fin designs A to D.

The test of Shot Numbers 531 to 538 was designed to be strictly a fin structural test of designs E to G. In this test a test slug design similar to the test slug used in the sabot development tests, was used to isolate the fin structural test from a test vehicle structural test. This test slug, as in previuos sabot development tests,

had front and rear non-discarding sabots. Also during this test, because of a short supply of the M30A1 propellant a double-base NQM propellant was used. A short internal ballistic test of the NQM propellant characteriestics is evident in Shots 527 to 530 of Table 9.

Although during this test no fin failures occurred among the fin designs E, F, and G, the F fin design was selected as the final fin design because of its added safety factor in design strength over the E design. As a sample, the smear camera results of Shot 536 are shown in Figure 56. Shot 538 of this structural fin test series was combined with a test vehicle fitted with fins of design G as shown in the smear photographs of Figure 57.

4.8.5 Testing of Sabot Performance

The performance of the sabots has been very good. In the figures supplied with this report so far the sabots have separated cleanly in a uniform fashion without causing instability or disturbance to the vehicle. In all cases the sabots have a very good radial displacement to sufficiently clear the fins. In all cases where the vehicle projection has not been complicated by a rear sabot carrier structural failure the sabots have discarded consistently exterior to the muzzle brake domain without any contact to the brake. In fact, with regard to these characteristics, the sabots have performed very consistently.

A design change was enacted at the beginning of this test vehicle test phase to improve the obturation of the projectile over the results obtained in the sabot development phase. To prevent the occurance of poor obturation evident in some shots of the sabot development tests (see Figure 29) a design change was made to the rear sabot components. These changes included a thicker main obturation, a steeper incline to the sabot-obturator ramp, and an intra-sabot pressure barrier.

A thicker main obturator (sliding plastic driving band) was used to prevent the obturator from fracturing early, within the bore

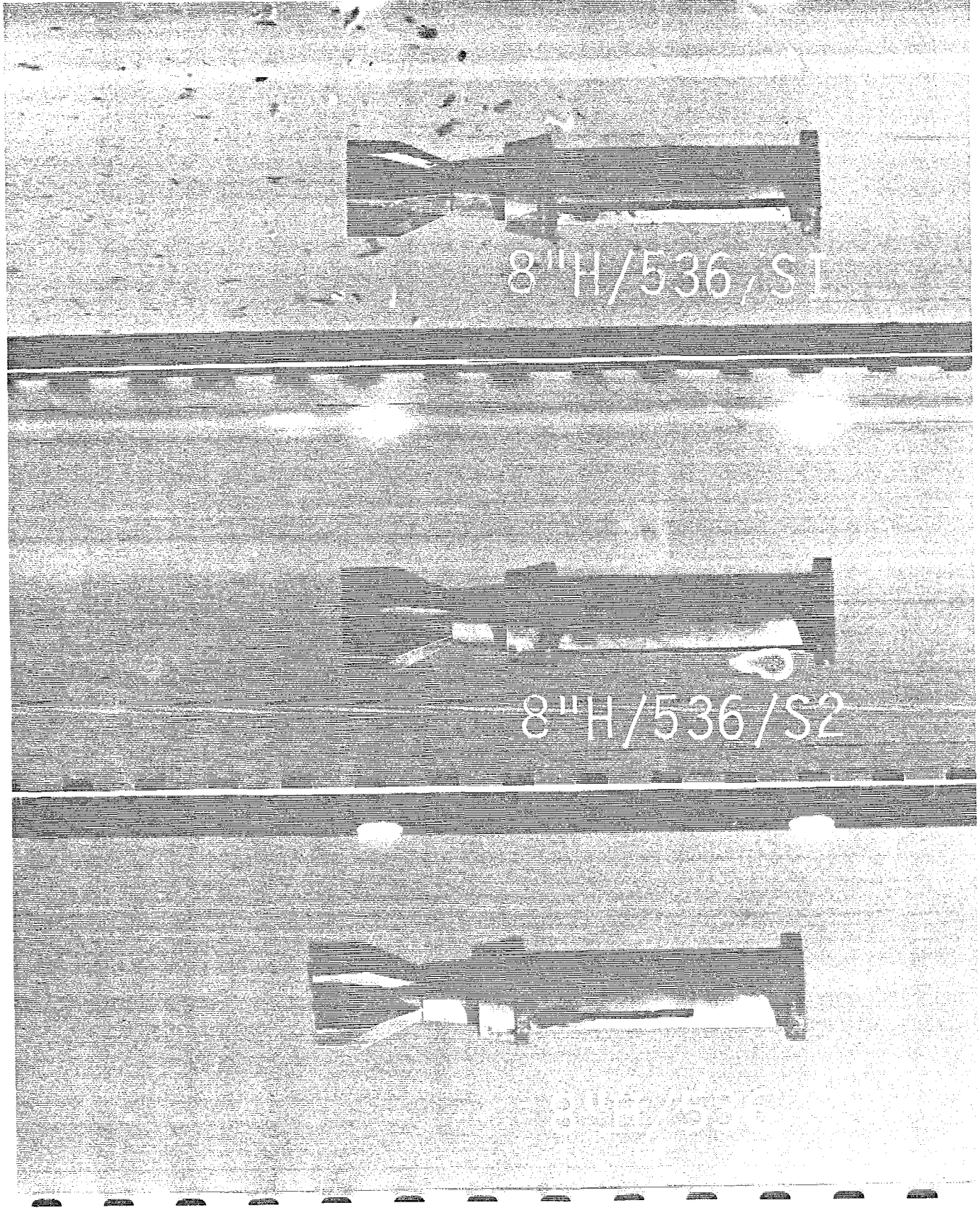

Figure 56. Smear Camera Photographs of Shot Number 536 showing Representative Results for the Structural Fin Tests

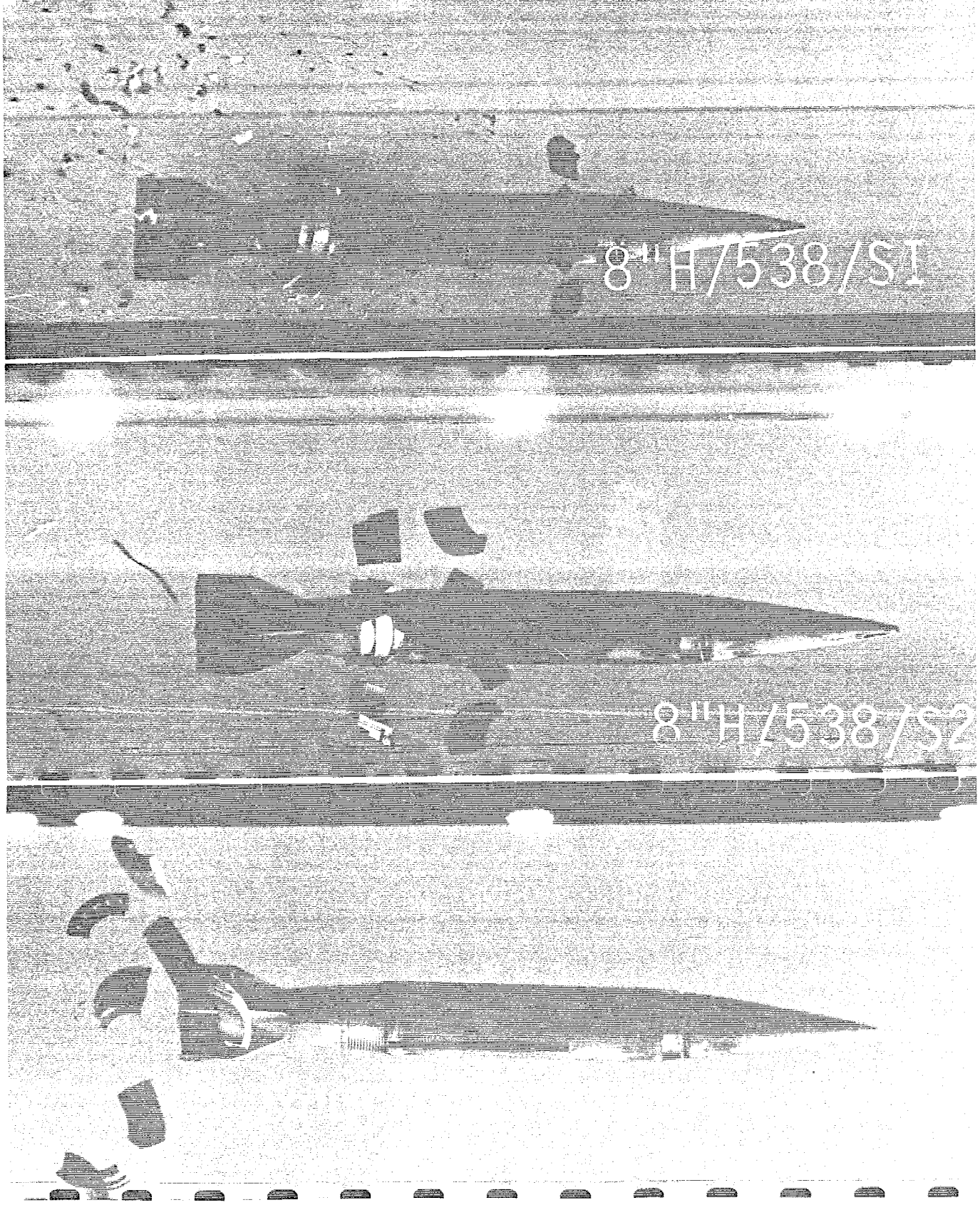

Figure 57. Test Vehicle of Shot No. 538 of the Structural Fin Test fitted with "G" Fins

of the gun tube. Also to improve the engraving and obturation quality of the main obturator, a steeper slope was given to the ramp of the rear sabot over which the main obturator slides. The steeper ramp insures that the obturator will not reach the end of the ramp and break obturation due to the abrasion of the obturator by the gun tube.

An intra-sabot pressure barrier was added as shown in Figure 31. This pressure barrier consists of a drilled passage at the inter-section of the sabot petal which is then filled with a room temperature vulcanizing silicone rubber. This then forms a silicone gasket between the sabot petals which effectively seals against any gas flow in this area. A significant improvement has been found in the quality of obturation since these changes were first tested in Shot 507. The obturation can be compared between Figures 15 to 18 and 54.

Another design change involved the front sabot and its guilding metal bore rider. As shown in Figure 51, during some shots the guilding metal front bore rider, swaged onto the front sabot petal, would separate from the petal either from aerodynamic forces or sabot-sabot impacts. While not serious, this problem was eliminated by a less expensive bore rider surface. The guilding metal bore rider was replaced by an appropriate change in the profile of the front sabot and a hardcoat anodized finish over the whole front sabot.

This design change was first tested in Shot 526 and again in Shots 538, and 542 to 544. Recovered front sabot petals showed the hardcoat anodized finish successfully resisted the abrasion of the gun tube.

4.9 FINAL DESIGN CONFIGURATION TEST

The last test (Shots 539 to 544) in this phase of testing had the objective of accepting the projectile design for subsequent tests at the U.S. Army Yuma Proving Ground under similar test conditions. This test involved three 8-inch subcaliber test vehicles.

The test was conducted with a M110E2 self-propelled howitzer, fitted with the standard muzzle brake, and test charges constructed from M30A1 MP .085 inch web propellant. This propellant was supplied through the ARRADCOM Project Engineer since this propellant was to be used during subsequent tests at YPG.

Various instrumentation were used in this test to obtain the data summarized in Table 9 and the following text. The breech pressure measurement was obtained from the average of three M-11 gages. Two piezoelectric gages were utilized (one being placed at the breech as shown in Figure 52 and one at the origin of rifling) to receive the breech and chamber pressure curve profiles. Photography instrumentation included a framing camera to record obturation results and three smear cameras, located 15, 35, and 55 feet down the gun line, to record the sabot discard sequence.

The test began with a M106 warming round and proceeded with a propellant safety check. In this propellant safety check a comparison was made between equal charge weights of propellant lot KAU 7/76, used in the past, and the newly supplied lot RAD-E-7, used for the first time here. The results of these shots (540 and 541) showed the RAD-E-7 lot to give a lower breech pressure than the KAU 7/76 lot, thus giving an indication of safe conditions to use equivalent quantities of the RAD-E-7 lot as used previously for the KAU 7/76 lot.

During this test the charge weights were increased, and some KAU 7/76 lot propellant was mixed with the RAD-E-7 lot to boost the breech pressures closer to 40 kpsi.

The smear camera results for the three test vehicles are shown in Figure 58 to 60 for Shots 542 to 544 respectively.

Figure 58 shows the first occurance of a sabot-fin impact in the third smear camera photograph. This impact has been caused by a sabot-sabot impact developing as shown in the second smear camera photograph. Otherwise Figures 58 to 60 show clean uniform sabot discard and indicate excellent structural performance.

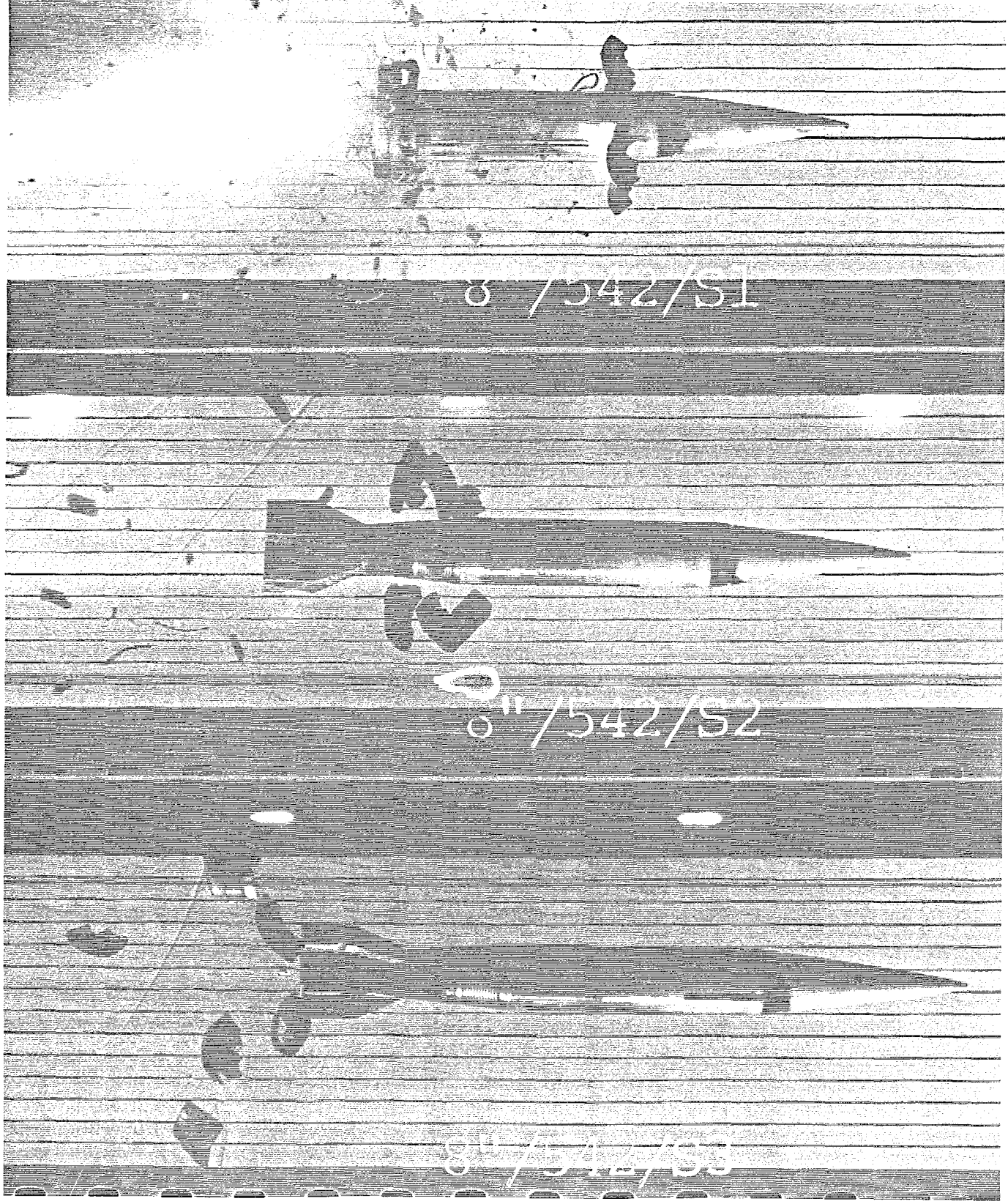

Figure 58. Smear Camera Photographs of Shot No. 542

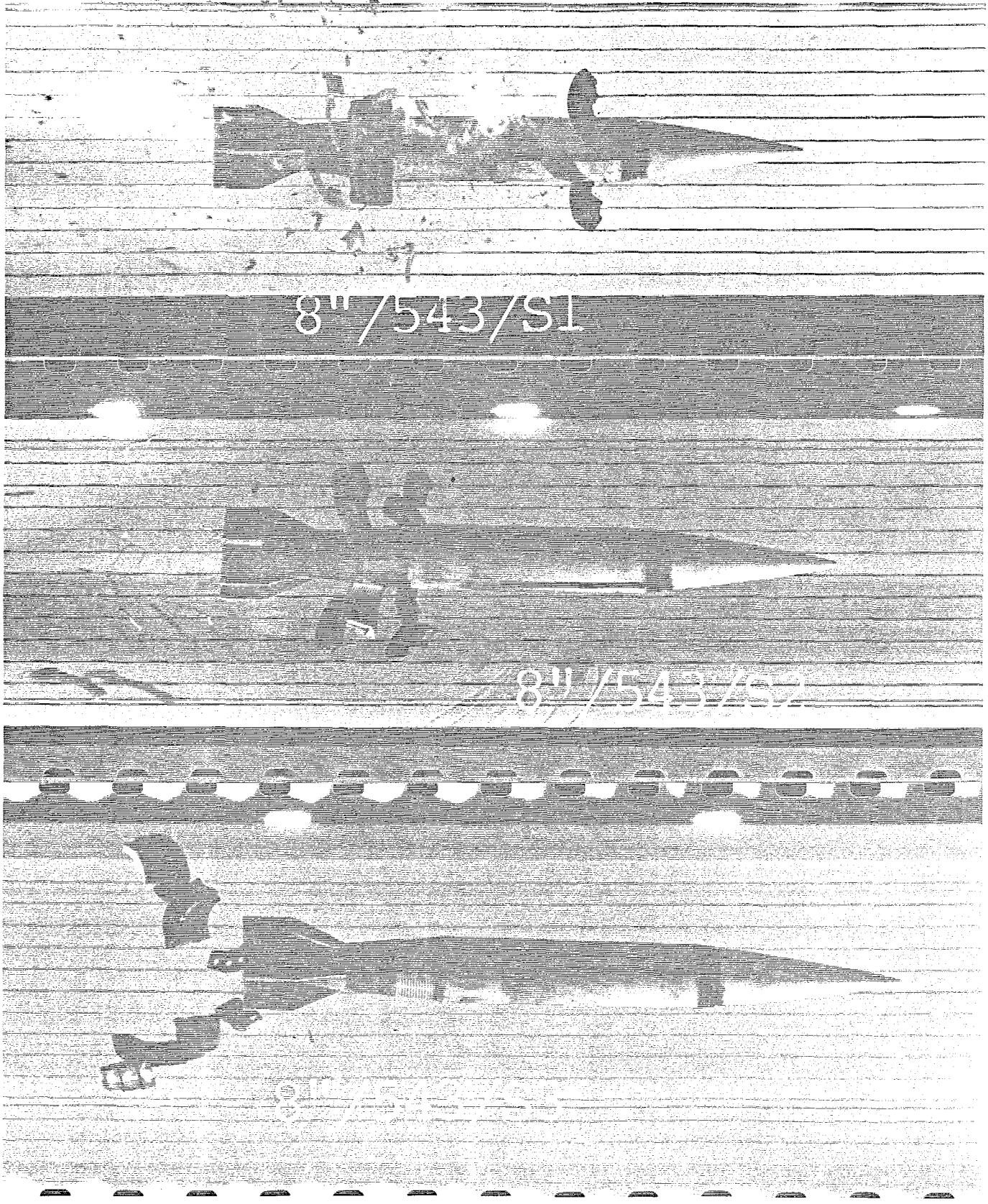

Figure 59. Smear Camera Photographs of Shot No. 543

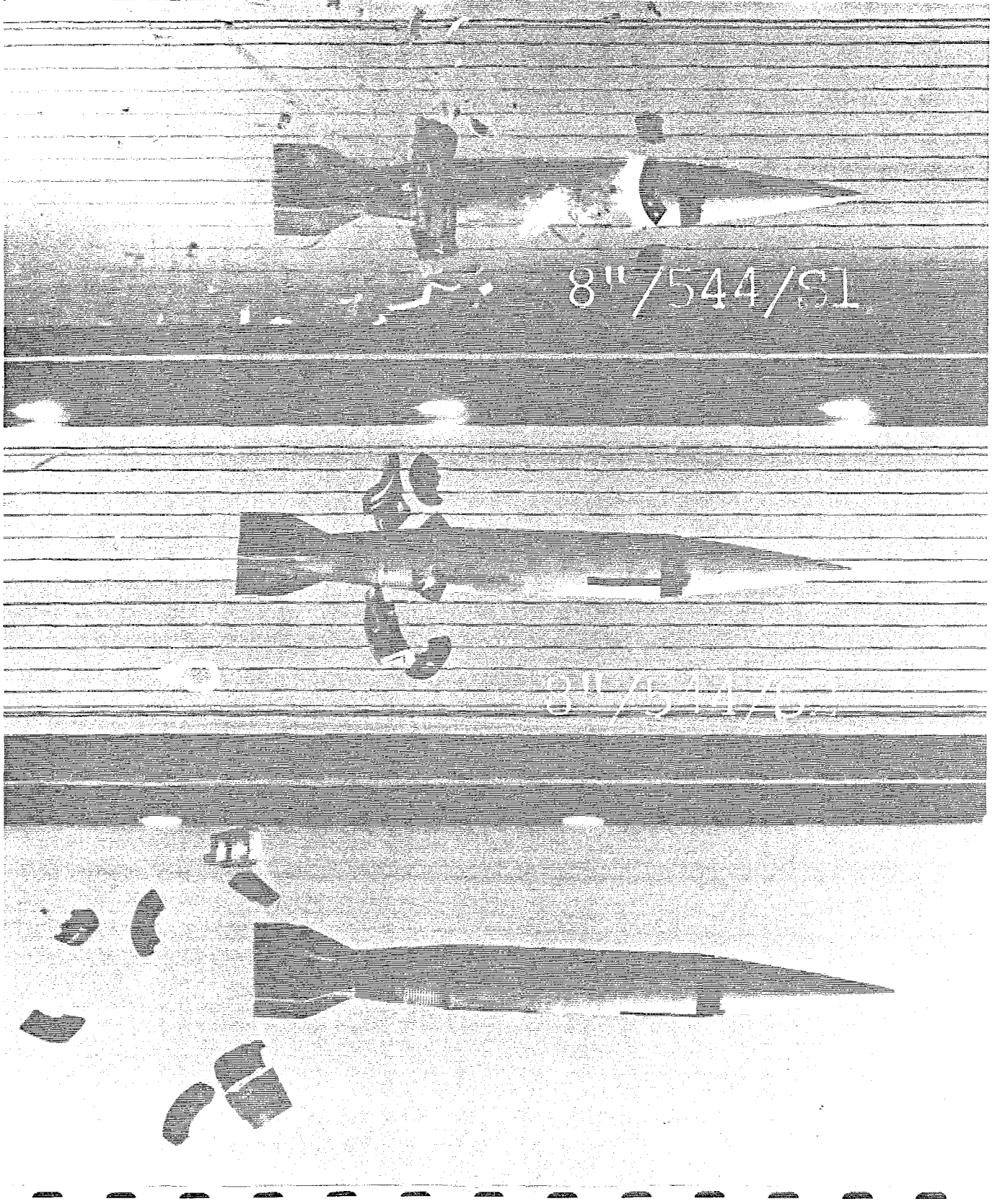

Figure 60. Smear Camera Photographs of Shot No.544

The framing camera photographs of Figure 61 show that in all cases the nose of the projectile emerges first from the muzzle ahead of the gas, indicating good obturation.

In this test additional instrumentation was used to satisfy three objectives; to accurately measure the breech and chamber pressures, to measure the time difference between the two pressures, and to show the pressure-time curves for the breech and chamber locations. To meet these objectives the gun was instrumented with two PCB piezoelectronics Model 109A2 piezoelectric gages; one mounted on the mushroom, shown in Figure 52, and one mounted at the start of the rifling to measure the breech and chamber pressures, respectively.

The piezoelectric gage outputs were linked to a dual-trace oscilliscope with a Polaroid camera for hard copy output of the peak pressures of the breech and chamber. The peak pressures of each curve were directly measured by a PCB Piezoelectronics Model 451A04 digital peak meter. The pressure curve profiles and the time interval between the curves were obtained by a second dual-trace scope with a Polaroid camera attachment. The time interval between the two curves was directly measured by a Hewelett-Packard Model HP5304A Time Counter with a Model HP5300A Measuring System. This instrument physically measures the interval of time which passes between the occurance of a specified triggering voltage associated with the positive slope of the first arriving curve and the occurance of the same specified triggering voltage associated with the positive slope of the last arriving curve. The digital data obtained from these instruments for Shots 539 to 544 are recorded in Table 12 and the photographs of the oscilloscope outputs are shown in Figures 62 to 67 respectively. The photograph at the top of each figure is the comparison of peak pressures where the breech pressure (A) is the lower trace and the chamber pressure (B) is shown inverted in the upper trace. The photograph in the lower half of each figure is the output for the comparison of pressure curve profiles and time interval measurement. It may be noted here that the vertical scale (voltage) sensitivity, of the oscilloscope, and the horizontal

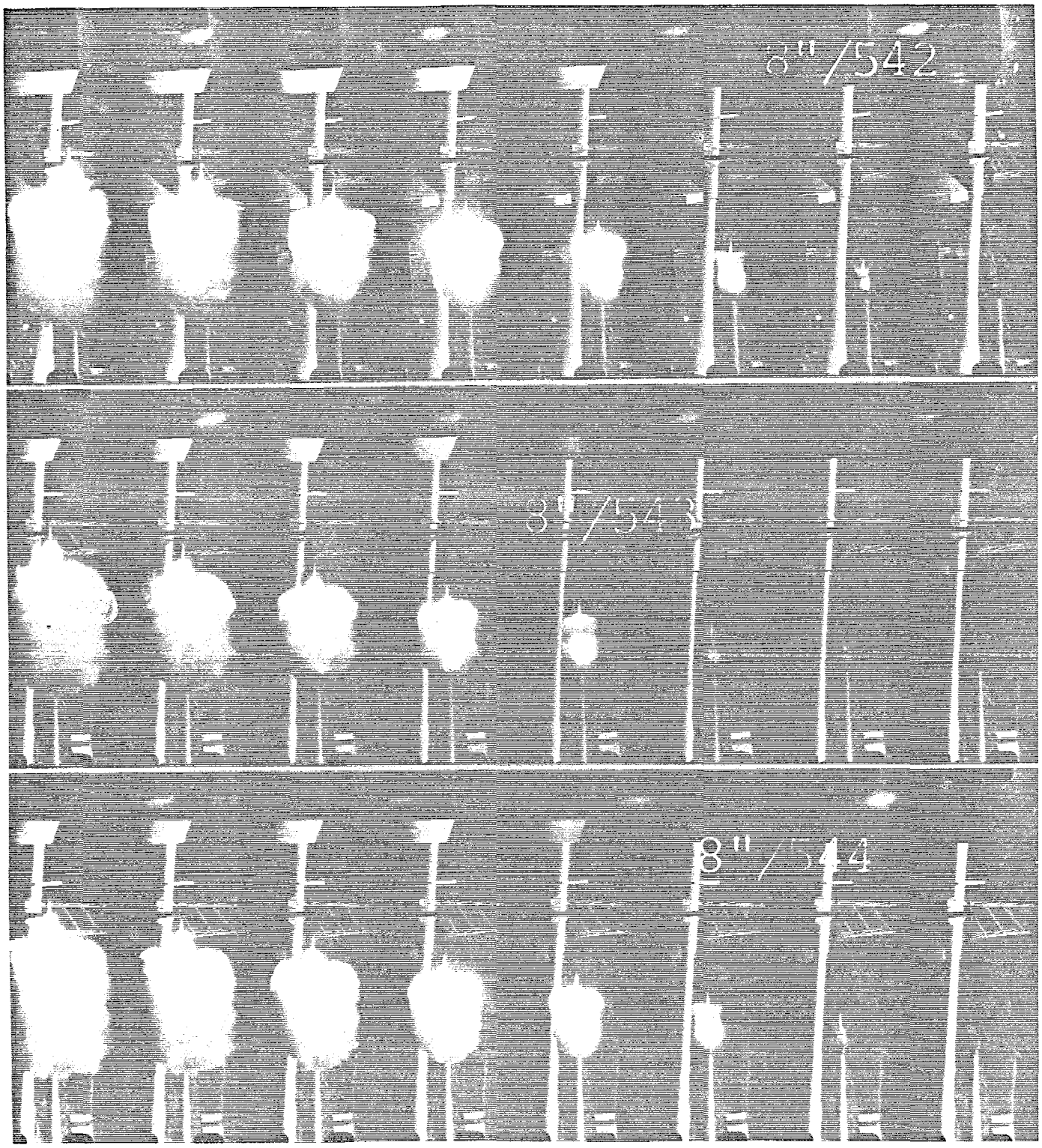

Figure 61. Framing Camera Photographs for Shot No. 542, 543, and 544 showing Quality of Obturation

TABLE 12. PRESSURE MEASUREMENTS FOR SHOTS 539 to 544

SHOT NO.	BREECH M-11 (kpsi)	BREECH PIEZO (kpsi)	CHAMBER PIEZO (kpsi)	TIME INTERVAL (Sec x 10^{-6})
539	23.1	22.5	27.3	-
540	28.2	27.4	-	-
541	24.7	23.4	27.6	392
542	32.0	31.6	40.3	-
543	33.3	33.0	40.1	246
544	35.3	35.6	40.2	-

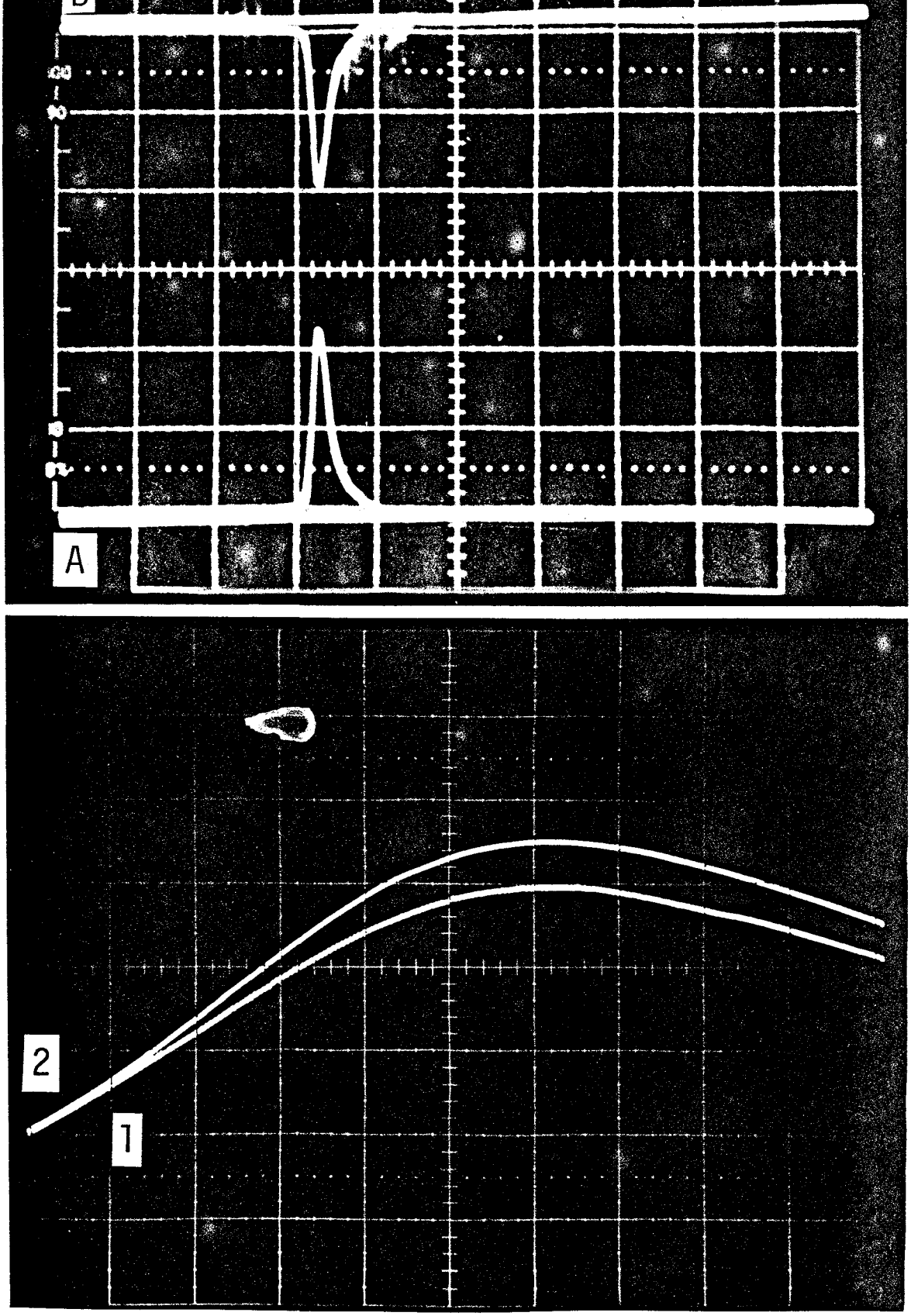

Figure 62. Oscilloscope Output for Shot 539 of the Breech Pressure (A) and Chamber Pressure (B) for Comparison of Peak Pressures (Top) and Profile-Time Correlation (Bottom). Top photo scale; 1 v/div., 50 ms/div. Bottom photo scale; .5v/div., 1 ms/div.

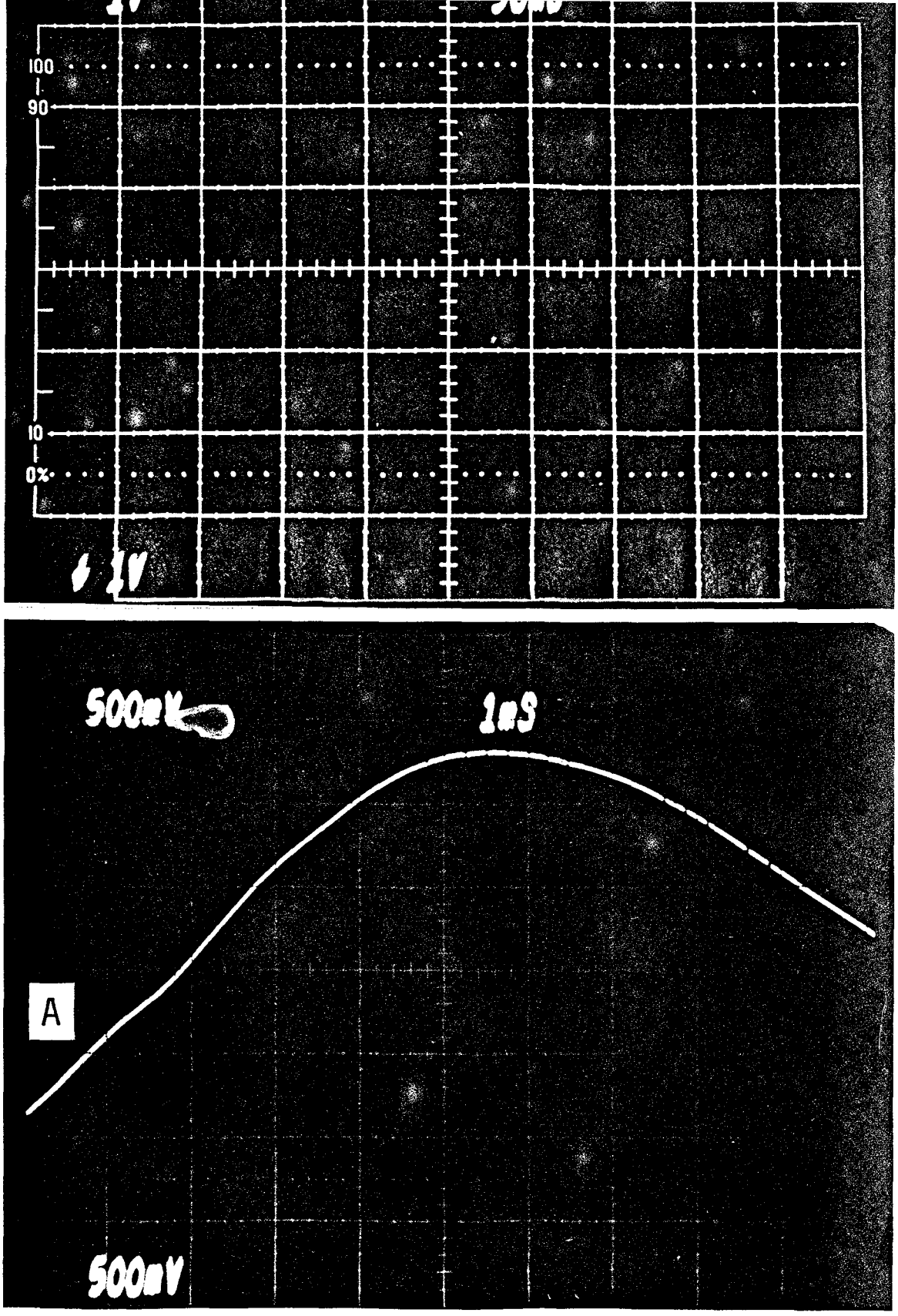

Figure 63. Oscilloscope Output for Shot 540

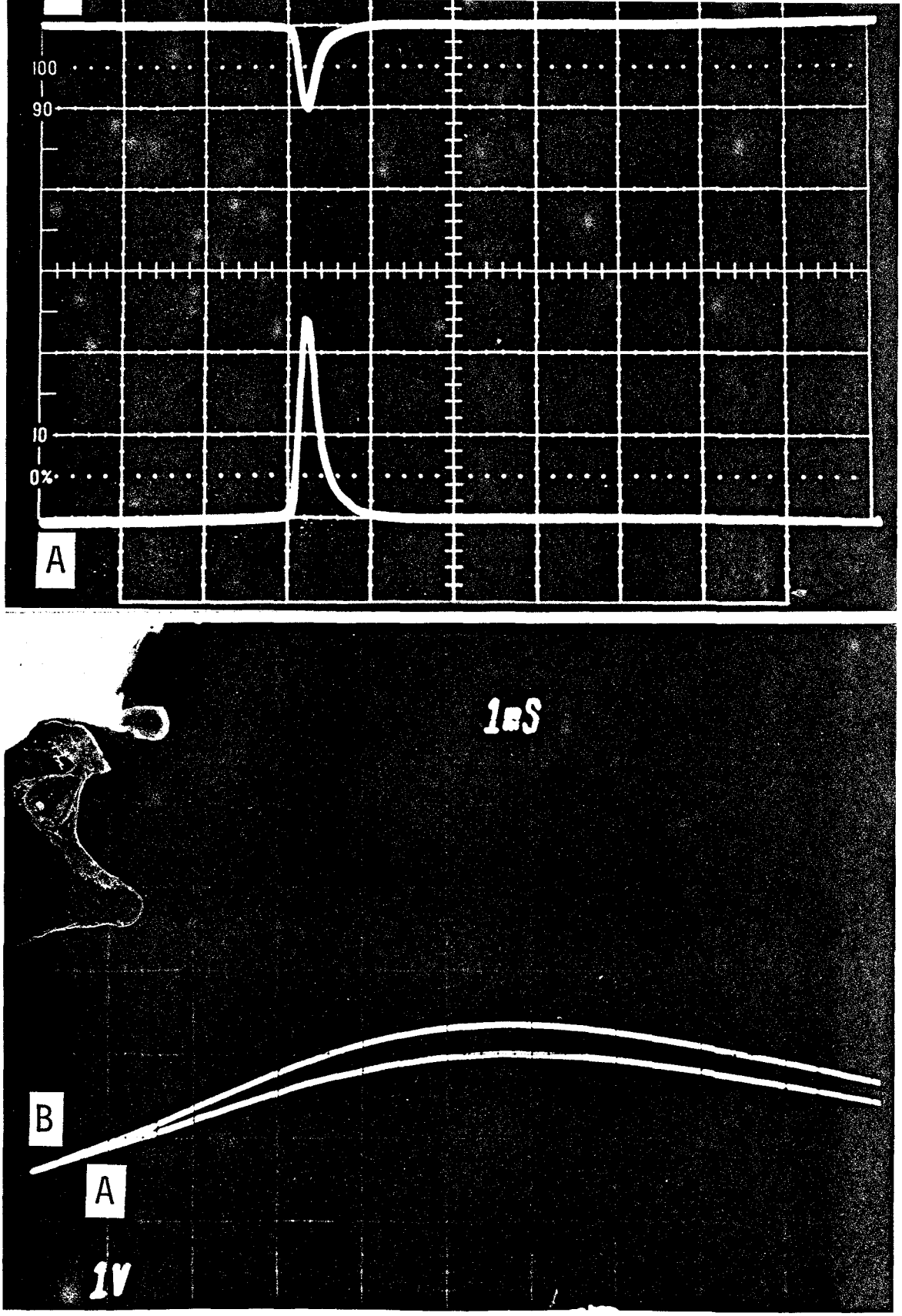

Figure 64. Oscilloscope Output for Shot 541. Scales for Top Photo; 1 v/div. for A, 2 v/div. for B., 50 ms/div.

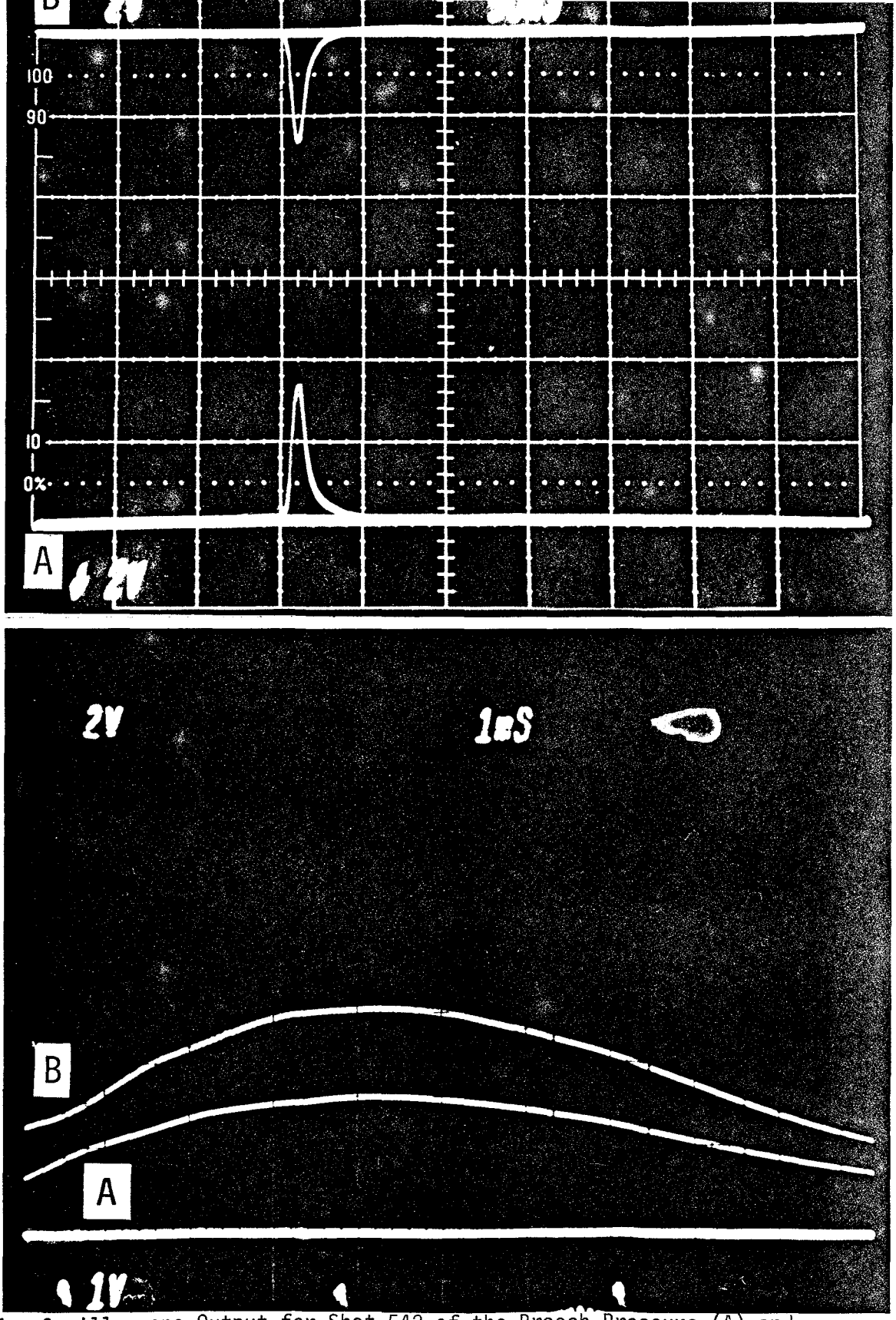

Figure 65. Oscilloscope Output for Shot 542 of the Breech Pressure (A) and Chamber Pressure (B) for Comparison of Peak Pressures (Top) and Profile-Time Correlation (Bottom).

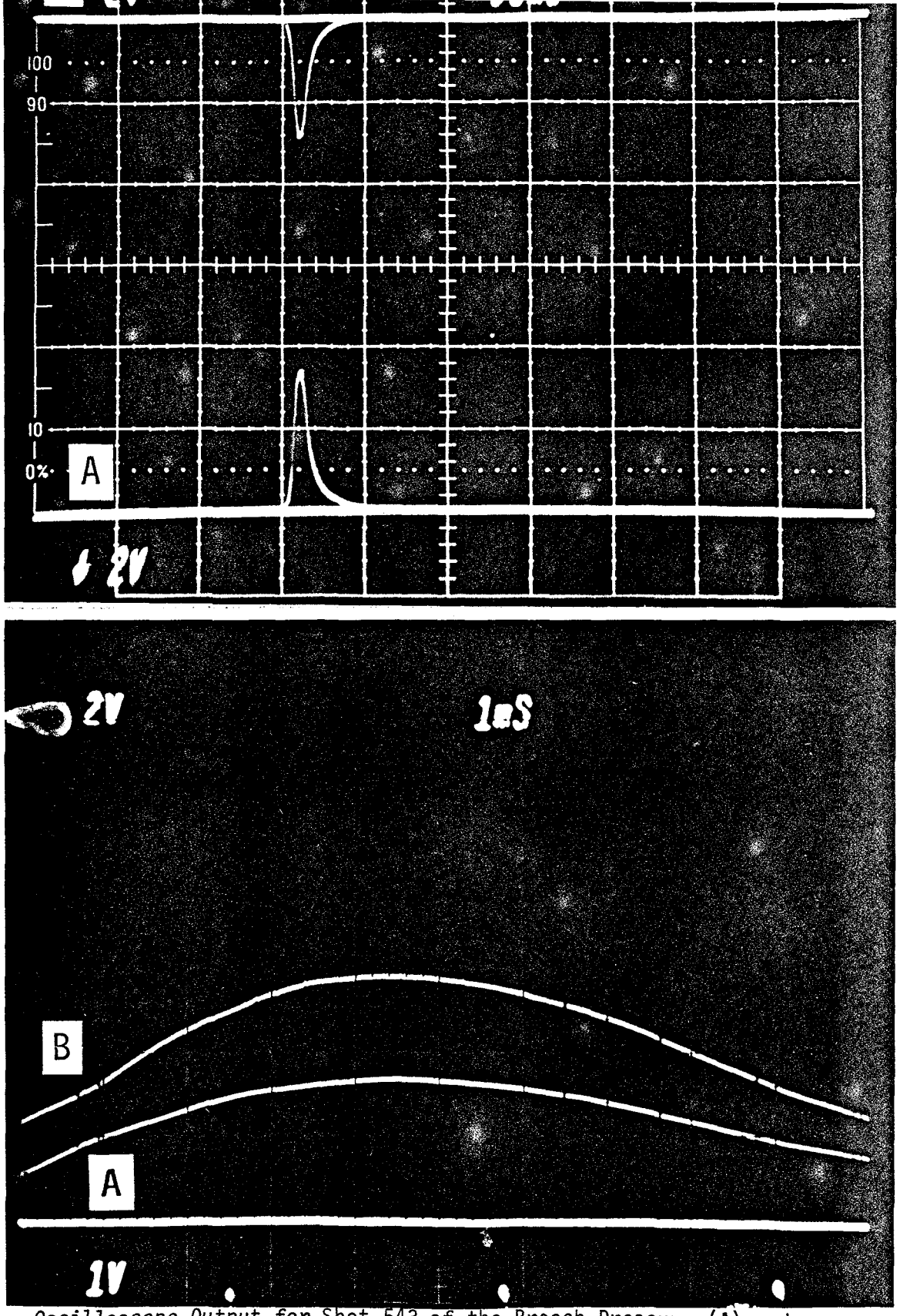

Figure 66. Oscilloscope Output for Shot 543 of the Breech Pressure (A) and Chamber Pressure (B) for Comparison of Peak Pressures (Top) and Profile-Time Correlation (Bottom).

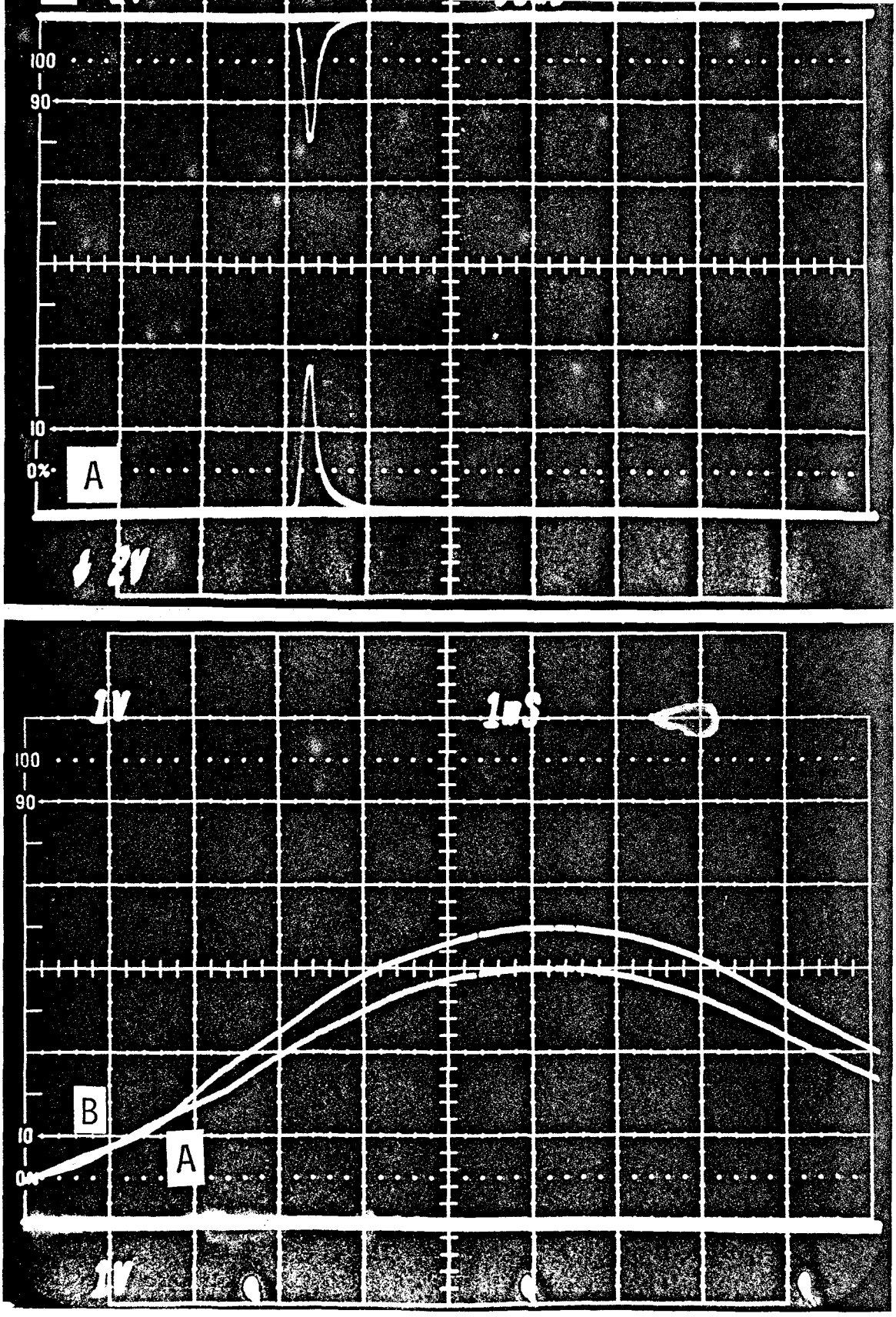

Figure 67. Oscilloscope Output for Shot 544 of the Breech Pressure (A) and Chamber Pressure (B) for Comparison of Peak Pressures (Top) and Profile-Time Correlation (Bottom).

scale (time) sensitivity are in most cases displayed within the boundaries of each photograph (see Figure 65). Here, the voltage sensitivity of the upper trace is shown in the upper left hand corner of each photograph, the voltage sensitivity of the lower trace is given in the lower left hand corner and the time sensitivity is given in the upper mid-section of each photograph.

(BLANK PAGE)

5.0 INITIAL FLIGHT TEST

5.1 HARDWARE FABRICATION

Fabrication of ten (10) 8-inch subcaliber test vehicles got underway early in 1979, since the basic vehicle design had been completed. Manufacture of the fin assembly was done after fin structural tests were completed and the final fin design was selected.

At the time the first ten flight vehicles were manufactured there existed a difference of opinion as to the best welding procedure for the fins. Two procedures had been recommended for welding the fins to the fin boom, differing primarily in the preheat temperature. The fin assemblies of test vehicles 1, 2, and 3 were welded using a higher preheat temperature. Subsequently the concern that the higher preheat would soften the aluminum excessively prevailed, although the weld penetration would be improved, and the remaining seven vehicles were welded according to the finalized welding procedure outlined earlier in this report. The test vehicles were identified according to welding procedure so that any differences in performance could be correlated with manufacturing process.

Twelve test charges composed of 62.0 lbs. of M30A1 MP .085 inch web propellant were supplied by this contractor during the summer of 1978 for this test. These charges had been delivered to Yuma Proving Ground earlier, so as to be available as soon as the test date was established, enabling the expedient conduct of the tests.

During May, 1979, ten (10) 8-inch subcaliber cargo shell test vehicles were completed. Physical measurements were made of the in-flight condition of the ten test vehicles at the Army Materials and Mechanics Research Center (AMMRC), Watertown, Massachusetts. The results of the measurements of the ten vehicles without sabots are given in Table 13. In-flight condition physical measurements were also taken on two vehicles fitted with spotting noses.

TABLE 13. 8-INCH SUBCALIBER CARGO SHELL MOD 4
TEST VEHICLE MASS PROPERTIES[2]

VEHICLE NO.	WGT (lbs)	Xcg[1] (in)	Iyy (lbs-in^2)	Ixx (lbs-in^2)
1	122.1	29.83	29,071	494.7
2	122.1	29.72	28,992	495.0
3	121.9	29.75	28,614	494.1
4	122.1	29.72	29,229	494.0
5	122.0	29.73	28,637	494.6
6	122.1	29.72	29,260	495.0
7	121.8	29.69	28,529	492.7
8	122.9	29.68	29,520	498.3
9	123.0	29.59	29,135	497.6
10	122.7	29.72	29,124	498.0
Avg.	122.3	29.71	29,011	495.4
WITH SPOTTING NOSE				
7	124.5	29.81	23,173	504.5
9	125.4	29.81	23,497	508.8

[1] Xcg is measured from the base of the projectile.

[2] Measurements made by AMMRC

On 29 May 1979 ten (10) 8-inch cargo shell Mod 4 test vehicles were shipped by GBL to Yuma Proving Ground with accessories consisting of eleven (11) spotting noses (Dwg. D24752) and ten (10) M51A1 inert fuzes. Twelve (12) retainers were provided to prevent the shell from falling back on the charge. The equipment listed above is shown in Figure 68. The retainer used to prevent shell fall back, shown in the foreground of Figure 68, was plywood, one-quarter inch thick, cut to a width of 1 inch and a length of 41 1/8 inches. The shell in the foreground of Figure 68 is a Mod 4 test vehicle (S/N 09) fitted with a spotting nose, a spin desensitized M54 fuze (Lot UST 1-157) supplied by ARRADCOM, and containing a T2 supplementary charge to produce a more visible signature upon impact for observers. The shell toward the rear of Figure 68 (S/N 01) is one of the prototype test vehicles with a standard nose. The charge in the background of Figure 68 is the 8-inch experimental charge used during the test. It is composed of 62.0 lbs. of M30A1 .085 inch web propellant of Lot KAU 7/76 and a 1 oz. Class A black powder base pad igniter and 5 oz. Class A black powder central core igniter. The charge measured 25 inches in circumference and 40 inches in length.

5.2 PROVING GROUND FLIGHT TEST RESULTS

The test date was established by the Army as 5 July 1979. Contractor personnel arrived at YPG in advance to prepare the hardware and assist with test coordination. Two test vehicles were converted to spotting rounds by removing the front sabot carrier-windshield nose with the enclosed M51A1 inert fuze and adding in its place a spotting nose with an exposed spin desensitized M564 fuze and T2 supplementary charge. Two of the twelve 8-inch experimental charges were reduced in weight from the original charge weight of 62.0 lbs. of M30A1 .085 inch web propellant (Lot KAU 7/76) to 58.0 lbs. in case the reduced charges would be needed. The remaining ten charges were unaltered.

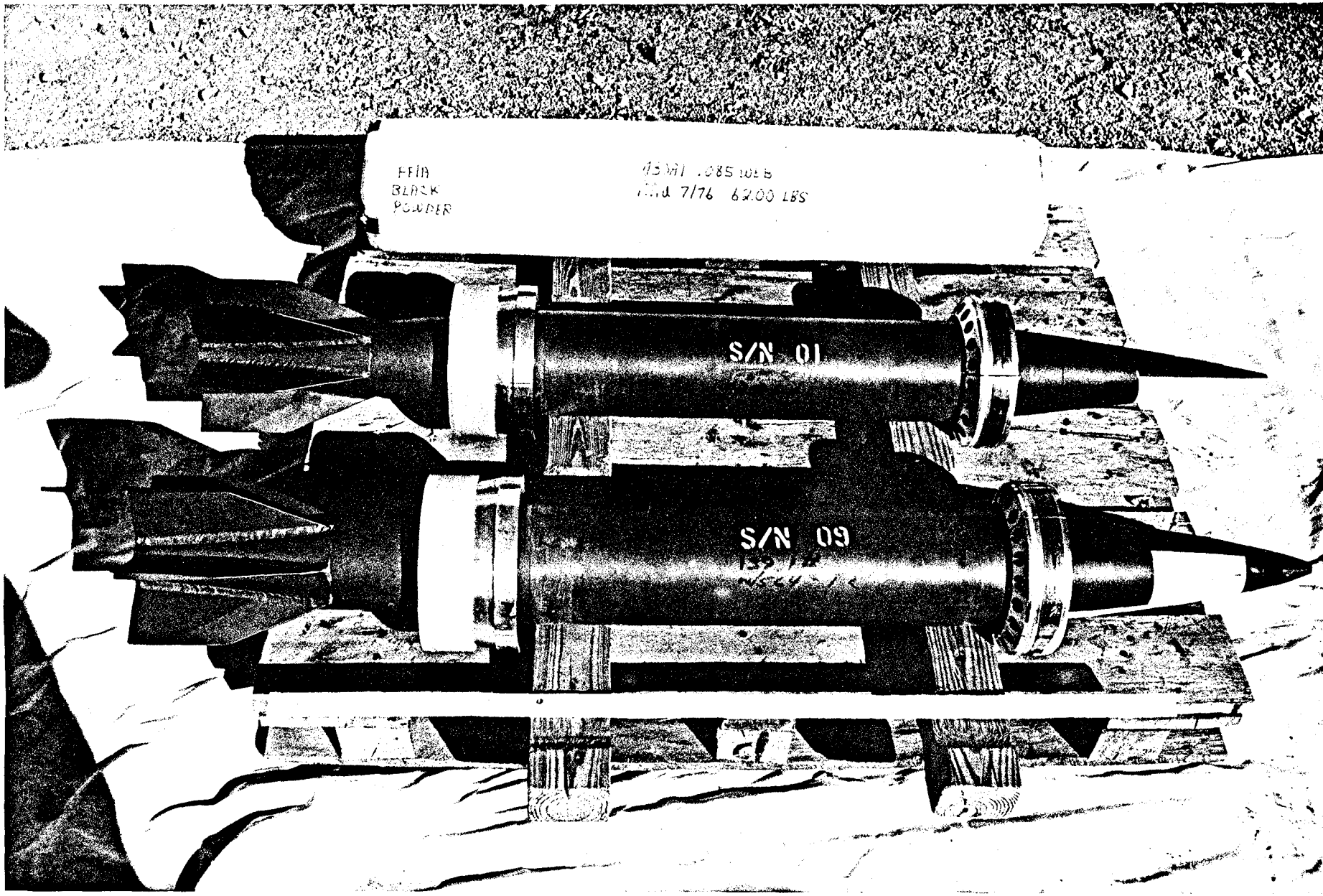

Figure 68. Flight Test Hardware at Yuma Proving Ground

The test began with three M106 warming rounds and during the test it was decided to fire one M106 warming round prior to each test vehicle. The results of the M106 warming rounds are not reported upon here as they have no significance to the objective of this test. All tests were fired at a QE of 51°.

Test data and results are included in Table 14. These data were collected by YPG personnel, evaluated by ARRADCOM, and supplied to the contractor[3]. Test vehicles 7 and 9 were converted to spotting rounds as denoted by the post script "s" in the table and thus have a different external configuration than the 8-inch subcaliber cargo shell Mod 4 test vehicle fired in the remainder of the test. The three rounds having suspected fin welding deficiencies were held until near the end of the series in case a problem developed. Figure 69 presents typical results from the two smear cameras located 25 and 50 feet from the muzzle. Shown in Figure 69 is test vehicle 8, Shot Number 871.

As can be noted by reference to the test results and smear photographs of vehicle numbers 4, 5, 6, 10, and 8, the ranges achieved were all in excess of 40 km, the test goal. Thus the capability of the new round in this initial flight test was well demonstrated. Rounds 7s and 9s, equipped with spotting noses and therefore having slightly different aerodynamic characteristics, produced nearly the same range as the standard rounds.

Test vehicles 1 and 2, having the higher preheat fin welds, were tested with the full charge of 62 lbs. When these vehicles were fired, flight characteristics were not observed by the radar nor were impacts sighted by observers. Information supplied by the framing camera shows an unusual flash of gases at the muzzle for each of these

---

3 Letter from ARRADCOM received 14 September 1979.

TABLE 14. JULY 1979 8-INCH SUBCALIBER CARGO SHELL MOD 4 TEST VEHICLE FLIGHT CHARACTERISTICS TEST AT YUMA PROVING GROUND

TUBE ROUND NO.	TEST VEHICLE NO.	TEST VEHICLE SHOT WEIGHT (lbs)	CHARGE[1] WEIGHT (lbs)	BREECH[2] PRESSURE (kpsi)	MUZZLE VELOCITY			RANGE (m)	DEFLECTION LEFT (m)	TIME OF FLIGHT (sec)
					Radar[4]	Smears[3]				
					(mps)	(fps)	(mps)			
856	7s	138.1	62	32.6	974	3198	975	40525	368	107.4
857	9s	139.1	62	37.6	917	3000	914	38125	354	-
859	4	135.2	62	39.4	991	3264	995	44728	522	120.3
861	5	135.2	62	34.1	941	3075	937	40321	495	-
863	6	135.4	62	35.4	947	3107	947	40506	425	115.5
865	10	136.1	62	40.4	993	3247	990	45214	509	-
867	2	135.3	62	36.2	-	-	-	-	-	-
869	1	135.4	62	40.3	-	-	-	-	-	-
871	8	136.2	62	40.6	994	3269	996	45229	430	-
872	3	135.3	58	29.8	897	2941	896	30660	547	103.6

[1] Propellant: M30A1 .085 Inch Web Lot KAU 7/76

[2] Average from two M11 Crusher Gages

[3] Measured from Smear Camera Films (±15 fps)

[4] YPG Radar Data

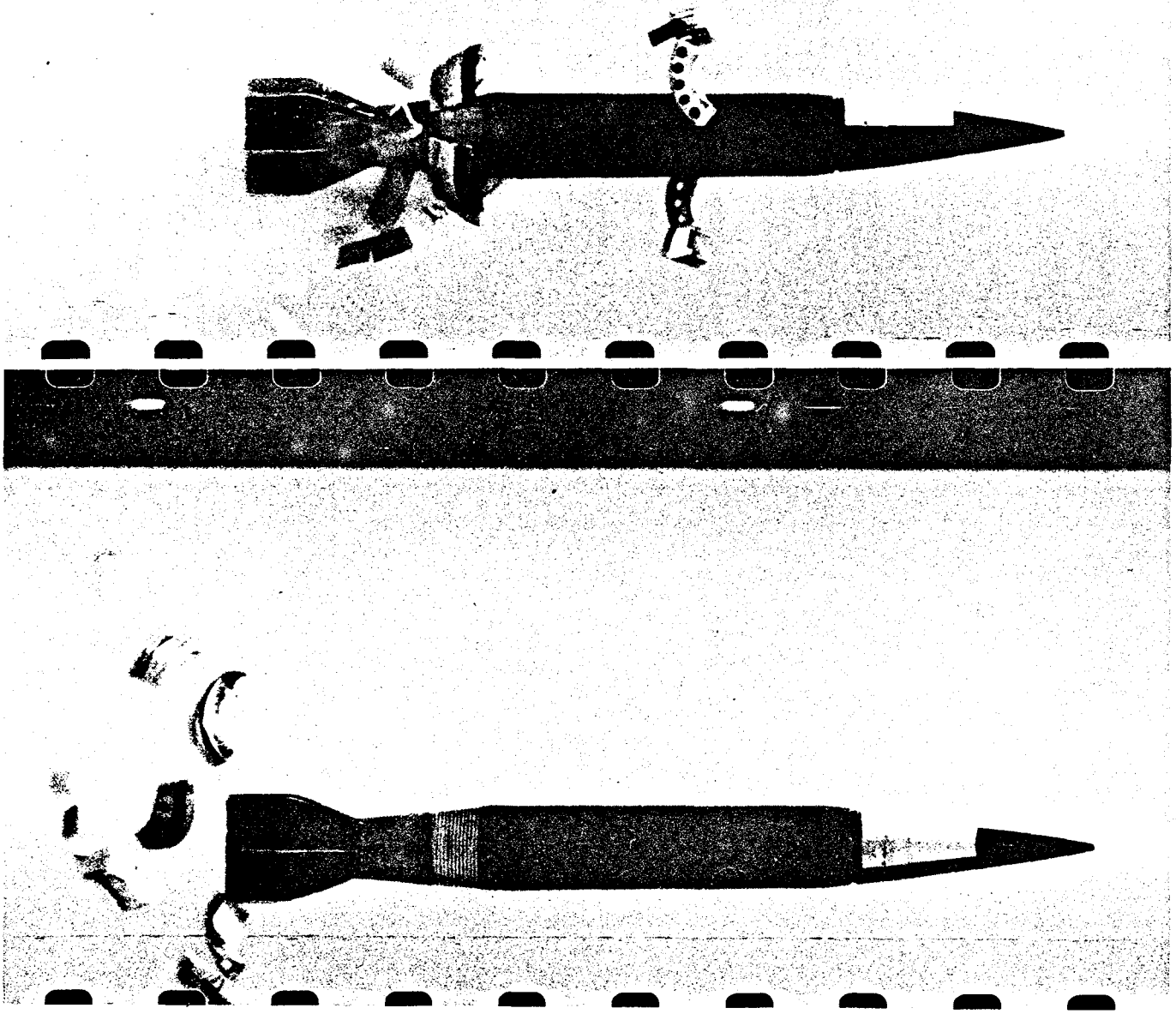

Figure 69. Typical results from the two smear cameras. Shown here is test vehicle 8 (tube round No. 871).

two shots. The smear camera record of Shot 867, test vehicle 2, shows the complete fin assembly removed from the rest of the shell, indicating the threads of the fin boom weldment had failed. In order to evaluate this problem further with the remaining shell from this lot, test vehicle 3 was fired using a reduced charge of 58.0 lbs. At the resultant reduced pressure, test vehicle 3 stayed structurally intact, although it achieved a shorter range, as would be expected. From the test results and observations, the correct procedure for welding the fins was verified and specified for use in fabricating the remaining lot of 20 projectiles.

The test results show a reasonable correlation between the breech pressures and the resulting ranges, and thus, even in this first flight test, show consistency in the performance of the round. Data tapes from the YPG tests were returned to ARRADCOM for reduction and evaluation, and the graphs in Figures 70-72 contain data generated from these tapes by ARRADCOM. Figure 70 demonstrates the relationship of peak chamber pressure (measured with piezoelectric gages) to muzzle velocity, showing excellent correlation. Figures 71 and 72 show muzzle velocity vs. range and velocity vs. time of flight, respectively, in comparison with computer simulation data. Agreement is generally good in all cases. The range data supplied in Table 14 are significant, for not only on the first effort do the measured ranges far exceed the range capabilities of present 8-inch ammunition in that gun system but also are substantially greater than the contract goal of 40 kilometers.

PAGE 160 IS MISSING FROM THE MASTER COPY

PAGE 161 IS MISSING FROM THE MASTER COPY

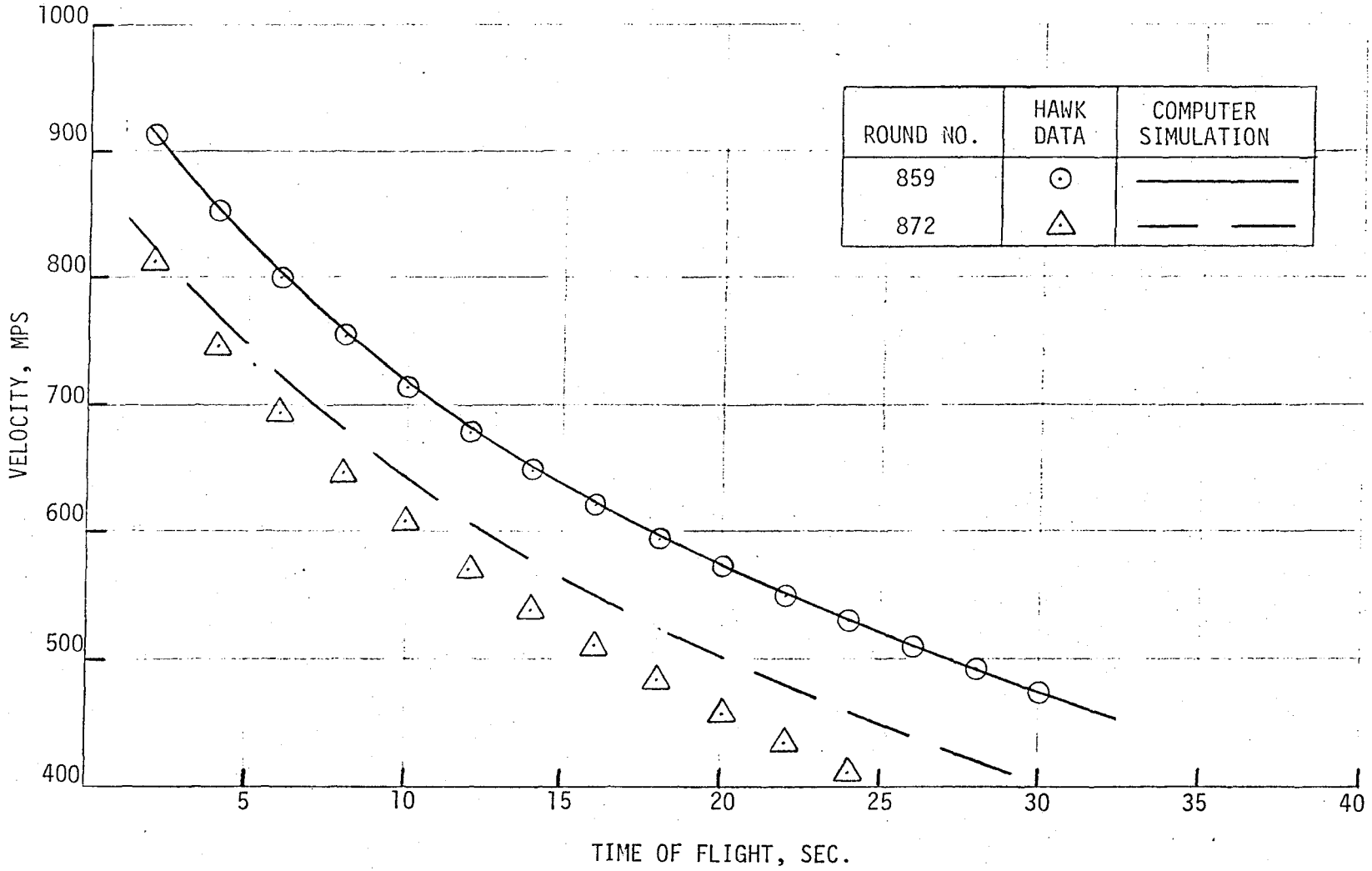

Figure 72. Velocity-Time of Flight Data from Selected Tests, Related to Simulation Results (YPG Firing, 5 July 1979)

6.0 FLIGHT TEST VEHICLE FINAL CONFIGURATION

Following the initial flight tests at YPG, it was possible to complete the final twenty (20) test vehicles required under this program. Figure 73 shows one of the Mod 5 vehicles prior to shipment to YPG. Only one minor change in configuration, relative to the Mod 4 vehicles tested at YPG, was required for the Mod 5 final configuration vehicles. This change was made to reflect the use of a hard anodize coating, rather than copper, for the front bore rider (this change was validated in gun testing prior to the YPG tests). The only design impact from the YPG tests was in regard to fin welding. The proven process, used on the successful flight test vehicles, has been carefully documented and included on the appropriate drawings for the Mod 5 test vehicle. One additional drawing note change was made to more accurately define the assembly procedure for the rear sabot. Table 15 contains a list of drawings for the final design. Reproducible drawings of this projectile have been supplied separately to the Army, and reduced prints of these drawings are shown in Figures 74-91.

The twenty (20) Mod 5 test vehicles described in this section have been delivered to YPG for further test and evaluation by the Army. These tests are not within the contractor's scope of work of the current contract. Early completion of these tests by the Army will provide significant additional data which will be useful in further development of the 8-inch Subcaliber Extended Range Cargo Vehicle. Additional recommendations for further work are discussed in the following section.

PAGE 164 IS MISSING FROM THE MASTER COPY

TABLE 15. FLIGHT TEST VEHICLE FINAL CONFIGURATION

PART	DRAWING NUMBER	REV	DATE
8" Cargo Shell, Mod 5	F24776	-	4 Oct 79
Windshield	D24733	A	9 Aug 78
Dummy Payload	C24737	A	9 Aug 78
Payload Ballast	C24738	A	9 Aug 78
Spacer, Body	B24758	A	30 Jan 79
Body	F24759	A	30 Jan 79
Fin Boom (Weldment)	D24777	-	4 Oct 79
Fin	D24762	-	5 Feb 79
Fin Boom	D24764	A	5 Feb 79
Front Sabot Ass'y	B24778	-	4 Oct 79
Front Sabot Carrier	D24732	B	9 Aug 78
Front Sabot	D24775	-	4 Oct 79
Retaining Ring	A24115	A	26 Jul 77
Rear Sabot Ass'y	B24779	-	4 Oct 79
Rear Sabot Carrier	D24757	A	30 Jan 79
Sabot, Rear	D24708	B	21 June 78
Band, Obturator	D24710	A	21 June 78
Obturator, Secondary	C24709	A	21 June 78

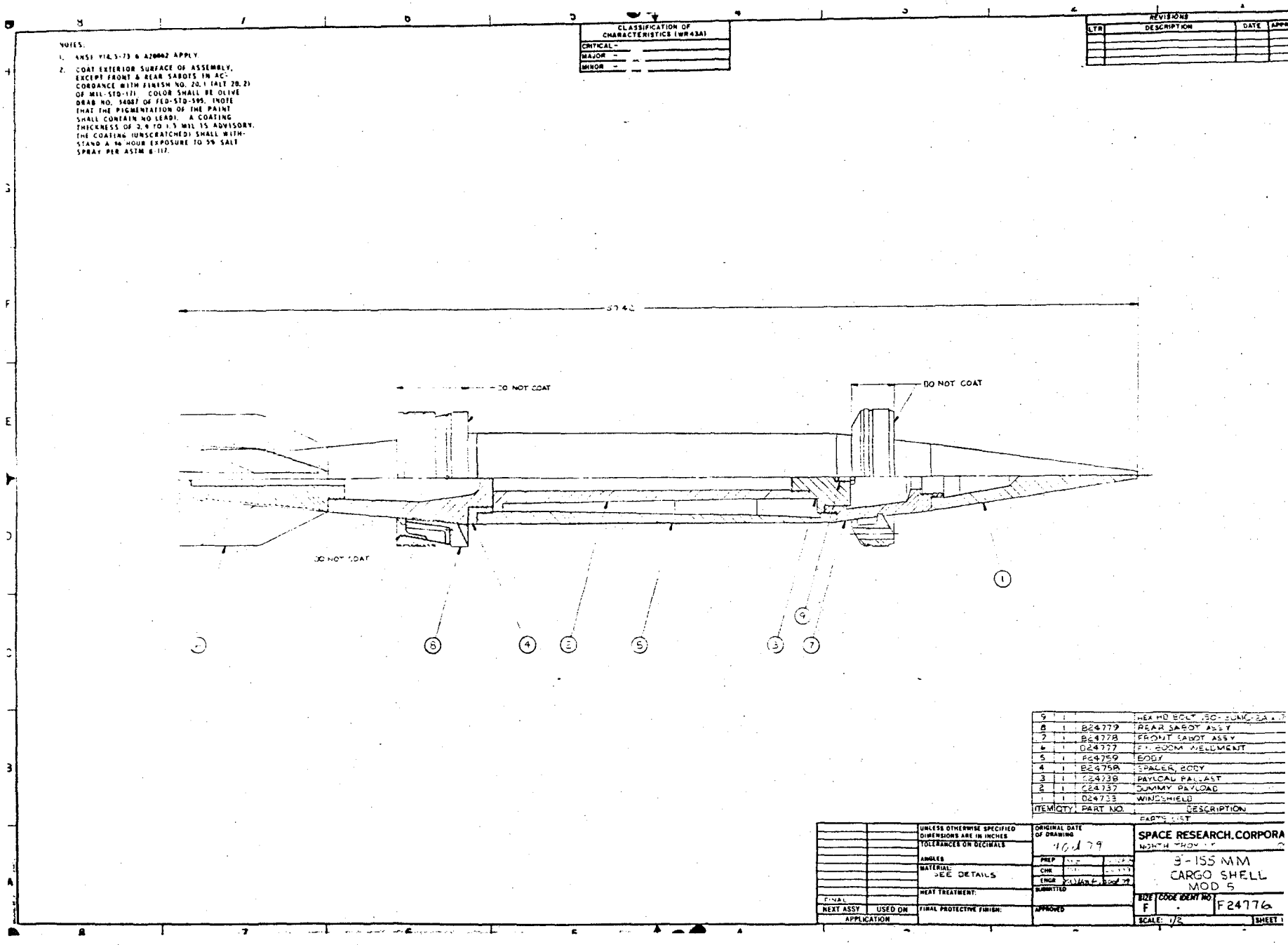
NOTES:
1. ANSI Y14.5-73 & A28662 APPLY.
2. COAT EXTERIOR SURFACE OF ASSEMBLY, EXCEPT FRONT & REAR SABOTS IN ACCORDANCE WITH FINISH NO. 20.1 (ALT 20.2) OF MIL-STD-171. COLOR SHALL BE OLIVE DRAB NO. 34087 OF FED-STD-595. NOTE THAT THE PIGMENTATION OF THE PAINT SHALL CONTAIN NO LEAD). A COATING THICKNESS OF 2.9 TO 3.5 MIL IS ADVISORY. THE COATING (UNSCRATCHED) SHALL WITHSTAND A 96 HOUR EXPOSURE TO 5% SALT SPRAY PER ASTM B-117.
CLASSIFICATION OF CHARACTERISTICS (WR43A)
CRITICAL –
MAJOR –
MINOR –
REVISIONS
LTR
DESCRIPTION
DATE
DO NOT COAT
DO NOT COAT
DO NOT COAT
1
2
3
4
5
6
7
8
9
ITEM
QTY
PART NO.
DESCRIPTION
9 1 HEX HD BOLT ISO-SUNC-2A x 7
8 1 B24779 REAR SABOT ASSY
7 1 B24778 FRONT SABOT ASSY
6 1 024777 FLOOM WELDMENT
5 1 B24759 BODY
4 1 B24758 SPACER, BODY
3 1 C24738 PAYLOAD BALLAST
2 1 C24737 DUMMY PAYLOAD
1 1 024733 WINDSHIELD
PARTS LIST
UNLESS OTHERWISE SPECIFIED DIMENSIONS ARE IN INCHES
TOLERANCES ON DECIMALS
ANGLES
MATERIAL: SEE DETAILS
HEAT TREATMENT:
FINAL PROTECTIVE FINISH:
FINAL
NEXT ASSY
USED ON
APPLICATION
ORIGINAL DATE OF DRAWING
10/1/79
PREP
CHK
ENGR
SUBMITTED
APPROVED
SPACE RESEARCH CORPORA
NORTH TROY
3-155 MM
CARGO SHELL
MOD 5
SIZE
F
CODE IDENT NO.
F24776
SCALE: 1/2
SHEET

Figure 74

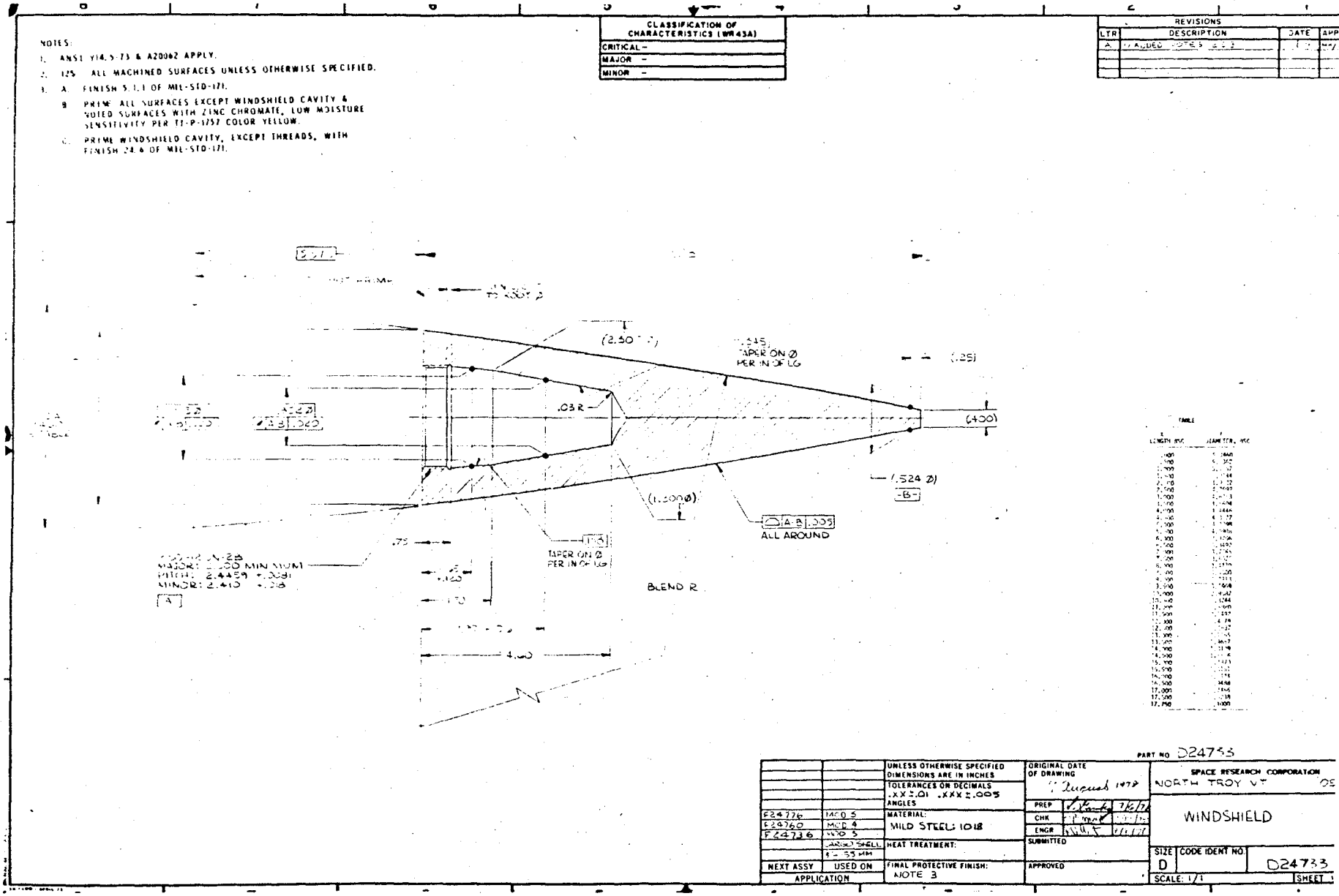
NOTES:
1. ANSI Y14.5-73 & A20062 APPLY.
2. 125 ALL MACHINED SURFACES UNLESS OTHERWISE SPECIFIED.
3. A FINISH 5.1.1 OF MIL-STD-171.
B PRIME ALL SURFACES EXCEPT WINDSHIELD CAVITY & NOTED SURFACES WITH ZINC CHROMATE, LOW MOISTURE SENSITIVITY PER TT-P-1757 COLOR YELLOW.
C PRIME WINDSHIELD CAVITY, EXCEPT THREADS, WITH FINISH 24.6 OF MIL-STD-171.
CLASSIFICATION OF CHARACTERISTICS (WR43A)
CRITICAL –
MAJOR –
MINOR –
REVISIONS
LTR DESCRIPTION DATE APP
A ADDED NOTES
(2.50 R)
.515 TAPER ON Ø PER IN OF LG
(.25)
.03 R
(.400)
.524 Ø
-B-
(1.500Ø)
.75
TAPER ON Ø PER IN OF LG
BLEND R
A-B .005 ALL AROUND
MAJOR: 2.500 MINIMUM
PITCH: 2.4459 +.0381
MINOR: 2.410 +.038
4.00
TABLE
LENGTH .XXX
DIAMETER .XXX
UNLESS OTHERWISE SPECIFIED DIMENSIONS ARE IN INCHES
TOLERANCES OR DECIMALS .XX ±.01 .XXX ±.005
ANGLES
MATERIAL:
MILD STEEL 1018
HEAT TREATMENT:
FINAL PROTECTIVE FINISH:
NOTE 3
F24776 MCD 5
F24760 MCD 4
F24736 MCD 3
NEXT ASSY
USED ON
APPLICATION
ORIGINAL DATE OF DRAWING
7 August 1979
PREP
CHK
ENGR
SUBMITTED
APPROVED
PART NO D24733
SPACE RESEARCH CORPORATION
NORTH TROY VT
WINDSHIELD
SIZE D
CODE IDENT NO.
D24733
SCALE: 1/1
SHEET

Figure 75

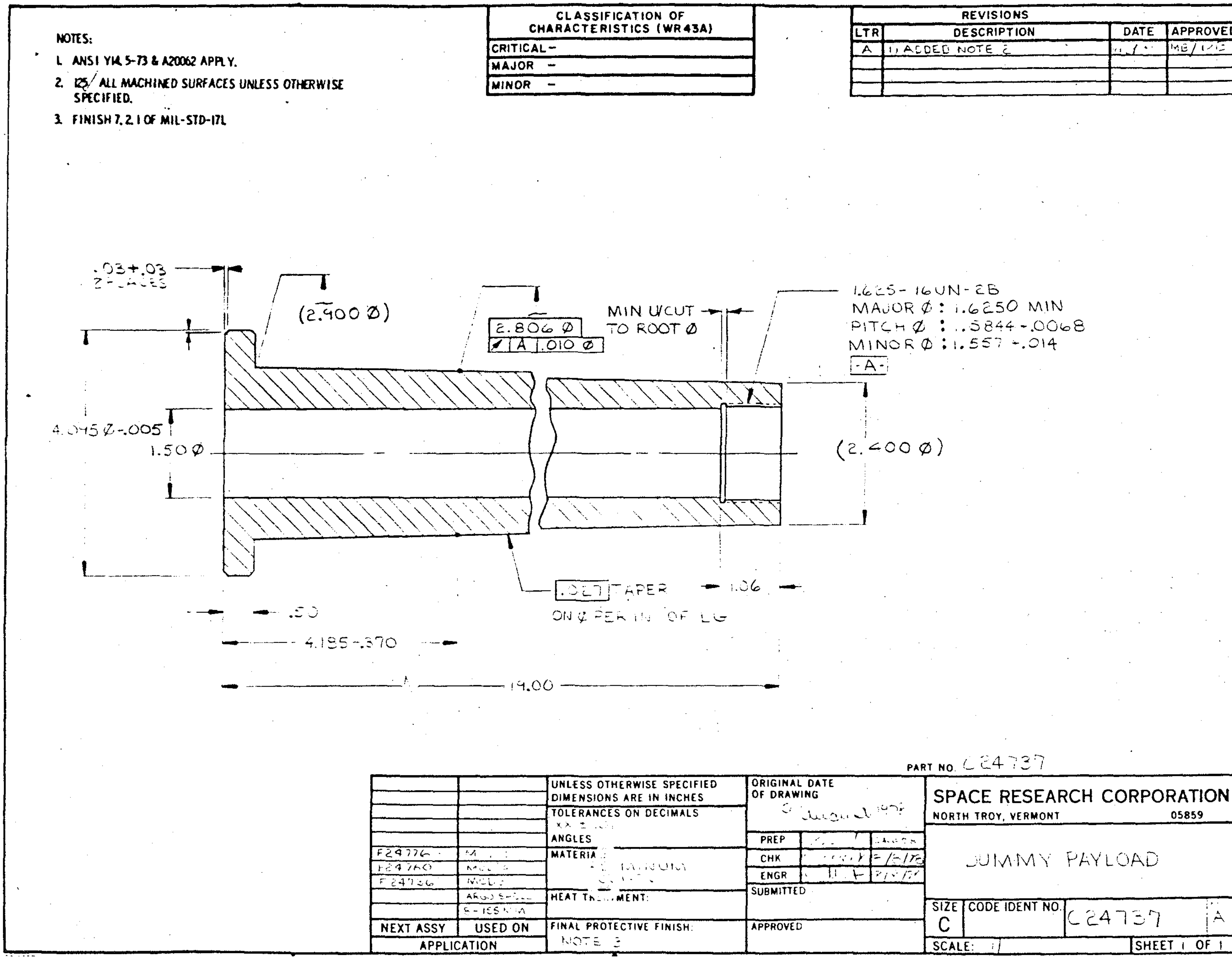
NOTES:
1. ANSI Y14.5-73 & A20062 APPLY.
2. 125/ ALL MACHINED SURFACES UNLESS OTHERWISE SPECIFIED.
3. FINISH 7.2.1 OF MIL-STD-171
CLASSIFICATION OF CHARACTERISTICS (WR43A)
CRITICAL -
MAJOR -
MINOR -
REVISIONS
LTR
DESCRIPTION
DATE
APPROVED
A
ADDED NOTE 2
.03+.03
(2.900 Ø)
2.806 Ø
A .010 Ø
MIN U/CUT TO ROOT Ø
1.625-16UN-2B
MAJOR Ø : 1.6250 MIN
PITCH Ø : 1.5844-.0068
MINOR Ø : 1.557-.014
-A-
4.045 Ø-.005
1.50 Ø
(2.400 Ø)
TAPER
ON Ø PER IN OF LG
1.06
.50
4.185-.370
19.00
PART NO. C24737
UNLESS OTHERWISE SPECIFIED
DIMENSIONS ARE IN INCHES
TOLERANCES ON DECIMALS
ANGLES
MATERIAL
HEAT TREATMENT:
FINAL PROTECTIVE FINISH:
NOTE 3
ORIGINAL DATE OF DRAWING
PREP
CHK
ENGR
SUBMITTED
APPROVED
NEXT ASSY
USED ON
APPLICATION
SPACE RESEARCH CORPORATION
NORTH TROY, VERMONT
05859
DUMMY PAYLOAD
SIZE
C
CODE IDENT NO.
C24737
A
SCALE:
SHEET 1 OF 1

Figure 76

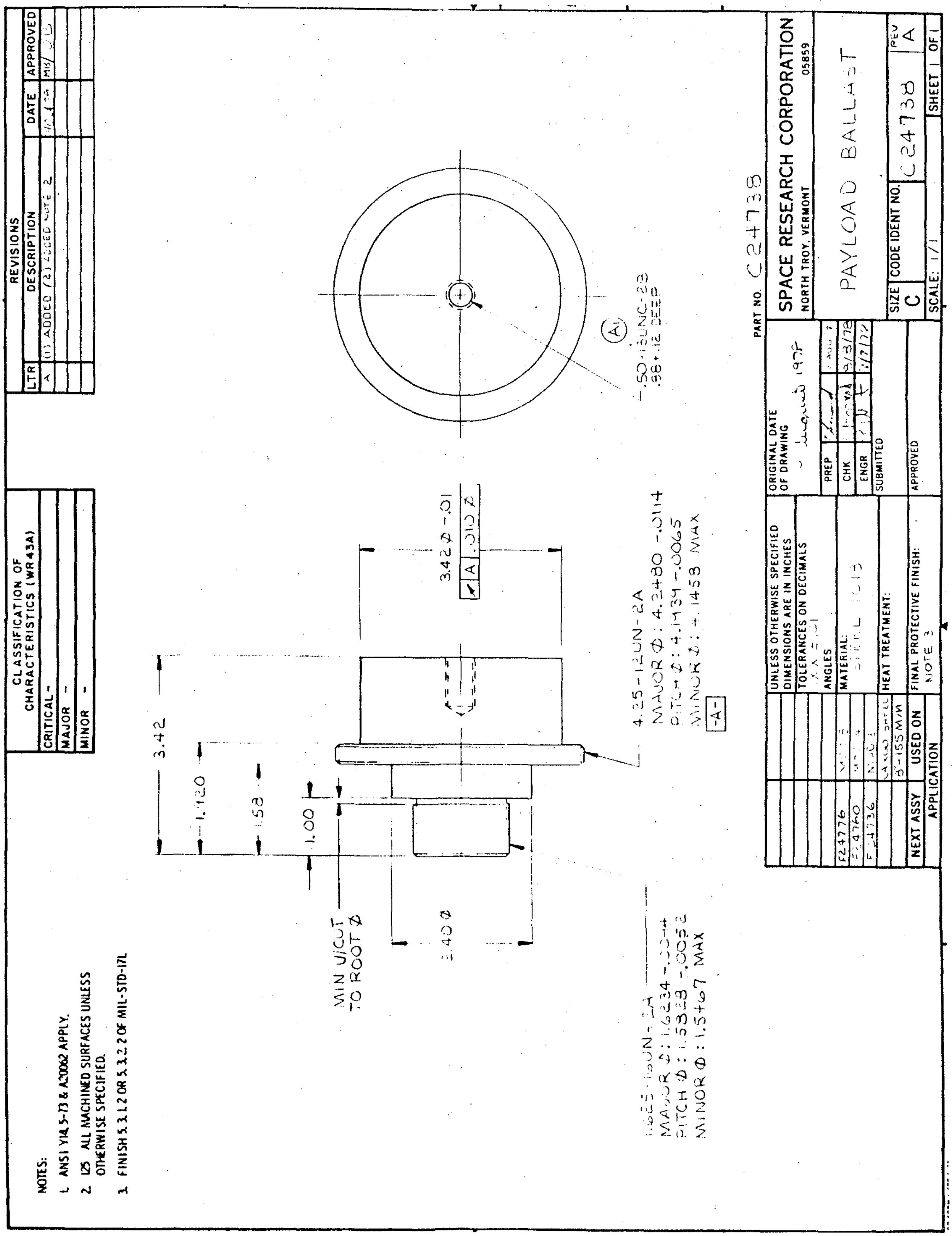
REVISIONS
LTR
DESCRIPTION
DATE
APPROVED
A
(1) ADDED (2) ADDED NOTE 2
CLASSIFICATION OF CHARACTERISTICS (WR 43A)
CRITICAL -
MAJOR -
MINOR -
NOTES:
1. ANSI Y14.5-73 & A20062 APPLY.
2. 125 ALL MACHINED SURFACES UNLESS OTHERWISE SPECIFIED.
3. FINISH 5.3.1.2 OR 5.3.2.2 OF MIL-STD-171.
3.42
1.120
.58
1.00
MIN U/CUT TO ROOT Ø
3.400
3.42 Ø -.01
A .010 Ø
4.25-12UN-2A
MAJOR Ø: 4.2480 -.0114
PITCH Ø: 4.1939 -.0065
MINOR Ø: 4.1453 MAX
-A-
MAJOR Ø: 1.6234 -.0094
PITCH Ø: 1.5833 -.0052
MINOR Ø: 1.5467 MAX
A1
.50-13UNC-2B
.88+.12 DEEP
PART NO. C24738
SPACE RESEARCH CORPORATION
NORTH TROY, VERMONT
05859
PAYLOAD BALLAST
SIZE C
CODE IDENT NO.
C24738
REV A
SCALE: 1/1
SHEET 1 OF 1
ORIGINAL DATE OF DRAWING
PREP
CHK
ENGR
SUBMITTED
APPROVED
UNLESS OTHERWISE SPECIFIED DIMENSIONS ARE IN INCHES
TOLERANCES ON DECIMALS
ANGLES
MATERIAL:
HEAT TREATMENT:
FINAL PROTECTIVE FINISH: NOTE 3
F24776
NEXT ASSY
USED ON
APPLICATION

Figure 77

REVISIONS				
ZONE	LTR	DESCRIPTION	DATE	APPROVED
	A	ADDED NOTE 4		

NOTES:

1. ANSI Y14.5-73 & A20062 APPLY.
2. MINIMUM YIELD STRENGTH 200 KPSI.
3. 125 ALL MACHINED SURFACES UNLESS OTHERWISE SPECIFIED.
4. A. FINISH 5.1.1 OF MIL-STD-171.
   B. PRIME NOTED SURFACES ONLY WITH ZINC CHROMATE LOW MOISTURE SENSITIVITY, PER TT-P-1757, COLOR YELLOW.

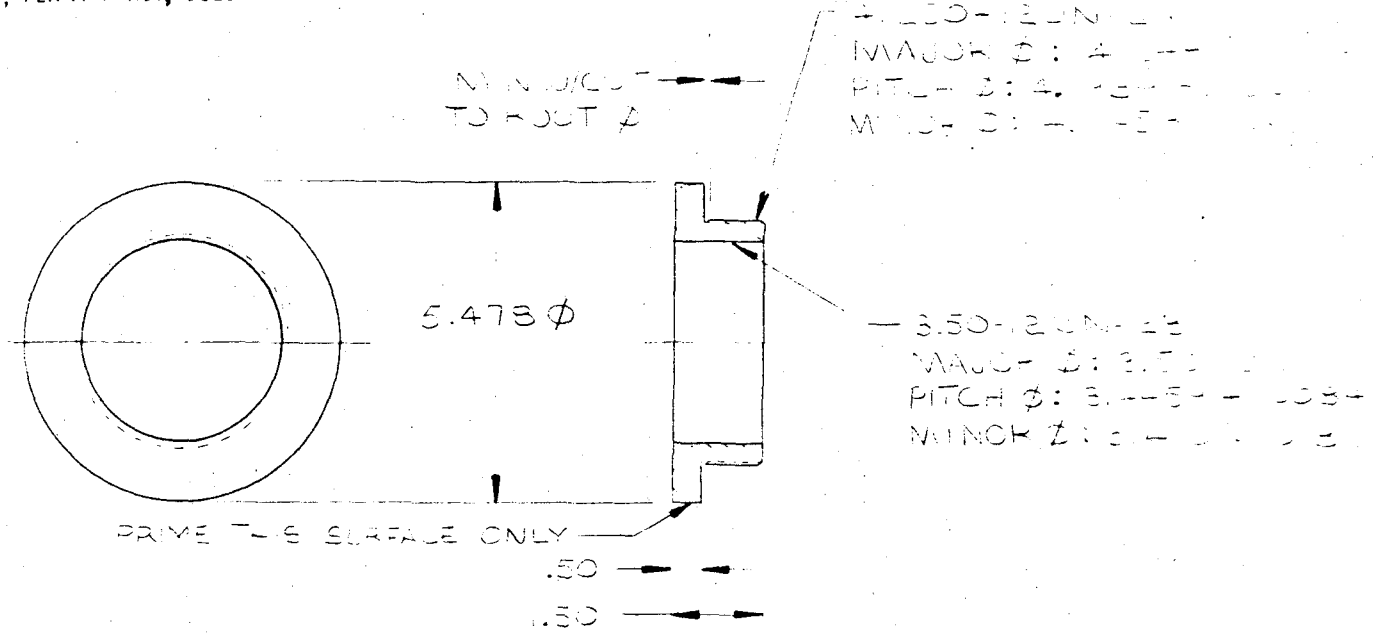

PART NO BLA[illegible]

		UNLESS OTHERWISE SPECIFIED DIMENSIONS ARE IN INCHES	ORIGINAL DATE OF DRAWING	SPACE RESEARCH CORPORATION
		TOLERANCES ON DECIMALS		
		ANGLES	PREP	
		MATERIAL	CHK	
			ENGR	
		HEAT TREATMENT	SUBMITTED	SIZE B / CODE IDENT NO. / BL-1.53
NEXT ASSY	USED ON	FINAL PROTECTIVE FINISH	APPROVED	SCALE / SHEET OF
APPLICATION				

Figure 78

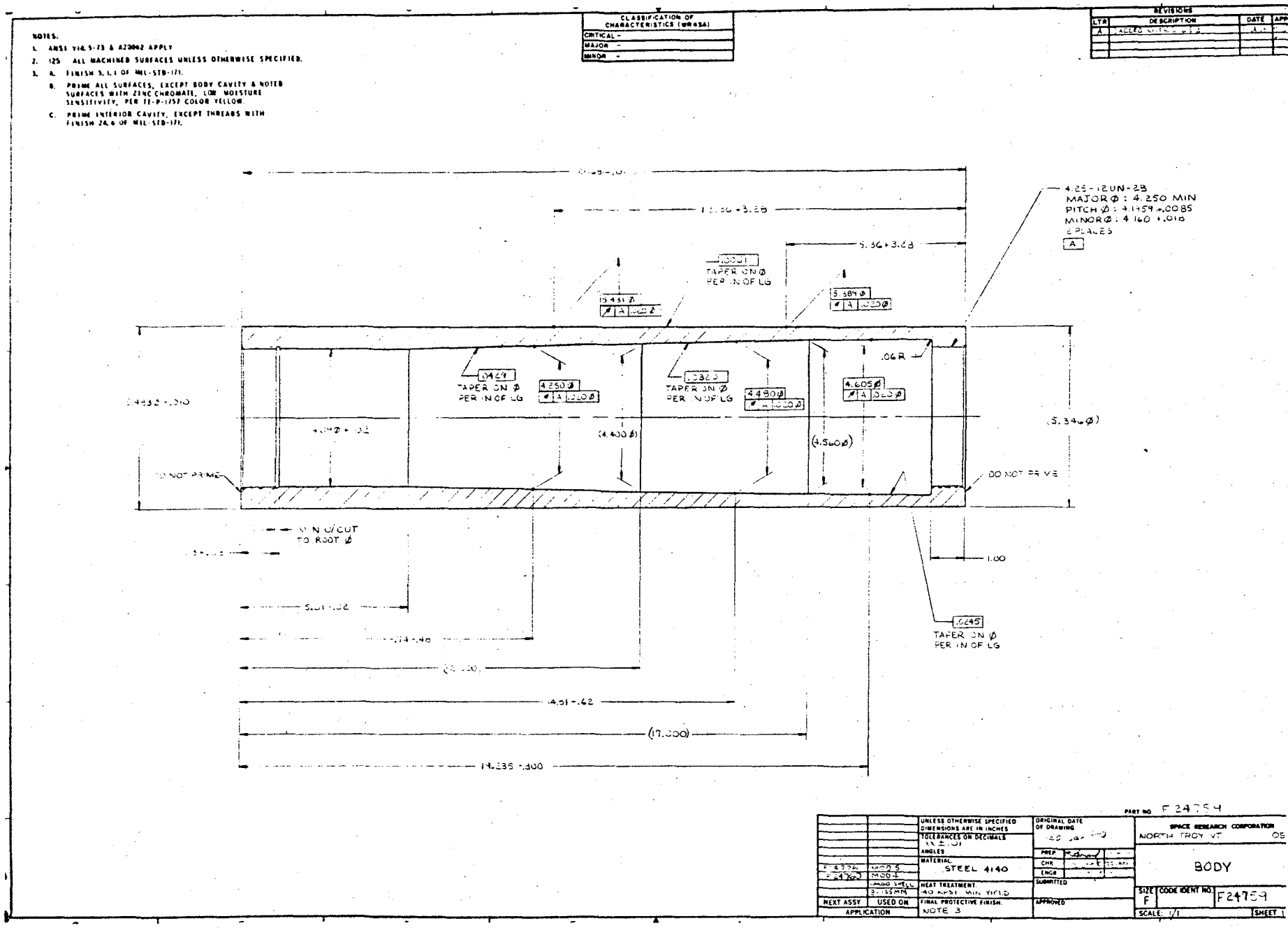
NOTES:
1. ANSI Y14.5-73 & A23002 APPLY
2. 125 ALL MACHINED SURFACES UNLESS OTHERWISE SPECIFIED.
3. A. FINISH 5.1.1 OF MIL-STD-171.
B. PRIME ALL SURFACES, EXCEPT BODY CAVITY & NOTED SURFACES WITH ZINC CHROMATE, LOW MOISTURE SENSITIVITY, PER TT-P-1757 COLOR YELLOW.
C. PRIME INTERIOR CAVITY, EXCEPT THREADS WITH FINISH 24.0 OF MIL-STD-171.
CLASSIFICATION OF CHARACTERISTICS (MIL-STD-1SA)
CRITICAL -
MAJOR -
MINOR -
REVISIONS
LTR
DESCRIPTION
DATE
4.25-12UN-2B
MAJOR Ø : 4.250 MIN
PITCH Ø : 4.1459 +.0085
MINOR Ø : 4.160 +.016
2 PLACES
A
TAPER ON Ø PER IN OF LG
TAPER ON Ø PER IN OF LG
TAPER ON Ø PER IN OF LG
.06R
DO NOT PRIME
DO NOT PRIME
(5.346Ø)
(4.400Ø)
(4.560Ø)
1.00
TAPER ON Ø PER IN OF LG
(17.000)
14.235 +.300
PART NO F24759
UNLESS OTHERWISE SPECIFIED DIMENSIONS ARE IN INCHES
TOLERANCES ON DECIMALS
ANGLES
MATERIAL
STEEL 4140
HEAT TREATMENT
140 KPSI MIN YIELD
FINAL PROTECTIVE FINISH
NOTE 3
NEXT ASSY
USED ON
APPLICATION
ORIGINAL DATE OF DRAWING
PREP
CHK
ENGR
SUBMITTED
APPROVED
SPACE RESEARCH CORPORATION
NORTH TROY VT
BODY
SIZE F
CODE IDENT NO. F24759
SCALE: 1/1
SHEET 1

Figure 79

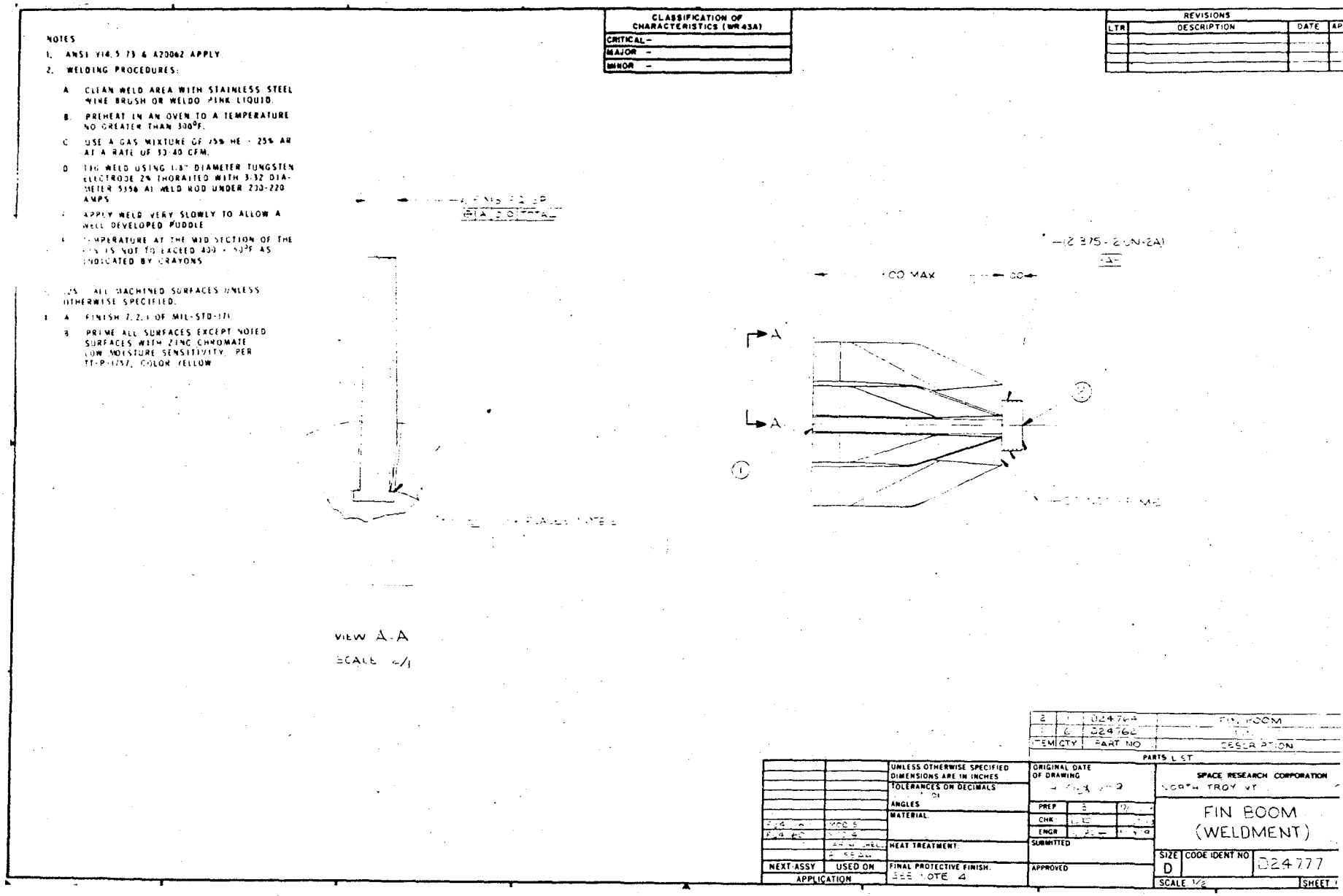
NOTES
1. ANSI Y14.5 73 & A20062 APPLY.
2. WELDING PROCEDURES:
A CLEAN WELD AREA WITH STAINLESS STEEL WIRE BRUSH OR WELDO PINK LIQUID.
B PREHEAT IN AN OVEN TO A TEMPERATURE NO GREATER THAN 300°F.
C USE A GAS MIXTURE OF 75% HE + 25% AR AT A RATE OF 30-40 CFM.
D TIG WELD USING 1/8" DIAMETER TUNGSTEN ELECTRODE 2% THORIATED WITH 3/32 DIAMETER 5356 AL WELD ROD UNDER 230-220 AMPS
E APPLY WELD VERY SLOWLY TO ALLOW A WELL DEVELOPED PUDDLE
F TEMPERATURE AT THE MID SECTION OF THE FIN IS NOT TO EXCEED 400 + 50°F AS INDICATED BY CRAYONS
3. ALL MACHINED SURFACES UNLESS OTHERWISE SPECIFIED.
A FINISH 7.2.1 OF MIL-STD-171.
B PRIME ALL SURFACES EXCEPT NOTED SURFACES WITH ZINC CHROMATE LOW MOISTURE SENSITIVITY, PER TT-P-1757, COLOR YELLOW
CLASSIFICATION OF CHARACTERISTICS (WR43A)
CRITICAL -
MAJOR -
MINOR -
REVISIONS
LTR DESCRIPTION DATE
100 MAX
30
A
A
VIEW A-A
SCALE 2/1
ITEM QTY PART NO DESCRIPTION
PARTS LIST
UNLESS OTHERWISE SPECIFIED DIMENSIONS ARE IN INCHES
TOLERANCES ON DECIMALS
ANGLES
MATERIAL
HEAT TREATMENT
FINAL PROTECTIVE FINISH
SEE NOTE 4
NEXT ASSY
USED ON
APPLICATION
ORIGINAL DATE OF DRAWING
PREP
CHK
ENGR
SUBMITTED
APPROVED
SPACE RESEARCH CORPORATION
NORTH TROY VT
FIN BOOM (WELDMENT)
SIZE D
CODE IDENT NO
024777
SCALE 1/2
SHEET

Figure 80

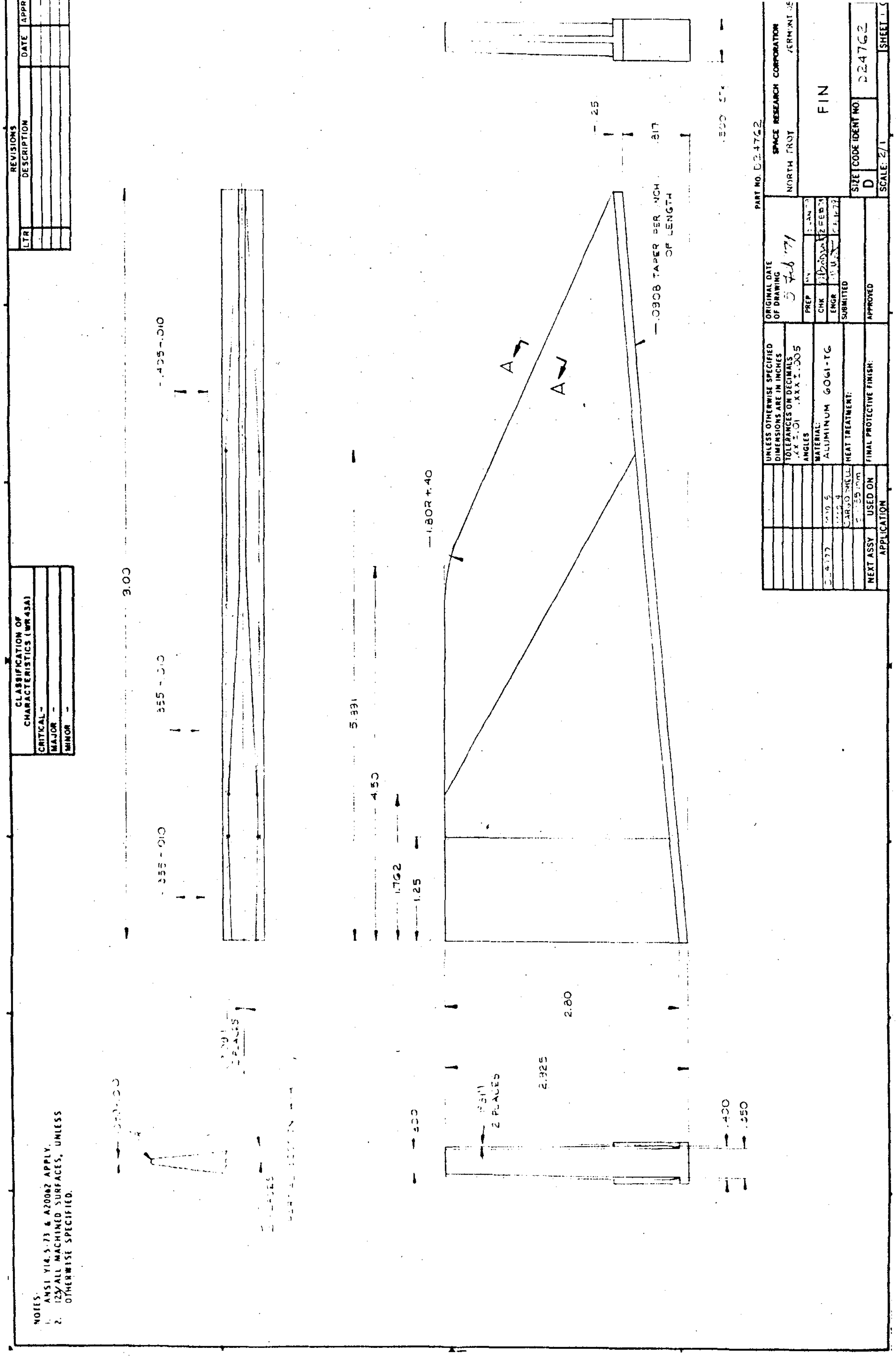

REVISIONS
LTR
DESCRIPTION
DATE
APPR
CLASSIFICATION OF CHARACTERISTICS (WR43A)
CRITICAL -
MAJOR -
MINOR -
NOTES:
1. ANSI Y14.5-73 & A200&2 APPLY.
2. 125/ALL MACHINED SURFACES, UNLESS OTHERWISE SPECIFIED.
3.00
5.331
2.80
2.925
1.762
1.25
.450
.400
.350
.817
.25
2 PLACES
-1.80R +.40
-.0308 TAPER PER INCH OF LENGTH
A
A
UNLESS OTHERWISE SPECIFIED DIMENSIONS ARE IN INCHES
TOLERANCES ON DECIMALS
ANGLES
MATERIAL:
ALUMINUM 6061-T6
HEAT TREATMENT:
FINAL PROTECTIVE FINISH:
NEXT ASSY
USED ON
APPLICATION
ORIGINAL DATE OF DRAWING
5 Feb '71
PREP
CHK
ENGR
SUBMITTED
APPROVED
PART NO. D24762
SPACE RESEARCH CORPORATION
NORTH TROY
VERMONT
FIN
SIZE
D
CODE IDENT NO.
D24762
SCALE: 2/1
SHEET

Figure 81

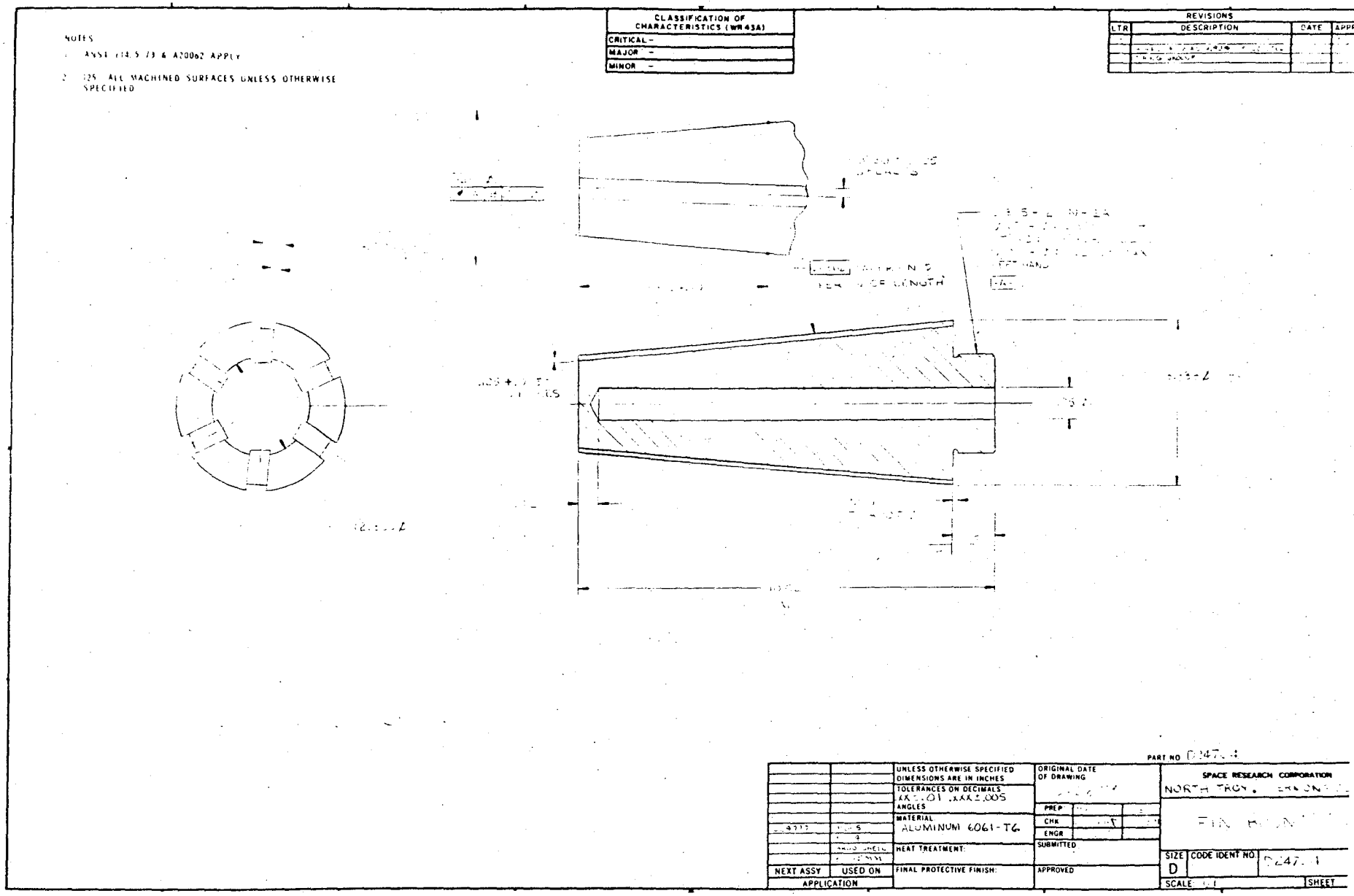
NOTES
CLASSIFICATION OF CHARACTERISTICS (WR43A)
CRITICAL –
MAJOR –
MINOR –
REVISIONS
LTR
DESCRIPTION
DATE
UNLESS OTHERWISE SPECIFIED DIMENSIONS ARE IN INCHES
TOLERANCES ON DECIMALS
ANGLES
MATERIAL
ALUMINUM 6061-T6
HEAT TREATMENT:
FINAL PROTECTIVE FINISH:
ORIGINAL DATE OF DRAWING
PREP
CHK
ENGR
SUBMITTED
APPROVED
NEXT ASSY
USED ON
APPLICATION
SPACE RESEARCH CORPORATION
SIZE
CODE IDENT NO.
D
SCALE
SHEET

Figure 82

NOTES:

1. ANSI Y14.5-73 & A20052 APPLY.
2. 125 ALL MACHINED SURFACES UNLESS OTHERWISE SPECIFIED.
3. FINISH SABOT ONLY, ITEM 2, WITH 7.5.1 OF MIL-STD-171 HARDCOAT TO BE .003 THICK.

REVISIONS				
ZONE	LTR	DESCRIPTION	DATE	APPROVE

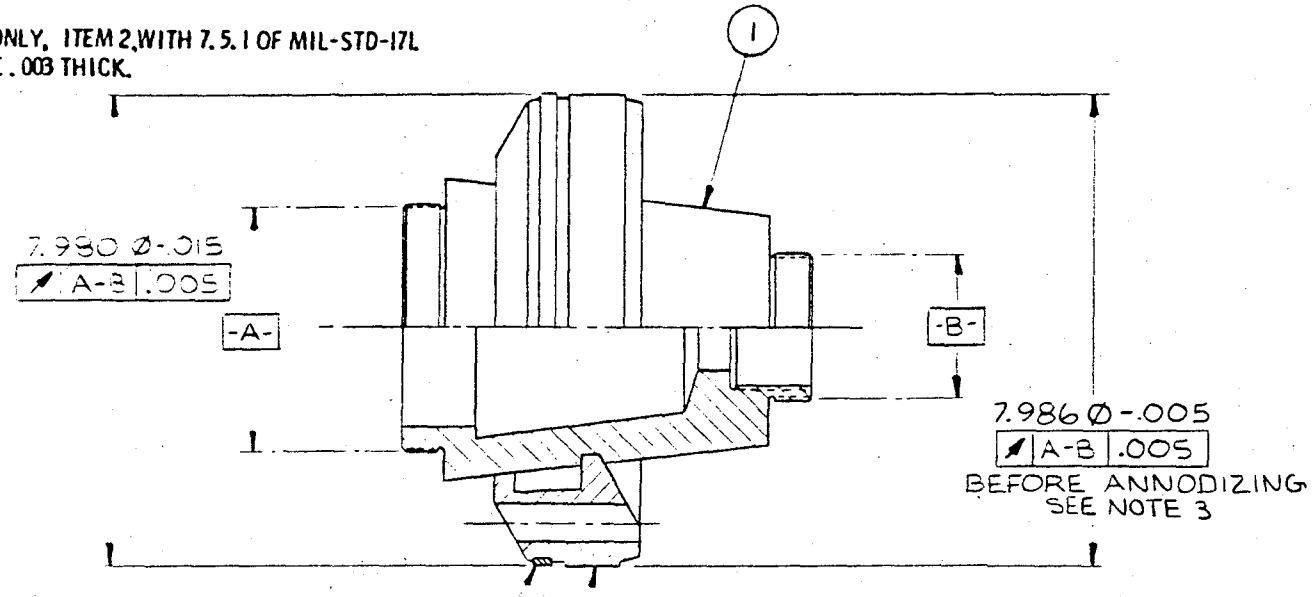

ITEM	QTY	PART NO.	DESCRIPTION
3	1	A24115	RETAINING RING
2	1	D24775	FRONT SABOT
1	1	D24732	FRONT SABOT CARRIER

PARTS LIST

NEXT ASSY	USED ON
F24776	MOD 5
	CARGO SHELL
	B .155 MM

APPLICATION

UNLESS OTHERWISE SPECIFIED DIMENSIONS ARE IN INCHES

TOLERANCES ON DECIMALS

ANGLES

MATERIAL:

HEAT TREATMENT:

FINAL PROTECTIVE FINISH: SEE DETAILS

ORIGINAL DATE OF DRAWING 4 Oct 79

PREP	MB	9/14/79
CHK	[illegible]	[illegible]
ENGR	[illegible]	[illegible]

SUBMITTED

APPROVED

SPACE RESEARCH CORPORATION
NORTH TROY VT 05859

FRONT SABOT ASS'Y

SIZE	CODE IDENT NO.		RE
B		B24778	

SCALE: 1/2 SHEET 1 OF 1

Figure 83

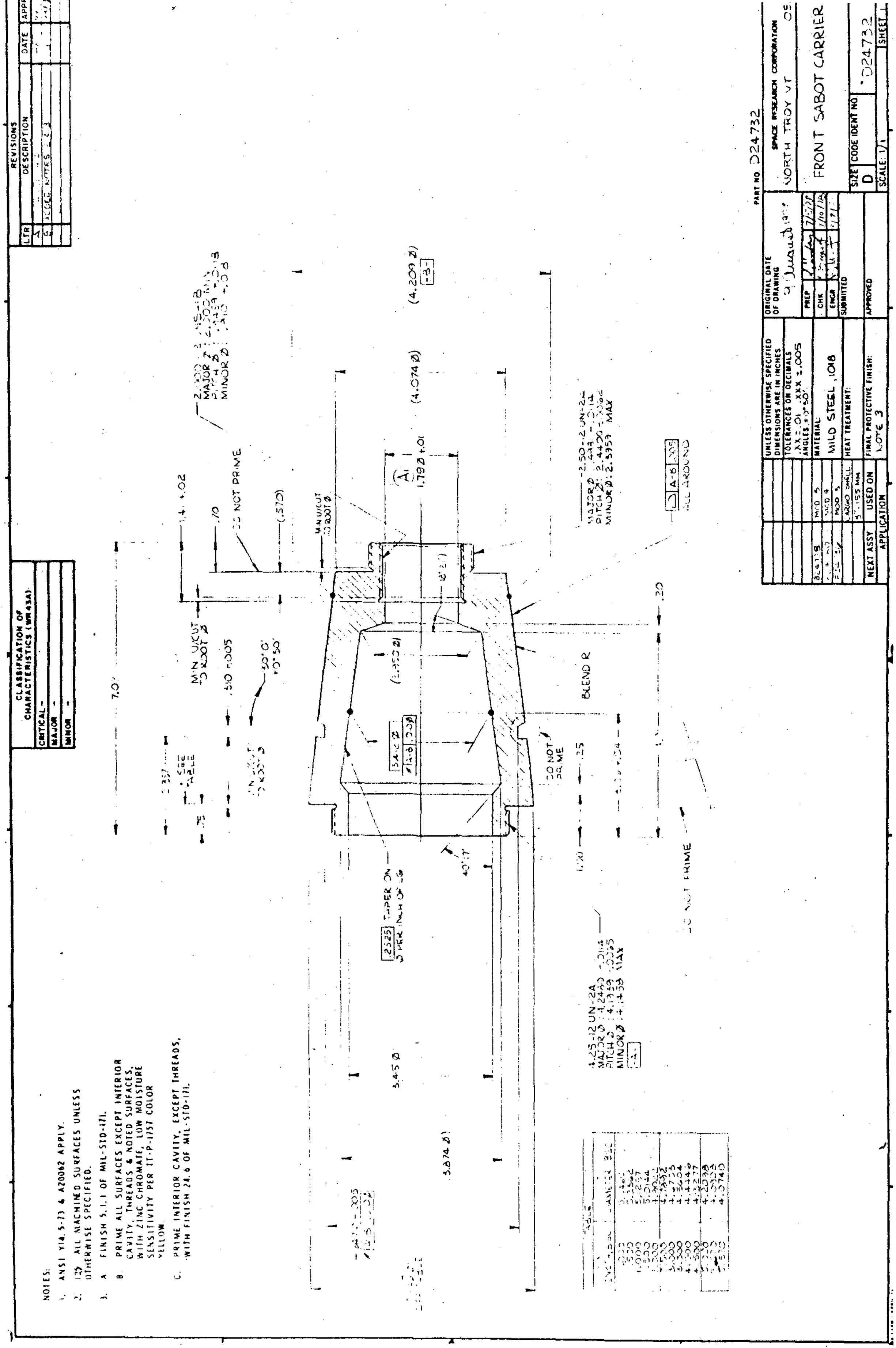
NOTES:
1. ANSI Y14.5-73 & A20062 APPLY.
2. 125 ALL MACHINED SURFACES UNLESS OTHERWISE SPECIFIED.
3. A FINISH 5.1.1 OF MIL-STD-171.
B. PRIME ALL SURFACES EXCEPT INTERIOR CAVITY, THREADS & NOTED SURFACES, WITH ZINC CHROMATE, LOW MOISTURE SENSITIVITY PER TT-P-1757 COLOR YELLOW.
C. PRIME INTERIOR CAVITY, EXCEPT THREADS, WITH FINISH 24.6 OF MIL-STD-171.
CLASSIFICATION OF CHARACTERISTICS (WR43A)
CRITICAL -
MAJOR -
MINOR -
REVISIONS
LTR
DESCRIPTION
DATE
DO NOT PRIME
BLEND R
UNLESS OTHERWISE SPECIFIED DIMENSIONS ARE IN INCHES
MATERIAL: MILD STEEL, 1018
FINAL PROTECTIVE FINISH: NOTE 3
NEXT ASSY
USED ON
APPLICATION
ORIGINAL DATE OF DRAWING
PREP
CHK
ENGR
SUBMITTED
APPROVED
PART NO. D24732
SPACE RESEARCH CORPORATION
NORTH TROY VT
FRONT SABOT CARRIER
SIZE D
CODE IDENT NO
D24732
SCALE 1/1
SHEET

Figure 84

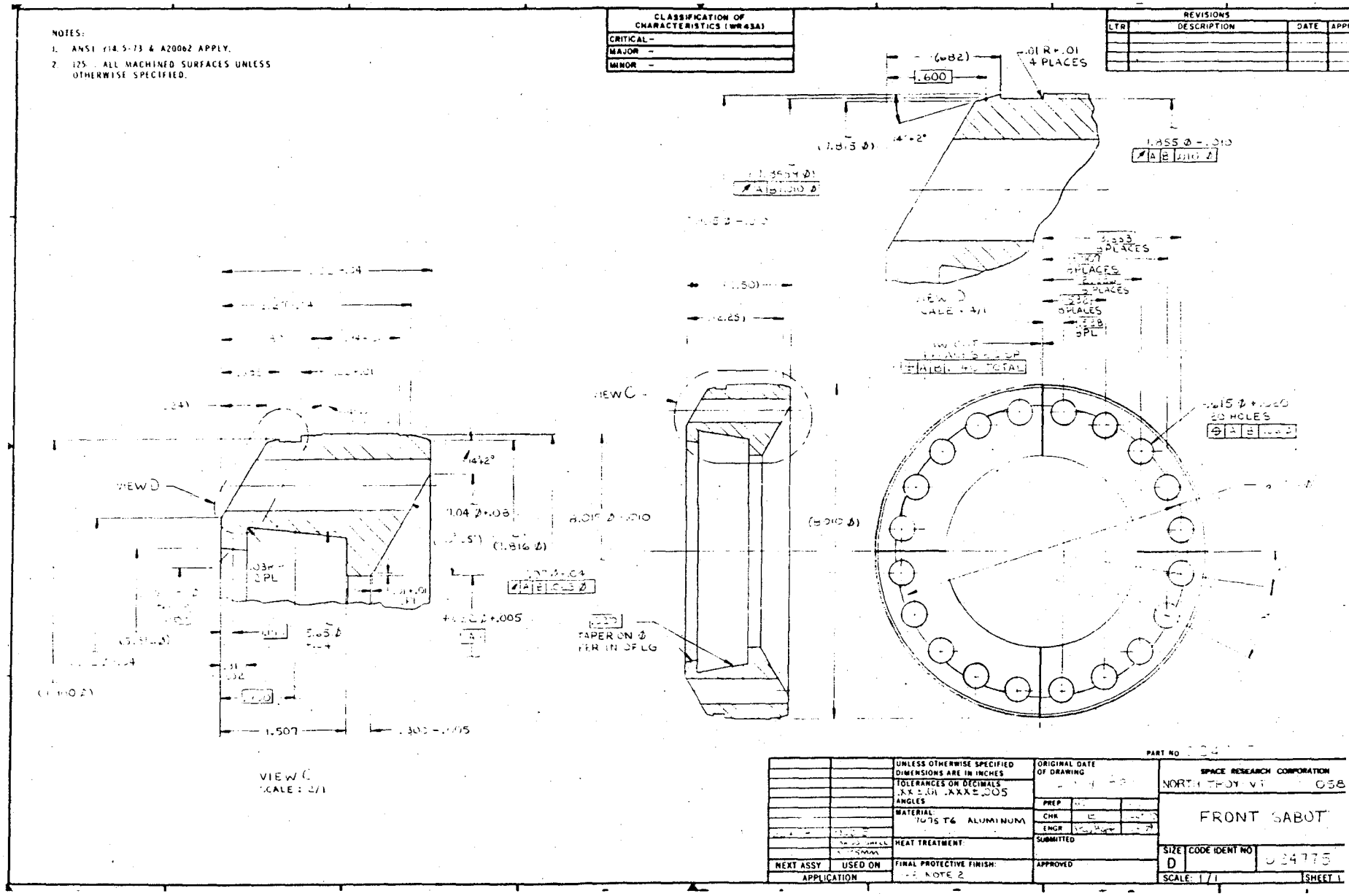
NOTES:
1. ANSI Y14.5-73 & A20062 APPLY.
2. 125 - ALL MACHINED SURFACES UNLESS OTHERWISE SPECIFIED.
CLASSIFICATION OF CHARACTERISTICS (MIL-STD-63A)
CRITICAL -
MAJOR -
MINOR -
REVISIONS
LTR
DESCRIPTION
DATE
1.600
VIEW D
SCALE : 4/1
VIEW C
SCALE : 2/1
TAPER ON Ø PER IN OF LG
20 HOLES
UNLESS OTHERWISE SPECIFIED DIMENSIONS ARE IN INCHES
TOLERANCES ON DECIMALS .XX ±.01 .XXX ±.005
ANGLES
MATERIAL 7075 T6 ALUMINUM
HEAT TREATMENT
FINAL PROTECTIVE FINISH:
NOTE 2
NEXT ASSY
USED ON
APPLICATION
ORIGINAL DATE OF DRAWING
PREP
CHK
ENGR
SUBMITTED
APPROVED
SPACE RESEARCH CORPORATION
NORTH TROY VT 058
FRONT GABOT
SIZE
D
CODE IDENT NO
SCALE: 1/1
SHEET 1

Figure 85

NEXT ASSY	USED ON	LTR	DESCRIPTION	DATE	APPROVED
	8"-155MM	A	[illegible] ADDED NOTE 2	[illegible]	[illegible]
C24119	[illegible]				
[illegible]	MOD [illegible]				
[illegible]	MOD [illegible]				
[illegible]	MOD 4				
B24778	MOD 5				

NOTES:

1. ANSI Y14.5-73 & A20062 APPLY.
2. 125/ ALL MACHINED SURFACES UNLESS OTHERWISE SPECIFIED.

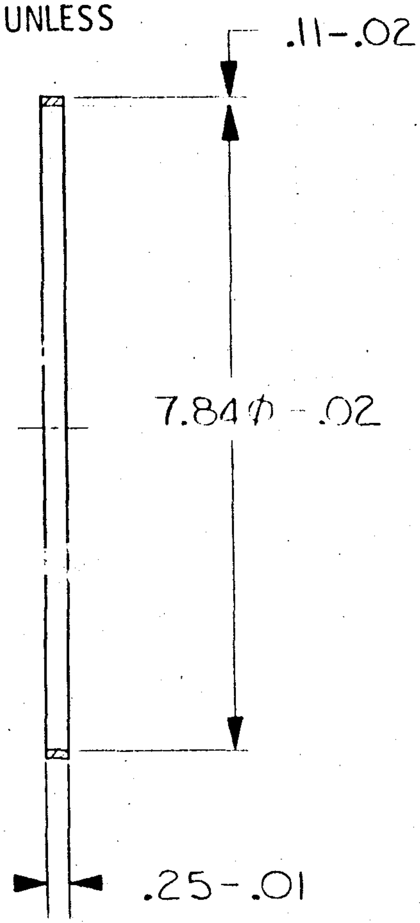

UNLESS OTHERWISE SPECIFIED DIMENSIONS ARE IN INCHES TOLERANCES FRACTIONS ANGLES 3 PLACE DECIMALS ± 2 PLACE DECIMALS ±	[illegible]		SPACE RESEARCH CORPORATION NORTH TROY VT 05859	
	PREP	S Douglas	25 July 77	RETAINING RING
MATERIAL: POLY PROPYLENE	CHK	D Brown	26 JULY 77	
	ENGR	[illegible]	[illegible]	
			SIZE A | CODE IDENT NO | DRAWING NO A24115 | REV A	
			SCALE: 1/2 | SHEET 1 OF 1	

Figure 86

REVISIONS				
ZONE	LTR	DESCRIPTION	DATE	APPRO

NOTES:

1. ANSI Y14.5-73 & A20062 APPLY.
2. SAW CUTS ON SECONDARY OBTURATOR AND REAR SABOT ARE NOT TO ALIGN AT ASSEMBLY.
3. PRESSURE BARRIER CAVITY SHOULD BE FILLED WITH GENERAL ELECTRIC RTV-II WITH NUOCURE 73.

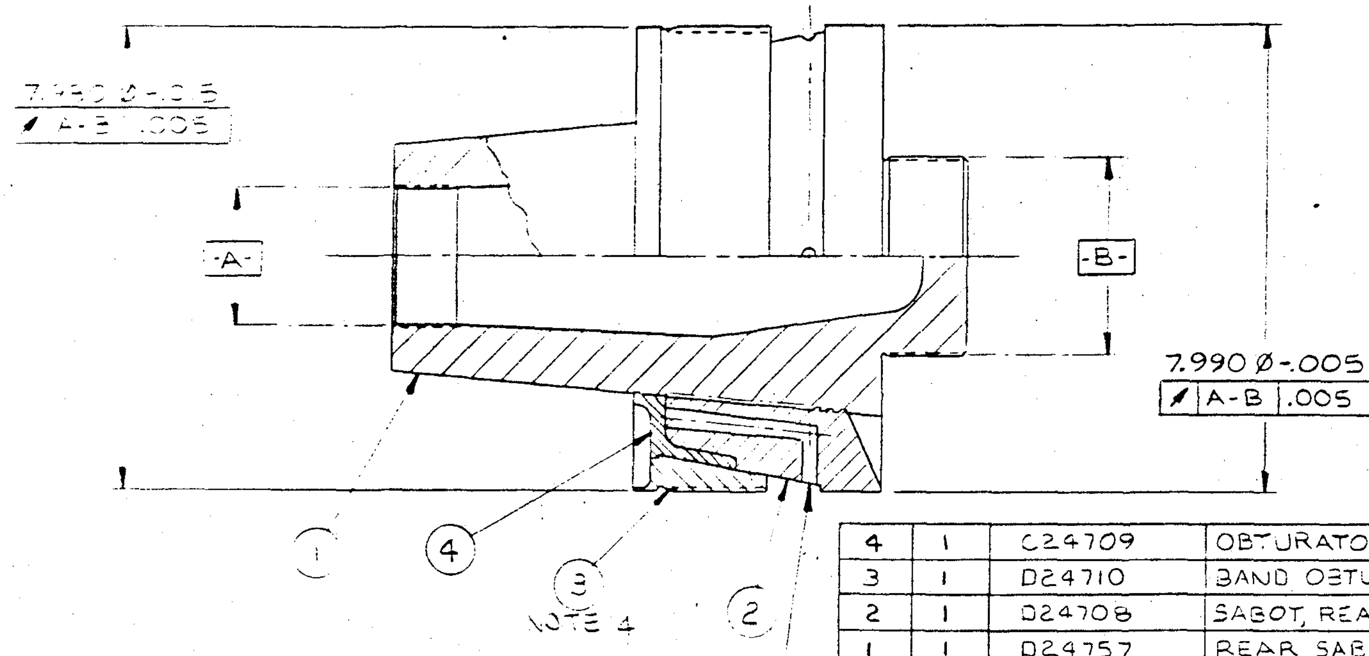

4. APPLY A THIN COAT OF SILICONE GREASE ON THE INSIDE DIA OF OBTURATOR BAND, ITEM 3 PRIOR TO ASSEMBLY.

ITEM	QTY	PART NO.	DESCRIPTION
4	1	C24709	OBTURATOR SECONDARY
3	1	D24710	BAND OBTURATOR
2	1	D24708	SABOT, REAR
1	1	D24757	REAR SABOT CARRIER

PARTS LIST

NEXT ASSY	USED ON
[illegible]	MOD 5 CARGO SHELL [illegible]

APPLICATION

UNLESS OTHERWISE SPECIFIED DIMENSIONS ARE IN INCHES

TOLERANCES ON DECIMALS

ANGLES

MATERIAL:

HEAT TREATMENT:

FINAL PROTECTIVE FINISH:

ORIGINAL DATE OF DRAWING: 4 Oct 79

PREP	[illegible]	9/14/79
CHK	DB	2 OCT 79
ENGR	[illegible]	[illegible]

SUBMITTED

APPROVED

SPACE RESEARCH CORPORATION
NORTH TROY VT 05859

REAR SABOT ASS'Y

SIZE: B | CODE IDENT NO. | B24779

SCALE: 1/2 | SHEET 1 OF

Figure 87

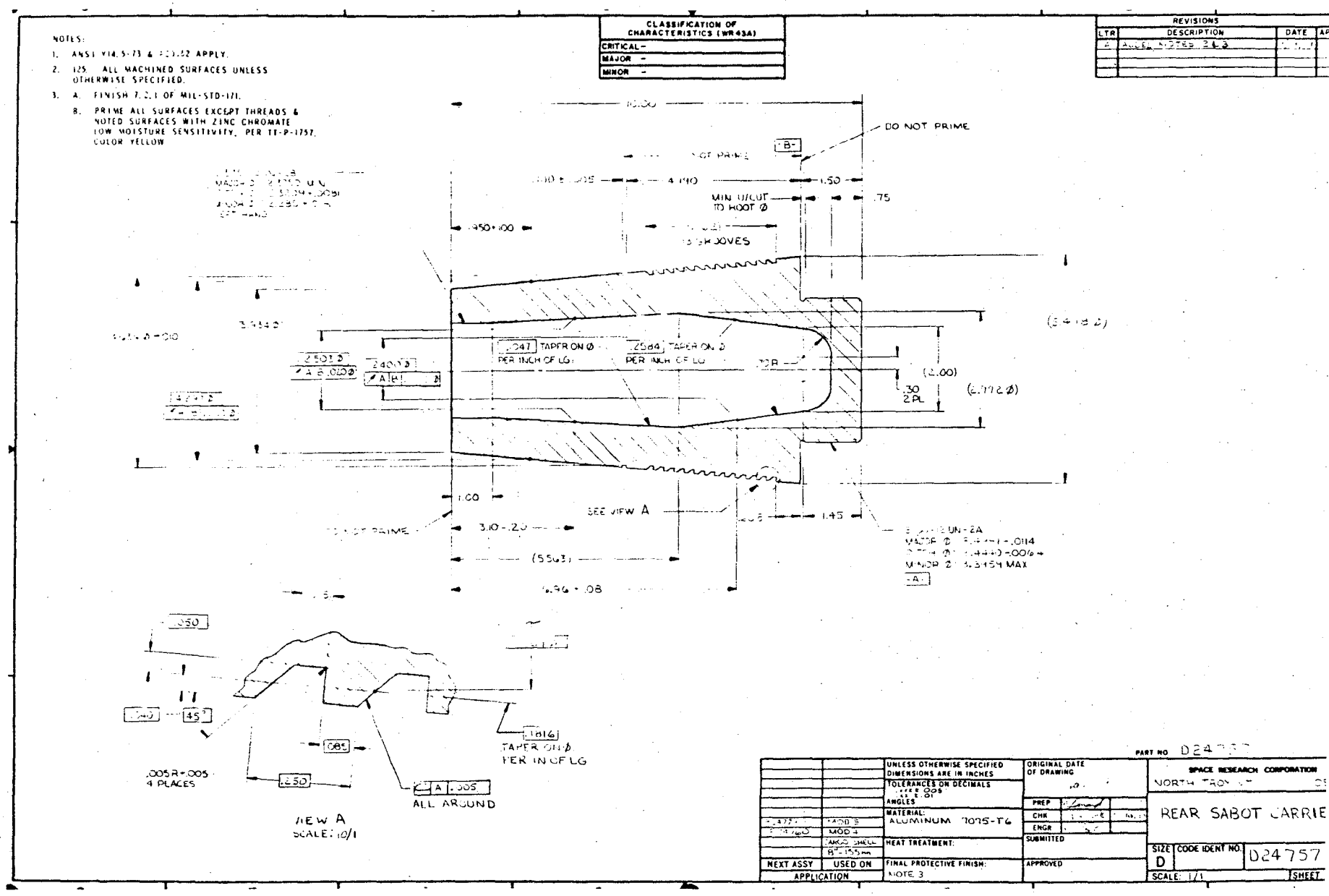

Figure 88

Copy available to DTIC does not permit fully legible reproduction

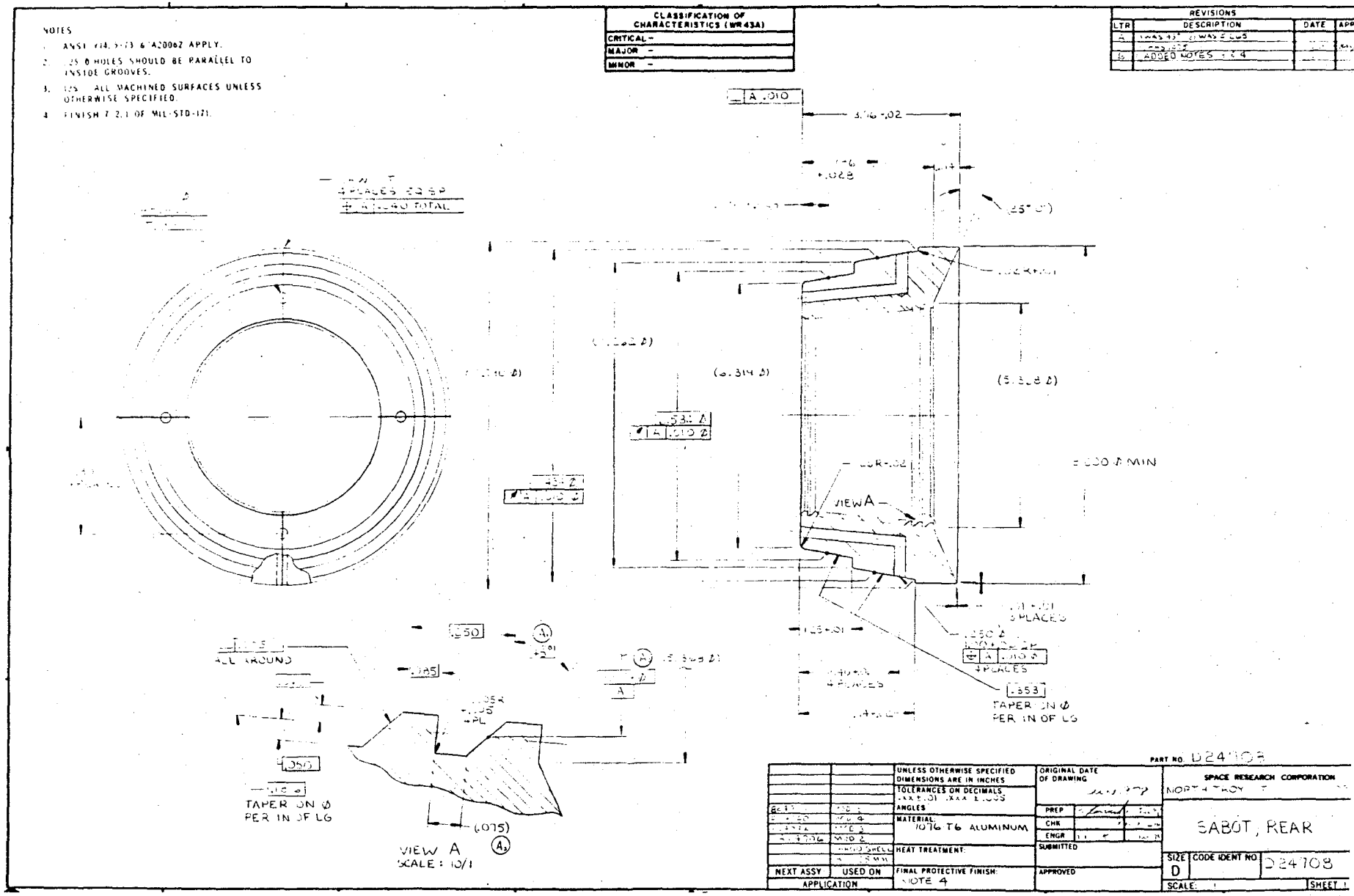

Figure 89

Copy available to DTIC does not permit fully legible reproduction

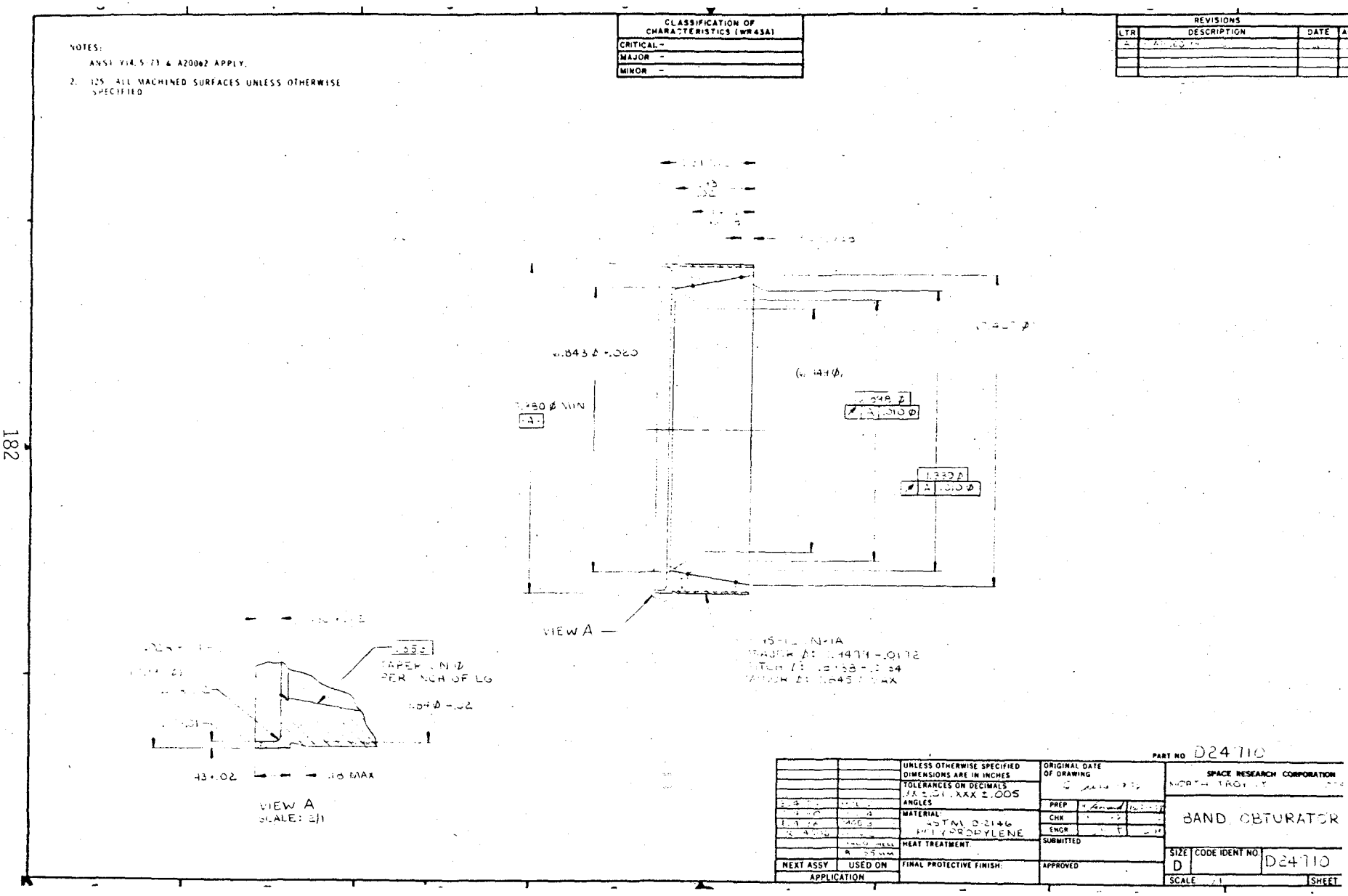

Figure 90

Copy available to DTIC does not permit fully legible reproduction

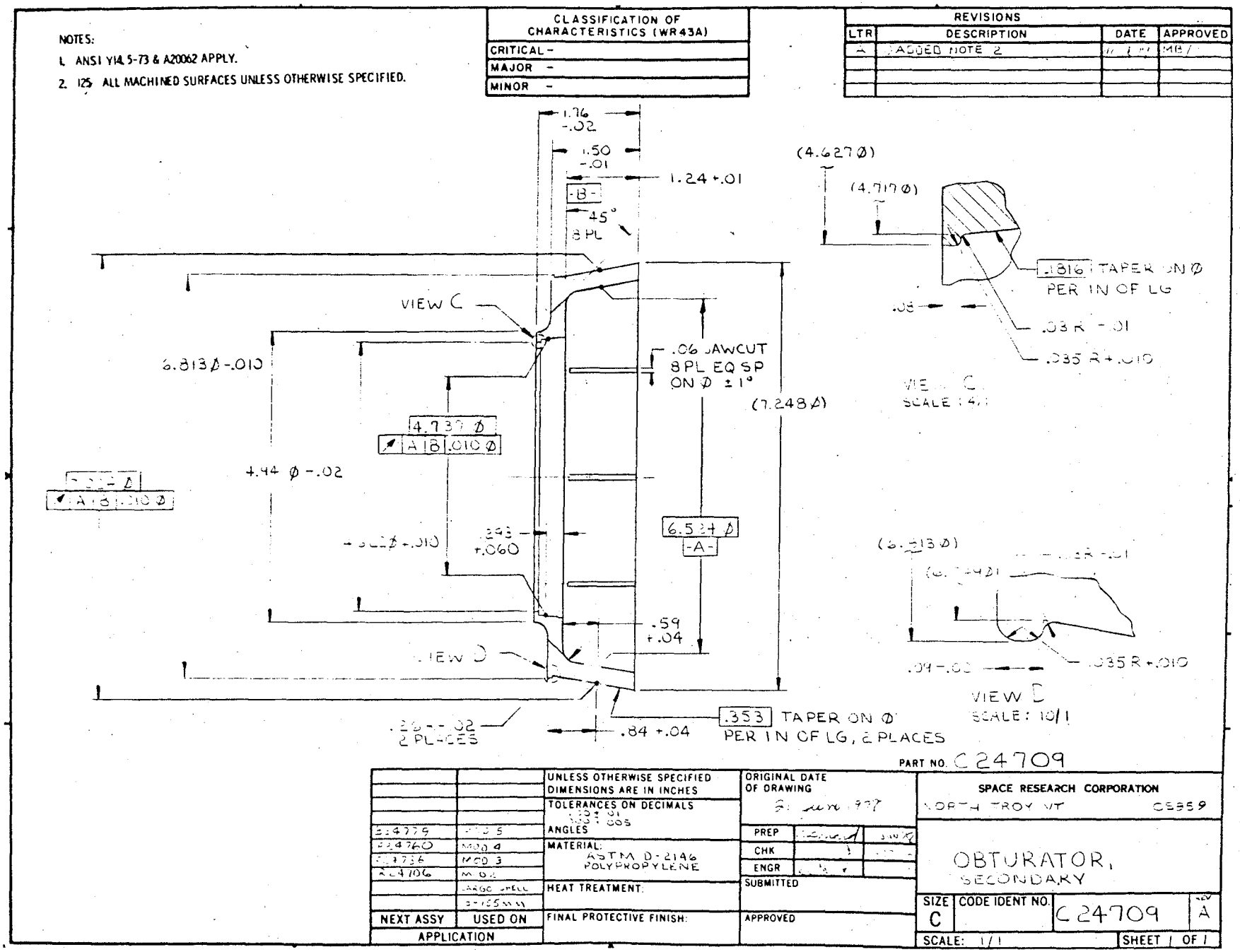

Figure 91

Copy available to DTIC does not permit fully legible reproduction

7.0 CONCLUSIONS AND RECOMMENDATIONS

The 8-inch subcaliber ammunition development program described in this report culminated in the successful flight tests at Yuma Proving Ground, during which the greatly enhanced range capability of the prototype hardware was demonstrated. The range goal of 40 km was exceeded, thereby doubling the range capability of the 8-inch weapon firing the standard M106 round with zone eight charge. Additional prototype rounds have been fabricated and delivered to the Army for further test and evaluation. Completion of this effort has resulted in several recommendations for future work, as outlined in this section.

a) Charge Development - Propelling charges used so far in testing prototype hardware were quickly assembled from available materials, since the contract scope of work did not include charge development and no other charges were available. They performed reasonably well but are not optimized for this application. Specific effort should be expended to develop an optimized charge for propelling the 8-inch subcaliber cargo ammunition.

b) Frangible Sabot - A goal of the current program was development of a sabot system which would permit effective and repeatable gun launch of the 8-inch subcaliber round and also cleanly discard without causing tipoff or fin interference. This goal was achieved as evidenced during the flight test program. However the sabot system contains some metal parts which brings up the question of a safety zone requirement in front of the gun. With relatively large discarding parts, current employment doctrine would require the 8-inch subcaliber round be listed as a special purpose item. Since work has been ongoing to develop a frangible sabot system, these efforts should be applied to the 8-inch subcaliber round.

c) Base Ejection - The 8-inch subcaliber round is designed to be used for delivery of various cargoes, including submunitions and mines which must be base ejected during projectile flight. Much experience is available from other programs using base eject and should be utilized in configuring the base eject concept for this round. The effort would include payload packaging, base design, ejection charge configuration, and delivery parameters.

d) Thin Body Shells - Prototype shells tested to date have utilized standard steels with relatively thick skins. It has been previously suggested that high strength steels be evaluated for the body. Successful employment of these high strength steels would result in reduced round weight and greater payload volume due to thinner skin. Manufacturing techniques using this new design would also require investigation.

e) Shot Start and Fall Back - The fin stabilized prototype projectile tested under this program is seated without interference in the tube for firing. Since the shell is not rammed, small variations have been observed in pressure data to due to lack of shot start. Further, at high QE, some external means (not part of the projectile) is required to prevent fall back of the shell prior to firing. These problem areas should be addressed to improve the performance of the projectile.

f) Field Handling - Since by design the 8-inch subcaliber shell has exposed fins and sabotry, it requires different handling to prevent damage prior to firing. Techniques for proper field handling must be devised to assure acceptance and resultant performance of the ammunition.

g) Fin Manufacture - For the prototype hardware fabricated so far, the fins have been welded to the tail boom. Although performance has been excellent, this technique is not considered best for production due to cost, potential welding induced structural problems, and delivery inaccuracies due to weld bead surface variation. Manufacturing methods should be investigated for fin fabrication in volume production. These methods would include impact extrusion, forging and casting.

h) Aerodynamic Data - During the initial flight tests of Yuma Proving Ground, Hawk radar data were collected which provide trajectory data for the test vehicle firings. These data should be analyzed to provide detailed projectile flight characteristics, such as drag, as well as other information useful in predicting trajectory and range data for future tests.

Completion of the above items of work, coupled with the demonstrated capability of the prototype hardware, will result in an 8-inch subcaliber cargo round that will meet performance requirements and provide the Army with an extended range cargo delivery vehicle which will greatly enhance its artillery inventory and capability.

APPENDIX A

This appendix presents the design drawings of the four test slug configurations used during this study. Table A1 presents the combination and drawing numbers of parts used to construct the four test slug configurations. The drawings are presented in Figures A1 to A15.

TABLE A1. 8-INCH SUBCALIBER TEST SLUG PARTS LIST

Drawing Number	Title
C22975	Test Slug Assembly (Vent Fin-Rear Sabot)
D22954	Vent Fin Boom
C22959	Body
C22972	Nose
D22973	Sabot
D22974	Band
C22955	Closure
C22976	Test Slug Assembly (Vent Fin-Center Sabot)
D22954	Vent Fin Boom
C22971	Body
C22972	Nose
D22973	Sabot
D22974	Band
C22956	Closure
C22977	Test Slug Assembly (Solid Fin-Rear Sabot)
D22958	Solid Fin Boom
C22959	Body
C22972	Nose
D22973	Sabot
D22974	Band
C22978	Test Slug Assembly (Solid Fin-Center Sabot)
D22957	Solid Fin Boom
D22971	Body
C22972	Nose
D22973	Sabot
D22974	Band

NOTES:

1. APPLY A LIGHT COATING OF SILICONE GREASE, MIL-C-21567, ON TAPERED SURFACE OF ITEM 4, PRIOR TO INSTALLATION OF ITEM 5.
2. HEAT ITEM 5 IN BOILING WATER FOR 10 TO 20 MINUTES PRIOR TO INSTALLATION. INSTALL ITEM 5 BY APPLYING A FORCE OVER ITS ENTIRE REAR FACE.

CLASSIFICATION OF CHARACTERISTICS (WR43A)
CRITICAL –
MAJOR –
MINOR –

REVISIONS		
LTR	DESCRIPTION	E

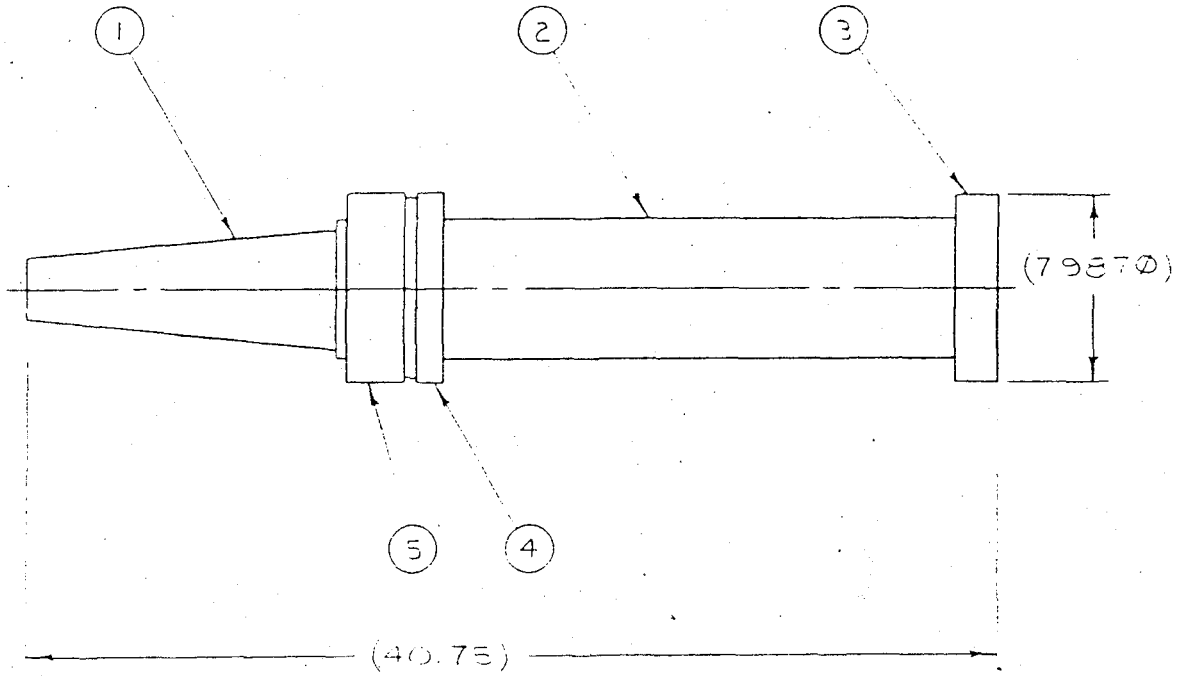

ITEM NO	PART NO.	TITLE
5	D22974	BAND
4	D22973	SABOT
3	C22972	NOSE
2	C22959	BODY
1	D22958	SOLID FIN S

PARTS LIST

Figure A1

		UNLESS OTHERWISE SPECIFIED DIMENSIONS ARE IN INCHES	ORIGINAL DATE OF DRAWING	SPACE RESEARCH CORPOR
		TOLERANCES ON DECIMALS		NORTH TROY, VERMONT
		ANGLES	PREP [signature] 4APR77	TEST SLUG ASSY
		MATERIAL	CHK	(SOLID FIN – REAR SA
			ENGR [signature] 4APR77	
	TEST SLUG	HEAT TREATMENT	SUBMITTED	SIZE C / CODE IDENT NO. 30478 / C22977
FINAL	8"-155mm			
NEXT ASSY	USED ON	FINAL PROTECTIVE FINISH	APPROVED	SCALE 1/4 / SHEET
APPLICATION				

NOTES:

1. APPLY A LIGHT COATING OF SILICONE GREASE, MIL-G-21567, ON TAPERED SURFACE OF ITEM 4, PRIOR TO INSTALLATION OF ITEM 5.
2. HEAT ITEM 5 IN BOILING WATER FOR 10 TO 20 MINUTES PRIOR TO INSTALLATION. INSTALL ITEM 5 BY APPLYING A FORCE OVER ITS ENTIRE REAR FACE.

CLASSIFICATION OF CHARACTERISTICS (WR43A)
CRITICAL –
MAJOR –
MINOR –

REVISIONS		
LTR	DESCRIPTION	DATE

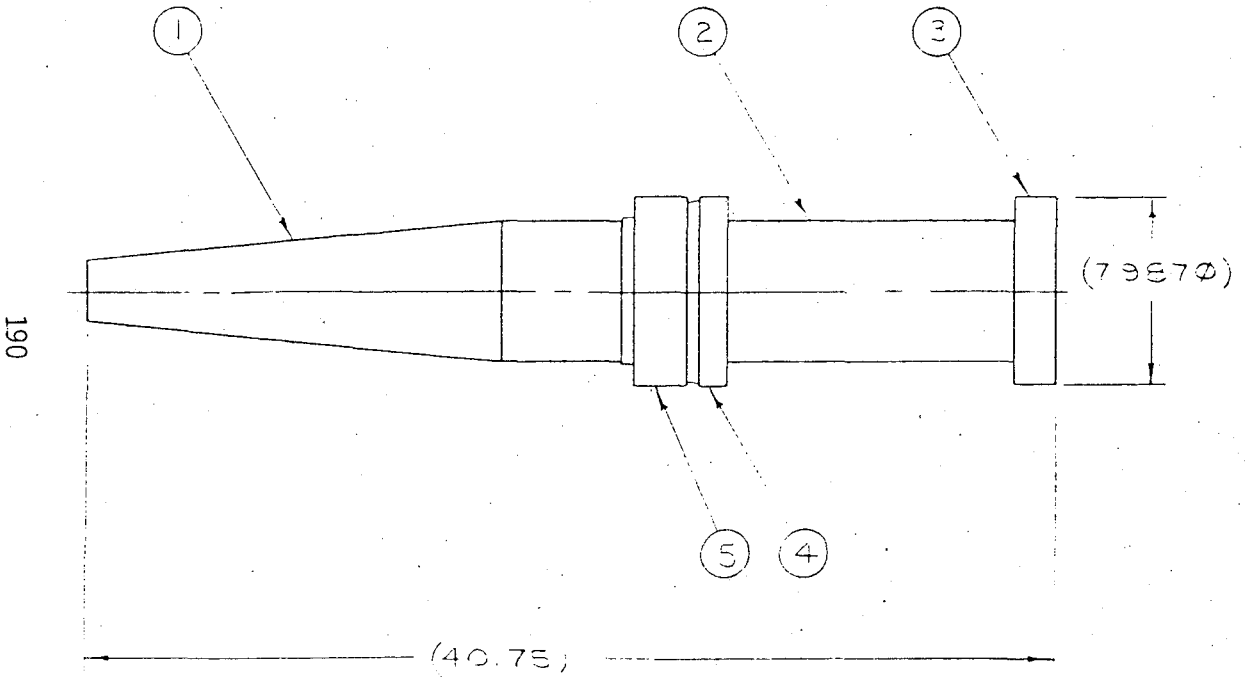

190

ITEM NO.	PART NO.	TITLE
5	D22974	SAND
4	D22973	SABOT
3	C22972	NOSE
2	D22971	BODY
1	D22957	SOLID FIN

PARTS LIST

Figure A2

		UNLESS OTHERWISE SPECIFIED DIMENSIONS ARE IN INCHES	ORIGINAL DATE OF DRAWING	SPACE RESEARCH CORP	
		TOLERANCES ON DECIMALS		NORTH TROY, VERMONT	
		ANGLES	PREP	SAPR77	TEST SLUG ASS
		MATERIAL	CHK		(SOLID FIN – CNTR
	TEST SLUG	HEAT TREATMENT	ENGR		
FINAL	8'-155mm		SUBMITTED	SIZE C	CODE IDENT NO. 30478
NEXT ASSY	USED ON	FINAL PROTECTIVE FINISH	APPROVED	SCALE 1/4	C2297
APPLICATION					SH

NOTES:

1. APPL[illegible] COATING OF SILICONE GREASE, [illegible] ON TAPERED SURFACE OF ITEM 4, PRIOR TO INSTALLATION OF ITEM 5.
2. HEAT ITEM 5 IN BOILING WATER FOR 10 TO 20 MINUTES PRIOR TO INSTALLATION. INSTALL ITEM 5 BY APPLYING A FORCE OVER ITS ENTIRE REAR FACE.

[illegible] CATION OF CHARACTER[illegible]CS (WR43A)
CRITICAL –
MAJOR –
MINOR –

LTR	DESCRIPTION	DATE

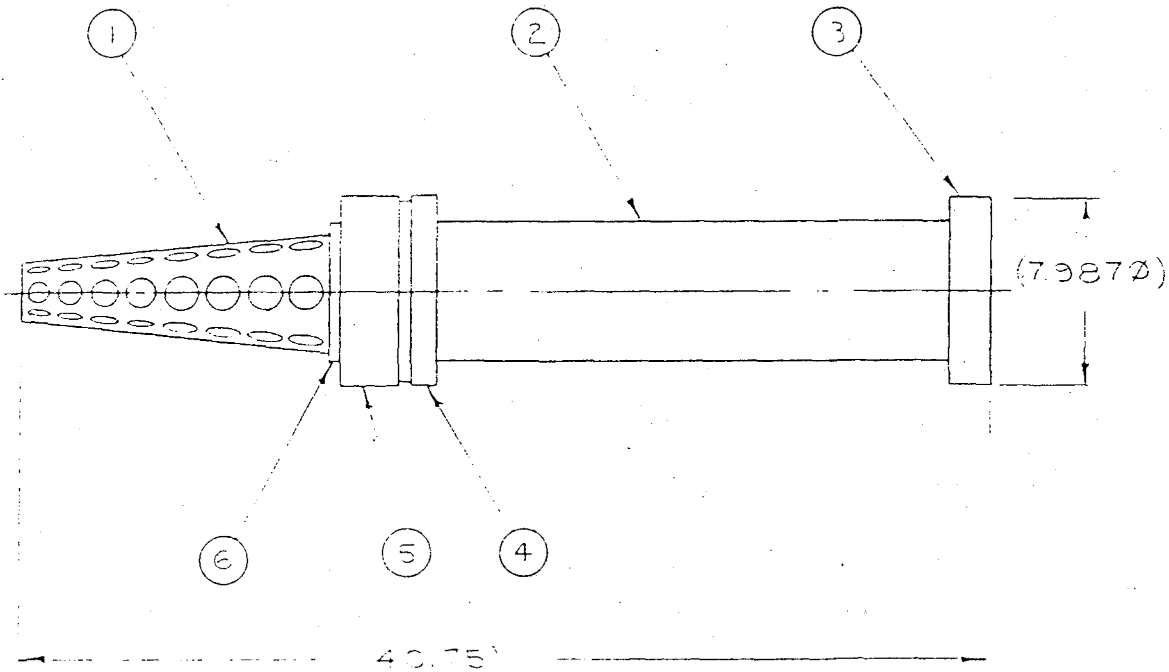

ITEM NO.	PART NO.	TITLE
6	C22955	CLOSURE
5	D22974	BAND
4	D22973	SABOT
3	C22972	NOSE
2	C22959	BODY
1	D22954	VENT. FIN 3

PARTS LIST

	TEST SLUG	UNLESS OTHERWISE SPECIFIED DIMENSIONS ARE IN INCHES TOLERANCES ON DECIMALS	ORIGINAL DATE OF DRAWING
		ANGLES	PREP 4 APR 77
		MATERIAL	CHK
			ENGR
FINAL	8-155MM	HEAT TREATMENT	SUBMITTED
NEXT ASSY	USED ON	FINAL PROTECTIVE FINISH.	APPROVED
APPLICATION			

SPACE RESEARCH CORPO[illegible]
NORTH TROY VERMONT

TEST SLUG ASS[illegible]
(VENT FIN - REAR SA

SIZE	CODE IDENT NO.	
C	30478	C2297[illegible]
SCALE 1/4		SHEE[illegible]

Figure A3

NOTES:

1. APPLY A LIGHT COATING OF SILICONE GREASE, MIL-C-21567, ON TAPERED SURFACE OF ITEM 4, PRIOR TO INSTALLATION, OF ITEM 5.
2. HEAT ITEM 5 IN BOILING WATER FOR 10 TO 20 MINUTES PRIOR TO INSTALLATION. INSTALL ITEM 5 BY APPLYING A FORCE OVER ITS ENTIRE REAR FACE.

CLASSIFICATION OF CHARACTERISTICS (WR43A)
CRITICAL –
MAJOR –
MINOR –

REVISIONS		
LTR	DESCRIPTION	E

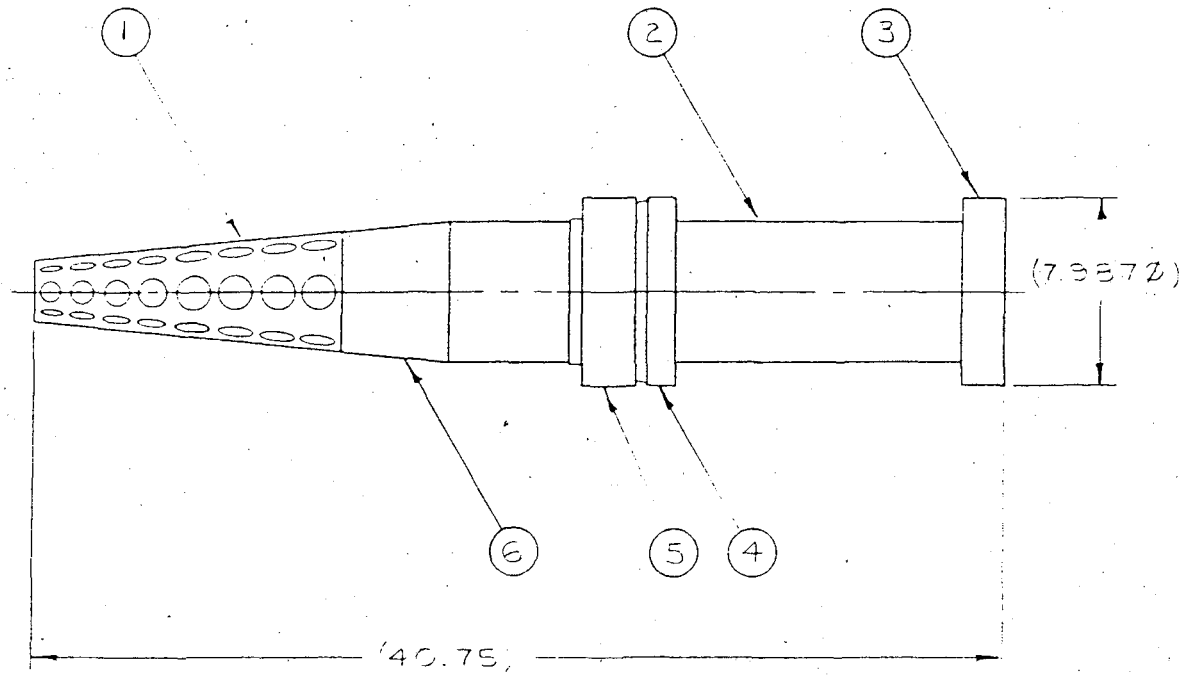

192

ITEM NO.	PART NO.	TITLE
6	C22956	CLOSURE
5	D22974	BAND
4	D22973	SABOT
3	C22972	NOSE
2	C22971	BODY
1	D22954	VENT. FIN 3

PARTS LIST

Figure A4

		UNLESS OTHERWISE SPECIFIED DIMENSIONS ARE IN INCHES	ORIGINAL DATE OF DRAWING 12 Oct 77	SPACE RESEARCH CORPOR	
		TOLERANCES ON DECIMALS		NORTH TROY, VERMONT	0
		ANGLES	PREP [illegible]	5 APR 77	TEST SLUG ASSY
		MATERIAL	CHK		(VENT FIN - CNTR SA
			ENGR [illegible]	15 APR 77	
	TEST SLUG	HEAT TREATMENT	SUBMITTED	SIZE / CODE IDENT NO.	C22976
FINAL	8-155MM			C / 30478	
NEXT ASSY	USED ON	FINAL PROTECTIVE FINISH.	APPROVED	SCALE 1/4	SHEET
APPLICATION					

NOTES:
1. ANSI Y14.5-73 & A20062 APPLY
2. ALL HOLES TO BE PERPENDICULAR TO EXTERNAL SURFACE.

CLASSIFICATION OF CHARACTERISTICS (WR43A)
CRITICAL -
MAJOR -
MINOR -

REVISIONS		
LTR	DESCRIPTION	DAT

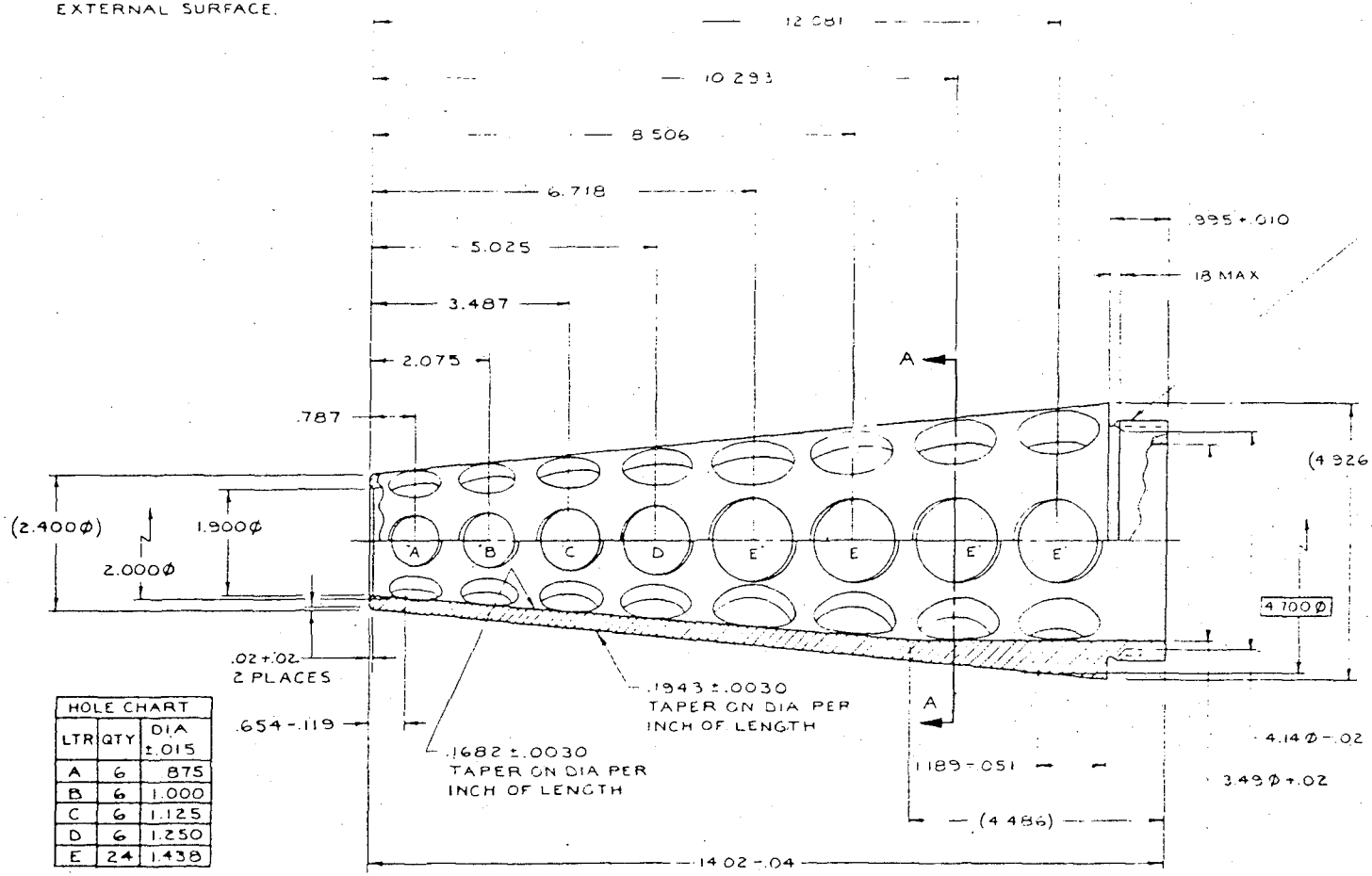

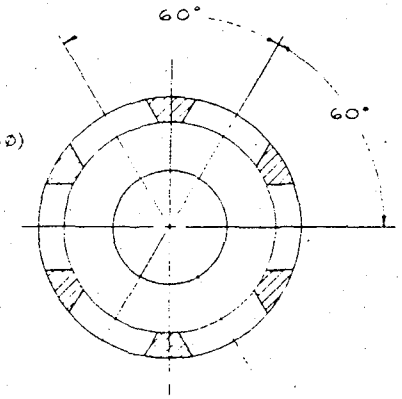

SECTION AA

HOLE CHART		
LTR	QTY	DIA ±.015
A	6	.875
B	6	1.000
C	6	1.125
D	6	1.250
E	24	1.438

(SEE NOTE 2)

Figure A5

		UNLESS OTHERWISE SPECIFIED DIMENSIONS ARE IN INCHES	ORIGINAL DATE OF DRAWING	SPACE RESEARCH COR NORTH TROY VERMONT
		TOLERANCES ON DECIMALS .XXX ±.030	PREP	
		ANGLES ±0°30'	CHK	
		MATERIAL ALUMINUM 7075T6	ENGR	VENTILATED FIN B
C22975	TEST SLUG	HEAT TREATMENT	SUBMITTED	
C22976	B .135MM			SIZE D / CODE IDENT NO 30478 / D229
NEXT ASSY	USED ON	FINAL PROTECTIVE FINISH	APPROVED	
APPLICATION				SCALE 1/1

PART NO D22954

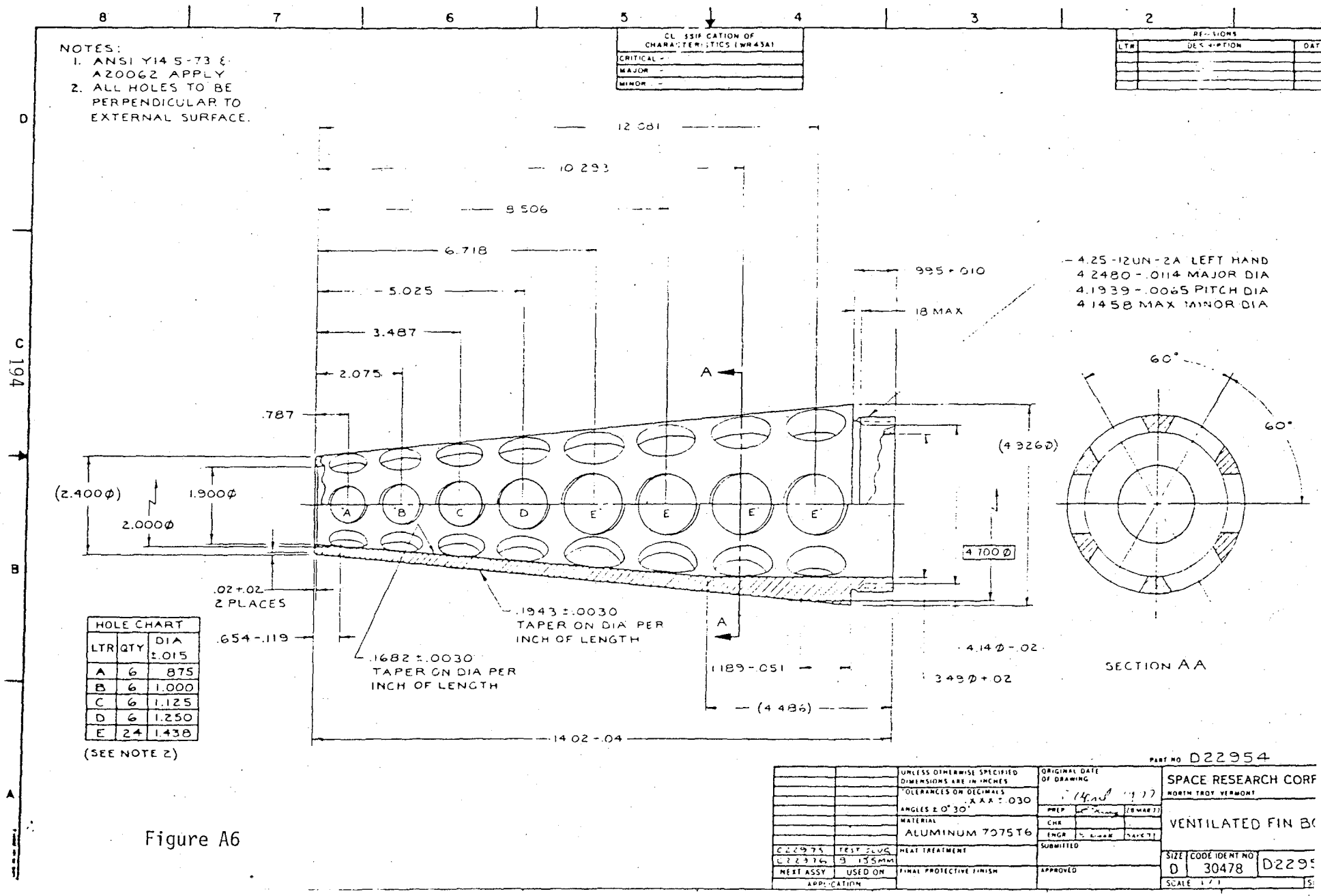
NOTES:
1. ANSI Y14.5-73 & A20062 APPLY
2. ALL HOLES TO BE PERPENDICULAR TO EXTERNAL SURFACE.
CLASSIFICATION OF CHARACTERISTICS (MIL-STD-453A)
CRITICAL -
MAJOR -
MINOR -
REVISIONS
LTR
DESCRIPTION
DATE
12.081
10.293
8.506
6.718
5.025
3.487
2.075
.787
995 ± .010
18 MAX
4.25-12UN-2A LEFT HAND
4.2480 - .0114 MAJOR DIA
4.1939 - .0065 PITCH DIA
4.1458 MAX MINOR DIA
(4.326Ø)
(2.400Ø)
1.900Ø
2.000Ø
4.100Ø
.02 ± .02
2 PLACES
.654 - .119
.1943 ± .0030
TAPER ON DIA PER
INCH OF LENGTH
.1682 ± .0030
TAPER ON DIA PER
INCH OF LENGTH
1.189 - .051
(4.486)
14.02 - .04
4.14Ø - .02
3.49Ø + .02
A
B
C
D
E
60°
60°
SECTION AA
HOLE CHART
LTR | QTY | DIA ±.015
A | 6 | .875
B | 6 | 1.000
C | 6 | 1.125
D | 6 | 1.250
E | 24 | 1.438
(SEE NOTE 2)
PART NO D22954
UNLESS OTHERWISE SPECIFIED DIMENSIONS ARE IN INCHES
TOLERANCES ON DECIMALS .XXX ± .030
ANGLES ± 0° 30'
MATERIAL
ALUMINUM 7075T6
HEAT TREATMENT
FINAL PROTECTIVE FINISH
ORIGINAL DATE OF DRAWING
PREP
CHK
ENGR
SUBMITTED
APPROVED
SPACE RESEARCH CORP
NORTH TROY, VERMONT
VENTILATED FIN BO
SIZE D
CODE IDENT NO 30478
D2295
SCALE 1/1
C22975 TEST PLUG
C22976 9.135MM
NEXT ASSY
USED ON
APPLICATION

Figure A6

CLASSIFICATION OF CHARACTERISTICS (WR43A)
CRITICAL -
MAJOR -
MINOR -

REVISIONS		
LTR	DESCRIPTION	DA
A	(1) NOTE 2 ADDED (2) CENTER HOLE ADDED	

NOTES:
1. ANSI Y-14.5-73 & A20062 APPLY.
2. MACHINE CENTER PERMISSIBLE .38 MAX DEEP.

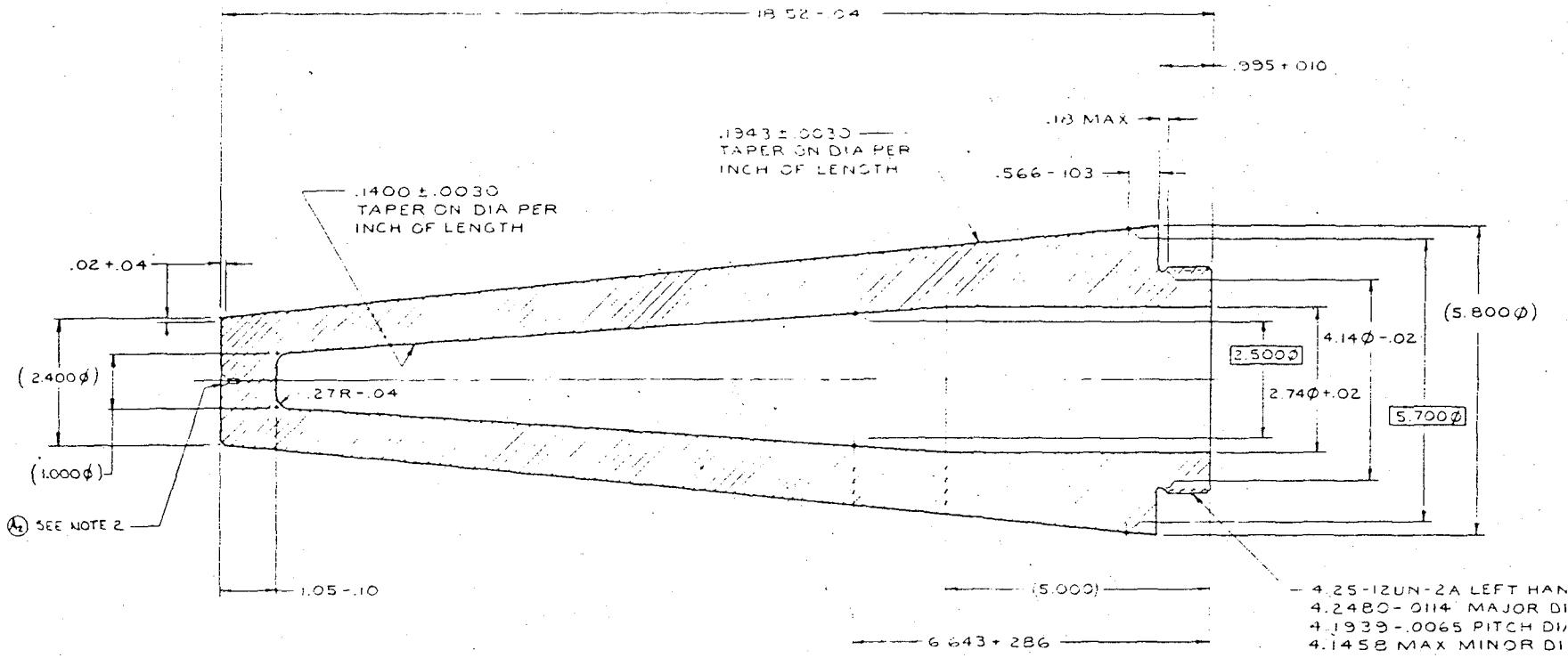

Figure A7

		UNLESS OTHERWISE SPECIFIED DIMENSIONS ARE IN INCHES	ORIGINAL DATE OF DRAWING	PART NO D22957	
		TOLERANCES ON DECIMALS	5 April 1977	SPACE RESEARCH COR	
		ANGLES	PREP	NORTH TROY VERMONT	
		MATERIAL ALUMINUM 7075T6	CHK	SOLID FIN BO	
			ENGR	(CENTER SAE	
		HEAT TREATMENT	SUBMITTED		
C22978	TEST SLUG 9.155MM			SIZE D	CODE IDENT NO 30478 D229
NEXT ASSY	USED ON	FINAL PROTECTIVE FINISH	APPROVED		
APPLICATION				SCALE 1/1	

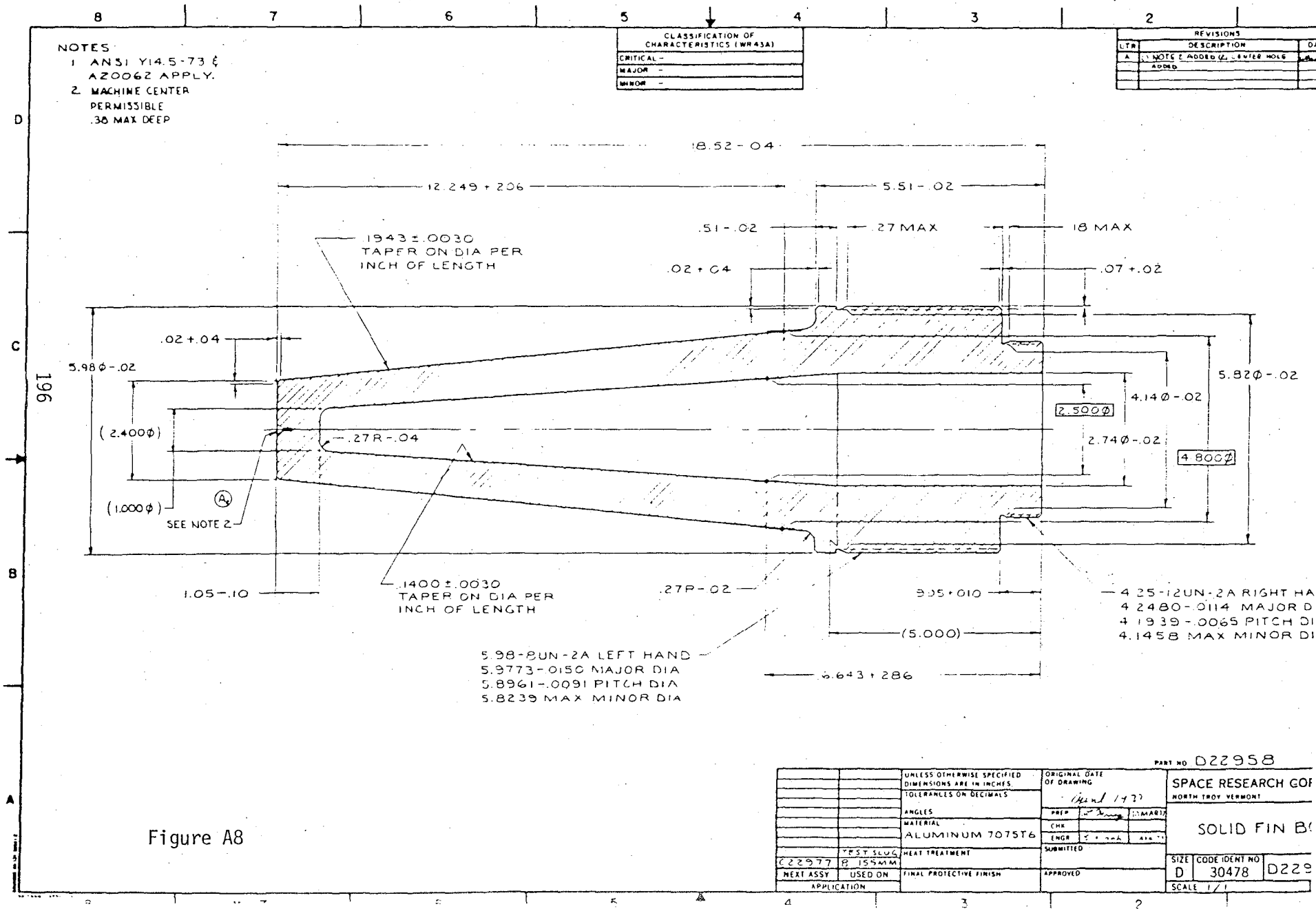
NOTES
1 ANSI Y14.5-73 & AZ0062 APPLY.
2. MACHINE CENTER PERMISSIBLE .38 MAX DEEP
CLASSIFICATION OF CHARACTERISTICS (WR43A)
CRITICAL –
MAJOR –
MINOR –
REVISIONS
LTR DESCRIPTION
A NOTE 2 ADDED & LETTER HOLE ADDED
18.52-.04
12.249+.206
5.51-.02
.51-.02
.27 MAX
18 MAX
.1943±.0030 TAPER ON DIA PER INCH OF LENGTH
.02+.04
.07+.02
.02+.04
5.98Ø-.02
(2.400Ø)
(1.000Ø)
SEE NOTE 2
.27R-.04
2.500Ø
4.14Ø-.02
2.74Ø-.02
4.800Ø
5.82Ø-.02
1.05-.10
.1400±.0030 TAPER ON DIA PER INCH OF LENGTH
.27R-.02
.505+.010
(5.000)
5.643+.286
5.98-8UN-2A LEFT HAND
5.9773-.0150 MAJOR DIA
5.8961-.0091 PITCH DIA
5.8239 MAX MINOR DIA
4.25-12UN-2A RIGHT HA
4.2480-.0114 MAJOR D
4.1939-.0065 PITCH DI
4.1458 MAX MINOR DI
196
PART NO D22958
UNLESS OTHERWISE SPECIFIED DIMENSIONS ARE IN INCHES
TOLERANCES ON DECIMALS
ANGLES
MATERIAL
ALUMINUM 7075T6
HEAT TREATMENT
FINAL PROTECTIVE FINISH
ORIGINAL DATE OF DRAWING
PREP
CHK
ENGR
SUBMITTED
APPROVED
TEST SLUG
C22977 B 155MM
NEXT ASSY
USED ON
APPLICATION
SPACE RESEARCH COR
NORTH TROY VERMONT
SOLID FIN B
SIZE D
CODE IDENT NO 30478
D229
SCALE 1/1

Figure A8

NOTES
1. ANSI Y14.5-73 & A20062 APPLY.

CHARACTERISTICS (WR43A)
CRITICAL –
MAJOR –
MINOR –

LTR	DESCRIPTION	DATE

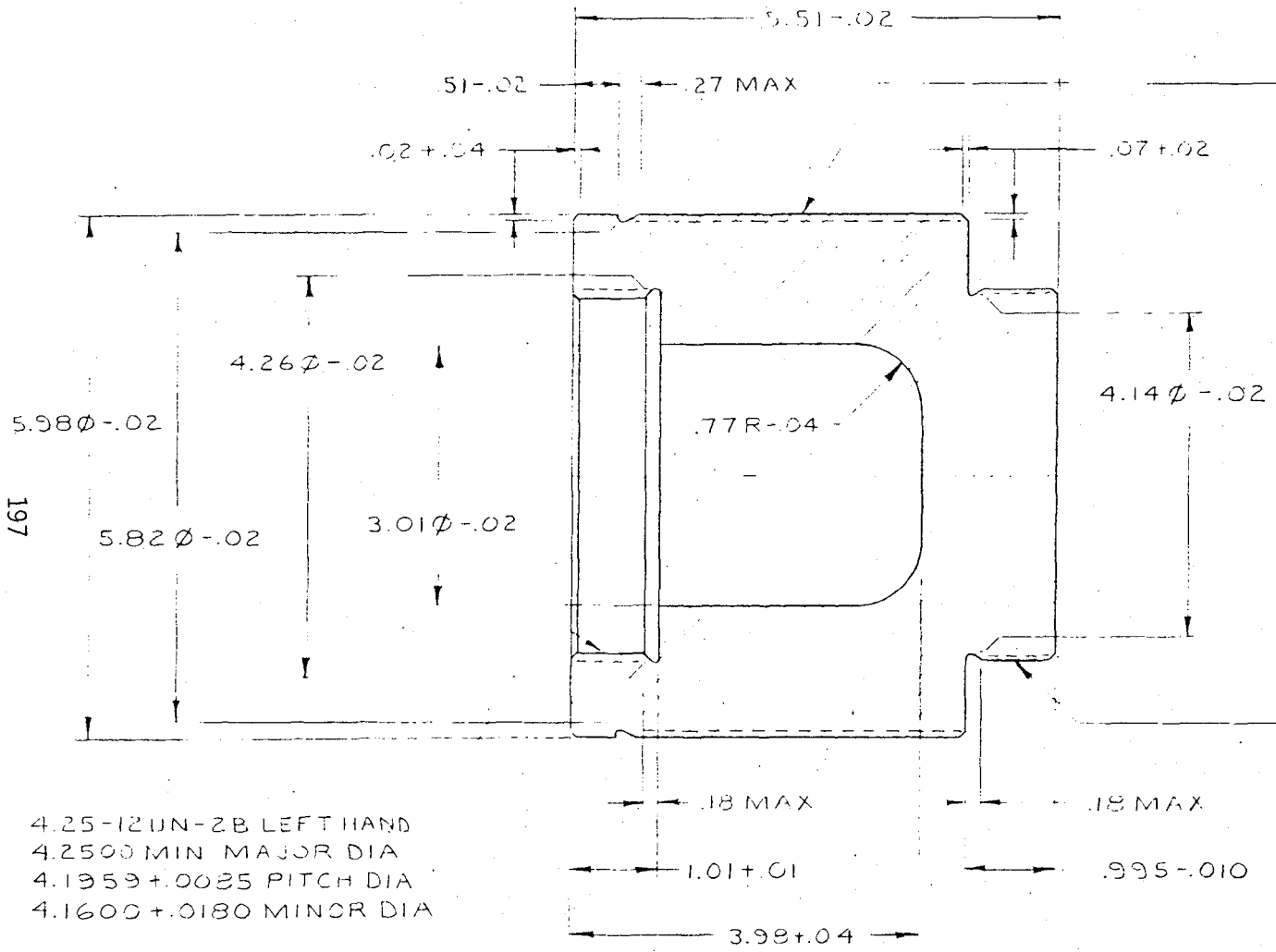

5.98-8UN-2A LEFT HA
5.9773-.0150 MAJOR D
5.8961-.0091 PITCH D
5.8239 MAX MINOR D

4.25-12UN-2A RIGHT H
4.2480-.0114 MAJOR DI
4.1939-.0065 PITCH DIA
4.1458 MAX MINOR DIA

4.25-12UN-2B LEFT HAND
4.2500 MIN MAJOR DIA
4.1959+.0085 PITCH DIA
4.1600+.0180 MINOR DIA

Figure A9

PART NO. C22955

		UNLESS OTHERWISE SPECIFIED DIMENSIONS ARE IN INCHES	ORIGINAL DATE OF DRAWING April 1977	SPACE RESEARCH CORPOR NORTH TROY, VERMONT
		TOLERANCES ON DECIMALS		
		ANGLES	PREP L. Krug 28MAR77	CLOSURE
		MATERIAL: ALUMINUM 7075 T6	CHK	
			ENGR E.L.nak 5APR77	
	TEST SLUG	HEAT TREATMENT:	SUBMITTED	SIZE C | CODE IDENT NO. 30478 | C22955
C22975	8"-155MM			
NEXT ASSY	USED ON	FINAL PROTECTIVE FINISH:	APPROVED	SCALE: 1/1 | SHEET
APPLICATION				

NOTES:
1. ANSI Y14.5-73 & A20062 APPLY.

CLASSIFICATION OF CHARACTERISTICS (WR43A)
CRITICAL -
MAJOR -
MINOR -

LTR	DESCRIPTION	DATE

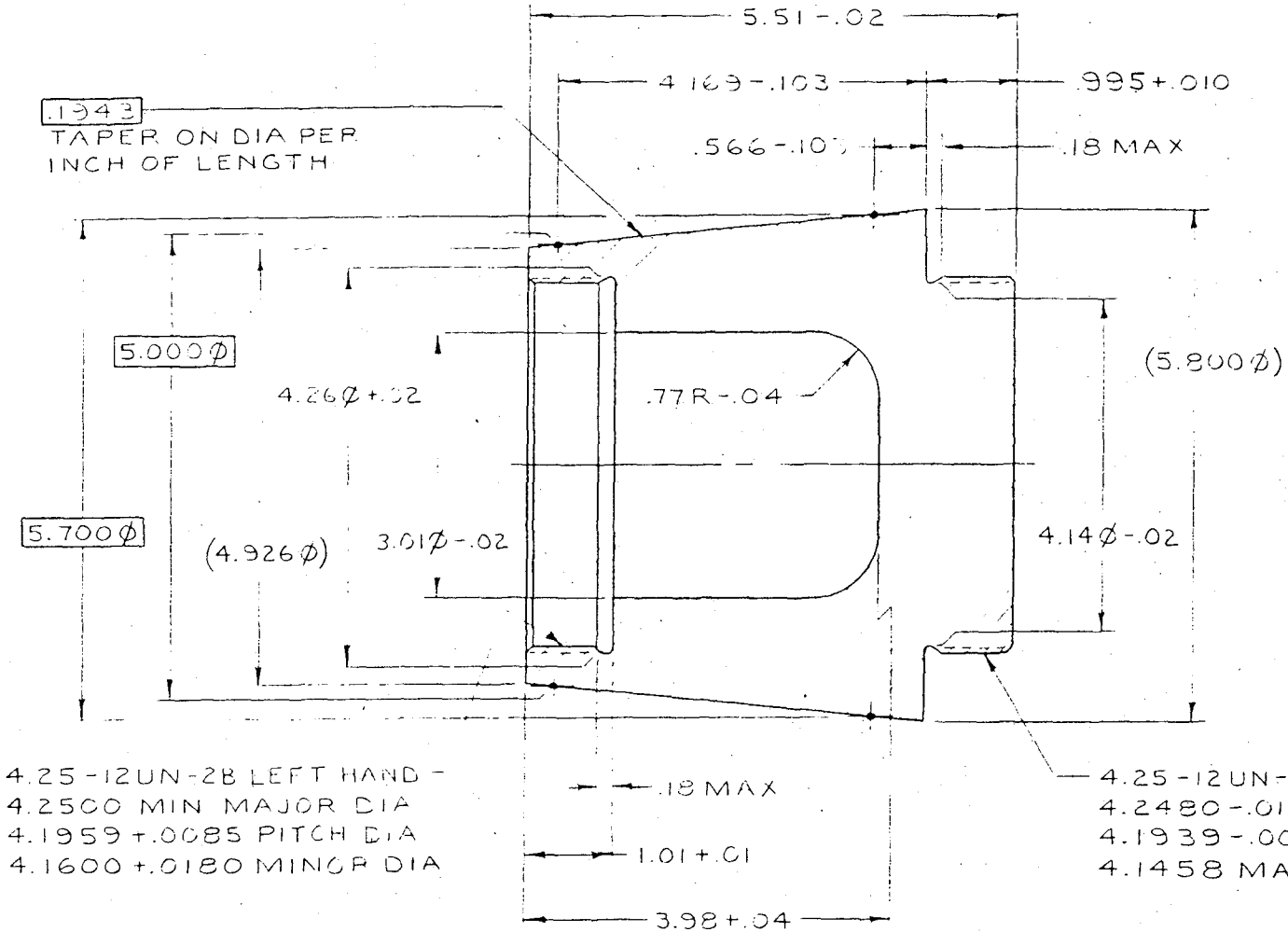

Figure A10

PART NO. C22956

		UNLESS OTHERWISE SPECIFIED DIMENSIONS ARE IN INCHES	ORIGINAL DATE OF DRAWING April 1977	SPACE RESEARCH CORPO NORTH TROY, VERMONT
		TOLERANCES ON DECIMALS		
		ANGLES	PREP [signature] 29MAR77	CLOSURE
		MATERIAL: ALUMINUM 7075 T6	CHK	(CENTER SABOT
			ENGR [signature] [illegible]	
	TEST SLUG	HEAT TREATMENT:	SUBMITTED	
C22976	8"-155 MM			SIZE C / CODE IDENT NO. 30478 / C22956
NEXT ASSY	USED ON	FINAL PROTECTIVE FINISH:	APPROVED	
APPLICATION				SCALE: 1/1 / SHE

NOTES:
1. ANS. Y14.5-73 & A20062 APPLY.

CLASSIFICATION OF CHARACTERISTICS (WR43A)
CRITICAL -
MAJOR -
MINOR -

LTR	DESCRIPTION	E

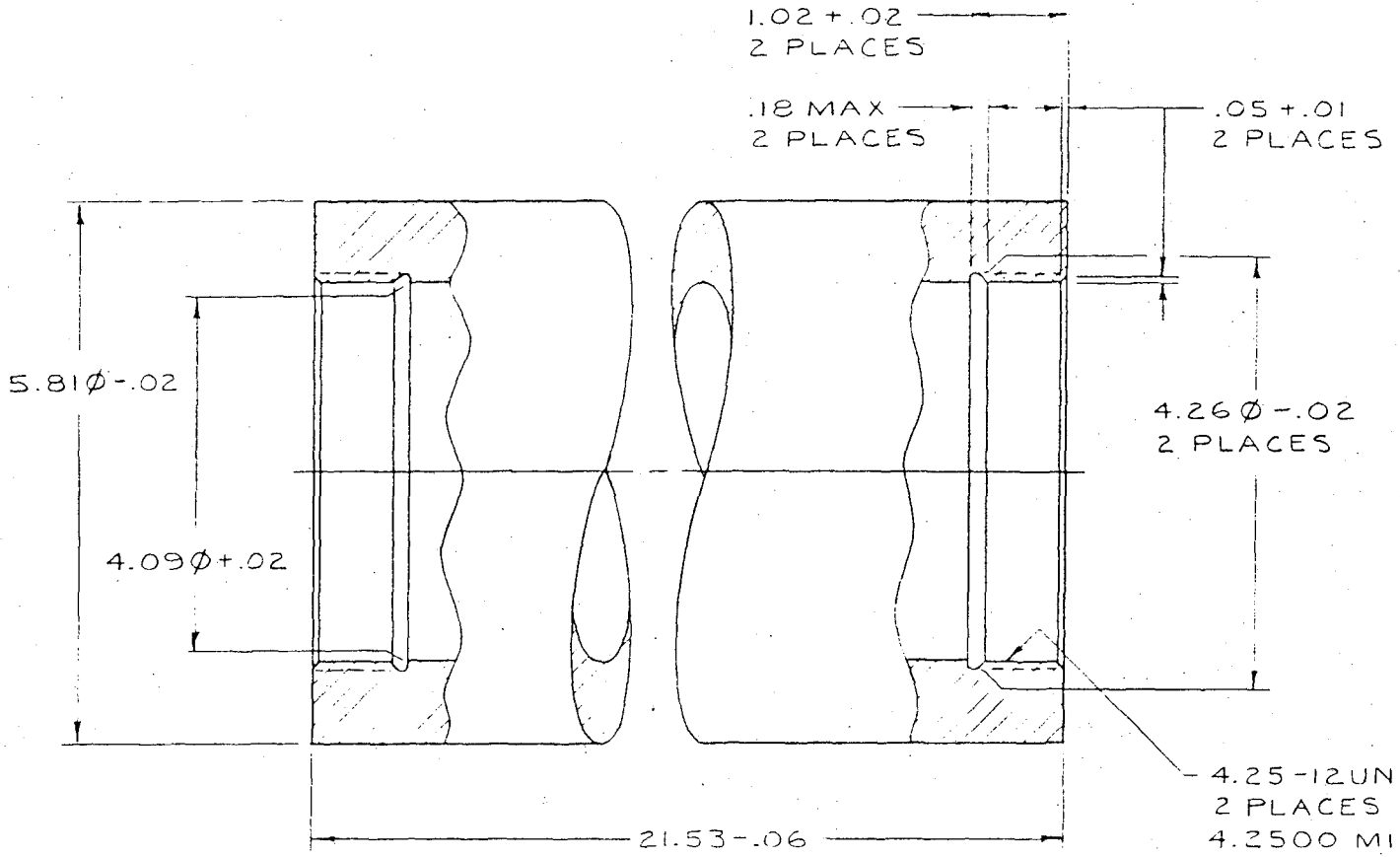

Figure A11

PART NO. C22959

		UNLESS OTHERWISE SPECIFIED DIMENSIONS ARE IN INCHES	ORIGINAL DATE OF DRAWING 5 April 77	SPACE RESEARCH CORPOR NORTH TROY, VERMONT
		TOLERANCES ON DECIMALS		
		ANGLES	PREP [illegible] 31MAR77	BODY
		MATERIAL: STEEL AISI 4140	CHK	
			ENGR S. Kmak 5APR77	
C22975	TEST SLUG	HEAT TREATMENT: NORMALIZED	SUBMITTED	
C22977	8"-155MM			SIZE C / CODE IDENT NO. 30478 / C2295
NEXT ASSY	USED ON	FINAL PROTECTIVE FINISH:	APPROVED	
APPLICATION				SCALE [illegible] / SHEE

MIL-STD-100 44 131 20041 2

NOTES
1 ANSI Y14.5-73 &
A20062 APPLY.

CLASSIFICATION OF CHARACTERISTICS (WR43A)
CRITICAL -
MAJOR -
MINOR -

REVISIONS		
LTR	DESCRIPTION	DA

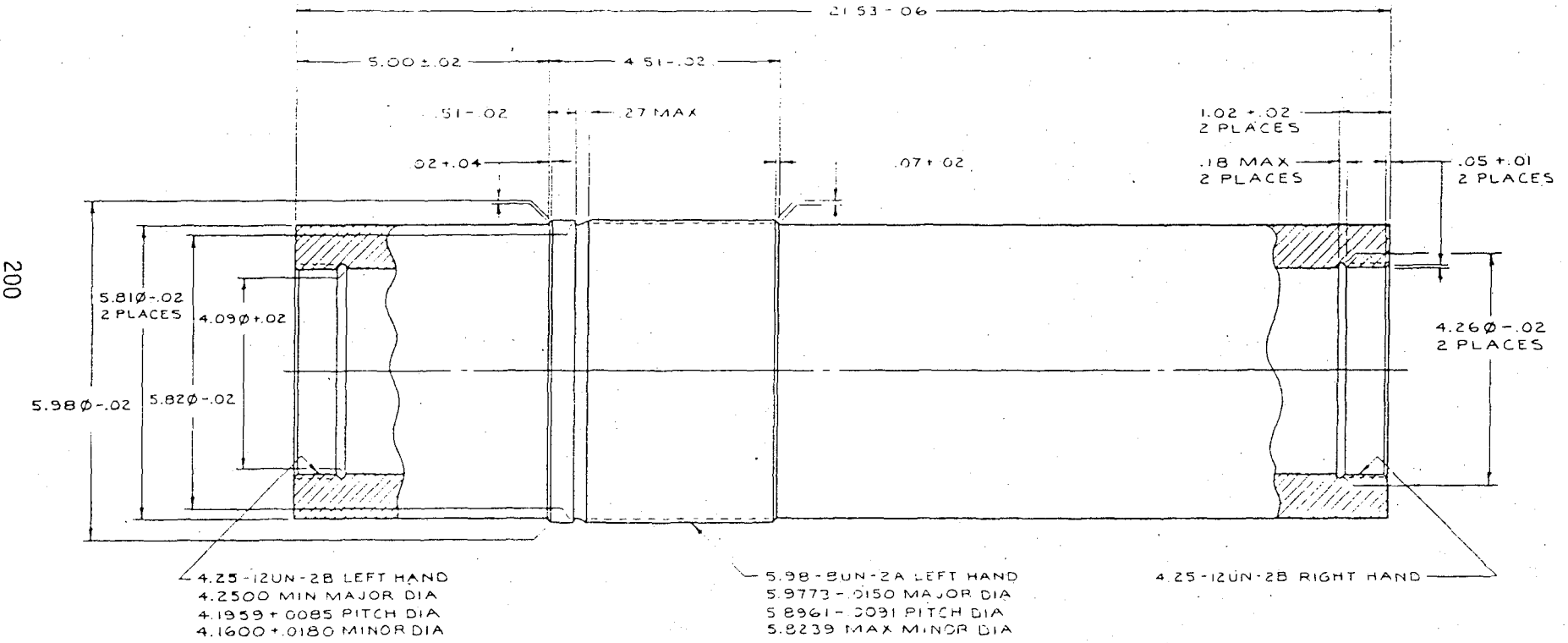

Figure A12

		UNLESS OTHERWISE SPECIFIED DIMENSIONS ARE IN INCHES	ORIGINAL DATE OF DRAWING April 1977
		TOLERANCES ON DECIMALS	
		ANGLES	PREP (11MAR77)
		MATERIAL STEEL AISI 4140	CHK
			ENGR (24MAR77)
C22976	TEST SLUG	HEAT TREATMENT NORMALIZED	SUBMITTED
C22978	B .155mm		
NEXT ASSY	USED ON	FINAL PROTECTIVE FINISH	APPROVED
APPLICATION			

PART NO D22971

SPACE RESEARCH COR
NORTH TROY, VERMONT

BODY
(CENTER SAB

SIZE	CODE IDENT NO	
D	30478	D229

SCALE 1/1

NOTES
1. ANSI Y14.5-73 & A20062 APPLY

CHARACTERISTICS (WR 43A)
CRITICAL –
MAJOR –
MINOR –

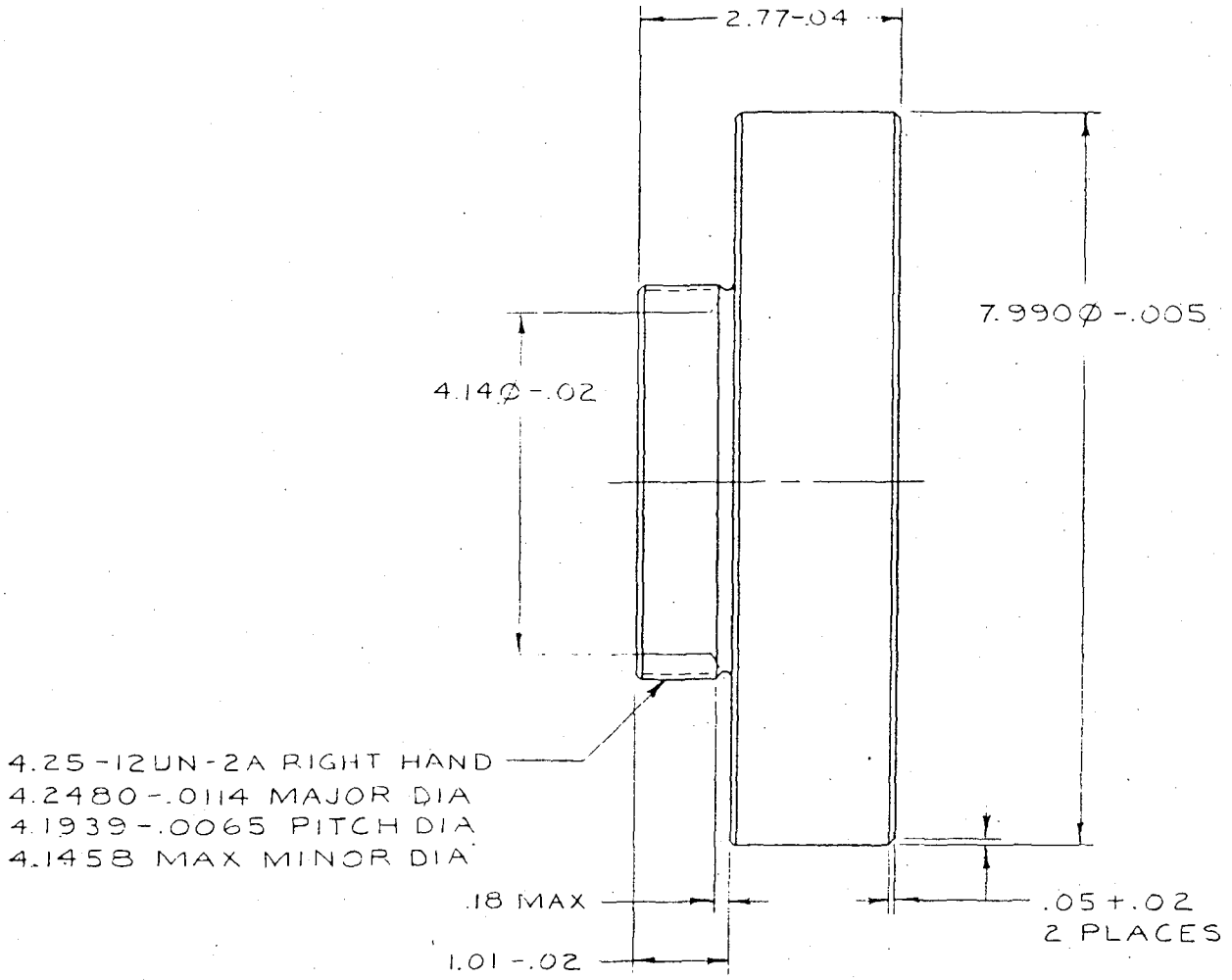

201

Figure A13

PART NO C22972

		UNLESS OTHERWISE SPECIFIED DIMENSIONS ARE IN INCHES	ORIGINAL DATE OF DRAWING 5 April 77	SPACE RESEARCH CORPORA NORTH TROY, VERMONT 058
		TOLERANCES ON DECIMALS		
		ANGLES	PREP [signature] 31MAR77	NOSE
		MATERIAL: MILD STEEL	CHK	
C22975			ENGR [signature] 5APR77	
C22976	TEST SLUG		SUBMITTED	
C22977	8"-155MM	HEAT TREATMENT:		SIZE C | CODE IDENT NO. 30478 | C22972
C22978				
NEXT ASSY	USED ON	FINAL PROTECTIVE FINISH:	APPROVED	SCALE: 1/1 | SHEET 1
APPLICATION				

4 3 2 1

NOTES:
1. ANSI Y14.5-73 & A20062 APPLY.

CLASSIFICATION OF CHARACTERISTICS (WR43A1)
CRITICAL –
MAJOR –
MINOR –

REVISIONS		
LTR	DESCRIPTION	DAT

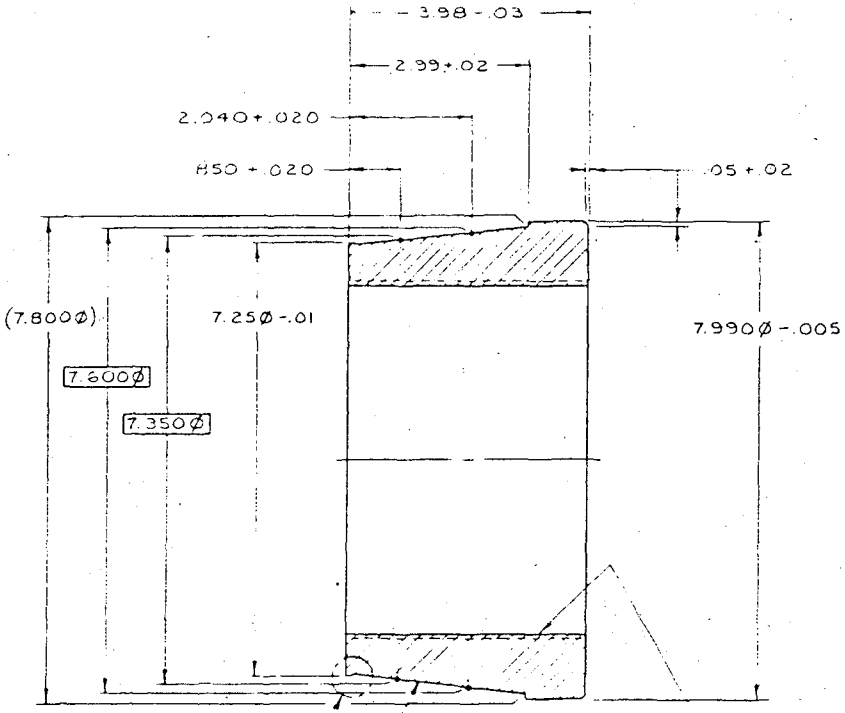

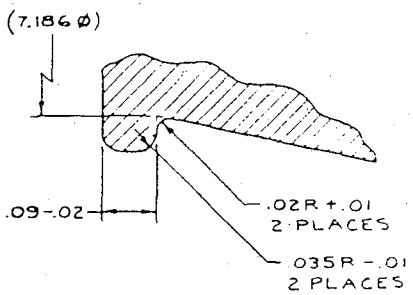

VIEW A
SCALE: 10/1

Figure A14

		UNLESS OTHERWISE SPECIFIED DIMENSIONS ARE IN INCHES	ORIGINAL DATE OF DRAWING
		TOLERANCES ON DECIMALS	
		ANGLES	PREP
		MATERIAL	CHK
C22975	TEST SLUG	ALUMINUM 7076 T6	ENGR
C22976	2 -155 MM		SUBMITTED
C22977		HEAT TREATMENT	
C22978			APPROVED
NEXT ASSY	USED ON	FINAL PROTECTIVE FINISH	
APPLICATION			

PART NO D22973

SPACE RESEARCH CORP
NORTH TROY, VERMONT

SABOT

SIZE	CODE IDENT NO	
D	30478	D229

SCALE 1/1 & AS NOTED

NOTES:
1. ANSI Y14.5-73 & A20062 APPLY.

CLASSIFICATION OF CHARACTERISTICS (WR43A)
CRITICAL -
MAJOR -
MINOR -

REVISIONS		
LTR	DESCRIPTION	D

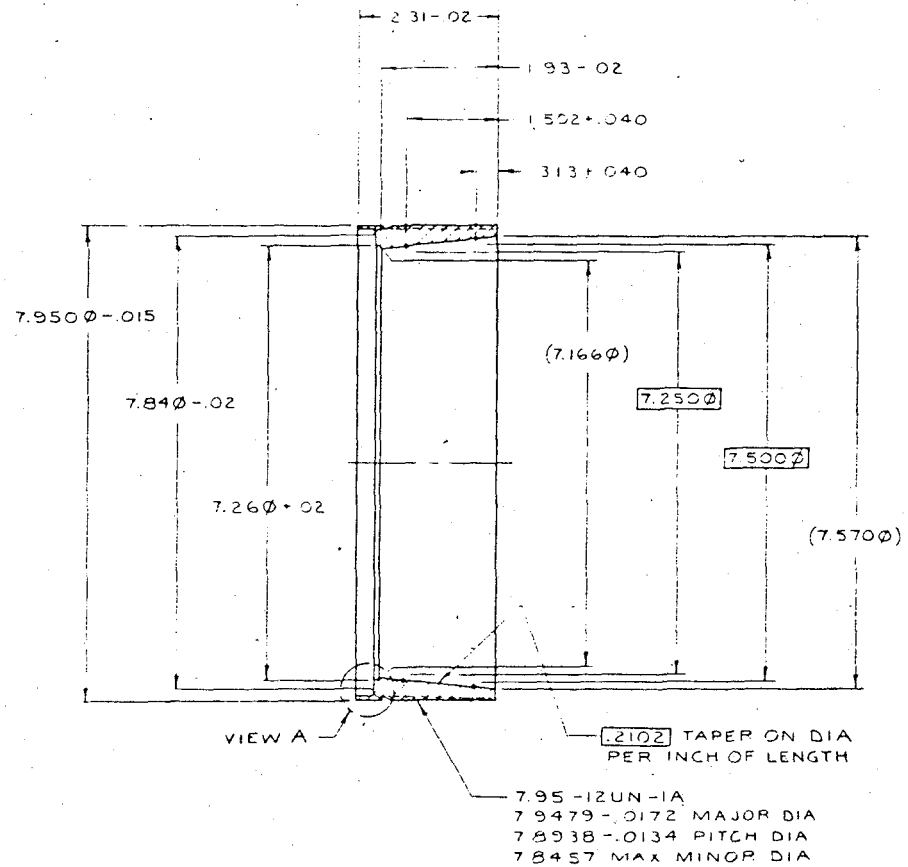

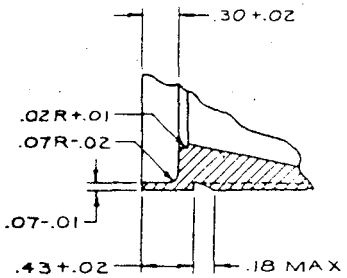

VIEW A
SCALE: 2/1

Figure A15

		UNLESS OTHERWISE SPECIFIED DIMENSIONS ARE IN INCHES	ORIGINAL DATE OF DRAWING	PART NO D22974
		TOLERANCES ON DECIMALS		SPACE RESEARCH COR NORTH TROY VERMONT
		ANGLES	PREP	7APR77
		MATERIAL	CHK	DRIVING BA
C22975	TEST SLUG	POLYPROPYLENE	ENGR	
C22976	Ø .155MM		SUBMITTED	
C22978		HEAT TREATMENT		SIZE D / CODE IDENT NO 30478 / D229
C22979			APPROVED	
NEXT ASSY	USED ON	FINAL PROTECTIVE FINISH		SCALE AS NOTED
APPLICATION				

203